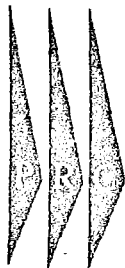


SECOND  
RELIABILITY ASSESSMENT  
FOR THE  
ORBETING GEOPHYSICAL  
OBSERVATORIES

PRC R-276

27 OCTOBER 1962

PREPARED FOR  
NATIONAL AERONAUTICS  
AND SPACE ADMINISTRATION  
GODDARD SPACE FLIGHT CENTER



PLANNING RESEARCH CORPORATION  
LOS ANGELES, CALIFORNIA WASHINGTON, D. C.

FACILITY FORM 602

N69-72324	
(ACCESSION NUMBER)	(THRU)
290	None
(PAGES)	(CODE)
CR 100614	
(NADA CR OR TMX OR AD NUMBER)	(CATEGORY)

SECOND RELIABILITY ASSESSMENT  
FOR THE  
ORBITING GEOPHYSICAL OBSERVATORIES

PRC R-276

27 October 1962

Prepared for  
National Aeronautics and Space Administration  
Goddard Space Flight Center  
Under Contract NAS 5-1692

George R. Grainger  
Project Manager

PLANNING RESEARCH CORPORATION  
LOS ANGELES, CALIF.      WASHINGTON, D.C.

## ACKNOWLEDGMENT

As in the preliminary reliability assessment of OGO, the work documented herein is a team effort. Accordingly, the project manager acknowledges with great appreciation the individual contributions of the members of the PRC study team: James D. Andrew, H. Bruce Battey, Eloise E. Bean, Charles E. Bloomquist, Norman E. Chudacoff, William E. Faragher, Richard K. Fox, Lloyd L. Philipson, George E. Monroe, Jr., Robert J. Mulvihill, Wilbur J. Myers, Richard G. Salter, and H. Scott Watson.

Special appreciation is expressed to James D. Andrew for his managerial assistance as leader of the assessment engineering team. Additional thanks are extended to the personnel of the PRC Publications Department for another outstanding publications effort, and particularly to Miss Peggy Kimball for her excellent editorial assistance.

Finally, the entire PRC study team gratefully acknowledges the cooperation of Mr. Jerome Joseph, of Space Technology Laboratories, and the effective support of Mr. Charles F. Rice, of NASA's Western Operations Office, in ensuring receipt by PRC of pertinent OGO design and test information.

## FOREWORD

This is the second of a series of reliability assessment reports on the Orbiting Geophysical Observatories (OGO). Working under prime contract NAS 5-1692, awarded by the Goddard Space Flight Center of the National Aeronautics and Space Administration, the Planning Research Corporation study team assists NASA in the over-all OGO development program by making independent estimates of OGO spacecraft system reliability, aiding in the establishment of reliability goals, and acting as a technical advisor to NASA in OGO reliability matters.

The first reliability assessment was preliminary in nature in that it was based on not-quite-finalized designs (in some areas), limited information about the experiments to be "serviced" by the OGO spacecraft, and broadly defined environmental and electrical stresses. The second assessment, which is reported herein, consists of a "second look" at the work of the first assessment, generally updating and refining the preliminary work. Specifically, to bring more realism into the second assessment, a number of simplifying assumptions that had of necessity been made in the preliminary assessment were eliminated, launch and POGO effects were brought into the assessment, each individual subsystem assessment was more detailed and incorporated the latest design changes, basic failure rates were revised based on new information, and the reliability models were revised to incorporate the greater depth of engineering analysis.

The third assessment, currently underway, will further refine and update the first two assessments. Primary emphasis is being placed on increased engineering analysis at the subsystem level, guided by the basic objective of achieving a complete assessment of all aspects of the spacecraft. To add to the completeness and realism of the assessment, applicable data arising from all OGO spacecraft and subsystem tests during this period will be incorporated into the assessment.



## ABSTRACT

This report is an after-the-fact publication of the second assessment findings in the sense that, because of OGO design changes and other perturbations in the development schedule, these findings have already been reported via a number of technical advisement memoranda (TAM's). The report's purpose, then, is to provide the reader with a single-entity report covering the work presented in these TAM's. In addition to bringing the second assessment TAM's together in one volume, this report also supplies introductory and summary sections to give the reader an over-all view of the assessment.

The report begins with the introduction and a summary of all TAM's prepared to date. It is well to note that summaries of the TAM's appearing in full in later sections of this report are included, thus providing the reader with a nondetailed description of the work reported in each such TAM.

Section II, "Parts Information," consists of two TAM's containing input information that is essential to the second assessment. More explicitly, the first TAM presents the component-part failure rates used in the second assessment system and subsystem reliability predictions, and the second TAM consists of a complete listing of the spacecraft's current parts complement.

Section III, "Subsystem Assessments," is the heart of the report, containing the TAM's describing the detailed aspects of the second reliability assessment of the five major spacecraft subsystems. Each of these TAM's references the corresponding preliminary subsystem assessment (e.g., in most cases, the subsystem description contains a description of subsystem design changes occurring since the first assessment) to a great degree, and emphasizes the refinements and greater depth of analysis introduced in the second assessment.

The subsystem assessment predictions are combined in Section IV, "Spacecraft System," in the form of a single TAM. This TAM restates the figure-of-merit (FOM) and classical reliability formulations

established in the preliminary assessment and then presents numerical evaluations of spacecraft system reliability using each of these models.

The final section, "Conclusions and Recommendations," was especially prepared, as was the first section, to give the reader an overall view of the assessment. With this as its goal, the final section presents, in summary form, the conclusions and recommendations reached during the second assessment. For the reader who is interested in more detail, the source of each conclusion is given in terms of the TAM in which it appears in detailed form.

## TABLE OF CONTENTS

TAM  
Number<sup>1</sup>

ACKNOWLEDGMENT

FOREWORD

ABSTRACT

I. INTRODUCTION

II. PARTS INFORMATION

III	A.	Parts Failure Rates	7
	B.	Parts Complement	10

III. SUBSYSTEM ASSESSMENTS

A.	Communications and Data Handling Subsystem	9
B.	Attitude Control and Stabilization Subsystem	12
C.	Power Supply Subsystem	11
D.	Thermal Control Subsystem	8
E.	Structure Subsystem	6

IV.	SPACECRAFT SYSTEM	13
-----	-------------------	----

V. CONCLUSIONS AND RECOMMENDATIONS

---

<sup>1</sup>The customary practice of giving page numbers cannot be followed here since this report is primarily a collection of previously published TAM's. For cross-referencing and other identification purposes, however, the TAM numbers corresponding to individual sections and subsections are presented. It should also be noted that each of the individual TAM's contains a table of contents.

## I. INTRODUCTION AND SUMMARY OF TAM'S

### A. Introduction

This document reports upon the second in a series of three independent reliability assessments of the Orbiting Geophysical Observatories (OGO). These assessments are being conducted by Planning Research Corporation (PRC) for the Goddard Space Flight Center, National Aeronautics and Space Administration.

The first assessment, intended to be of a preliminary nature, culminated in PRC report R-243, Preliminary Reliability Assessment for the Orbiting Geophysical Observatories, dated 1 February 1962 (Unclassified). As a result of certain complexities not foreseen at the outset, the first assessment entered into greater detail in certain areas (notably the Communications and Data Handling Subsystem) than had originally been envisioned for the initial assessment effort. This, in effect, shifted portions of the second assessment effort into the preliminary assessment. At the same time, design changes by STL had occasioned some slippage in the development schedule and, consequently, caused a slippage in PRC's preliminary assessment schedule due to the concomitant delays in delivery to PRC of essential drawings and other pertinent information.

Considering all these factors, the net result was a reduction in the time scale and budgeting allocations for the second assessment in order to devote the necessary increased attention to the preliminary assessment. Further design changes occurred early in the second assessment that necessitated the sequential (i. e., by subsystem) accomplishment of the assessment. When the desirability of this course of action became evident, GSFC and PRC representatives agreed that the subsystem and system second assessments would be reported on sequentially, as they were completed, through the use of technical advisement memoranda (TAM's). Since other TAM's pertaining to specialized problems were also issued during the second assessment, it was felt that a single document summarizing all the second assessment work and incorporating

the subsystem and system TAM's in toto is desirable. This report, then, is an after-the-fact publication, as a single-entity report, of the work of the second assessment.

The second assessment work has consisted, in the main, of a "second look" at the work of the first assessment. In order to bring more realism into the second assessment, considerable effort was devoted to the elimination of a number of simplifying assumptions made as a matter of economic and temporal necessity in the first effort. It should be realized that the elimination of some of these assumptions has entailed considerable detailed engineering activity at the subsystem level, while others have involved changes in the over-all system reliability model. Each instance, however, has resulted in worthwhile increases in the realism and practicality of the study.

At this writing, the third assessment already is well underway. That assessment will be devoted primarily to increased engineering analysis at the subsystem level. In addition, it is anticipated that partial results of STL's test program on the OGO spacecraft will be available as data inputs for the third assessment, increasing the realism and utility of the assessment results to a considerable degree.

This second assessment report has been written under the assumption that it need not be repetitive of the contents of the first assessment report (PRC R-243). Hence, the reader is encouraged to consult that report (as well as the referenced TAM's summarized herein) when further clarification or additional details are required.

The report is organized in the following fashion: The second half of this section (subsection I.B) contains a brief summary of each of the TAM's published in the second assessment effort. Section II consists of information concerning parts being utilized in OGO. First, failure rates for use in the reliability analysis are discussed (TAM No. 7) and, second, a parts complement for the spacecraft is presented (TAM No. 10). As concerns TAM No. 10, this is believed to be the only complete parts complement that has been prepared for the OGO system. Hence, it should prove valuable in many activities over and above those related to reliability considerations.

Section III contains complete copies of the TAM's reporting on the second assessment for each subsystem. The TAM's presented are No. 9, Communications and Data Handling; No. 12, Attitude Control and Stabilization; No. 11, Power Supply; No. 8, Thermal Control; and No. 6, Structure.<sup>1</sup> It should be noted that not all of the TAM's summarized in subsection I.B are reprinted in their entirety in Section III. Rather, only those TAM's considered essential to an understanding of the second assessment results are reprinted; other more specialized TAM's are omitted, but have been summarized in subsection I.B.

Next, Section IV reports the calculated over-all OGO spacecraft system reliability, synthesizing the results of the foregoing TAM's through use of the PRC figure-of-merit reliability model.

Finally, a summary of the conclusions and recommendations arising from the second assessment activity is contained in Section V. This section reports findings from the TAM's contained in their entirety in the body of this report, as well as those from TAM's given only summary treatment herein.

#### B. Summary of TAM's

During the course of the OGO reliability studies, 13 technical advisement memoranda have been issued by PRC. Actually, certain of these TAM's were published during the period of the first assessment, but in order to provide a complete picture all of them are summarized in this subsection. Also, 8 of the 13 TAM's (those essential to the mechanics of the second assessment) are published in their entirety in subsequent sections of this document.

In summary, the contents of the TAM's are as follows:

##### 1. TAM No. 1, "Technical Advisement Memoranda"

TAM No. 1 establishes the policy for issuance of TAM's by PRC and recommends a procedure for review and comment by STL and GSFC. Since this TAM is nontechnical in nature, no further summary discussion of it will be presented here.

---

<sup>1</sup>TAM's are numbered in the order published; however, for ease of cross-reference, subsystems are listed in the order established in PRC R-243.

2. TAM No. 2, "Communications and Data Handling (CDH) Subsystem, Main Commutator Matrix (MCM) Reliability,"

TAM No. 2 first evolves a generalized functional description of the MCM, as presently designed, in which the main commutator counter (MCC) is identified as a seven-stage binary counter the function of which is to drive the MCM. The driving mechanism is based on true or false logic states that are transformed into 128 word-time signals by the MCM. The MCC is configured in a row-column matrix with a four-stage counter driving a three-stage counter to achieve the seven stages. The state signals drive 16 four-input diode "AND" gates in the four-stage counter and 8 three-input diode "AND" gates in the three-stage counter. Suitable buffer amplifiers are also provided.

A parts count is made based on the above configuration. This is followed by an analysis of types of failures wherein it is shown (with calculated probabilities of occurrence) that certain failures can cause either loss of signal or garbling of signal for entire rows or columns. Other failures are serious in nature in that single-word losses result.

In view of the seriousness of certain failures (occurring with non-negligible probability) with this row-column design, two alternate designs are evolved in the TAM and parts counts are calculated for them. One of these is called the "direct" scheme, in which 128 seven-input "AND" gates are used (i. e., one for each word) in the MCM. More parts are involved with this configuration, but no gate failure causing multiple-word loss can occur. The second scheme is called the "3-wire" scheme; this involves an 8-row-by-16-column matrix portioned into 8 submatrices with 4-row-by-4-column configurations.

It is clear that, in the above configurations (as well as in several others that can be envisioned), the effects of failure are subject to wide variation. This points up the importance of the figure-of-merit (FOM) approach and highlights the inadequacy of the "classical" reliability analysis for an application of this type. Three types of analyses are made for each of the three configurations: (1) FOM, (2) classical, and (3) parts-count classical. For the classical analysis, it is assumed that success is defined as having two-thirds or more of the 128 words in an operable

state. The parts-count classical analysis assumes that all parts are in series, reliability-wise, and that any failure results in system loss. (The FOM approach, having been discussed in depth in PRC's first assessment report, will not be further discussed here.)

Clearly, an analysis of type (2)--and, even more so, type (3)--would be unrealistic for this application, but, for purposes of comparison, these are included in the following table. The table presents 1-year reliability estimates for an MCM configured in the three schemes mentioned above.

	Type of Analysis		
	<u>FOM</u>	<u>Classical</u>	<u>Parts-Count Classical</u>
Present Design	0.898	0.980	0.082
Direct	0.975	~ 1.00	0.042
3-Wire	0.983	0.997	0.170

It is first concluded that the present design is the least reliable of the three schemes considered. Then, additional consideration is centered upon the "unpluggability" feature of the direct scheme, and it is finally concluded that this "tailoring to the mission" possibility makes the direct scheme the superior one.

### 3. TAM No. 3, "Determination of Average Power Generated by Solar Cells Under Conditions of Random Tumbling"

The preliminary investigation reported in TAM No. 3 was performed at the request of GSFC. The purpose of the investigation was to determine whether, in a tumbling state, the solar cells of the OGO spacecraft would "see" the sun for an adequate percentage of time to generate sufficient power to keep the craft in some state of useful, though highly degraded, operation.

Since the investigation is preliminary in nature, the general approach is to establish an optimistic methodology wherein the maximum expected solar cell generation efficiency and the minimum spacecraft



power requirements are assumed. Then, the calculations indicate either (1) that the spacecraft definitely cannot survive in the tumbling state or (2) that it cannot be determined on the basis of this preliminary investigation that survival is possible. With answer (2), further investigation might be warranted at the descretion of GSFC.

The basic relation utilized in the analysis is

$$p(\theta) = p_m \cos \theta$$

where  $p(\theta)$  is the power generated by a single solar cell at any angle  $\theta$  from the sun, and  $p_m$  is the maximum power generation capability of the cell when the sun's rays impinge upon its face at a  $90^\circ$  angle.

From the above relation it follows that the total power,  $P(\theta)$ , for an entire array of cells is

$$P(\theta) = P_m \cos \theta$$

where  $P_m = n \bar{p}_m$  ( $\bar{p}_m$  being the average  $p_m$  of the individual cells comprising the array and  $n$  being the number of cells).

For a randomly tumbling spacecraft, TAM No. 3 derives an equation for the average power,  $P_{avg}$ , generated by the solar array. This equation is

$$P_{avg} = \frac{P_m}{\pi} = 0.318 P_m$$

Using the above equation and required OGO power system data, the following table is prepared:

Time in Orbit (Months)	$P_m$ (Watts) for a Perfectly Oriented OGO Vehicle	$P_{avg}$ (Watts) for a Randomly Tumbling OGO Vehicle	Watt-Hours Per EGO Orbit for a Randomly Tumbling OGO Vehicle
0	423	135	5130
3	402	128	4860
6	380	121	4600
9	358	114	4330
12	337	107	4070

To investigate the capability of the spacecraft to survive in the randomly tumbling state, it is necessary to estimate the minimum power requirements for it to "keep alive" (i. e., perform any useful function as a data-gathering device). In making this investigation it is assumed that all unneeded equipment can be deactivated by command so that only essential power requirements are satisfied.

Based on published STL data, it is determined that 1765 watt-hours per EGO orbit are required for the "keep-alive" randomly tumbling condition. Thus, it is seen that answer (2) is obtained; i. e., it cannot be stated whether survival is possible. A more definitive resolution would require more detailed analysis, not only of the power generation system and spacecraft power requirements, but of the capabilities of other subsystems in the tumbling state (e. g., the Thermal Control Subsystem).

4. TAM No. 4, "Critique of STL's OGO Reliability Report Number II, Dated 29 January 1962"

At the request of GSFC, PRC reviewed the subject STL report and prepared a critique in the form of a TAM. Essentially, this TAM compares PRC's first assessment findings with those of STL and discusses the major points of difference. In summary, the major differences are as follows:

- a. Generally, STL's failure rates are lower than those used by PRC.
- b. STL uses a classical reliability model, while PRC uses a figure-of-merit model plus a classical model for comparative purposes.
- c. Numerous differences (generally of little importance) exist in the way the various subsystems are assumed to be redundant, the effects of failure, etc.

The resulting classical reliability estimates (for 1 year of operation) are summarized in the following table. The predominant factor contributing to the differences in PRC's and STL's classical estimates (PRC's figure-of-merit estimates cannot be compared with the STL estimate) is the difference in the failure rates used by the two corporations.

<u>Subsystem</u>	<u>STL Estimate From Subject Report</u>	<u>PRC Estimate From PRC R-243</u>
Communications and Data Handling	0.408	0.0574
Attitude Control and Stabilization	0.665	0.0698
Power Supply	0.936	0.8840
Thermal Control	0.980	0.9968
Structure	0.985	1.0000
System Reliability	0.25	0.0037

5. TAM No. 5, "Structure Subsystem, Weight Reduction"

At the request of GSFC, PRC devotes a modest effort to reliability/weight tradeoffs for the OGO spacecraft; that is, studies are made of areas where savings in weight might be achieved, perhaps with a consequent reduction in system reliability. The first such study is reported in TAM No. 5, where a possible weight saving in the Structure Subsystem is considered. Specifically, attention is given to the appendage deployment release mechanism.

The design configuration (at the time of publication of the TAM) of the appendage deployment release mechanism consists of two assemblies: assembly A, actuating six double-ended appendage release latches, and assembly B, actuating six other double-ended appendage release latches. Each of these assemblies contains completely redundant gas pressure bottles, explosive valves, and plumbing.

In estimating the reliability of the deployment release mechanism, it is first assumed that the reliability of the gas pressure bottles and the plumbing is equal to unity. Then, the STL failure probabilities<sup>1</sup> of 0.008 and 0.007 for an explosive valve and for one end of a double-ended release latch, respectively, are employed in the calculations. Using an expression describing the design configurations, it is then determined that the probability of success for the deployment release mechanism is 0.9981.

---

<sup>1</sup> STL's failure rates for structural items are being used by PRC in the second assessment.

Next, an alternative configuration is considered consisting of assemblies A' and B'. Each of these assemblies actuates six release latches, as before, but the modified version is redundant only as concerns the double-ended feature of the release latches. In other words, the redundant bottles, explosive valves, and plumbing are eliminated. The probability of success for this alternate configuration (using the same failure probabilities) is calculated to be 0.9835.

This reduction in reliability (i. e., from 0.9982 to 0.9836) "buys" an estimated weight savings of 0.78 pounds. However, it is shown that, by further modifying the configuration, this reliability loss can be recovered with essentially no weight penalty. This can be accomplished by adding redundant charges in the valves. The deployment mechanism, with this additional configuration change, has a calculated reliability of 0.9993.

6. TAM No. 6, "Second Reliability Assessment for the OGO Structure Subsystem"

As indicated in TAM No. 6, the second assessment differs from the preliminary one in two primary areas. First, the subsystem design changes subsequent to the preliminary assessment are discussed, and the differences are described in the form of changes in subsystem descriptions, failure modes, and model equations. The principal changes are in the interstage release mechanisms and the gas-actuated appendage release mechanism. The failure modes and model equations are revised to account for the redesign changes. Second, the failure rates used in the numerical calculations are appropriately increased to reflect the effects of launch-phase dynamics on the failure probabilities of the various components.

The strengths and weaknesses of the subsystem are reviewed in the light of existing STL specifications, test reports, and drawings. Analysis indicates that a significant weight saving could result at a very small cost in reliability if the redundant deployment springs in the appendage joints are replaced with one spring per joint.

The conclusions reached in TAM No. 6 are as follows:

a. If the Hinshelwood report<sup>1</sup> accurately predicts the maximum acceleration, shock, and vibration loads, then the specifications and qualification test requirements adequately provide for the design of a highly reliable Structure Subsystem. This conditional conclusion is drawn by PRC although an acceleration test is not included, nor its exclusion justified, in the environmental-type test. It is PRC's judgment that the exclusion of the acceleration test is a low-order risk.

b. It is certain that variations around the maximum acceleration, shock, and vibration loads called out in the Hinshelwood report will exist with some hopefully small, but finite, probability of occurrence.

c. The above conclusion notwithstanding, it is felt that the two environmental qualification test specifications, D13351 and D13353, are sufficiently severe to define adequately most significant structural problem areas during the performance of the prescribed tests, if these problem areas have not already been located during development testing.

d. The design of the boom deployment hinges and springs appears to be adequate.

e. It is felt that vibration inputs to the spacecraft during the launch phase will very likely be transmitted through the experiment mounting panels at levels which will expose the experiment packages to acceleration levels higher than their design specifications require.

f. It is considered possible that the vibration levels experienced by the folded solar arrays during the launch phase will be high enough to cause damage to the arrays due to large elastic excursions. The most probable failure mode is expected to be the loosening or damaging of the solar cells due to twisting or bowing of the substrates.

g. There are several approaches to solving each of the potential problems cited in e and f, and, since any solution invariably results in a weight penalty, it is considered unwise to apply solutions

---

<sup>1</sup> G. D. Hinshelwood, Estimated Shock, Acceleration, and Vibration Environments for Atlas-Agena B and Thor-Agena B Spacecraft, AGENA-SAV-1, NASA, 1 August 1961.

before the existence of the problems themselves is verified (e. g., by appropriate testing).

7. TAM No. 7, "Parts Failure Rates, OGO Second Reliability Assessment"

The purpose of TAM No. 7 is to arrive at failure rates to be used in PRC's second assessment. The general approach is to survey all available data sources in order to determine whether failure rates used by PRC in its preliminary assessment should again be used "as is" or should be revised in the light of new information.

First, it is concluded that maximum value can be realized by confining the reexamination to the four most common classes of parts--resistors, capacitors, diodes, and transistors. On that basis, it is decided that, with the exception of structural items, all other parts (in the main, low-population items) will be assigned the same failure rates as were used in the preliminary assessment--a decision of small consequence as concerns resultant changes in the magnitude of the system and subsystem reliability calculations. For structural items, STL's failure rates are adopted by PRC because STL's more conservative numbers seem the more realistic considering the effects of launch dynamics.

For the four most common parts, then, some 12 sources of data are examined which were not available to PRC at the time that preliminary assessment rates were derived. Certain of these sources are of a "laboratory" nature, leading to a side study in which it is concluded that the inherent differences between "laboratory" and "assembled hardware" applications justifies the assignment of a failure rate of 0.01 failure per  $10^6$  hours to parts demonstrating a "laboratory" failure rate lower than that amount.

In the study of these 12 sources, a new position is taken in some instances on rates to be employed in the second assessment. In the main, the new set of rates agrees closely with the set contained in MIL Handbook 217, seemingly the best source of failure-rate data currently available.

8. TAM No. 8, "Second Reliability Assessment for the OGO Thermal Control Subsystem"

TAM No. 8 begins by noting nine significant changes in the subsystem configuration occurring since the preliminary assessment. Briefly, these changes involve (1) adjusting the fully open and fully closed angles of selected louver actuators, (2) adding sunshades to protect one radiating side panel, (3) cancelling plans to incorporate angle sensors for the louvers, and (4) adding various materials and/or use of special processes to various portions of the subsystem to improve its thermal control capabilities.

Subsystem states and modes are next reviewed and/or defined. A review of the 36 failure modes delineated by STL revealed that the one-by-one enumeration method of failure modes does not guarantee that all important failure modes are identified. Hence, because they provide a more logical and accurate delineation of failure modes, the failure modes used in the PRC preliminary assessment (modified slightly to identify louver actuator failures either as "stuck open" or "not stuck open" failures) are also used in the second assessment.

The model equations, except for the new interpretation of failure modes, remain unchanged. Component part failure rates used in the models are higher than before, based on test experience gained thus far in the OGO development program and taking into account the dynamic and thermal stresses to which the louver actuators are subjected during launch. The resulting reliability predictions for the Thermal Control Subsystem at the four quarters of a year are 0.995, 0.988, 0.972, and 0.944, respectively.

Apprehension expressed by PRC in the first assessment report concerning the use of  $\text{MoS}_2$  as a lower bearing lubricant have been dispelled by subsequent information. It appears that use of this lubricant in the space environment will present no problems.

Subsystem strengths and weaknesses are noted. An additional strength is achieved in the recent louver design modifications in that they ensure a reasonable probability of surviving the launch-phase vibration

environment. The most critical areas are still the areas over the battery packs and the transmitters.

The TAM concludes with a preliminary quantitative assessment of the Thermal Control Subsystem under tumbling conditions. Based on the assumption of a slowly tumbling spacecraft, it is shown that the steady-state average temperature of the spacecraft would be in an acceptable range; however, examination of a local "hot spot" (viz, the radiating panel over the battery pack) reveals that the steady-state temperatures reached by this panel would cause battery failure. Although removal of such hot spots might be effected, it is concluded that (1) the design effort to do so is not justifiable in view of existing spacecraft design constraints (e. g., maximum weight) and (2) a more detailed study involving a thorough dynamic heat balance analysis of the tumbling state is of questionable value at this time.

9. TAM No. 9, "Second Reliability Assessment for the OGO Communications and Data Handling Subsystem"

The major portion of TAM No. 9 is devoted to an engineering explanation of the operation of the command equipment. The functions of the command receivers and associated antennas are discussed, and the manner in which the receivers are squelched is brought out in detail. The redesigned tone decoder is examined, and its operation is explained to the extent that it is possible to understand exactly how a specific sequence of three tones will produce an unambiguous command output. The digital decoder is treated in considerable depth, and attention is focused on its functions and on the scheme used to address and decode the commands. Details of word synchronization, parity checks, and interlocking with the tone decoder are presented in an organized fashion. The command distribution unit is discussed briefly.

Such considerations as initial states of command relays and the effects of mission time-profile events on the execution of commands are the subject of a separate section of the TAM. The importance of these considerations is demonstrated by a series of examples illustrating the necessity of knowing the time-event sequence with reasonable accuracy



and of accounting for the impact of the events on the usefulness and effectiveness of the commands. These ideas are extended to include failure effects in a broad sense; i. e., the consequences of failures in the command equipment, with full consideration being given to the operational configuration of the vehicle.

The TAM concludes with a reevaluation of the first numerical assessment of reliability. Only one significant change is made in the model equations, and this reflects the added capability of the redesigned tone decoder. Except for this change, the first assessment model is used; however, revised failure rates are employed throughout. Because of these new failure rates, the second assessment classical reliability increases to 0.383 (for a full year) as against the 0.059 arrived at in the first assessment. It is shown that the tone decoder revision is not a major factor in this rather dramatic increase in reliability.

10. TAM No. 10, "OGO Spacecraft Parts Complement, Second Reliability Assessment"

TAM No. 10 documents the OGO parts complement underlying PRC's second reliability assessment. In order to attain a high order of accuracy in the parts tabulation for use in the second assessment, as well as to facilitate the continuation of this level of accuracy in subsequent assessments with a minimum of effort, the parts counts given in the TAM (with a few exceptions) are derived from the most recently released drawings currently available to PRC.

The information given in the TAM includes, in addition to the parts count for each of the major subsystems, a definition of the parts according to military or STL specifications and other available information separating them from similar parts which may be different from a reliability viewpoint. The TAM also sets forth the assumptions made regarding parts quality and cites the basis (e. g., specific STL documents) for these assumptions.

11. TAM No. 11, "Second Reliability Assessment for the OGO Power Supply Subsystem"

The Power Supply Subsystem has been substantially redesigned since the first assessment. Therefore, TAM No. 11 is a complete

assessment in itself. It describes the subsystem as it is now designed and considers its ability to handle POGO and EGO loads during the course of their missions. The several modes of failure that can occur and the methods provided to overcome their effect on subsystem operation and reliability are defined, described, and used as the basis for the reliability model equations and numerical assessment.

The many strong points of the second design are noted. Perhaps the principal strong point of this design is that no solar array output power is dissipated in the shunt-type regulator when full output power is demanded by the combination of system loads and battery recharging requirements. The counterpart of this strength is the weakness that such power conservation has not been used to reduce OGO weight by reducing the number of solar cells. This could only be done, of course, if OGO power requirements have not increased.

Though the reliability of the second design is high (0.91 after 1 year), it could be still higher if subsystem redundancy were increased by making both the batteries and the regulators individually redundant. As the design now stands, the combination of a battery and a regulator is redundant to the other battery and regulator; i. e., regulators are not interchangeable after assembly.

The recommendations made in TAM No. 11, in condensed form, are as follows:

- a. The capability of one battery to handle the entire load should be established with statistical confidence.
- b. Switching circuits to provide full redundancy of regulators and batteries should be employed.
- c. Ground-station location studies should include the fact that many subsystem failure modes are correctable only by ground command.
- d. The use of latching-type relays throughout the subsystem should be considered.
- e. The possibility of utilizing the increased subsystem efficiency to reduce subsystem weight should be considered.

12. TAM No. 12, "Second Reliability Assessment for the OGO Attitude Control and Stabilization Subsystem"

The second assessment of the Attitude Control and Stabilization Subsystem (reported in TAM No. 12) considers the effects of the five distinct modes of operation in which the subsystem functions. Up-to-date circuit diagrams (whenever available) are the sources for the new analysis model, and new failure rates (reported in TAM No. 7) are used.

In addition to consideration of five operational modes, the assessment considers the ACS as composed of four separate servo channels: the solar array channel; the yaw channel; the pitch channel; and the roll channel. In TAM No. 12, calculations are presented for each of the four channels in each operating mode. Also, the subsystem numbers versus mode are presented.

During construction of the second assessment ACS model, it was recognized that "compartmenting" the model by assembly interfaces is unrealistic. The separation of circuits into assemblies is often a packaging expedient, and interfaces between such assemblies are not (in general) the interfaces between functional circuit groups. Definition of some of the "more natural" interfaces has been performed and is discussed in TAM No. 12. All natural interfaces will be considered in the third assessment model. Such "in-depth" study of functions in the ACS has effected several recommendations, which are included in TAM No. 12.

Using the revised model and the revised failure rates, predicted ACS reliability values are 0.328, 0.148, 0.066, and 0.028, corresponding respectively to the four quarters of the 1-year OGO mission. This decrease in over-all ACS reliability is directly related to the increased detail of analysis of the subsystem.

13. TAM No. 13, "OGO Spacecraft System Reliability"

In TAM No. 13 the implications to spacecraft system reliability of the subsystem assessments are evaluated. Graphs of two PRC figure-of-merit (FOM) system reliability measures are presented along with a graph of a classical reliability measure. The classical measure

$R(t)$  expresses the probability as a function of mission time that spacecraft equipment operation will be "satisfactory" in a defined (though necessarily somewhat arbitrary) sense. The first FOM  $V(t)$  measures, as a function of mission time, the expected value of performance of OGO experiments--taking possible spacecraft equipment failures into account--relative to the ideal value of the experiments that would accrue if no such failures occurred. The second FOM  $V(\tau)$  is the time average over the interval  $(0, \tau)$  of the first. Either of the two FOM measures is a more "realistic" measure of spacecraft system reliability by virtue of its obviation of the arbitrary definitions inherent in the classical measure.

The following table excerpts values from the graphs of the three measures at four mission time points of interest.

Spacecraft Reliability Measure	Mission Time, $t$ or $\tau$ (hours)			
	2190	4380	6570	8760
$V(t)$	0.290	0.100	0.030	0.088
$V(\tau)$	0.580	0.376	0.270	0.208
$R(t)$	0.303	0.109	0.034	0.009

## II. PARTS INFORMATION

This section comprises two subsections, each consisting of a TAM. The first subsection is TAM No. 7, "Parts Failure Rates--OGO Second Reliability Assessment." This TAM, in essence, represents a re-examination of the failure rates used in the preliminary assessment in the light of failure rate reference sources not employed in the preliminary assessment. Potential areas for revision are delineated, a philosophical discussion of the use of "laboratory" failure rates is presented, a discussion of the new sources is presented together with failure rate comparisons, and a list of the failure rates selected for use in the second assessment is given.

The second subsection is TAM No. 10, "OGO Spacecraft Parts Complement." This TAM is the first complete delineation of the component parts constituting the spacecraft and its major subsystems. Such a complete listing is an indispensable input to the detailed second assessment reliability predictions; however, it is well to note that such a tabulation should prove to be quite useful for non-reliability purposes.

The tabulation itself is presented in the appendix to the TAM; it is broken down first by major subsystems, each of the five subsystems representing a suitably (but arbitrarily) indexed section. Each section, in turn, is further broken down and appropriately indexed, consistent with a hardware breakdown into units and subunits. In short, the tabulation evolves as an indentured listing (or indexing) of the inherent hierarchy of hardware items making up the spacecraft and its major subsystems.

For each specific item in the tabulation (in addition to its index), its name or description, the applicable drawing or part number (or, in some cases, the Mil specification number), the quantity required, and a "Remarks" column are given.

TECHNICAL ADVISEMENT MEMORANDUM NO. 7

PARTS FAILURE RATES-  
GO SECOND RELIABILITY ASSESSMENT

---

## TABLE OF CONTENTS

	<u>Page</u>
1. Introduction . . . . .	1
2. Area for Revision . . . . .	2
3. Philosophy on the Use of "Laboratory" Failure Rates . . . .	2
4. Failure Rate Determination . . . . .	6
5. Discussion of Additional Data Sources . . . . .	6
6. Additional Data and Selected Second Assessment Failure Rates . . . . .	9
a. Capacitors . . . . .	10
b. Resistors . . . . .	10
c. Transistors . . . . .	10
d. Diodes . . . . .	10

---

## TECHNICAL ADVISEMENT MEMORANDUM NO. 7

To: Assistant OGO Project Manager, GSFC, NASA  
From: PRC OGO Assessment Team  
Subject: Parts Failure Rates--OGO Second Reliability Assessment

### 1. Introduction

In PRC's first assessment of OGO reliability, a set of part and component failure rates were employed which, for the most part, differed considerably from those being used by STL. In general, STL's failure rates were more optimistic (i. e., lower) than those used by PRC, thus resulting in a higher figure for predicted system reliability.

The reasoning on which PRC based its failure-rate estimates is discussed in the First Assessment Report (PRC R-243). Subsequent to this report, however, PRC has been directed by GSFC to re-examine the failure rates used, with a view toward reaching agreement (or agreeing to disagree) with STL on a common set of rates to be employed in future assessments.

Study of additional data on which to base reasonable failure-rate estimates has been accomplished by PRC. However, PRC believes that across-the-table determinations with STL--leading to a commonly acceptable set of rates for all parts--are not practicable at this time. This belief is based on STL's position that failure rates are a subject for corporate decision and are not determined on the project level. According to STL representatives, then, the only room for negotiation would be in the "K factor" multipliers used to adjust data to the space environment. This means that a prerequisite for agreement would be that PRC arrive at a set of failure rates which stand in approximately the same relation to one another as do those in the set used by STL.

Unfortunately, PRC cannot agree with the relative standings of failure rates used by STL for many classes of the four most commonly used types of parts in the OGO spacecraft: capacitors, resistors, diodes, and transistors.



PRC believes that across-the-table determinations cannot lead to agreement on a set of aligning "K factors" and that, in fact, this is not in the best interests of the OGO program, but alternatively proposes that GSFC and STL consider the failure rates contained in this memo. Following study of the adjustments made in PRC's originally used rates, and the reasons therefore, it is requested that STL comment on PRC's revised estimates. It is further requested that GSFC then (1) approve these rates for use in PRC's subsequent OGO reliability assessments, (2) suggest additional data sources on which to base further adjustments, or (3) redirect PRC to enter into across-the-table discussions with STL.

## 2. Area for Revision

It is clear that four types of parts dominate computations of OGO reliability (as was previously mentioned, these are capacitors, resistors, diodes, and transistors). Therefore, although PRC has continued to study additional sources of failure-rate data on all of the parts originally assigned failure rates in PRC R-243, this TAM will concern itself only with these four types of parts. To this end, it has already been decided (and reported to GSFC) that PRC will employ STL's failure rates for structural items,<sup>1</sup> at least until such time as meaningful OGO structural test data become available. For other items, PRC will continue to use its original rates, appropriately adjusted to include other factors such as launch dynamics, etc., until other data are available that materially change the background against which the estimates originally were made.

## 3. Philosophy on the Use of "Laboratory" Failure Rates

The failure rate ( $\lambda$ ) of a part can be broken down in a number of ways wherein  $\lambda$  is considered to be the sum of a number of contributing factors of a similar kind. For example,  $\lambda$  can be considered as the sum of the various modes of failure where the modes are the ways in which basic physical and chemical capabilities of the part can be exceeded in terms of geometric or material properties. Or,  $\lambda$  may

---

<sup>1</sup>Reported in PRC's progress report (OGO), dated 23 April 1962.

be considered as the sum of various failure mechanisms (therbligs)<sup>1</sup> where the mechanisms are the failures of functional capabilities; i.e., shorts, drift, leaks, etc. The interrelationship of these concepts is obvious; however, discrete definition of the failure rate by one or the other is possible.

The third approach, most useful in the present situation, considers the failure rate to be a function of its application regime. In predicting system reliability, PRC takes the stand that part failure data obtained from "laboratory" reliability testing<sup>2</sup> should be considered separately from that obtained in field experience with operational equipments. To this end, it will be recalled that the sources primarily employed by PRC in estimating the failure rates used in PRC R-243 were of the field-data variety (RCA's TR 54-416-1, Martin-Marietta's Reliability Analyses Guide, PRC's R-235). The belief that field experience is more valid (in spite of the fact that control is loose) for systems reliability predictions is based on the fact that this type of data reflects the reliability of parts as applied in actual design and fabrication situations, rather than the "ultimate" or "ideal" part reliabilities.

Actually, many authorities have recognized this problem and have given attention to it. A most notable effort in this regard may be found in work done by Paul H. Zorger of Martin-Marietta. Dr. Zorger has concluded that over-all system reliability  $P_{ov}$  is a product of three parameters, viz,

$$P_{ov} = P_d P_f P_c$$

where  $P_d$  = reliability of the design parameters

$P_f$  = reliability of processes and assembly operations

$P_c$  = reliability of the parts

---

<sup>1</sup>Failure Therblig Failure Rates, D. R. Earles and M. F. Eddins, Avco Corporation.

<sup>2</sup>"Laboratory" parts reliability testing is defined here as any test program where the reliability of parts is determined through testing of the parts themselves rather than through observation of parts reliability in operating equipments. Accelerated testing may or may not be employed.

What Dr. Zorger infers here is that  $P_{ov}$  is likely to be less than the reliability indicated by combinatorial exercises involving reliability numbers reflecting the capabilities of the parts alone ( $P_c$ ).

Applying this concept at the part level and writing in terms of the failure rate yields the following expression:

$$\lambda = \lambda_a + \lambda_c$$

where  $\lambda$  is the failure rate from the over-all part reliability obtained from field testing data,  $\lambda_c$  is the ideal rate obtained from part tests in controlled laboratory conditions, and  $\lambda_a$  is the failure contribution due to application factors associated uniquely with the design and fabrication of the part into practical systems. Experimentally,  $\lambda_a$  can be determined only as the difference between field and laboratory test data of appropriate consistency in conditions.

Design practice and production quality control procedures are obviously aimed at minimizing  $\lambda_a$  while realizing other design requirements. However, the problems in establishing trends and values for  $\lambda_a$  are significant.

Consider first the design and production trends that might affect  $\lambda_a$ , particularly in the area of spacecraft electronic equipment. In the past few years, especially in this area, the packing densities of equipment designs have increased tremendously. At the same time, chassis have given way to circuit cards, eliminating a heat sink which served to stabilize temperature excursions.

To offset these problems in modern design, increased use of very low-power digital logic circuits and marked reduction in the power dissipation requirements of analog devices have reduced the amount of heat which must be dissipated. However, modern spacecraft do have heat-generating equipments (notably batteries) and it is unlikely that "hot spots" can be entirely avoided. Certainly, modern circuitry has a lesser capability for enduring these "hot spot" situations if they exist.

Next, consider the inherent manufacturing reliability of modern equipments. Fabrication processes have also undergone a revolution

in recent years. Automatic circuit welding devices have supplanted much of the soldering done in the past, and circuit potting has become more widely used. These techniques have served to achieve greater uniformity and stability in equipments.

However, the parts which are being employed, although they have become inherently more reliable in the "laboratory" sense, have become very much smaller. The fear arises, therefore, that much of the reliability built into the parts may be taken out of them in equipment fabrication. Modern "miniature" resistors, capacitors, diodes, and transistors obviously have very poor heat capacity. Therefore, welding and potting temperature transients possibly could cause quite severe internal stresses.

To counter these effects, it must be recognized that quality control has improved in the past few years.

An estimate, then, in the trend of  $\lambda_a$  would necessarily be arbitrary and qualitative, since quantitative data are not known to exist. However, even if we assume that  $\lambda_a$  has not changed and that the above factors are in balance, we can examine the significance of considering  $\lambda_a$  as an element of  $\lambda$  in the light of increasing part "laboratory" reliabilities (decreasing  $\lambda_c$ ).

Let us assume that over a period of time, say 10 years,  $\lambda_a$  has remained constant at  $0.01/10^6$  hours. This corresponds to an effect factor of 0.916 in the reliability of a 1,000-part system for 1 year of operation. In the same period we can estimate that the laboratory failure rate  $\lambda_c$  has decreased an order of magnitude from, say, 0.15 to 0.015. It is obvious that the effect of neglecting  $\lambda_a$  when computing  $\lambda$  and knowing only  $\lambda_c$  results in an error that has increased from 6 percent to 40 percent.

PRC will summarize this philosophical discussion, then, by pointing out that the recent marked improvements in parts failure rates, as observed under "laboratory" conditions, must result in improvement of system reliability. However, these same parts improvements make it important to realize that field-type failure data, reflecting actual experience with actual equipments, are much more realistic for predicting system reliability than "laboratory" parts failure experience.

#### 4. Failure-Rate Determination

It now becomes necessary to combine the best available data, field or laboratory, with engineering judgment in order to evolve the most plausible failure rate for each class of parts considered here. A number of approaches are possible.

One such approach has been suggested independently in MIL Handbook 217 and by a PRC investigator. In essence this approach involves the use of field data ( $\lambda$ ), or laboratory data ( $\lambda_c$ ) if no field data are available, with a minimum or "floor" failure rate of  $0.01/10^6$  hours where laboratory data indicate a lower value of  $\lambda_c$ . As values of  $\lambda$  (based on field data) lower than 0.01 become available, they would of course be applied.

The final failure rates (recommended for the Second Assessment) for the classes of equipment considered here are chosen by a variation of the above approach--using the concept of the previously discussed relationship,  $\lambda = \lambda_a + \lambda_c$ . The variation consists of using an estimated value of  $\lambda_a$  to combine with  $\lambda_c$  when only the latter type of data are available. The nominal rate that PRC has assigned to  $\lambda_a$  is  $0.01/10^6$  hours. This figure could be varied in either direction if specific application knowledge with respect to the design and fabrication of the utilization is available and so indicates.

The reasonableness of the chosen value must be inferred from experience; for example, consider again the 1,000-part, 1-year system. A  $\lambda_a$  of 0.01 contributes a factor to the reliability calculation of 0.916 which, in PRC's experience, seems appropriate. Experimental evidence contained in the data tabulated for this TAM indicates considerable scatter. From the best data group, that for capacitors, the average value obtained for  $\lambda_a$  is 0.013.

#### 5. Discussion of Additional Data Sources

In the tabulations to be presented later in this paper, failure-rate reference sources in addition to those employed in PRC's First Assessment are enumerated. Tabulations of data from sources leading to the First Assessment estimates are not repeated, except in one instance where a revised issue of one of these sources is included.

failure rates (primarily of the "laboratory" type) used by STL OGO reliability assessments are included because they represent information not available to PRC during the First Assessment.

Some general remarks are in order concerning the sources of general data (data sources peculiar to one type of part will be discussed when the tabulations are presented). First, failure rates used by PRC in the First Assessment have been discussed in PRC R-243 and, with one exception, this source does not seem to require further discussion. That exception is the data from Source No. 1 of PRC R-243. These data have since been revised, updated, and reissued as MIL Handbook 217. In many cases a considerable improvement in failure rates has been recognized; the final Second Assessment rates are considerably influenced by these improvements, particularly where Source No. 1 was the predominating influence in establishing the rates for the First Assessment.

Next, several of STL's data sources have been studied, including their OGO reliability assessment reports of 15 August 1961 and 29 January 1962 as well as reliability studies conducted by two principal OGO subcontractors: ATL (Horizon Scanner) and RCA (Tape Recorder). These latter studies are included as "STL sources" because the failure rates used by ATL and RCA were as directed by STL and hence agree with those used by STL.

Also, data from a paper given by an STL reliability authority<sup>1</sup> are included in the general category of STL data sources. Here it is interesting to note that, where this paper disagrees with failure rates used in STL's OGO reports, the OGO numbers are usually higher.

A third general data source included in the tabulations is a recent report of Autonetics reliability improvement activities in connection with the Minuteman program.<sup>2</sup> This report seems to be the best recent source of "laboratory"-type failure-rate data because of the statistically meaningful sample sizes and testing durations used. It appears that

---

<sup>1</sup>Morrison, S. C., "Maximizing Reliability for One-Shot Space Missions," Paper No. 61-95-1789, presented to a joint meeting of the IAS and ARS, 13-16 June 1961.

<sup>2</sup>Autonetics Report No. EM-2496-3, undated (but known to be very recent).

good correlation of data for tests being conducted under accelerated conditions has been realized, and that valid statistical inferences may be made for the OGO application.

The test results reported by Autonetics are treated in two different ways in PRC's tabulations. For those items which were not manufactured under special Minuteman process controls (i.e., were manufactured under conventional specifications) the most recent results are tabulated. However, for those items being subjected to strict Minuteman reliability process controls, it should be realized that general procurement is not yet possible. To account for this, PRC has made the assumption that about 1-1/2 years will be required for the realization of Minuteman-induced reliability improvements in parts procurable under conventional specifications. In these instances, therefore, the observed failure rates of like parts, not manufactured under Minuteman controls, are used as indicators of the reliability that may be procured today.

Another general source is data published in a recent issue of the Bell Systems Technical Journal.<sup>1</sup> Although these data duplicate, to some extent, a source already considered by both PRC and STL in arriving at their original sets of failure rates (BTL's general failure rate document), the article represents an updating which should be taken into account. However, the failure rates quoted from this source are nominal for the various classes of parts, and there is no way of determining a relationship of the stresses under which these data were obtained to the OGO environment. As a result, the data can only be used as a general guideline.

Two other general sources are an article distributed by IBM<sup>2</sup> and a recent paper given by representatives of the Space-General Corporation.<sup>3</sup>

---

<sup>1</sup>Ross, I. M., "Reliability of Components for Communications Satellites," Bell Systems Technical Journal, Volume XLI, No. 2, March 1962.

<sup>2</sup>Digital Computer Characteristics for Space Applications, IBM, Federal Systems Division, Report No. 59-504-1, 9 June 1959.

<sup>3</sup>Doshay, I., and Shuken, H. L., Predicting Space Mission Success Through Time-Stress Analysis, Space-General Corporation (presented at Seventh Military-Industry Missile and Space Reliability Symposium, 18-21 June 1962).

The IBM article makes general predictions of "ultimate" reliabilities (circa 1970) of certain parts in the space environment, while the Space-General paper reports on data obtained from airborne fire control equipment. Both of these sources are "broad-brush" treatments and are suitable only as general trend guidelines.

Thus it is seen that, of the general sources considered, only MIL Handbook 217, STL's OGO documents, and the Autonetics report constitute additional sources of sufficiently "solid" data on which to base any revisions of PRC's parts failure rates.

One general source which will not be shown in the tabulations is a report on ARINC's recently completed study of the observed reliability of some 15 spacecraft.<sup>1</sup> Based on observed spacecraft performance, ARINC estimated reliability on an Active Element Group (AEG) basis, and, when PRC's First Assessment failure rates are suitably combined to predict AEG reliability, very close agreement with ARINC's estimates is realized. These results have already been orally presented to STL and GSFC and will not be repeated here. ~~However, they do contribute in some measure to PRC's confidence in a conservative approach to selection of failure rates.~~

#### 6. Additional Data and Selected Second Assessment Failure Rates

In the tabulations now to be presented, the data sources are coded as follows:

<u>Code Number</u>	<u>Source</u>
1	PRC R-243
2	STL OGO Reliability Report No. 1 (15 August 1961)
3	STL OGO Reliability Report No. 2 (29 January 1962)
4	Autonetics Report No. EM-2496-3
5	Didinger, G. H., "On the Reliability of Solid Tantalum Capacitors," <u>Electronic Components Conference Proceedings</u> , 1961

<sup>1</sup>Willard, C. F., Satellite Reliability Spectrum, ARINC Research Corporation, Publication No. 173-5-280, 30 January 1962.



<u>Code Number</u>	<u>Source</u>
6	"Capacitor Reliability Brochure," Corning Glass Works, undated (but known to be recent)
7	Morrison's paper presented to IAS/ARS
8	"Annual Report on Reliability, Silicon Transistors--1960," Texas Instruments, Inc.
9	Article in March 1962 <u>Bell Systems Technical Journal</u>
10	IBM Report No. 59-504-1
11	Doshay/Shuken paper (see footnote 3 on page 8)
12	MIL Handbook 217

a. Capacitors

Exhibit 1 summarizes failure rates gleaned from 10 sources available to PRC. For glass capacitors, a special data source (No. 6) was available; this was a "laboratory"-type source which closely agreed with STL's figure. The Autonetics data, however, showed an even more conservative result than PRC's original estimates. Hence, PRC has chosen to remain with its original failure rate estimate for this part.

In the case of paper capacitors, Autonetics data indicate a "laboratory" failure rate twice that of the field-type data in MIL Handbook 217 and only about 50 percent lower than PRC's original estimate. However, for consistency, PRC will use the field figure.

b. Resistors

Failure-rate data for resistors are summarized in Exhibit 2, where eight different sources are quoted.

c. Transistors

Failure data on transistors (10 sources) are given in Exhibit 3.

d. Diodes

Exhibit 4 summarizes failure-rate information on diodes.

# EXHIBIT 1 - CAPACITORS--FAILURES PER 10<sup>6</sup> HOURS

Class	Source										Second Assessment Final
	<u>1</u>	<u>2</u>	<u>3</u>	<u>4<sup>(1)</sup></u>	<u>5</u>	<u>6</u>	<u>7</u>	<u>9<sup>(2)</sup></u>	<u>11<sup>(3)</sup></u>	<u>12</u>	
Aluminum, electrolytic	1.2	-	-	-	-	-	-	-	-	0.40	0.40
Ceramic, fixed	0.06	0.004	-	-	-	-	-	-	-	0.01	0.01
Ceramic, variable	0.15	-	-	-	-	-	-	-	-	0.015	0.015
Glass	0.01	-	0.004	0.05	-	0.003	-	-	-	0.01	0.01
Mica, button or foil	0.02	-	0.003	-	-	-	-	0.005	-	0.01	0.01
Mica, molded	0.01	0.003	0.003	-	-	-	-	-	-	0.01	0.01
Paper	0.05	0.003	0.003	0.02	-	-	0.003	-	-	0.01	0.01
Tantalum, solid	-	0.04	0.04	-	0.00002	-	-	-	-	0.08	0.08
Tantalum, foil	1.0	0.08	-	0.08	-	-	-	-	-	0.09	0.09
Undefined class from airborne fire control systems	-	-	-	-	-	-	-	-	-	-	N/A

- Notes: (1) Failure rate as of January 1961 (see text)--60 percent confidence.  
(2) Nominal for class of parts shown.  
(3) Divided by 10 to derate from manned aircraft to GSE environment.

# EXHIBIT 2 - RESISTORS--FAILURES PER 10<sup>6</sup> HOURS

Class	Source							Second Assessment Final
	<u>1</u>	<u>2</u>	<u>3</u>	<u>4<sup>(1)</sup></u>	<u>7<sup>c</sup></u>	<u>9<sup>(2)</sup></u>	<u>11<sup>(3)</sup></u>	
Composition, fixed	0.17	0.018	0.018	-	0.005	-	-	0.01
Composition, variable	-	0.038	-	-	-	-	-	0.05
Film, signal, fixed	0.37	0.008	0.008	0.02	-	0.005	-	0.23
Film, power, fixed	1.08	-	-	-	-	-	-	1.08
Wirewound, accurate, fixed	1.38	0.044	-	-	0.05	-	-	1.03
Wirewound, variable	-	0.064	-	-	-	-	-	0.07
Wirewound, power, fixed	1.08	0.054	-	0.015	-	-	-	0.22
Undefined class from airborne fire control systems	-	-	-	-	-	-	0.27	N/A

Notes: (1) Failure rate as of January 1961 (see text)--60 percent confidence.

(2) Nominal for class of parts shown.

(3) Divided by 10 to derate from manned aircraft to GSE environment.

# EXHIBIT 3 - TRANSISTORS--FAILURES PER 10<sup>6</sup> HOURS

Class	Source											Second Assessment Final
	1	2	3	4	7	8	9 <sup>(1)</sup>	10 <sup>(2)</sup>	11 <sup>(3)</sup>	12		
Germanium, signal	0.45	0.218	-	0.31 <sup>(4)</sup>	-	-	0.01	-	--	0.30	0.30	
Silicon, signal	0.45	0.153	0.153	0.05 <sup>(4)</sup>	0.06	4.0	-	0.1	-	0.30	0.30	
Silicon, medium power	-	-	-	0.31	-	-	-	-	-	-	0.32	
Silicon, power	-	-	-	0.22 <sup>(4)</sup>	-	-	-	-	-	-	0.23	
Germanium, power	-	-	-	0.07 <sup>(4)</sup>	-	-	-	-	-	-	0.08	
Undefined class from airborne fire control systems	-	-	-	-	-	-	-	-	2.7	-	N/A	

Notes: (1) Nominal for class of parts shown.

(2) Estimate of ultimate (1970) in space application.

(3) Divided by 10 to derate from manned aircraft to GSE environment.

(4) Failure rate as of January 1961 (see text)--60 percent confidence.

# EXHIBIT 4 - DIODES--FAILURES PER $10^6$ HOURS

Class	Source							Second Assessment Final
	1	2	3	4 <sup>(1)</sup>	7	9 <sup>(2)</sup>	11 <sup>(3)</sup>	
Germanium, signal	0.35	0.073	-	0.01	-	0.01	-	0.15
Silicon, signal	0.35	0.051	0.051	0.01	0.013	-	-	0.15
Silicon, zener (reference)	-	-	0.073	0.25	-	-	-	0.26
Double based, low power	-	-	-	0.03	-	-	-	0.04
Medium power (500m A)	-	-	-	0.0035	-	-	-	0.01
Power (20 A)	-	-	-	0.025	-	-	-	0.03
High power (200 A)	-	-	-	0.12	-	-	-	0.13
Undefined class from airborne fire control systems	-	-	-	-	-	-	0.15	N/A

Notes: (1) Sixty percent confidence.

(2) Nominal for class of parts shown.

(3) Divided by 10 to derate from manned aircraft to GSE environment.

TECHNICAL ADVISEMENT MEMORANDUM NO. 10

---

OGO SPACECRAFT  
PARTS COMPLEMENT

## TABLE OF CONTENTS

	<u>Page</u>
1. Introduction . . . . .	1
2. Description of OGO Parts Complement Tabulation . . .	2
a. Communications and Data Handling (CDH) Subsystem . . . . .	4
b. Attitude Control and Stabilization (ACS) Subsystem . . . . .	4
c. Power Supply (PS) Subsystem . . . . .	5
d. Thermal Control Subsystem . . . . .	5
e. Structure Subsystem . . . . .	5
3. Parts Quality . . . . .	6
References . . . . .	8
Appendix I: OGO Parts Complement . . . . .	9

---

## TECHNICAL ADVISEMENT MEMORANDUM NO. 10

To: Assistant OGO Project Manager, GSFC, NASA  
From: PRC OGO Assessment Team  
Subject: OGO Spacecraft Parts Complement

### 1. Introduction

An indispensable input to the assessment of OGO spacecraft system and subsystem reliability is a delineation of the component parts comprising the spacecraft and its major subsystems. For the preliminary assessment of OGO reliability, the parts complement used by PRC was based on information gleaned from a variety of sources; e.g., preliminary drawings and schematics, discussions with STL engineers, wire tab runs, etc. This gross identification of the parts complement was sufficient for the preliminary assessment; however, the current second assessment and following third assessment demand a more complete and accurate parts complement tabulation.

The primary purpose, then, of this memorandum is to document the OGO parts complement underlying PRC's second OGO reliability assessment. The information given herein includes, in addition to the parts count for each of the major subsystems, a definition of the parts according to military or STL specifications and other available information which separates them from similar parts which may be different from a reliability viewpoint. For the reader's convenience,<sup>1</sup> the parts tabulation is presented in Appendix I. Background information on the tabulation is given in section 2 below. It is important to note that in order to attain a high order of accuracy in the tabulation for the second assessment, thereby facilitating the continuation of this level of accuracy in subsequent assessments with a minimum of effort, all<sup>2</sup> parts counts given in Appendix I were derived from the most recently released drawings currently available to PRC. Section 2 discusses and identifies,

---

<sup>1</sup>It is anticipated that the tabulation will also be used for non-reliability purposes by various GSFC personnel.

<sup>2</sup>With a few exceptions as noted in Appendix I.



for each major subsystem, the deficiencies in the tabulations given in Appendix I.

Section 3 of this memorandum briefly discusses another important aspect of the reliability assessments, namely, parts quality. This aspect is very pertinent in that the final assigned failure rate for each part is dependent on the inherent quality of the part as well as on its classification (e.g., via Appendix I) and its expected use environment. The environmental, electrical, and mechanical stresses have been fairly well defined in the second assessment, but the parts quality level has, in the main, been assumed. The purpose of section 3, therefore, is to set forth the assumptions made regarding parts quality and cite the basis (e.g., STL documents) for these assumptions. It is anticipated that the generalized assessment of parts quality presented in section 2 will be superseded by a more detailed parts quality assessment to be conducted by PRC during the third OGO reliability assessment.

## 2. Description of OGO Parts Complement Tabulation

The parts complement tabulation given in Appendix I is based on the OGO Spacecraft System Tree shown in Exhibit 1.

The columns of the tree are identified with subsystems, and the elements of each column are the subsystem units. The units, in turn, are composed of parts; these parts are tabulated in Appendix I. In some instances subunits can be separately identified, and this has been done wherever possible.

This breakdown is a composite of numerous breakdowns listed by STL. A completely authoritative and current listing of subsystems, etc., has not yet been received by PRC. Thus somewhat arbitrary classifications are used. As mentioned above, the complement list will be revised as more complete information becomes available.

A particular subsystem analysis may or may not include all items listed for the subsystem in Exhibit 1. Each analysis will, of course, indicate which of the items are considered in that assessment and, where current information on a unit is unavailable, an estimate of the parts breakdown will be made.

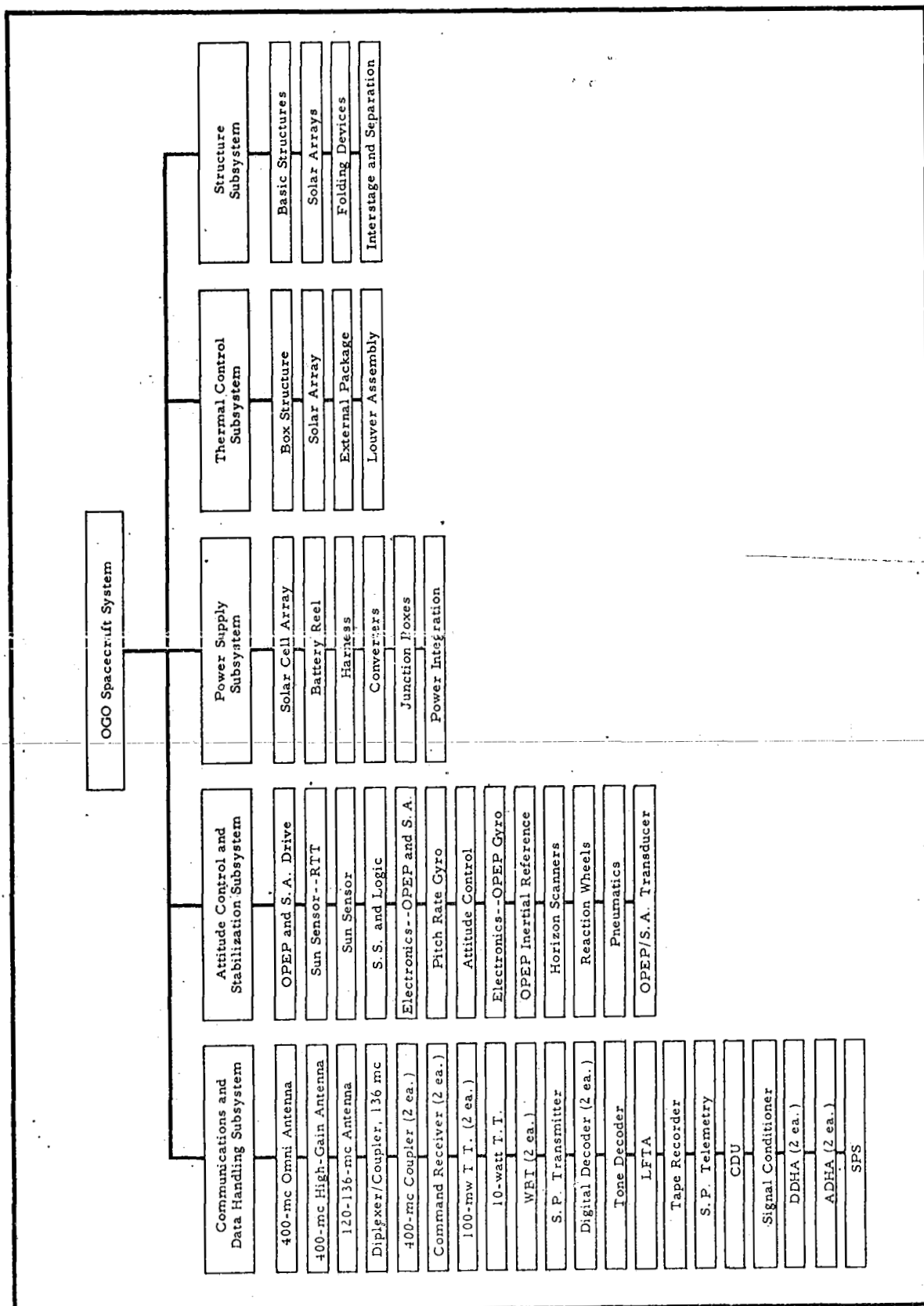


EXHIBIT 1 - OGO SPACECRAFT SYSTEM TREE

Information not available at this time consists, typically, of drawings not released, information not received from subcontractors, and information needed to request specific documentation. This unavailable information is generally in the interface area and much of it is currently being forwarded. The major items have been covered quite well, particularly in the CDH and ACS Subsystems. It is estimated that Appendix I lists between 90 and 95 percent of the parts<sup>1</sup> included in the OGO vehicle. Deficiencies in the listings and appropriate comments for each of the major subsystems follow.

a. Communications and Data Handling (CDH) Subsystem

Although this is by far the most complicated subsystem, it also appears to be the most completely documented at the present time. The over-all CDH Subsystem is covered by Drawing X200393. This block diagram is the basis for the first breakdown under the subsystem level. From this level, top assembly drawings exist for each item; these make it possible to carry the analysis to the part level. At the present time the top assembly drawings, or reasonable substitutes, are not available for the Diplexers and Couplers or the Spacecraft Performance Sensors. In addition, a few lower level drawings for the Digital Decoder, Low-Frequency Timing Assembly, and Digital Data Handling Assembly have not yet been acquired. (The Converters have been included in the Power Supply Subsystem.) However, even allowing for the units for which no information is available, the parts tabulation for this subsystem is estimated to be 95 percent complete.

b. Attitude Control and Stabilization (ACS) Subsystem

An up-to-date definition of the major units comprising the ACS Subsystem has not yet been discovered. The units shown in Exhibit 1 and Appendix I were derived for a number of sources and are subject to change. Each unit, however, is covered by a top assembly drawing, with the exception of the Reaction Wheels. One lower level drawing is missing for the Sun Sensor and Logic Assembly. Assuming

---

<sup>1</sup>Excluding only such nonmoving parts as bolts, nuts, frames, etc.

that each unit is accounted for and well defined, the parts complement for this subsystem is approximately 95 percent complete.

c. Power Supply (PS) Subsystem

This subsystem, in particular, lacks complete assembly drawing definition. There are indications that power supply and integration are separate subsystems. A completely definitive interface has not yet been received by PRC; hence, power integration has been included as a unit of this subassembly. In addition, because of the recent relatively major redesign of this subsystem, it has the largest proportion of nonreleased drawings. Due primarily to a lack of converter drawings (which have also been placed, somewhat arbitrarily, in this subsystem) and junction box drawings, it is estimated that the parts complement is only 50-75 percent complete.

d. Thermal Control Subsystem

The parts that are listed for this subsystem have been restricted generally to those parts considered in the subsystem assessments. Although this is true to some extent for all subsystems, it is more noticeable in this section because of the smaller number of such parts. The only parts listed are those which make up the lower assembly. The thermal control for the basic box structure comprises just five strips of Mylar and the method of construction; hence no detailed breakdown of the subsystem is given. The solar array thermal control is achieved by the use of black paint and judicious design, and, hence, no detailed parts breakdown is given. The external package thermal control is known to consist of thermostatically controlled heating elements in addition to Mylar strips and thermal design, but no drawings on this section are presently available. The Thermal Control Subsystem parts complement is approximately 90 percent complete.

e. Structure Subsystem

The only items in this subsystem that have been detailed are the Folding Devices and Interstage and Separation unit. The remaining items have not been broken down, since they consist only

of nonmoving parts such as bolts, nuts, frames, etc. The two items mentioned have been detailed only to the extent necessary to include the moving or electronic parts. The parts listing for this subsystem is 90-95 percent complete.

### 3. Parts Quality

In the effort, for second assessment purposes, to arrive at the inherent quality of the electronic piece parts used in the OGO vehicle, Reference 1 was used as the primary source of information. It must be emphasized that this section makes no attempt to assess parts reliabilities conditioned by the actual use of the parts, but rather to indicate the quality--and hence reliability--of OGO parts as they are observed independent of application. The reliability of the parts as they are applied in a particular subsystem is discussed in the assessment of that subsystem.

The factors that affect the nonapplied reliability of parts can be divided into two areas: (1) purchaser's specifications and (2) vendor's compliance. This division makes it clear that the inherent quality of a part is determined by how well the part corresponds to its specification. Writing specifications is the user's responsibility, whereas complying with the specification is the responsibility of the vendor.

One method of assuring adequate specifications and vendor compliance is the QPL system. Under this system a vendor qualifies his part to an applicable military specification under government supervision, and the user adjusts his design to utilize parts delineated by that specification. The advantages of this system are clear: the vendor produces a standard item; the engineer has an adequate specification. Moreover, the QPL system has a history of satisfactory results when consistently applied. A large majority of the resistors and capacitors used on OGO, as well as a sizable portion of the remaining parts such as diodes and transistors, are purchased via the QPL system.

The main deficiency in the QPL system is its failure to keep pace with the state-of-the-art in regard to part performance and, in some cases, reliability itself. Many of the OGO non-QPL parts are minor

variations of QPL items such as size, performance, and reliability. These items exhibit the same or better reliability levels than their QPL counterparts. Where no QPL items exist or improvements on QPL items have been made, the parts have an STL specification prepared with vendor commitment required prior to purchase.

The preceding discussion has been concerned primarily with procurement practices when given an adequate specification. Other factors to be considered are the adequacy of the specification and proof of compliance. The latter is generally a part of the specification itself. Reviewing the adequacy of specifications is beyond the scope of this assessment; however, a typical high-population item was briefly checked. "

The PT4-7 (STL specification) resistor, a non-QPL item, is a metal film resistor available from three excellent sources. Its temperature range is from  $-55^{\circ}\text{C}$  to  $165^{\circ}\text{C}$ . Stability is 25 parts/million/ $^{\circ}\text{C}$ , and metal film resistors have an excellent failure rate record: 17 to 58 failures per billion hours, as compared to carbon-deposited types with a failure rate of 110 to 570 failures per billion hours. Fully comparable results are obtained when the QPL items are checked.

In summary, the parts used appear to be qualitatively the best obtainable consistent with over-all program goals.

## REFERENCES

1. OGO Electronic Specification Development Guide, STL IOC 9301.1-145, from D. L. Stern to distribution, 5 April 1962.
2. OGO Program Specifications, STL 2311-0003-OU-000, 15 September 1961.
3. OGO Engineering Data Book, STL 2311-0010-OU-000, revised to 16 March 1962.

## APPENDIX I

### OGO PARTS COMPLEMENT

The parts tabulation which follows is grouped first by major subsystem, each subsystem comprising a section indexed as indicated below:

Communications and Data Handling Subsystem	Section 1.0
Attitude Control and Stabilization Subsystem	Section 2.0
Power Supply Subsystem	Section 3.0
Thermal Control Subsystem	Section 4.0
Structure Subsystem	Section 5.0

To facilitate the location of a specific item, these sections are preceded by a unit index which lists each primary unit together with its associated assembly drawing number, data list (DL) number, or specification (D) number. Where no drawing, DL, or D number is given, the reason for its absence is in the "Remarks" column. The unit index contains a column showing the status of the collection of drawings or other documents necessary for the identification of a parts complement. The percentage figure heading the status column for each subsystem indicates the proportion of documentation on hand from which a parts breakdown can be made. The notation "Need \_\_\_\_" in the status column specifies the number of drawings, including lower level drawings, required to complete the documentation of a particular unit. An entry of "0%" shows a complete lack of documentation on a particular unit. It should be noted that status estimates are based on available knowledge of the requirements for drawings, etc., and cannot reflect an accurate estimate if PRC is unaware of the existence of certain documents.

Next, in the sectional tabulations for each subsystem, the individual units are broken down, where suitable, into subunits, and these are indexed with decimal extensions of the unit number. Thus the Command Receiver is listed as unit 1.6 and the R.F. Board as subunit 1.6.1. Where this kind of unit portioning has been done, it is noted in the column



headed "Remarks." The name of each part is given along with the applicable drawing or part number and, in some instances, a Mil specification number. The required quantity is shown, with the notation "AR" indicating "as required" for parts which are not readily measured. At least one page of the Appendix is allotted to each unit, and it is intended that revisions, additions, and deletions can be handled by a page substitution scheme. This accounts for the presence of some pages which are currently blank except for the unit title. The appearance of the letter "N" opposite a parts entry means that the drawing or part number has been identified, but that the drawing must be obtained to ascertain the basic parts complement. Assemblies which are otherwise electronic in their makeup sometimes include nonelectronic parts. These are generally identified through the use of the word "Mechanical" opposite the parts entry. This is not done, of course, for structural or mechanical assemblies.

---

# OGO PARTS COMPLEMENT

## UNIT INDEX

<u>PRC Index</u>	<u>Description</u>	<u>Assembly Drawing No.</u>	<u>Status</u>
1.0	Communications and Data Handling Subsystem	X200393	98%
1.1	400-mc Omni Antenna Assembly	200593	Complete
1.2	400-mc High-Gain Antenna Assembly	200867	Complete
1.3	120-136-mc Omni Antenna Assembly	201418	Complete
1.4	Dual Diplexer/136-mc Coupler	(Subcontracted--No Information)	0%
1.5	400-mc Coupler (2 ea.)	(Subcontracted--No Information)	0%
1.6	Command Receiver (2 ea.)	201456	Complete
1.7	100-mw Tracking Transmitter (2 ea.)	201000	Complete
1.8	10-watt Tracking Transmitter	201458	Complete
1.9	400-mc Wideband Telemetry Transmitter (2 ea.)	201460	Complete
1.10	Special-Purpose Transmitter	201459	Complete
1.11	Digital Command Decoder (2 ea.)	201506	Complete
1.12	Tone Decoder	(Preliminary Parts List and Schematics)	Complete
1.13	Low-Frequency Timing Assembly	201441	Need 2
1.14	Tape Recorder (2 ea.)	(Subcontracted--Parts List Available)	Complete
1.15	Special-Purpose Telemetry DHU	202650	Complete

PRC Index	Description	Assembly Drawing No.	Status
1.16	Command Distribution Unit	201529	Complete
1.17	Signal Conditioner	201738	Complete
1.18	Digital Data Handling Assembly (2 ea.)	201348	Need 5
1.19	Analog Data Handling Assembly (2 ea.)	201140	Complete
1.20	Spacecraft Performance Sensors	(No Information)	0%
2.0	Attitude Control and Stabilization Subsystem		95%
2.1	OPEP and Solar Array Drive	202540	Complete
2.2	Sun Sensor Assembly--Radiation Tracking Transducer	202384	Complete
2.3	Sun Sensor Assembly	202744	Complete
2.4	Sun Sensor Electronics and Logic Assembly	200932	Complete
2.5	Electronics Assembly, OPEP and Solar Array Drive	200934	Complete
2.6	Pitch Rate Gyro Assembly	200935	Complete
2.7	Assembly Attitude Control Unit	200833	Complete
2.8	OPEP Gyro Electronics Assembly	202163	Complete
2.9	OPEP Inertial Reference Assembly	201371	Complete
2.10	Horizon Scanners	(Subcontracted--Parts List Available)	Complete
2.11	Reaction Wheels	(Subcontracted--No Information)	0%
2.12	Pneumatic System Installation--Attitude Control	100012	Complete?
2.13	Transducer--OPEP and Solar Array	C200979	0%

<u>PRC Index</u>	<u>Description</u>	<u>Assembly Drawing No.</u>	<u>Status</u>
3.0	Power Supply Subsystem		60%
3.1	Solar Array Installation	100022	Complete
3.2	Battery Pack (2 ea.)	204593	Complete
3.3	Harness	D13404	0%
3.4	Converters	D13405	Need 8
3.5	Junction Boxes	D13407	Need 4
3.6	Power Integration Unit	201543	Need 9
4.0	Thermal Control Subsystem		90%
4.1	Box Structure (Insulation)	100472	Complete
4.2	Solar Array (Insulation)	DL100825	Complete
4.3	External Package T.C.	DL100826	0%
4.4	Louver Assembly	100023	Complete
5.0	Structure Subsystem		95%
5.1	Basic Box Structure	DL100823	Complete
5.2	Solar Array (Main Frame)	DL100825	Complete
5.3	Folding Devices	DL100826	Complete
5.4	Interstage and Separation	DL100823	Complete

# 1.0: CDH PARTS COMPLEMENT

<u>PRC Index</u>	<u>Item</u>	<u>Quantity</u>	<u>Remarks</u>
1.1	400-mc Omni Antenna Assembly, 200593		
	Balun, 200455	1	
	Element Assembly, 201503	1	See 1.1.2
	Collar, Coaxial Assembly, 200590	2	
	Base, Connector Clamp, 201293	1	
	Clamp Connector, 201282	2	
	Crossover, 201239-2	1	
	Stub, Mounting, 201318	1	
	Crossover, 201239-1	1	
	Conductor, Coaxial, 54001-8	AR	
	Connector, PT2-14-4	2	
	Gusset, Balun, 203548	1	
	Coaxial Switch, 400 mc, C207437	1	
1.1.2	Element Assembly, 201503		
	Element, Inner Conductor, 200591	2	
	Element, Outer Conductor, 200592	2	

<u>PRC Index</u>	<u>Item</u>	<u>Quantity</u>	<u>Remarks</u>
1.2	400-mc High-Gain Antenna Assembly, 200867		
	Boom Assembly, 200863-1	1	
	Element Assembly, 202171-1	1	See 1.2.2
	Reflector Assembly, 201263-1	1	
	Balun Assembly, 200865-1	1	
	Element, Driver, 200858-1	4	
	Collar, Coaxial Connector, 200590-1	2	
	Crossover, 201435-1	2	
	Conductor, Coaxial, 54001-7 STL	AR	
	Connector, Coaxial Plug, 502002-4	2	
1.2.2	<u>Element Assembly, 202171-1</u>		
	Element, Inner Conductor, 200866-1	2	
	Element, Outer Conductor, 202172-1	2	

<u>PRC Index</u>	<u>Item</u>	<u>Quantity</u>	<u>Remarks</u>
1.3	120-136-mc Omni Antenna Assembly, 201418		
	Element Assembly, 200896	1	
	Balun, 201419	1	Tubing
	Conductor, Coaxial, 54001-8	AR	
	Crossover, 201424-2	2	Mechanical
	Collar, Coaxial Connector, 200590	2	
	Crossover, 201424-1	1	Mechanical
	Connector, 502002-4	2	
	Conductor, Coaxial, 54001-7	AR	
	Coaxial Switch, 136 mc, C207438	1	

Quantity      Remarks

PRC Index      Item  
1.4      Dual Diplexer 1136-mc Coupler



Remarks

Quantity

Item

PRC Index

400-mc Coupler (2 ea.)

1.5

<u>PRC Index</u>	<u>Item</u>	<u>Quantity</u>	<u>Remarks</u>
1.6	Command Receiver, 201456		
	R.F. Board, 202025	1	See 1.6.1
	Audio Board, 202860	1	See 1.6.2
	Panel, Connector, 202117	1	
	Shield, Connector, 202257	1	
	Connector, PT2-14-L, J1	1	
	Connector, PT2-5-3, J2	1	
	Connector, PT2-7-2, J3	1	
	Contacts, Coaxial, PT2-7-55, J3	5	
	Filter, PT4-1016, FL2	1	
1.6.1	R.F. Board Assembly, Command Receiver, 202025		
	Terminal Assembly, R.F. Board, 201795	1	Printed Circuit Board
	Transformer, 201808 (T1)	1	
	Transformer, 201809 (T2)	1	
	Transformer, 201810 (T3)	1	
	Transformer, 201811 (T4)	1	
	Transformer, 201812 (T5)	1	
	Transformer, 201813 (T6)	1	
	Transformer, 201814 (T7)	1	
	Transformer, 201815 (T8)	1	
	Transformer, 201816 (T9)	1	
	Transformer, 201817 (T10)	1	

<u>PRC Index</u>	<u>Item</u>	<u>Quantity</u>	<u>Remarks</u>
1.6.1	R.F. Board Assembly, Command Receiver, 202025 (Continued)		
	Transformer, 201818 (T12)	1	
	Transformer, 201819 (T18)	1	
	Inductor, 201820 (L1)	1	
	Inductor, 201821 (L3)	1	
	Capacitor, Mil-C-11015B, CK05CW102M	18	
	Capacitor, Mil-C-11015B, CK06CW___M	17	
	Capacitor, Mil-C-11272B, CY10C___	12	
	Capacitor, Mil-C-11272B, CY10C___J	6	
	Capacitor, Mil-C-26655A, CS13AE___K	6	
	Capacitor, Variable, PT4-1000 (C39)	1	
	Resistor, Mil-R-11C, RC07GF___J	47	
	Resistor, Mil-R-11C, RC20GF240J	4	
	Thermistor, PT4-1	2	
	Transistor, PT4-7015	1	
	Transistor, PT4-7016	8	
	Transistor, PT4-7004	5	
	Diode, PT4-2003	2	
	Diode, Mil-S-19500/127, IN755A	1	
	Diode, PT4-2012	1	
	Choke, R.F., PT6-1-3	1	
	Crystal, 503001-4, -5	2	
	Filter, Crystal, PT4-13002	1	

<u>PRC Index</u>	<u>Item</u>	<u>Quantity</u>	<u>Remarks</u>
1.6.2	Audio Board Assembly, Command Receiver, 202860		
	Terminal Assembly, Audio Board, 202474	1	Printed Circuit Board
	Transformer, 202864 (T14)	1	
	Transformer, 202865 (T15)	1	
	Transformer, 202866 (T16)	1	
	Transformer, 202867 (T17)	1	
	Transformer, 202868 (T19)	1	
	Transistor, PT4-7003	1	
	Transistor, Mil-S-19500/177, 2N1132	1	
	Transistor, PT4-7001	2	
	Transistor, PT4-7021	1	
	Transistor, PT4-7004	8	
	Transistor, PT4-7020	1	
	Transistor, PT4-7016	2	
	Diode, Mil-S-19500/117(USN), 1N965B	1	
	Diode, PT4-2001	2	
	Diode, Mil-S-19500/115A, 1N3027B	1	
	Diode, Mil-S-19500/159, 1N821	1	
	Diode, PT4-2044	1	
	Diode, PT4-2003	1	
	Diode, PT4-2012	2	
	Thermistor, PT4-1-2	2	

PRC Index

1.6.2

Audio Board Assembly, Command Receiver, 202860  
(Continued)

<u>Item</u>	<u>Quantity</u>	<u>Remarks</u>
Resistor, Mil-R-11C, RC07GF __ J	66	
Resistor, Mil-R-26C, RW59V202	1	
Capacitor, Mil-C-11015B, CK05CW102K	2	
Capacitor, Mil-C-11015B, CK06CW __ K	20	
Capacitor, Mil-C-11272B, CY10C131J	2	
Capacitor, Mil-C-11272B, CY15C __ J	3	
Capacitor, PT4-1011-G104M	8	
Capacitor, Mil-C-26655A, C513AF6REK	3	
Capacitor, Mil-C-26655A, C513AD220K	1	
Inductor, PT6-3-7	1	
Inductor, PT6-3-8	2	
Relay, PT2-1012	1	

<u>PRC Index</u>	<u>Item</u>	<u>Quantity</u>	<u>Remarks</u>
1.7	100-mw Tracking Transmitter, 201000		
	Transformer, 201468-1	1	
	Transformer, 208588-1	1	
	Transformer, 208587-1	1	
	Transformer, 201471-1	1	
	Inductor, 201472-1	1	
	Inductor, 201473-1	1	
	Filter, PT4-1016	1	
	Capacitor, Mil-C-11272, CY12C510J-AF.	1	
	Capacitor, Mil-C-11272, CY12C270J-AF.	1	
	Capacitor, Mil-C-11272, CY12C___J-AF.	5	
	Capacitor, Mil-C-11015/18, CK05CW102M	11	
	Capacitor, Mil-C-11272, CY10C200G	1	
	Capacitor, Mil-C-11272, CY12C100J-AF.	1	
	Capacitor, Mil-C-11272, CY12C100J-AF.	1	
	Capacitor, Mil-C-11272, CY10C620G	1	
	Capacitor, PT4-1000	3	
	Capacitor, Mil-C-11015/19, CK06CW103.	1	
	Connector, PT2-18-2	1	
	Connector, PT2-17-3	1	
	Choke, PT6-1-1	2	
	Choke, PT6-1-3	2	
	Crystal, 503001-1	1	
	Diode, PT4-2053	1	

<u>PRC Index</u>	<u>Item</u>	<u>Quantity</u>	<u>Remarks</u>
1.7	100-mw Tracking Transmitter, 201000 (Continued)		
	Diode, PT4-2001	1	
	Diode, PT4-2004	2	
	Resistor, Mil-R-11, RC07GF J	11	
	Transistor, 2N697, Mil-S-19500/99A	1	
	Transistor, PT4-7000	4	

<u>PRC Index</u>	<u>Item</u>	<u>Quantity</u>	<u>Remarks</u>
1.8	10-watt Tracking Transmitter, 201458		
	R.F. Input Assembly, 205000	1	See 1.8.1
	Power Amplifier Assembly, 204934	1	See 1.8.2
	Capacitor, CK05CW102K	1	
	Resistor, PT4-15-6R2J, 6.2 $\Omega$ , 1/4 w, $\pm 5\%$	1	
	Connector, PT2-14-2	1	
	Thermistor, PT4-6	1	
	Filter, PT4-1016	2	
	Transistor, PT4-7067	3	
	Connector, PT2-5-6	1	
	Connector, PT2-5-1	1	
1.8.1	R.F. Input Assembly, 205000		
	Terminal Assembly, 205049	1	
	Inductor, 201472 (L5)	1	
	Inductor, 202587 (L9)	1	
	Transformer, 202590 (T1)	1	
	Transformer, 202469 (T2)	1	
	Transformer, 202593 (T3)	1	
	Transformer, 202597 (T4)	1	
	Transformer, 202591 (T5)	1	
	Capacitor, Mil-C-11015B, CK05CW102K, 1000 $\mu$ uf	15	
	Capacitor, Mil-C-11272B, CY12C J	10	
	Capacitor, PT4-1000	2	



<u>PRC Index</u>	<u>Item</u>	<u>Quantity</u>	<u>Remarks</u>
1.8.1	R.F. Input Assembly, 205000 (Continued)		
	Resistor, Mil-R-11C, RC07GF __ J, $\pm 5\%$ , 1/4 w	12	
	Transistor, PT4-7000	6	
	Coil, PT6-1-1	4	
	Diode, PT4-2004	2	
	Crystal, 503001, 68.1 mc (Y1)	1	
1.8.2	Driver and Power Amplifier Assembly, 204934		
	Transformer, 203130 (T7, T8)	2	
	Inductor, 204462 (L12)	1	
	Capacitor, PT4-1000	8	
	Capacitor, Mil-C-11272B, CY12C __ J	5	
	Capacitor, Mil-C-11015, GK05CW102K	12	
	Inductor, 206241 (L17)	1	
	Resistor, Mil-R-11C, RC076F100J, 1/4 w, $\pm 5\%$	3	
	Resistor, PT4-15- __ J, 1/4 w, $\pm 5\%$	3	
	Inductor, PT6-1-X (X = $\mu$ h)	6	

<u>PRC Index</u>	<u>Item</u>	<u>Quantity</u>	<u>Remarks</u>
1.9	400-mc Wideband Telemetry Transmitter, 201460		
	R.F. Input Assembly, 204642	1	See 1.9.1
	Multiplier Assembly, 203040	1	See 1.9.2
	Filter Assembly, 203724	1	See 1.9.3
	Thermistor, PT4-7067	1	
	Filter, PT4-1016	2	
	Transistor, PT4-6	3	
	Connector, PT2-5-6	1	
	Connector, PT2-5-1	1	
	Connector, PT2-14-2	1	
	Resistor, PT4-15-6R2J, 6.2, 1/4 w, $\pm 5\%$	1	
	Capacitor, CK05CW102K, 1000 $\mu$ uf, 10%, 200 v	1	
1.9.1	R.F. Input Assembly, 204642		
	Terminal Assembly, 203226 (56 Terminals)	1	
	Inductor, 204393 (L6)	1	
	Inductor, 202587 (L9)	1	
	Transformer, 202590 (T1)	1	
	Transformer, 202648 (T3)	1	
	Transformer, 202592 (T6)	1	
	Transformer, 202589 (T2, T4)	2	
	Transformer, 205675 (T5)	1	
	Capacitor, Mil-C-11015B, CK05CW102K	15	
	Capacitor, Mil-C-11272B, CY12C J	13	

<u>PRC Index</u>	<u>Item</u>	<u>Quantity</u>	<u>Remarks</u>
1.9.1	<u>R.F. Input Assembly, 204642 (Continued)</u>		
	Capacitor, Mil-C-26655A, C513AE100K	2	
	Capacitor, PT4-1000	1	
	Varactor, PT4-2033 (CV1)	1	
	Resistor, Mil-R-11C, RC07GF J	18	
	Transistor, PT4-7000	6	
	Coil, PT6-1-4	6	
	Diode, PT4-2004	3	
	Crystal, 503001-3 (Y1)	1	
1.9.2	<u>Multiplier Assembly, 203040</u>		
	Inductor, 202926 (L18)	1	
	Inductor, 202927 (L15)	1	
	Inductor, 202928 (L20)	1	
	Inductor, 202929 (L21)	1	
	Inductor, 202930 (L22)	1	
	Inductor 202931 (L23)	1	
	Terminal, Plain, 204478-1, -2 (Tie-Down Type)	5	
	Terminal, SP0026-2 (Little Post)	1	
	Terminal, SP0006-1, -2 (Little Post)	3	
	Terminal, SP0005-2 (Little Post)	1	
	Terminal, SP0030-2 (Little Post)	1	
	Capacitor, Mil-C-11272B, CY12C101J	2	
	Capacitor, Mil-C-11272B, CY16C471J	2	

<u>PRC Index</u>	<u>Item</u>	<u>Quantity</u>	<u>Remarks</u>
1.9.2	<u>Multiplier Assembly, 203040 (Continued)</u>		
	Capacitor, Mil-C-11272B, CY10C J	4	
	Capacitor, Variable, 1-10 $\mu$ f, PT4-1006	4	
	Capacitor, Variable, .8-10 $\mu$ f, PT4-1007	2	
	Resistor, Mil-R-11C; RC07GF124J	2	
	Varactor, PT4-2034	1	
1.9.3	<u>Filter Assembly, 203724</u>		
	Filter Board No. 2, 203726	1	Mechanical
	Filter Board No. 1, 203725	1	Mechanical
	Ground Plane, 204050-1, -2	2	Mechanical
	Feedthrough, SP0005-2	2	
	Ground Terminal, SP0050-3	1	

<u>PRC Index</u>	<u>Item</u>	<u>Quantity</u>	<u>Remarks</u>
1.10	<u>Special-Purpose Transmitter, 201459</u>		
	R.F. Input Assembly, 204642	1	See 1.9.1
	Multiplier Assembly, 204443	1	See 1.10.2
	Filter Assembly, 203724	1	See 1.9.3
	Connector, PT2-14-2	1	
1.10.2	<u>Multiplier Assembly, 204443</u>		
	Transformer, 203891 (T13)	1	
	Transformer, 203890 (T14)	1	
	Transformer, 203888 (T15)	1	
	Transformer, 203887 (T16)	1	
	Inductor, 203889 (L17)	1	
	Diode, PT4-2033	1	
	Diode, PT4-2036	1	
	Capacitor, PT4-1006, 1-10 $\mu$ uf, 500 v	6	
	Capacitor, Mil-C-11015B, CK05CW102K	2	
	Capacitor, Mil-C-11272B, CY10C__J + C	3	
	Resistor, Mil-R-11C, RC07GF__J	2	
	Terminal, SP0006-1 (Just a part to tie the wire on)	10	
	Terminal, SP0025-2 (Just a part to tie the wire on)	7	

<u>PRC Index</u>	<u>Item</u>	<u>Quantity</u>	<u>Remarks</u>
1.11	<u>Digital Command Decoder (2 ea.), 201506</u>		
	Decoder, Subassembly, 202988	1	See 1.11.1
1.11.1	<u>Decoder, Subassembly, 202988</u>		
	Assembly Board No. 1, 202955-1	1	See 1.11.1.1
	Assembly Board No. 2, 203000-1	1	See 1.11.1.2
	Transistor, 2N1721	1	
	Connector, PT2-5-5	1	
	Connector, PT2-5-10	1	
	Connector, PT2-5-8	1	
	Receptacle, PT2-14-2	2	
1.11.1.1	<u>Assembly Board No. 1, 202995</u>		
	Module Assembly, Shift Key, 203224-1	10	See 1.11.1.1.1
	Module Assembly, Matrix Pulses, 203231-1	32	See 1.11.1.1.2
	Module Assembly No. 1, Blocking Oscillator, 203261-1	2	See 1.11.1.1.3
	Module Assembly, Combiner, 203235-1	1	See 1.11.1.1.4
	Module Assembly, Logic Gate, 203239-1	2	See 1.11.1.1.5
	Terminal, Feedthrough, 204678-1	92	
	Resistor, Mil-R-11C, RC07GF104J	1	
1.11.1.1.1	<u>Module Assembly, Shift Register, 203224</u>		
	Component Assembly, Shift Register, 203229-1	1	See 1.11.1.1.1.1

<u>PRC Index</u>	<u>Item</u>	<u>Quantity</u>	<u>Remarks</u>
1.11.1.1.1.1	<u>Component Assembly, Shift Register, 203229</u>		
	Transistor, PT4-7059, 2N708	2	
	Diode, Mil-S-19500/144, 1N3064	6	
	Capacitor, CK06CW__K, Mil-C-11015B	4	
	Resistor, PT4-7-C__F, 1/8 w, ±1%	11	
1.11.1.1.2	<u>Module Assembly, Matrix Pulser, 203231</u>		
	<u>Component Assembly, Matrix Pulser, 203232-1</u>	1	See 1.11.1.1.2.1
1.11.1.1.2.1	<u>Component Assembly, Matrix Pulser, 203232</u>		
	Capacitor, CK06CW__K, Mil-C-11015B	3	
	Capacitor, CK05CW__K, Mil-C-11015B	2	
	Diode, Mil-S-19500/144, 1N3064	6	
	Resistor, PT4-7-C__F, 1/8 w, ±1%	9	
	Transistor, PT4-7003, 2N722	1	
	Transistor, PT4-7010, 2N834	1	
	Transformer, TF4RX13YY, UTC (D1-T37)	1	
1.11.1.1.3	<u>Module Assembly No. 1, Blocking Oscillator, 203261-1</u>		
	<u>Component Assembly, Blocking Oscillator, 203262-1</u>	1	See 1.11.1.1.3.1
1.11.1.1.3.1	<u>Component Assembly No. 1, Blocking Oscillator, 203262</u>		
	Capacitor, CS13AF010K, Mil-C-26655A	1	
	Capacitor, CK05CW470K, Mil-C-11015B	1	
	Diode, Mil-S-19500/144, 1N3064	6	
	Resistor, PT4-7-C__F, 1/8 w, ±1%	7	

<u>PRC Index</u>	<u>Item</u>	<u>Quantity</u>	<u>Remarks</u>
1.11.1.1.3.1	<u>Component Assembly No. 1, Blocking Oscillator, 203262 (Continued)</u>		
	Transistor, PT4-7034, 2N910	1	
	Transistor, PT4-7063, 2N834	1	
	Transformer, PT6-1014	1	
1.11.1.1.4	<u>Module Assembly, Combiner, 203235</u>		
	<u>Component Assembly, Combiner, 203236-1</u>	1	See 1.11.1.1.4.1
1.11.1.1.4.1	<u>Component Assembly, Combiner, 203236</u>		
	Resistor, PT4-7-C F, 1/8 w, $\pm 1\%$	12	
	Transistor, PT4-7034, 2N910	12	
1.11.1.1.5	<u>Module Assembly, Logic Gate, 203239-1</u>		
	<u>Component Assembly, Logic Gate, 203240-1</u>	1	See 1.11.1.1.5.1
1.11.1.1.5.1	<u>Component Assembly, Logic Gate, 203240</u>		
	Diode, Mil-S-19500/144, 1N3064	48	
1.11.1.2	<u>Assembly Board No. 2, 203000</u>		
	<u>Component Assembly, Demodulator, 203003-1</u>	1	See 1.11.1.2.1
	<u>Module Assembly No. 1, Demodulator, 203245-1</u>	1	See 1.11.1.2.2
	<u>Module Assembly No. 2, Demodulator, 203247-1</u>	1	See 1.11.1.2.3
	<u>Module Assembly No. 3, Demodulator, 203249-1</u>	1	See 1.11.1.2.4
	<u>Module Assembly No. 4, Demodulator, 203251-1</u>	1	See 1.11.1.2.5
	<u>Module Assembly, Voltage Regulator, 203253-1</u>	1	See 1.11.1.2.6
	<u>Module Assembly, Enable, 203255-1</u>	1	See 1.11.1.2.7



<u>PRC Index</u>	<u>Item</u>	<u>Quantity</u>	<u>Remarks</u>
1.11.1.2	Assembly Board No. 2, 203000 (Continued)		
	Module Assembly, Decoder Address, 203259-1	1	See 1.11.1.2.8
	Module Assembly No. 1, Blocking Oscillator, 203261-1	3	See 1.11.1.1.3
	Module Assembly, Word Command, 203265-1	11	See 1.11.1.2.10
	Module Assembly, Programmer, 203267-1	6	See 1.11.1.2.11
	Module Assembly, Delay, 203269-1	1	See 1.11.1.2.12
	Module Assembly, Data Available, 203271-1	1	See 1.11.1.2.13
	Module Assembly, Word Sampling Timing, 203273-1	1	See 1.11.1.2.14
	Module Assembly, Programmer Reset Pulser, 203275-1	1	See 1.11.1.2.15
	Module Assembly, Parity, 203277-1	1	See 1.11.1.2.16
	Module Assembly, Programmer Reset Timing, 203281-1	1	See 1.11.1.2.17
	Module Assembly, Internal Address, 203283-1	2	See 1.11.1.2.18
	Module Assembly, Timing Gate Logic, 203285-1	1	See 1.11.1.2.19
	Module Assembly, Gate A and B, 203350-1	1	See 1.11.1.2.20
	Terminal, Feedthrough, 204628-1	76	
	Terminal, Standoff, 204627-1	46	
	Transistor, 2N1721	1	
	Resistor, Mil-R-11C, RC07GF__J	7	
	Resistor, PT4-7, 1/8 w, 1%	5	
	Capacitor, PT4-1004, 800 pf, 300 vdc, 1%	2	
	Capacitor, Mil-C-11015B, CK06CW103K	2	
	Diode, Mil-S-19500, 1N3064	10	

<u>PRC Index</u>	<u>Item</u>	<u>Quantity</u>	<u>Remarks</u>
1.11.1.2.1	Component Assembly, Demodulator, 203003		
	Board Assembly, 203004 (PCB)	1	
	Capacitor, Mil-C-26655A, CS13AF220K	2	
	Capacitor, PT4-1004, 300 vdc, 1%	3	
	Capacitor, PT4-1010, 50 vdc, 20%	1	
	Capacitor, Mil-C-27287, CTM274VAJ	1	
	Inductor, PT6-3	4	
1.11.1.2.2	Module Assembly No. 1, Demodulator, 203245		
	Component Assembly, 203246-1	1	See 1.11.1.2.2.1
1.11.1.2.2.1	Component Assembly No. 1, Demodulator, 203246		
	Capacitor, Mil-C-11015B, CK06CW103K, .01 $\mu$ f	4	
	Diode, Mil-S-19500/118, 1N485B	1	
	Resistor, PT4-7-C__F, 1/8 w, $\pm$ 1%	11	
	Transistor, PT4-7034, 2N910	4	
1.11.1.2.3	Module Assembly No. 2, Demodulator, 203247		
	Component Assembly, 203248-1	1	See 1.11.1.2.3.1
1.11.1.2.3.1	Component Assembly No. 2, Demodulator, 203248		
	Sensistor, PT4-2-102J, 1.0 k, $\pm$ 5%	1	
	Resistor, PT4-7-C__F, 1/8 w, $\pm$ 1%	7	
	Resistor, RC07GF104J, Mil-R-11C, 100k, 1/4 w, $\pm$ 5%	3	
	Capacitor, Mil-C-26655A, CS13AF__K	4	
	Diode, Mil-S-19500, 1N485B	4	
	Transistor, PT4-7003, 2N722	2	
	Transistor, PT4-7034, 2N910	1	

<u>PRC Index</u>	<u>Item</u>	<u>Quantity</u>	<u>Remarks</u>
1.11.1.2.4	Module Assembly No. 3, Demodulator, 203249		
	Component Assembly, 203250-1	1	See 1.11.1.2.4.1
1.11.1.2.4.1	Component Assembly No. 3, Demodulator, 203250		
	Resistor, PT4-7-C __ F, 1/8 w, 1%	13	
	Capacitor, Mil-C-26655A, CS13AF __ K, 35 vdc, ±10%	3	
	Capacitor, Mil-C-11015B, CK05CW __ K, 200 vdc, ±10%	2	
	Diode, Mil-S-19500/118, 1N485B	2	
	Transistor, PT4-7034, 2N910	4	
1.11.1.2.5	Module Assembly No. 4, Demodulator, 203251		
	Component Assembly, 203252-1	1	See 1.11.1.2.5.1
1.11.1.2.5.1	Component Assembly No. 4, Demodulator, 203252		
	Resistor, PT4-7-C __ F, 1/8 w, ±1%	19	
	Capacitor, Mil-C-11015B, CK06CW __ K, 200 vdc, 10%	6	
	Capacitor, Mil-C-11015B, CK05CW __ K, 200 vdc, 10%	2	
	Diode, Mil-C-19500/118, 1N485B	2	
	Transistor, PT4-7013, 2N869	1	
	Transistor, PT4-7034, 2N910	2	
	Transistor, PT4-7003, 2N722	2	
1.11.1.2.6	Module Assembly, Voltage Regulator, 203253		
	Component Assembly, Voltage Regulator, 203254	1	See 1.11.1.2.6.1

<u>PRC Index</u>	<u>Item</u>	<u>Quantity</u>	<u>Remarks</u>
1.11.1.2.6.1	Component Assembly, Voltage Regulator, 203254		
	Resistor, PT4-7-C___F, 1/8 w, ±1%	4	
	Resistor, RC07GF104J, Mil-R-11C	2	
	Capacitor, CK06CW103K, Mil-C-11015B	4	
	Diode, Mil-S-19500/127, 1N756A	1	
	Diode, Mil-S-19500/127, 1N757A	2	
	Diode, Mil-S-19500/118, 1N485B	2	
	Choke, PT6-1-7, 100 µh	1	
	Transistor, PT4-7034, 2N910	2	
1.11.1.2.7	Module Assembly, Enable, 203255		
	Component Assembly, Enable, 203256	1	See 1.11.1.2.7.1
1.11.1.2.7.1	Component Assembly, Enable, 203256		
	Capacitor, CK06CW103K, Mil-C-11015B	2	
	Capacitor, CK05CW102K, Mil-C-11015B	2	
	Diode, Mil-S-19500/144, 1N3064	13	
	Resistor, PT4-7-C___F, 1/8 w, ±1%	13	
	Resistor, RC07GF103J, Mil-R-11C	1	
	Transistor, PT4-7034, 2N910	1	
	Transistor, PT4-7059, 2N708	2	
1.11.1.2.8	Module Assembly, Decoder Address, 203259		
	Component Assembly, Decoder Address, 203260	1	See 1.11.1.2.8.1

<u>PRC Index</u>	<u>Item</u>	<u>Quantity</u>	<u>Remarks</u>
1.11.1.2.8.1	Component Assembly, Decoder Address, 203260		
	Resistor, PT4-7-C__F, 1/8 w, ±1%	10	
	Capacitor, CK06CW103K, Mil-C-11015B	2	
	Capacitor, CK05CW102K, Mil-C-11015B	2	
	Diode, Mil-S-19500/144, 1N3064	10	
	Transistor, PT4-7059, 2N708	2	
1.11.1.2.10	Module Assembly, Word Command, 203265		
	Component Assembly, Word Command, 203266	1	See 1.11.1.2.10.1
1.11.1.2.10.1	Component Assembly, Word Command, 203266		
	Capacitor, CK06CW103K, Mil-C-11015B	2	
	Capacitor, CK05CW__K, Mil-C-11015B	2	
	Diode, Mil-S-19500/144, 1N3064	8	
	Resistor, PT4-7-C__F, 1/8 w, ±1%	8	
	Transistor, PT4-7003, 2N722	1	
	Transistor, PT4-7010, 2N834	1	
	Transistor, TF4RX13YY (D1-T11, UTC)	1	
1.11.1.2.11	Module Assembly, Programmer, 203267		
	Component Assembly, Programmer, 203268	1	See 1.11.1.2.11.1
1.11.1.2.11.1	Component Assembly, Programmer, 203268		
	Resistor, PT4-7-C__F	10	
	Capacitor, CK06CW103K, Mil-C-11015B	2	
	Capacitor, CK05CW102K, Mil-C-11015B	2	
	Diode, Mil-S-19500/144, 1N3064	6	
	Transistor, PT4-7059, 2N708	2	

<u>PRC Index</u>	<u>Item</u>	<u>Quantity</u>	<u>Remarks</u>
1.11.1.2.12	<u>Module Assembly, Delay, 203269</u>		
	Component Assembly, Delay, 203290	1	See 1.11.1.2.12.1
1.11.1.2.12.1	<u>Component Assembly, Delay, 203290</u>		
	Capacitor, CK05CW __ K, Mil-C-11015E	3	
	Resistor, PT4-7-C __ F, 1/8 w, $\pm 1\%$	9	
	Transistor, PT4-7010, 2N834	2	
	Diode, Mil-S-19500/144, 1N3064	3	
1.11.1.2.13	<u>Module Assembly, Data Available, 203271</u>		
	Component Assembly, Data Available, 203272	1	See 1.11.1.2.13.1
1.11.1.2.13.1	<u>Component Assembly, Data Available, 203272</u>		
	Capacitor, CK06CW __ K, Mil-C-11015E	2	
	Capacitor, CK05CW __ K, Mil-C-11015E	2	
	Diode, Mil-S-19500/144, 1N3064	6	
	Resistor, PT4-7-C __ F, 1/8 w, $\pm 1\%$	5	
	Transistor, PT4-7003, 2N722	1	
	Transistor, PT4-7010, 2N834	1	
	Transformer, TF4RX13YY (D1-T11, UTC)	1	
1.11.1.2.14	<u>Module Assembly, Word Sampling Timing, 203273</u>		
	Component Assembly, Word Sampling Timing, 203274	1	See 1.11.1.2.14.1
1.11.1.2.14.1	<u>Component Assembly, Word Sampling Timing, 203274</u>		
	Diode, Mil-S-19500/144, 1N3064	20	
	Resistor, PT4-7-C1002F, 1/8 w, $\pm 1\%$	5	

<u>PRC Index</u>	<u>Item</u>	<u>Quantity</u>	<u>Remarks</u>
1.11.1.2.15	<u>Module Assembly, Programmer Reset Pulser, 203275</u>		
	Component Assembly, Programmer Reset Pulser, 203276	1	See 1.11.1.2.15.1
1.11.1.2.15.1	<u>Component Assembly, Programmer Reset Pulser, 203276</u>		
	Capacitor, CK06CW103K, Mil-C-11015E	2	
	Capacitor, CK05CW__K, Mil-C-11015E	2	
	Diode, Mil-S-19500/144, 1N3064	6	
	Diode, Mil-S-19500/127, 1N754A	1	
	Resistor, PT4-7-C__F, 1/8 w, $\pm 1\%$	12	
	Transistor, PT4-7003, 2N722	1	
	Transistor, PT4-7010, 2N834	1	
	Transistor, PT4-7034, 2N910	2	
	Transformer, TF4RX13YY (D1-T22, UTC)	1	
1.11.1.2.16	<u>Module Assembly, Parity, 203277</u>		
	Component Assembly, Parity, 203278	1	See 1.11.1.2.16.1
1.11.1.2.16.1	<u>Component Assembly, Parity, 203278</u>		
	Resistor, PT4-7-C__F, 1/8 w, $\pm 1\%$	12	
	Capacitor, CK06CW__F, Mil-C-11015E	2	
	Capacitor, CK05CW__F, Mil-C-11015E	2	
	Diode, Mil-S-19500/144, 1N3064	10	
	Transistor, PT4-7059, 2N708	2	
1.11.1.2.17	<u>Module Assembly, Programmer Reset Timing, 203281</u>		
	Component Assembly, Programmer Reset Timing, 203282	1	See 1.11.1.2.17.1

<u>PRC Index</u>	<u>Item</u>	<u>Quantity</u>	<u>Remarks</u>
1.11.1.2.17.1	<u>Component Assembly, Programmer Reset Timing, 203282</u>		
	Diode, Mil-S-19500/144, 1N3064	21	
	Resistor, PT4-7-C___F, 1/8 w, ±1%	5	
1.11.1.2.18	<u>Module Assembly, Internal Address, 203283</u>		
	<u>Component Assembly, Internal Address, 203284</u>	1	See 1.11.1.2.18.1
1.11.1.2.18.1	<u>Component Assembly, Internal Address, 203284</u>		
	Resistor, PT4-7-C___F, 1/8 w, ±1%	11	
	Resistor, RC07GF104J, Mil-R-11C	1	
	Capacitor, CK06CW103K, Mil-C-11015B	2	
	Capacitor, CK05CW102K, Mil-C-11015B	2	
	Diode, Mil-S-19500/144, 1N3064	10	
	Transistor, PT4-7059, 2N708	2	
1.11.1.2.19	<u>Module Assembly, Timing Gate Logic, 203285</u>		
	<u>Component Assembly, Timing Gate Logic, 203286</u>	1	See 1.11.1.2.19.1
1.11.1.2.19.1	<u>Component Assembly, Timing Gate Logic, 203286</u>		
	Diode, Mil-S-19500/144, 1N3064	48	
1.11.1.2.20	<u>Module Assembly, Gate A and B, 203350</u>		
	<u>Component Assembly, Gate A and B, 203351</u>	1	See 1.11.1.2.20.1
1.11.1.2.20.1	<u>Component Assembly, Gate A and B, 203351</u>		
	Resistor, PT4-7-C___F, 1/8 w, ±1%	6	
	Diode, Mil-S-19500/144, 1N3064	16	



PRC Index

1.12

<u>Item</u>	<u>Quantity</u>	<u>Remarks</u>
<u>Tone Decoder (from Schematic and Preliminary Parts List)</u>		
Resistor, PT4-7-C___F, 1/8 w, 1%	172	
Resistor, Mil-R-9444(N416), Tapped, 1.6 $\Omega$ , .8 $\Omega$ , .4 $\Omega$ , 1/8 w, 1%	1	
Capacitor, PT4-1004, 200 vdc, $\pm 10\%$	19	
Capacitor, PT4-1004, 300 vdc, $\pm 10\%$	49	
Capacitor, PT4-1010, 50 vdc, $\pm 10\%$	6	
Capacitor, PT4-1014, 35 vdc, $\pm 10\%$	1	
Capacitor, Mil-C-11015B, CK06CW___K	8	
Capacitor, Mil-C-11015B, CK05CW___K	1	
Capacitor, Mil-C-26655A, C513AF___K	17	
Diode, PT4-2003, 1N459	23	
Diode, Mil-S-19500/127, 1N756A, Zener	1	
Diode, Mil-S-19500/127, 1N752A, Zener	1	
Diode, Mil-S-19500/127, 1N746A, Zener	2	
Diode, PT4-2039	1	
Transistor, PT4-7034, 2N910	62	
Transistor, PT4-7003, 2N722	7	
Relay, PT2-1005-3 (Iron Fireman)	12	
Transformer, PT6-1009-6, DO-T6 UTC, 4-pin, 10 k $\rightarrow$ 3.6 $\Omega$	1	
Inductor, PT6-1009, DO-T8 UTC	1	
Inductor, PT6-3	14	

<u>PRC Index</u>	<u>Item</u>	<u>Quantity</u>	<u>Remarks</u>
1.12	Tone Decoder (from Schematic and Preliminary Parts List) (Continued)		
	Connector, PT2-5-4, Cannon DCM-37P-NM-4 (Many Pins)	1	
	Connector, PT2-5-8, Cannon DBM-25S-NM-1 (Many Pins)	1	

<u>PRC Index</u>	<u>Item</u>	<u>Quantity</u>	<u>Remarks</u>
1.13	<u>Low-Frequency Timing Assembly, 201441</u>		
	Board Assembly No. 1, 205872	1	See 1.13.1
	Board Assembly No. 2, 205873	1	See 1.13.2
	Board Assembly No. 3, 205874	1	See 1.13.3
	Connector, PT2-5-5	4	
1.13.1	<u>Board Assembly No. 1, Module, 205872</u>		
	Strip Assembly, 205875	1	Mechanical
	Module Assembly, 203153, FF-2	31	See 1.13.1.2
	Module Assembly, 203154, FF-3	11	See 1.13.1.3
	Module Assembly, 202197, IV-2	7	See 1.13.1.4
	Module Assembly, 202250, SC-2	2	See 1.13.1.5
	Module Assembly, 205400, AG-7	1	See 1.13.1.6
	Module Assembly, 205376, 3G-1	1	See 1.13.1.7
	Module Assembly, 205380, JG-3	1	See 1.13.1.8
	Module Assembly, 205382, JG-4	1	See 1.13.1.9
	Module Assembly, 205384, JG-5	2	See 1.13.1.10
	Module Assembly, 205410, LG-4	1	See 1.13.1.11
	Module Assembly, 205412, LG-5	5	See 1.13.1.12
	Module Assembly, 205414, LG-6	31	See 1.13.1.13
1.13.1.2	<u>Module Assembly, 64-kc Toggle Flip-Flop (FF-2), 203153</u>		
	Transistor, PT4-7014	2	
	Transistor, PT4-7059	2	

<u>PRC Index</u>	<u>Item</u>	<u>Quantity</u>	<u>Remarks</u>
1.13.1.2	Module Assembly, 64-kc Toggle Flip-Flop (FF-2), 203153 (Continued)		
	Diode, PT4-2009	5	
	Capacitor, CY10C221J, Mil-C-11272B	2	
	Resistor, PT4-7-C___F, 1/8 w, $\pm 1\%$	1	
1.13.1.3	Module Assembly, 64-kc J-K Flip-Flop (FF-3), 203154		
	Transistor, PT4-7014	2	
	Transistor, PT4-7059	2	
	Diode, PT4-2009	5	
	Capacitor, CY10C221J, Mil-C-11272B	2	
	Resistor, PT4-7-C1872F, 1/8 w, $\pm 1\%$	10	
1.13.1.4	Module Assembly, Logic Inverter (IV-2), 202197		
	Transistor, PT4-7059	6	
	Resistor, PT4-7-C___F, 1/8 w, $\pm 1\%$	9	
1.13.1.5	Module Assembly, Slave Clock (SC-2), 202250		
	Transistor, PT4-7059	2	
	Resistor, PT4-7-C8450F, 1/8 w, $\pm 1\%$	2	
1.13.1.6	Module Assembly, Logic Gate (AG-7), 205400		
	Resistor, PT4-7-C___F, 1/8 w, $\pm 1\%$	8	
	Diode, PT4-2009	20	
1.13.1.7	Module Assembly, Logic Gate (JG-1), 205376		
	Resistor, PT4-7-C___F, 1/8 w, $\pm 1\%$	9	
	Diode, PT4-2009	37	

<u>PRC Index</u>	<u>Item</u>	<u>Quantity</u>	<u>Remarks</u>
1.13.1.8	Module Assembly, Logic Gate (JG-3), 205380 Resistor, PT4-7-C___F, 1/8 w, $\pm 1\%$ Diode, PT4-2009	7 17	
1.13.1.9	Module Assembly, Logic Gate (JG-4), 205382 Resistor, PT4-7-C___F Diode, PT4-2009	4 7	
1.13.1.10	Module Assembly, Logic Gate (JG-5), 205384 Resistor, PT4-7-C___F, 1/8 w, $\pm 1\%$ Diode, PT4-2009	4 13	
1.13.1.11	Module Assembly, Logic Gate (LG-4), 205410 Resistor, PT4-7-C___F, 1/8 w, $\pm 1\%$ Diode, PT4-2009	1 11	
1.13.1.12	Module Assembly, Logic Gate (LG-5), 205412 Resistor, PT4-7-C___F, 1/8 w, $\pm 1\%$ Diode, PT4-2009	1 8	
1.13.1.13	Module Assembly, Logic Gate (LG-6), 205414 Resistor, PT4-7-C___F, 1/8 w, $\pm 1\%$ Diode, PT4-2009	1 5	
1.13.2	Board Assembly No. 2, 205873 Strip Assembly, 205875 Module Assembly, 202202, AM-1	1 3	Mechanical See 1.13.2.2

<u>PRC Index</u>	<u>Item</u>	<u>Quantity</u>	<u>Remarks</u>
1.13.2	Board Assembly No. 2, 205873 (Continued)		
	Module Assembly, 202248, AM-2	3	See 1.13.2.3
	Module Assembly, 206915, BN-1	1	See 1.13.2.4
	Module Assembly, 200263, FF-1	5	See 1.13.2.5
	Module Assembly, 203153, FF-2	22	See 1.13.1.2
	Module Assembly, 203154, FF-3	2	See 1.13.1.3
	Module Assembly, 202250, SC-2	2	See 1.13.1.5
	Module Assembly, 205390, AG-2	2	See 1.13.2.9
	Module Assembly, 205402, AG-8	0	See 1.13.2.10
	Module Assembly, 205382, JG-4	1	See 1.13.1.9
	Module Assembly, 205384, JG-5	1	See 1.13.1.10
	Module Assembly, 205366, KG-2	3	See 1.13.2.13
	Module Assembly, 205408, LG-3	5	See 1.13.2.14
	Module Assembly, 205410, LG-4	1	See 1.13.1.11
	Module Assembly, 205412, LG-5	2	See 1.13.1.12
	Module Assembly, 205414, LG-6	14	See 1.13.1.13
	Module Assembly, 205374, MG-1	5	See 1.13.2.18
	Module Assembly, 205400, AG-7	1	N
	Sensing Assembly, 208779	1	N
1.13.2.2	Module Assembly, Amplifier Driver (AM-1), 202202		
	Resistor, PT4-7-C__F, 1/8 w, ±1%	12	
	Transistor, PT4-7059	6	

<u>PRC Index</u>	<u>Item</u>	<u>Quantity</u>	<u>Remarks</u>
1.13.2.3	<u>Module Assembly, Buffer Amplifier (AM-2), 202248</u>		
	Transistor, PT4-7014	2	
	Transistor, PT4-7059	2	
	Diode, PT4-2009	4	
	Diode, PT4-2010	2	
	Resistor, PT4-7-C___F, 1/8 w, $\pm 1\%$	8	
1.13.2.4	<u>Module Assembly, Bias Network (BN-1), 206915</u>		
	Diode, PT4-2010	36	
	Resistor, PT4-7-C___F, 1/8 w, $1\%$	12	
1.13.2.5	<u>Module Assembly, 256-kc Flip-Flop (FF-1), 200263</u>		
	Capacitor, CY10C___J, Mil-C-11272B	4	
	Diode, PT4-2009	5	
	Resistor, PT4-7-C___F, 1/8 w, $\pm 1\%$	11	
	Transistor, PT4-7014	2	
	Transistor, PT4-7059	2	
1.13.2.9	<u>Module Assembly, Logic Gate (AG-2), 205390</u>		
	Resistor, PT4-7-C___F, 1/8 w, $\pm 1\%$	7	
	Diode, PT4-2009	29	
1.13.2.10	<u>Module Assembly, Logic Gate (AG-8), 205402</u>		
	Resistor, PT4-7-C___F, 1/8 w, $\pm 1\%$	5	
	Diode, PT4-2009	21	

<u>PRC Index</u>	<u>Item</u>	<u>Quantity</u>	<u>Remarks</u>
1.13.2.13	Module Assembly, Logic Gate (KG-2), 205366		
	Resistor, PT4-7-C__F, 1/8 w, $\pm 1\%$	2	
	Diode, PT4-2009	12	
1.13.2.14	Module Assembly, Logic Gate (LG-3), 205408		
	Resistor, PT4-7-C__F, 1/8 w, $\pm 1\%$	2	
	Diode, PT4-2009	11	
1.13.2.18	Module Assembly, Logic Gate (MG-1), 205374		
	Resistor, PT4-7-C__F, 1/8 w, $\pm 1\%$	2	
	Diode, PT4-2009	9	
1.13.3	Board Assembly No. 3, Modular, LFTA, 205874		
	Strip Assembly, 205875-1	1	Mechanical
	Module Assembly, 202199, IV-1	3	See 1.13.3.2
	Module Assembly, 202202, AM-1	9	See 1.13.2.2
	Module Assembly, 202248, AM-2	2	See 1.13.2.3
	Module Assembly, 205368, KG-3	2	See 1.13.3.5
	Module Assembly, 205394, AG-4	8	See 1.13.3.6
	Module Assembly, 205400, AG-7	1	See 1.13.1.6
	Module Assembly, 203154, FF-3	6	See 1.13.1.3
	Module Assembly, 202250, SC-2	1	See 1.13.1.5
	Module Assembly, 205382, JG-4	4	See 1.13.1.9
	Module Assembly, 205384, JG-5	2	See 1.13.1.10
	Thermistor, PT4-1-2	5	



<u>PRC Index</u>	<u>Item</u>	<u>Quantity</u>	<u>Remarks</u>
1.13.3.2	Module Assembly, Inverting Driver (IV-1), 202199		
	Transistor, PT4-7014	2	
	Transistor, PT4-7059	2	
	Resistor, PT4-7-C__F, 1/8 w, $\pm 1\%$	10	
1.13.3.5	Module Assembly, Logic Gate (KG-3), 205368		
	Resistor, PT4-7-C__F, 1/8 w, $\pm 1\%$	3	
	Diode, PT4-2009	8	
1.13.3.6	Module Assembly, Logic Gate (AG-4), 205394		
	Resistor, PT4-7-C__F, 1/8 w, $\pm 1\%$	11	
	Diode, PT4-2009	27	

<u>PRC Index</u>	<u>Item</u>	<u>Quantity</u>	<u>Remarks</u>
1.14	<u>Tape Recorder (from RCA Design Review)</u>		
	Record Elements	1	See 1.14.1
	Common Elements	1	See 1.14.2
	Playback Elements	1	See 1.14.3
1.14.1	<u>Record Elements</u>		
	OCW Controls, R-1	1	See 1.14.1.1
	OEW End of Tape, R-2	1	See 1.14.1.2
	OMR Record Motor, Hysteresis 28 v, 400 cps, Synchronous, 8000 rpm	1	Vendor: MAR
	OAW Record Amplifier and Logic, R-5	1	See 1.14.1.4
	DW-309 Record Head, R-6, 9-Coil	1	
1.14.1.1	<u>OCW Controls, R-1</u>		
	Resistor, Film, $\pm 1\%$ , 1/8 w	4	
	Capacitor, Dry Tantalum, 39 mf, 35 v, $\pm 10\%$ , Sprague	4	
1.14.1.2	<u>OEW End of Tape, R-2</u>		
	Diode, 1N1126A, TI	1	
	Resistor, $\pm 1\%$ , 1/8 w	2	
	Switch, Micro, 7 amps, Vendor: MIN	2	
1.14.1.4	<u>OAW Record Amplifier and Logic</u>		
	4-Input NOR Gate	1	See 1.14.1.4.1
	2-Input NOR Gate	4	See 1.14.1.4.2
	Write Amplifier and Logic	1	See 1.14.1.4.3
	Line Receiver	4	See 1.14.1.4.4

<u>PRC Index</u>	<u>Item</u>	<u>Quantity</u>	<u>Remarks</u>
1.14.1.4.1	<u>4-Input NOR Gate</u>		
	Capacitor, Mica, 51 mmf, 500 v, $\pm 5\%$ , EMM	5	
	Resistor, Film, $\pm 1\%$ , 1/8 w	9	
	Transistor, 2N708, FA	4	
1.14.1.4.2	<u>2-Input NOR Gate</u>		
	Capacitor, Mica, 51 mmf, 500 v, $\pm 5\%$	2	
	Resistor, Film 1/8 w, $\pm 1\%$	5	
	Transistor, 2N708, FA	2	
1.14.1.4.3	<u>Write Amplifier and Logic</u>		
	Emitter Follower	1	See 1.14.1.4.3.1
	Write Amplifier Switch	1	See 1.14.1.4.3.2
	Standard Inverter	3	See 1.14.1.4.3.3
	Write Amplifier	9	See 1.14.1.4.3.4
1.14.1.4.3.1	<u>Emitter Follower</u>		
	Diode, 1N658, FA	1	
	Transistor, 2N708, FA	1	
	Resistor, Film, 1/8 w, $\pm 1\%$	1	
1.14.1.4.3.2	<u>Write Amplifier Switch</u>		
	Resistor, Film, 1/8 w, $\pm 1\%$	4	
	Transistor, 2N708, FA	1	
	Transistor, 2N722, FA	1	
	Diode, 1N658, FA	1	

<u>PRC Index</u>	<u>Item</u>	<u>Quantity</u>	<u>Remarks</u>
1.14.1.4.3.3	<u>Standard Inverter</u>		
	Capacitor, Mica, 120 mmf, 500 v, $\pm 2\%$	1	
	Transistor, 2N708	1	
	Resistor, Film, 1/8 w, $\pm 1\%$	3	
1.14.1.4.3.4	<u>Write Amplifier</u>		
	Diode, 1N658	2	
	Resistor, Film, 1/8 w, $\pm 1\%$	5	
	Transistor, 2N708	2	
1.14.1.4.4	<u>Line Receiver</u>		
	Capacitor, Mica, 51 mmf, 500 v, $\pm 5\%$ , ENIM	1	
	Resistor, Film, 1/8 w, $\pm 1\%$	4	
	Transistor, 2N708	1	
1.14.2	<u>Common Elements</u>		
	OL Logic, C-1	1	See 1.14.2.1
	OD D.C. Converter, C-2	1	See 1.14.2.2
	OV Overload Protection, C-3	1	See 1.14.2.3
	OI Motor Inverter, C-4	1	See 1.14.2.4
	ON Enclosure Connector, C-5, 41-pin Connector	2	DTK07H-20-41P-Deutsch
	OF Time Delay, C-6	1	See 1.14.2.6
	OS Servo, C-7	1	See 1.14.2.7
1.14.2.1	<u>Logic, C-1</u>		
	Standard Flip-Flop	13	See 1.14.2.1.1
	NAND Gate	2	See 1.14.2.1.2

<u>PRC Index</u>	<u>Item</u>	<u>Quantity</u>	<u>Remarks</u>
1.14.2.1.1	Standard Flip-Flop		
	Transistor, 2N708, FA	9	
	Capacitor, Mica, 500 v, $\pm 2\%$	5	
	Diode, 1N658, FA	2	
	Resistor, Film, 1/8 w, $\pm 1\%$	17	
1.14.2.1.2	NAND Gate		
	Capacitor, Mica, 500 v, $\pm 5\%$	2	
	Resistor, Film, 1/8 w, $\pm 1\%$	4	
	Resistor, Film, 1/4 w, $\pm 1\%$	1	
	Transistor, 2N708	2	
54 1.14.2.2	D.C. Converter, C-2		
	Capacitor, Mica, 300 v, $\pm 5\%$ , EMM	3	
	Capacitor, Mica 500 v, $\pm 5\%$ , EMM	3	
	Capacitor, Dry Tantalum, 35 v, $\pm 10\%$ , Sprague	17	
	Diode, 1N485B, FA	3	
	Diode, 1N1126A, TI	4	
	Diode, 1N3016B, MOT	2	
	Relay, SL110C, P and B	1	
	Resistor, Film, 1/8 w, $\pm 1\%$	13	
	Resistor, Film, 1/2 w, $\pm 1\%$	5	
	Resistor, Film, 1 w, $\pm 1\%$	6	
	Resistor, Film, 1/4 w, $\pm 1\%$	3	
	Resistor, Variable, Wirewound, .8 v, $\pm 10\%$ , Bourns	2	

<u>PRC Index</u>	<u>Item</u>	<u>Quantity</u>	<u>Remarks</u>
1.14.2.2	<u>D.C. Converter, C-2 (Continued)</u>		
	Transformer, INT	1	
	Transistor, 2N708, FA	4	
	Transistor, 2N697, FA	2	
	Transistor, 2N1016B, WST	4	
	Transistor, 2N722, FA	2	
	Transistor, 2N1132, FA	1	
	Transistor, 2N174A, FA	2	
1.14.2.3	<u>Overload Protection C-3</u>		
	Capacitor, Dry Tantalum, 35 v, $\pm 10\%$ , Sprague	4	
	Relay, Signal Type	1	
	Relay, SL1DC-24, P and B	1	
	Resistor, Wirewound 1/2 w, $\pm 1\%$	1	
	Resistor, Film 1/8 w, $\pm 1\%$	4	
1.14.2.4	<u>Motor Inverter, C-4</u>		
	Resistor, Wirewound	3	
	Resistor, Film, 1/4 w, $\pm 1\%$	2	
	Transformer, TOR	2	
	Transformer, Toroidal, TOR	2	
	Transistor, 2N697	2	
	Transistor, 2N1011	5	
	Transistor, 2N1514	1	
	Diode, Zener, 1N3028	1	

<u>PRC Index</u>	<u>Item</u>	<u>Quantity</u>	<u>Remarks</u>
1.14.2.5	<u>Time Delay, C-6</u>		
	Resistor, Film, 1/8 w	6	
	Resistor, Film, 1/4 w	1	
	Resistor, Film, 1/2 w	1	
	Resistor, Film, 1 w	1	
	Transistor, 2N708	2	
	Transistor, 2N697	1	
	Diode, Zener, IN756A	1	
	Capacitor, Solid Tantalum, 35 v	5	
1.14.2.7	<u>Servo, C-7</u>		
	Resistor, Film, 1/8 w	15	
	Resistor, Film, 1/4 w	2	
	Transistor, 2N708	6	
	Capacitor, Solid Tantalum, 35 v	1	
	Capacitor, Mica, 300 v	1	
1.14.3	<u>Playback Elements</u>		
	OCR Controls, P-1	1	See 1.14.1.1
	OER End of Tape, P-2	1	See 1.14.1.2
	ESR Servo, P-3	1	See 1.14.3.3
	OMR Playback Motor, P-4, Hysteresis 28 v, 400 cps, Synchronous, 6000 rpm	1	
	OAR Read Amplifier and Logic, P-5	1	See 1.14.3.5
	DR-259 Playback Head, P-6, 9-coil	1	

<u>PRC Index</u>	<u>Item</u>	<u>Quantity</u>	<u>Remarks</u>
1.14.3.3	Servo, P-3		
	Resistor, Film, 1/8 w	60	
	Resistor, Film, 1/4 w	5	
	Resistor, Film, 1/2 w	1	
	Resistor, Variable, .8 w	1	
	Capacitor, Mica, 100 vdc	2	
	Capacitor, Mica, 500 vdc	7	
	Capacitor, Cerafil, 100 vdc	7	
	Capacitor, Solid Tantalum, 35 vdc	6	
	Capacitor, Solid Tantalum, 20 vdc	2	
	Diode, 1N485B	5	
	Diode, 1N658B	2	
	Transistor, 2N708	14	
1.14.3.5	Read Amplifier and Logic, P-5		
	2-Input NOR Gate	1	See 1.14.1.4.2
	3-Input NOR Gate	1	See 1.14.3.5.2
	4-Input NOR Gate	1	See 1.14.1.4.1
	Hybrid Gate No. 1	1	See 1.14.3.5.4
	Hybrid Gate No. 2	1	See 1.14.3.5.4
	Hybrid Gate No. 3	1	See 1.14.3.5.6
	Phase Detector	1	See 1.14.3.5.7
	Line Driver	1	See 1.14.3.5.8



<u>PRC Index</u>	<u>Item</u>	<u>Quantity</u>	<u>Remarks</u>
1.14.3.5	Read Amplifier and Logic, P-5 (Continued)		
	Standard Flip-Flop	7	See 1.14.2.1.1
	Oscillator	1	See 1.14.3.5.10
	Standard Inverter	3	See 1.14.1.4.3.1
	Buffer	1	See 1.14.3.5.12
	Emitter Follower	1	See 1.14.1.4.3.1
	Read Amplifier	9	See 1.14.3.5.14
1.14.3.5.2	Three-Input NOR Gate		
	Capacitor, Mica, 500 v, $\pm 5\%$ , EMM	3	
	Resistor, Film, 1/8 w, $\pm 1\%$	7	
	Transistor, 2N708, FA	3	
1.14.3.5.4	Hybrid Gate No. 1		
	Capacitor, Mica, 500 v, $\pm 5\%$	7	
	Resistor, Film, 1/8 w, $\pm 1\%$	15	
	Transistor, 2N708	7	
1.14.3.5.6	Hybrid Gate No. 3		
	Capacitor, Mica, 500 v, $\pm 5\%$	4	
	Resistor, Film, 1/8 w, $\pm 1\%$	9	
	Transistor, 2N708	4	

<u>PRC Index</u>	<u>Item</u>	<u>Quantity</u>	<u>Remarks</u>
1.14.3.5.7	<u>Phase Detector</u>		
	Resistor, Film, 1/8 w, $\pm 1\%$	24	
	Transistor, 2N722, FA	1	
	Transistor, 2N697, FA	1	
	Transistor, 2N708, FA	1	
	Varicap, PAC		
	Pot, Wirewound, .8 w, $\pm 10\%$ , Bourns	1	
	Diode, 1N65B	3	
	Capacitor, Cerafil, 100 v, $\pm 20\%$	3	
	Capacitor, Mica, 300 v, $\pm 2\%$	1	
	Capacitor, Dry Tantalum, 35 v, $\pm 10\%$	3	
1.14.3.5.8	<u>Line Driver</u>		
	Capacitor, Mica, 500 v, $\pm 5\%$ EMM	1	
	Diode, 1N658, FA	1	
	Resistor, Film, 1/8 w, $\pm 1\%$	3	
	Transistor, 2N708, FA	2	
1.14.3.5.10	<u>Oscillator</u>		
	Capacitor, Mica, 500 v, $\pm 2\%$ ELM	3	
	Capacitor, Dry Tantalum, 35 v, $\pm 10\%$ , Sprague	1	
	Capacitor, Cerafil, 100 v, $\pm 20\%$ AEK	2	
	Trimmer, Glass, 1000 v, JFD	1	
	Resistor, Film, 1/8 w, $\pm 1\%$	11	
	Transistor, 2N708, FA	3	

<u>PRC Index</u>	<u>Item</u>	<u>Quantity</u>	<u>Remarks</u>
1.14.3.5.12	<u>Buffer</u>		
	Capacitor, Dry Tantalum, 35 v, $\pm 10\%$ , Sprague	4	
	Resistor, Film 1/8 w, $\pm 1\%$	11	
	Transistor, 2N697, FA	2	
1.14.3.5.14	<u>(Read Amplifier)</u>		
	Capacitor, Cerafil, 100 v, $\pm 20\%$ , AER	4	
	Capacitor, Dry Tantalum, 35 v, $\pm 10\%$ , Sprague	1	
	Resistor, Film, 1/8 w, 1%, (IRC)	14	
	Pot, Wirewound, .8 w, $\pm 10\%$ , Bourns	1	
	Transistor, 2N708, FA	5	

<u>PRC Index</u>	<u>Item</u>	<u>Quantity</u>	<u>Remarks</u>
1.15	<u>Special-Purpose Telemetry DHU, 202650</u>		
	Module Board Assembly, 203354	1	See 1.15.1
1.15.1	<u>Module Board Assembly, 203354</u>		
	<u>(from Schematic 202963)</u>		
	Connector, 6-pin	1	
	Connector, 50-pin	1	
	Diodes, IN485B	9	
	Diodes, 1N757A, Selected	2	
	Resistors, 1/8 w, 1%, Various Values	52	
	Resistors, 1/4 w, 5%, Various Values	10	
	R.T., 1.2 k, 5%	1	
	Capacitors, 35 v, Various Values, $\pm 10\%$	21	
	Transistors, 2N910	9	
	Transistors, 2N834	2	
	Transistors, 2N722	1	

<u>PRC Index</u>	<u>Item</u>	<u>Quantity</u>	<u>Remarks</u>
1.16	<u>Command Distribution Unit, 201529</u>		
	Connector, PT2-5-10	1	
	Connector, PT2-5-5	1	
	Connector, PT2-5-4	1	
	Connector, PT2-5-9	1	
	Connector, PT2-5-3	1	
	Connector, PT2-5-8	12	
	Relay, Non-Latching, PT2-1008	1	
	Diode Board Assembly, 203423-1	1	See 1.16.8
	Interharness Matrix, 201623-1	1	See 1.16.9
	Matrix Driver, 202035-1	16	See 1.16.10
	Relay Driver, 201749-1	1	See 1.16.11
	Relay Module 10, 201539-1	1	See 1.16.12
	Relay Module 8, 201538-1	1	See 1.16.13
	Relay Modules 6 and 9, 201537-1	2	See 1.16.14
	Relay Module 5, 201536-1	1	See 1.16.15
	Relay Modules 3, 4, and 7, 201535-1	3	See 1.16.16
	Relay Module 2B, 201534-1	1	See 1.16.17
	Relay Module 2A, 201533-1	1	See 1.16.18
	Relay Module 1B, 201532-1	1	See 1.16.19
	Relay Module 1A, 201531-1	1	See 1.16.20

<u>PRC Index</u>	<u>Item</u>	<u>Quantity</u>	<u>Remarks</u>
1.16.8	Diode Board Assembly (1), 203423		
	Diode, 1N270	1	
	Diode, 1N647	9	
	Resistor, 2.8 k, 1/8 w, 1%, Mil-R-10509, RN60G2801F	1	
1.16.9	Interharness Matrix, 201623		
	Matrix Subassembly 1, 201624-1	4	Mechanical
	Matrix Subassembly 2, 201627-1	1	Mechanical
	Matrix Subassembly 3, 203049-1	1	Mechanical
1.16.10	Matrix Driver, 202035		
	Diode, PT4-2027	2	
	Diode, PT4-2001	3	
	Resistor, RN60G46R4F, Mil-R-10509D	2	
	Capacitor, CK06CW103K, Mil-C-11015B	2	
1.16.11	Relay Driver, 201799		
	Transistor, 2N718A	2	
	Diode, 1N647	1	
	Terminal, Silver Plated, Subminiaturized, 5010A, Lerco	4	
	Resistor, RN60G, 100 k, 1/8 w, 1%, Mil-R-10509D	1	
	Diode, 1N749A, 4.3 v Zener, Mil-S-195C0	1	
	Resistor, 215 k, 1/8 w, 1%, RN60G, Mil-R-10509D	1	

<u>PRC Index</u>	<u>Item</u>	<u>Quantity</u>	<u>Remarks</u>
1.16.12	Relay Module 10, 201539		
	Terminal Board No. 1, 206990-1	1	See 1.16.12.1
	Terminal Board No. 2, 203526-1	1	See 1.16.12.2
	Board Assembly, TB3, 202873-1	1	See 1.16.12.3
	Board Assembly TB4, 202874-1	1	See 1.16.12.4
	Relay, Latching, PT2-1011	10	
	Relay, Non-Latching, PT2-1008	1	
	Timer Oscillator, PT2-1020	1	
	Timer Record Counter, PT2-1021	3	
	Timer Relay Driver, PT2-1022	1	
	Connector, PT2-5-8	1	
	Connector, PT2-5-3	1	
	Diode, 1N916, PT4-2012	2	
	Diode, 1N647, PT4-2001	2	
1.16.12.1	Terminal Board No. 1, 206990		
	Terminal Board, 203525 (PCB)	1	
	Diode, 1N647, PT4-2001	1	
1.16.12.2	Terminal Board No. 2, 203526		
	Terminal Board, 203526-2 (PCB)	1	
	Terminal, 590310-6, Split Lug	5	
	Terminal, 590310-2, Split Lug	43	

<u>PRC Index</u>	<u>Item</u>	<u>Quantity</u>	<u>Remarks</u>
1.16.12.3	Board Assembly, TB3, 202873	1	
	Terminal Board, 201451 (PCB)		
	Diode, 1N647, PT4-2001	16	
1.16.12.4	Board Assembly, TB4, 202874	1	
	Terminal Board, 201451 (PCB)		
	Diode, 2N647, PT4-2001	5	
1.16.13	Relay Module 8, 201538		
	Terminal Board No. 1, 203521-1	1	See 1.16.13.1
	Terminal Board No. 2, 203484-1	1	See 1.16.13.2
	Board Assembly TB3, 202513-1	1	See 1.16.13.3
	Board Assembly TB4, 202512-1	1	See 1.16.13.4
	Relay, Latching, PT2-1011, DPDT 2A	2	
	Relay, Non-Latching, PT2-1008, DPDT 2A	14	
	Connector, PT2-5-3	1	
	Connector, PT2-5-10	1	
1.16.13.1	Terminal Board No. 1, 203521		
	Terminal Board 203521-2 (PCB)	1	
	Terminal, 590310-2, Split Lug	8	
	Terminal, 590310-6, Split Lug	24	
1.16.13.2	Terminal Board No. 2, 203484		
	Terminal Board, 203484-2 (PCB)	1	
	Terminal, 590310-2	2	
	Terminal, 590310-6	34	



<u>PRC Index</u>	<u>Item</u>	<u>Quantity</u>	<u>Remarks</u>
1.16.13.3	<u>Board Assembly, TB3, 202513</u> Terminal Board, 201451-1 (PCB) Diode, 1N647, PT4-2001	1 8	
1.16.13.4	<u>Board Assembly, TB4, 202512</u> Terminal Board, 201451-2 (PCB) Diode, 1N647, PT4-2001	1 10	
1.16.14	<u>Relay Modules 6 and 9, 201537</u> Terminal Board No. 1, 203521-1 Terminal Board No. 2, 203522-1 Board Assembly TB3, 202378-1 Board Assembly TB4, 202379-1 Relay, Non-Latching, PT2-1008 Connector, PT2-5-3 Connector, PT2-5-10	1 1 1 1 1 16 1 1	See 1.16.13.1 See 1.16.14.2 See 1.16.14.3 See 1.16.14.4
1.16.14.2	<u>Terminal Board No. 2, 203522</u> Terminal Board, 203522-2 (PCB) Terminal, 590310-2, Split Lug Terminal, 590310-6, Split Lug	1 7 25	
1.16.14.3	<u>Board Assembly, TB3, 202378</u> Terminal Board, 201451-1 (PCB) Diode, 1N647, PT4-2001	1 8	

<u>PRC Index</u>	<u>Item</u>	<u>Quantity</u>	<u>Remarks</u>
1.16.14.4	Board Assembly, TB4, 202379		
	Terminal Board, 201451-2 (PCB)	1	
	Diode, 1N647, PT4-2001	8	
1.16.15	Relay Module 5, 201536		
	Board Assembly TB1, 203852	1	See 1.16.15.1
	Board Assembly TB2, 203853	1	See 1.16.15.2
	Board Assembly TB3, 203181-1	1	See 1.16.15.3
	Board Assembly TB4, 203180-1	1	See 1.16.15.4
	Data Logic, 203506-1	1	See 1.16.15.5
	Relay, Latching, PT2-1011	15	
	Connector, PT2-5-4	1	
	Connector, PT2-5-10	1	
1.16.15.1	Board Assembly, TB1, Relay Module 5, 203852		
	Terminal Board, 203519-1	1	
	Diode, PT4-2001, 1N647	2	
	Diode, Mil-S-19500/200, 1N720	1	
	Resistor, RN60G__F, Mil-R-10509D	2	
	Resistor, RC20GF__J, Mil-R-11/3	1	
1.16.15.2	Board Assembly, TB2, Relay Module 5, 203853		
	Terminal Board, 203520	1	
	Diode, PT4-2001, 1N647	1	
	Resistor, RN60G__F, Mil-R-10509D	1	
	Capacitor, CS13AG__M, Mil-C-26655	1	

<u>PRC Index</u>	<u>Item</u>	<u>Quantity</u>	<u>Remarks</u>
1.16.15.3	<u>Board Assembly, TB3, Relay Module 5, 203181</u> Terminal Board, 201451 Diode, PT4-2001, 1N647	1 19	
1.16.15.4	<u>Board Assembly, TB4, Relay Module 5, 203180</u> Terminal Board, 207077 Diode, PT4-2001	1 32	
1.16.15.5	<u>Data Logic, 203506</u> Resistor, RC07GF__J, Mil-R-11 Resistor, RC20GF__J, Mil-R-11 Transistor, PT4-7004, 2N718A Diode, PT4-2001, 1N647	5 1 2 14	
1.16.16	<u>Relay Modules 3, 4, and 7, 201535</u> Terminal Board No. 1, 203517-1 Terminal Board No. 2, 203518-1 Board Assembly TB3, 202389-1 Board Assembly TB4, 202388-1 Relay, Latching, 2PDT 2A, PT2-1011 Connector, PT2-5-3 Connector, PT2-5-10	1 1 1 1 16 1 1	See 1.16.16.1 See 1.16.16.2 See 1.16.16.3 See 1.16.16.4
1.16.16.1	<u>Terminal Board No. 1, 203517</u> Terminal Board, 203517-2 (PCB) Terminal, 590310-2, Split Lug Terminal, 590310-6, Split Lug	1 11 30	

<u>PRC Index</u>	<u>Item</u>	<u>Quantity</u>	<u>Remarks</u>
1.16.16.2	Terminal Board No. 2, 203518		
	Terminal Board, 203518-2 (PCB)	1	
	Terminal, 590310-2, Split Lug	11	
	Terminal, 590310-6, Split Lug	30	
1.16.16.3	Board Assembly, TB3, 202389		
	Terminal Board, 201451-1 (PCB)	1	
	Diode, 1N647, PT4-2001	16	
1.16.16.4	Board Assembly, TB4, 202388		
	Terminal Board, 201451-2 (PCB)	1	
	Diode, 1N647, PT4-2001	16	
1.16.17	Relay Module 2B, 201534		
	Terminal Board No. 1, 203515-1	1	See 1.16.17.1
	Terminal Board No. 2, 203516-1	1	See 1.16.17.2
	Board Assembly TB3, 202922-1	1	See 1.16.17.3
	Board Assembly TB4, 202923-1	1	See 1.16.17.4
	Relay, Latching, PT2-1011	10	
	Relay, Non-Latching, PT2-1008	3	
	Connector, PT2-5-3	1	
	Connector, QT2-5-10	1	
1.16.17.1	Terminal Board No. 1, 203515		
	Terminal Board, 203515-2 (PCB)	1	
	Terminal, 590310-2, Split Lug	9	
	Terminal, 590310-6, Split Lug	31	

<u>PRC Index</u>	<u>Item</u>	<u>Quantity</u>	<u>Remarks</u>
1.16.17.2	<u>Terminal Board No. 2, 203516</u>		
	Board Detail, 203516-2 (PCB), Mil-P-13949	1	
	Terminal, SP0013-2, Split Lug	11	
	Terminal, SP0013-6, Split Lug	24	
1.16.17.3	<u>Board Assembly, TB3, 202922</u>		
	Terminal Board, 201451-1 (PCB)	1	
	Diode, 1N647, PT4-2001	16	
1.16.17.4	<u>Board Assembly, TB4, 202923</u>		
	Terminal Board, 201451-2 (PCB)	1	
	Diode, 1N647, PT4-2001	12	
1.16.18	<u>Relay Module 2A, 201533</u>		
	Board Assembly TB1, 204203-1	1	See 1.16.18.1
	Board Assembly TB2, 204204-1	1	See 1.16.18.2
	Time Delay Unit, 516002-1	3	
	Relay, Latching, PT2-1011	4	
	Relay, Non-Latching, PT2-1008	2	
	Relay, Latching, PT2-1001	3	
	Relay, Non-Latching, PT2-1000	2	
	Connector, PT2-5-3	1	
	Connector, PT2-5-10	1	

<u>PRC Index</u>	<u>Item</u>	<u>Quantity</u>	<u>Remarks</u>
1.16.18.1	Board Assembly, TB1, 204203		
	Terminal Board, 203513-1 (PCB)	1	
	Diode, 1N647, PT4-2001	7	
	Resistor, Mil-R-105090, RN60G__F	8	
	Resistor, Mil-R-26, RW59V1R0	3	
	Diode, 1N968B, Mil-S-19500/117	1	
	Diode, 1N970B, Mil-S-19500/117	1	
	Diode, 1N969B, Mil-S-19500/117	1	
	Diode, 1N916, PT4-2012	3	
1.16.18.2	Board Assembly, TB2, 204204		
	Terminal Board, 203514-1 (PCB)	1	
	Diode, 1N647, PT4-2001	12	
	Diode, 1N916, PT4-2012	1	
	Diode, 1N971B, Mil-S-19500/117	1	
	Resistor, RN60G__F, Mil-R-10509D	4	
	Capacitor, CS13AG010K, Mil-C-26655	3	
1.16.19	Relay Module 1B, 201532		
	Board Assembly TB1, 204201-1	1	See 1.16.19.1
	Board Assembly TB2, 204202-1	1	See 1.16.19.2
	Board Assembly TB3, 202924-1	1	See 1.16.19.3
	Board Assembly TB4, 202925-1	1	See 1.16.19.4
	Undervoltage Sensor, 202672-1	1	See 1.16.19.5

<u>PRC Index</u>	<u>Item</u>	<u>Quantity</u>	<u>Remarks</u>
1.16.19	<u>Relay Module 1B, 201532 (Continued)</u>		
	Time Delay Unit, 516002-1	1	
	Relay, Latching, PT2-1011	10	
	Relay, Non-Latching, PT2-1008	4	
	Connector, PT2-5-4	1	
	Connector, PT2-5-8	1	
1.16.19.1	<u>Board Assembly, TB1, 204201</u>		
	Terminal Board, 203511-1 (PCB)	1	
	Diode, 1N647, PT4-2001	2	
	Capacitor, CS13AG010K, Mil-C-26655	1	
1.16.19.2	<u>Board Assembly, TB2, 204202</u>		
	Terminal Board, 203512-1 (PCB)	1	
	Diode, 1N647, PT4-2001	4	
	Resistor, 1.5 k to 2.5 k, 1/8 w, Mil-R-105090	1	
1.16.19.3	<u>Board Assembly, TB3, 202924</u>		
	Terminal Board, 201451-1 (PCB)	1	
	Diode, 1N647, PT4-2001	14	
	Resistor, RN60G9093F, Mil-R-10509D	1	
1.16.19.4	<u>Board Assembly, TB4, 202925</u>		
	Terminal Board, 201451-2 (PCB)	1	
	Diode, 1N647, PT4-2001	11	

<u>PRC Index</u>	<u>Item</u>	<u>Quantity</u>	<u>Remarks</u>
1.16.19.5	<u>Undervoltage Sensor, 202672</u>		
	Printed Circuit Board, Mil-P-18177	4	
	Sensistor, PT4-16-102K	1	
	Resistor, Mil-R-10509, RN60G__F	2	
	Resistor, PT4-8-1, 1/8 w, ±1%	1	
	Capacitor, Mil-C-26655, CS13AF__K	1	
	Capacitor, Mil-C-11015/18, CK05CW__K	1	
	Capacitor, PT4-1012, 35 v, ±10%	1	
	Diode, Zener, Mil-S-19500/127, 1N759H	2	
	Capacitor, Zener, Mil-S-19500/127, 1N755H	1	
	Diode, Silicon, PT4-2001	1	
	Rectifier, Silicon, 2N887, PT4-7061	1	
	Transistor, Unijunction, PT4-7060, 2N492	1	
	Transistor, Silicon, NPN, PT4-7001, 2N720H	1	
1.16.20	<u>Relay Module 1A, 201531</u>		
	Board Assembly TB1, 204197-1	1	See 1.16.20.1
	Board Assembly TB2, 204198-1	1	See 1.16.20.2
	Board Assembly TB3, 203179-1	1	See 1.16.20.3
	Board Assembly TB4, 203178-1	1	See 1.16.20.4
	Timer Relay Driver, 303-4021, General Time 24733	1	
	Timer Decode Counter, 308-4022, General Time 24733	1	
	Relay, Latching, PT2-1011	11	
	Relay, Non-Latching, PT2-1008	2	



<u>PRC Index</u>	<u>Item</u>	<u>Quantity</u>	<u>Remarks</u>
	<u>Relay Module 1A, 201531 (Continued)</u>		
	Timer Oscillator, 308-4023, General Time 24733	1	
	Connector, PT2-5-4	1	
	Connector, PT2-5-10	1	
1.16.20.1	<u>Board Assembly, TB1, 204197</u>		
	Terminal Board, 203509-1 (PCB)	1	
	Diode, 1N647, PT4-2001	4	
	Resistor, RN60G1001F, Mil-R-10509D	1	
1.16.20.2	<u>Board Assembly, TB2, 204198</u>		
	Terminal Board, 203510-1 (PCB)	1	
	Diode, 1N647, PT4-2001	6	
	Resistor, RN60G1002F, Mil-R-10509D	2	
	Capacitor, CS13AG220M, Mil-C-26655	4	
1.16.20.3	<u>Board Assembly, TB3, 203179</u>		
	Terminal Board, 204199-1 (PCB)	1	
	Diode, 1N647, PT4-2001	21	
1.16.20.4	<u>Board Assembly, TB4, 203178</u>		
	Terminal Board, 204200-1 (PCB)	1	
	Diode, 1N647, PT4-2001	18	

<u>PRC Index</u>	<u>Item</u>	<u>Quantity</u>	<u>Remarks</u>
1.17	Signal Conditioner, 201738		
	Z1 Module, 204076	4	See 1.17.1
	Z2 Module, 204183	1	See 1.17.2
	Z3 Module, 204184	1	See 1.17.3
	Connector, PT2-5-10, 50-pin, 0 spares, 8 spares, 8 spares	3	
	Connector, PT2-5-9, 37-pin, 5 spares, 12 spares	2	
	Connector, PT2-5-8, 25-pin, 2 spares, 7 spares, 9 spares	3	
	Connector, PT2-5-7, 15-pin, 1 spare	1	
	Connector, PT2-5-6, 9-pin, 2 spares	1	
1.17.1	Z1 Module (from 201754, Signal Conditioner Schematic)		
	Resistor, 1/8 w, 1%, 5.11 k	10	
	Resistor, 1/8 w, 1%, 13 k	10	
1.17.2	Z2 Module (from 201754)		
	Resistor, 1/8 w, 1%, 8.06 k	5	
	Resistor, 1/8 w, 1%, 4.02 k	5	
	Resistor, 1/8 w, 1%, 2 k	5	
	Resistor, 1/8 w, 1%, 1 k	6	
	Capacitor, 2.2 $\mu$ f, $\pm 10\%$ , 20 v	7	

<u>PRC Index</u>	<u>Item</u>	<u>Quantity</u>	<u>Remarks</u>
1.17.3	Z3 Module (from 201754)	12	
	Resistor, 4.02 k, .5%, 1/8 w	1	
	Resistor, 2 k, 1/8 w, 1%	4	
	Resistor, 13 k, 1/8 w, 1%	4	
	Resistor, 5.11 k, 1/8 w, 1%	1	
	Resistor, 100 k, 1/8 w, 1%	1	
	Resistor, 45.3 k, 1/8 w, 1%	1	
	Resistor, 40.2 k, 1/8 w, 1%	1	
	Resistor, 19.6 k, 1/8 w, 1%	1	
	Diodes, 1N759	Z	

<u>PRC Index</u>	<u>Item</u>	<u>Quantity</u>	<u>Remarks</u>
1.18	<u>Digital Data Handling Assembly, 201348</u>		
	Board Assembly No. 1, 205866	1	See 1.18.1
	Board Assembly No. 2, 205867	1	See 1.18.2
	Board Assembly No. 3, 205868	1	See 1.18.3
	Board Assembly No. 4, 205869	1	See 1.18.4
	Board Assembly No. 5, 205871	1	See 1.18.5
	Connector, PT2-5-5	13	
1.18.1	<u>Board Assembly No. 1, 205866</u>		
	Strip Assembly, 205876	1	Mechanical
	Module Assembly, 202204, AM-5	15	See 1.18.1.1
	Module Assembly, 202256, NE-1	2	See 1.18.1.2
	Module Assembly, 202254, NE-2	1	See 1.18.1.3
	Module Assembly, 203138, GM-1	1	See 1.18.1.4
	Module Assembly, 203155, GM-2	1	See 1.18.1.5
	Module Assembly, 202240, TG-1	10	See 1.18.1.6
	Thermistors, PT4-1-2	5	
1.18.1.1	<u>Module Assembly, Matrix Line Driver (AM-5), 202204</u>		
	Capacitor, CY10C___J, Mil-C-11272B	6	
	Resistor, PT4-7-C___F, 1/8 w, ±1%	16	
	Diode, PT4-2009	12	
	Transistor, PT4-7014	4	
	Transistor, PT4-7059	4	
1.18.1.2	<u>Module Assembly, NAND Element (NE-1), 202256</u>		
	Transistor, PT4-7059	16	

<u>PRC Index</u>	<u>Item</u>	<u>Quantity</u>	<u>Remarks</u>
1.18.1.3	Module Assembly, NAND Element (NE-2), 202254 Transistor, PT4-7059	16	
1.18.1.4	Module Assembly, Matrix Gate (GM-1), 203138 Diode, PT4-2009 Resistor, PT4-7-C___F, 1/8 w, $\pm 1\%$	72 15	
1.18.1.5	Module Assembly, Matrix Gate (GM-2), 203155 Transistor, PT4-7059 Resistor, PT4-7-C___F, 1/8 w, $\pm 1\%$	9 19	
1.18.1.6	Module Assembly, Transmission Gate (TG-1), 202240 Resistor, PT4-7-C___F, 1/8 w, $\pm 1\%$ Diode, PT4-2009 Transistor, PT4-7074	17 24 4	
1.18.2	Board Assembly No. 2, 205867 Strip Assembly, 205876 Module Assembly, 202204, AM-5 Module Assembly, 206915, BN-1 Module Assembly, 203138, GM-1 Module Assembly, 203155, GM-2 Module Assembly, 202256, NE-1 Module Assembly, 202199, IV-1 Module Assembly, 202250, SC-2 Module Assembly, 202202, AM-1	1 7 1 1 1 2 1 1 1 3	Mechanical See 1.18.1.1 See 1.13.2.4 See 1.18.1.4 See 1.18.1.5 See 1.18.1.2 See 1.13.3.2 See 1.13.1.5 See 1.13.2.2

<u>PRC Index</u>	<u>Item</u>	<u>Quantity</u>	<u>Remarks</u>
1.18.2	<u>Board Assembly No. 2, 205867 (Continued)</u>		
	Module Assembly, 203153, FF-2	5	See 1.13.1.2
	Module Assembly, 203154, FF-3	7	See 1.13.1.3
	Module Assembly, 202197, IV-2	4	See 1.13.1.4
	Module Assembly, 205392, AG-3	4	See 1.18.2.13
	Module Assembly, 205396, AG-5	2	See 1.18.2.14
	Module Assembly, 205398, AG-6	1	See 1.18.2.15
	Module Assembly, 205382, JG-4	5	See 1.13.1.9
	Module Assembly, 205386, JG-6	2	See 1.18.2.17
	Module Assembly, 205404, LG-1	5	See 1.18.2.18
	Module Assembly, 202240, TG-1	8	See 1.18.1.6
1.18.2.13	<u>Module Assembly, Logic Gate (AG-3), 205392</u>		
	Diode, PT4-2009	29	
	Resistor, PT4-7-C__F, 1/8 w, $\pm 1\%$	13	
1.18.2.14	<u>Module Assembly, Logic Gate (AG-5), 205396</u>		
	Diode, PT4-2009	36	
	Resistor, PT4-7-C__F, 1/8 w, $\pm 1\%$	9	
1.18.2.15	<u>Module Assembly, Logic Gate (AG-6), 205398</u>		
	Diode, PT4-2009	28	
	Resistor, PT4-7-C__F, 1/8 w, $\pm 1\%$	8	
1.18.2.17	<u>Module Assembly, Logic Gate (JG-6), 205386</u>		
	Diode, PT4-2009	14	
	Resistor, PT4-7-C__F, 1/8 w, $\pm 1\%$	5	

<u>PRC Index</u>	<u>Item</u>	<u>Quantity</u>	<u>Remarks</u>
1.18.2.18	Module Assembly, Logic Gate (LG-1), 205404		
	Diode, PT4-2009	28	
	Resistor, PT4-7-C F, 1/8 w, ±1%	5	
1.18.3	Board Assembly No. 3, 205868		
	Strip Assembly, 205876	1	Mechanical
	Module Assembly, 202204, AM-5	13	See 1.18.1.1
	Module Assembly, 202256, NE-1	3	See 1.18.1.2
	Module Assembly, 202254, NE-2	1	See 1.18.1.3
	Module Assembly, 205931, GM-3	1	See 1.18.3.5
	Module Assembly, 202240, TG-1	12	See 1.18.1.6
	Module Assembly, 203155, GM-2	1	See 1.18.1.5
	Module Assembly, 202250, SC-2	1	See 1.13.1.5
	Module Assembly, 202202, AM-1	3	See 1.13.2.2
	Module Assembly, 202197, IV-2	2	See 1.13.1.4
	Module Assembly, 203153, FF-2	9	See 1.13.1.2
	Module Assembly, 203154, FF-3	2	See 1.13.1.3
	Module Assembly, 205402, AG-8	2	See 1.13.2.10
	Module Assembly, 205388, AG-1	3	See 1.18.3.14
	Module Assembly, 205414, LG-6	3	See 1.13.1.13
	Module Assembly, 205412, LG-5	4	See 1.13.1.12
	Module Assembly, 205410, LG-4	1	See 1.13.1.11
	Module Assembly, 205406, LG-2	1	See 1.18.3.18
	Module Assembly, 205382, JG-4	1	See 1.13.1.9
	Module Assembly, 205384, JG-5	1	See 1.13.1.10

<u>PRC Index</u>	<u>Item</u>	<u>Quantity</u>	<u>Remarks</u>
1.18.3.5	Module Assembly, Matrix Gate (GM-3), 205931		
	Resistor, PT4-7-C__F, 1/8 w, ±1%	9	
	Diode, PT4-2010	9	
	Capacitor, CY10C121J, Mil-C-11272B	3	
1.18.3.14	Module Assembly, Logic Gate (AG-1), 205388		
	Diode, PT4-2009	26	
	Resistor, PT4-7-C__F, 1/8 w, ±1%	6	
1.18.3.18	Module Assembly, Logic Gate (LG-2), 205406		
	Resistor, PT4-7-C__F, 1/8 w, ±1%	3	
	Diode, PT4-2009	28	
1.18.4	Board Assembly No. 4, Modular, 205869		
	Strip Assembly, 205876	1	
	Module Assembly, 202199, IV-1	4	See 1.13.3.2
	Module Assembly, 202250, SC-2	1	See 1.13.1.5
	Module Assembly, 202202, AM-1	8	See 1.13.2.2
	Module Assembly, 206916, BN-2	1	N
	Module Assembly, 203153, FF-2	12	See 1.13.1.2
	Module Assembly, 203154, FF-3	12	See 1.13.1.3
	Module Assembly, 205400, AG-7	2	See 1.13.1.6
	Module Assembly, 205402, AG-8	1	See 1.13.2.10
	Module Assembly, 205406, LG-2	7	See 1.18.3.18
	Module Assembly, 205408, LG-3	1	See 1.13.2.14



<u>PRC Index</u>	<u>Item</u>	<u>Quantity</u>	<u>Remarks</u>
1.18.4	<u>Board Assembly No. 4, Modular, 205869 (Continued)</u>		
	Module Assembly, 205414, LG-6	4	See 1.13.1.13
	Module Assembly, 205378, JG-2	8	N
	Module Assembly, 205380, JG-3	2	See 1.13.1.8
	Module Assembly, 205382, JG-4	2	See 1.13.1.9
	Module Assembly, 205398, AG-6	4	See 1.18.2.15
	Module Assembly, 205394, AG-4	1	See 1.13.3.6
	Sensing Assembly, 208779	1	
1.18.5	<u>Board Assembly No. 5, Modular, DDHA, 205871</u>		
	Strip Assembly, 205876	1	
	Module Assembly, 202202, AM-1	2	See 1.13.2.2
	Module Assembly, 202248, AM-2	7	See 1.13.2.3
	Module Assembly, 202582, AM-6	3	See 1.18.5.4
	Module Assembly, 200263, FF-1	5	See 1.13.2.5
	Module Assembly, 203153, FF-2	3	See 1.13.1.2
	Module Assembly, 203154, FF-3	3	See 1.13.1.3
	Module Assembly, 203155, GM-2	1	See 1.18.1.5
	Module Assembly, 202199, IV-1	3	See 1.13.3.2
	Module Assembly, 202197, IV-2	1	See 1.13.1.4
	Module Assembly, 202214, MC-1	2	See 1.18.5.11
	Module Assembly, 202244, MV-1	1	See 1.18.5.12
	Module Assembly, 202216, MV-2	1	See 1.18.5.13
	Module Assembly, 203161, MV-3	2	See 1.18.5.14

PRC Index

1.18.5 Board Assembly No. 5, Modular, DDHA, 205871  
(Continued)

<u>Item</u>	<u>Quantity</u>	<u>Remarks</u>
Module Assembly, 202250, SC-2	1	See 1.13.1.5
Module Assembly, 203734, OS-1A	1	See 1.18.5.16
Module Assembly, 203740, OS-1B	1	See 1.18.5.17
Module Assembly, 203738, OS-1C	1	See 1.18.5.18
Module Assembly, 203736, OS-1D	1	See 1.18.5.19
Module Assembly, 202218, SP-1	2	See 1.18.5.20
Module Assembly, 205390, AG-2	1	See 1.13.2.9
Module Assembly, 205364, KG-1	1	See 1.18.5.22
Module Assembly, 203163, HG-5	1	See 1.18.5.23
Module Assembly, 205927, HG-6	1	See 1.18.5.24
Module Assembly, 205929, HG-7	1	See 1.18.5.25
Module Assembly, 205376, JG-1	2	See 1.13.1.7
Module Assembly, 205382, JG-4	1	See 1.13.1.9
Module Assembly, 205366, KG-2	2	See 1.13.2.13
Module Assembly, 205368, KG-3	1	See 1.13.3.5
Module Assembly, 205370, KG-4	5	See 1.18.5.30
Module Assembly, 205408, LG-3	1	See 1.13.2.14
Module Assembly, 205414, LG-6	2	See 1.13.2.13
Module Assembly, 205374, MG-1	2	See 1.13.2.18
Module Assembly, 210249, BN-3	1	N
Thermistor, PT4-1-2	4	

<u>PRC Index</u>	<u>Item</u>	<u>Quantity</u>	<u>Remarks</u>
1.18.5.4	<u>Module Assembly, Buffer, Analog Data (AM-6), 202582</u>		
	Diode, PT4-2009	12	
	Resistor, PT4-7-C__F, 1/8 w, $\pm 1\%$	24	
	Transistor, PT4-7059	6	
1.18.5.11	<u>Module Assembly, Master Clock Generator (MC-1), 202214</u>		
	Resistor, PT4-7-C__F, 1/8 w, $\pm 1\%$	8	
	Capacitor, CK06CW103K, Mil-C-11015E	1	
	Transistor, PT4-7059	1	
	Transistor, PT4-7014	1	
	Transistor, Mil-S-19500/99A	1	
	Diode, PT4-2009	4	
	Diode, PT4-2010	5	
1.18.5.12	<u>Module Assembly, 0.2-<math>\mu</math>sec Monostable Multivibrator (MV-1), 202244</u>		
	Capacitor, CY10C__J, Mil-C-11272B	4	
	Diode, PT4-2009	2	
	Resistor, PT4-7-C__F, 1/8 w, $\pm 1\%$	9	
	Transistor, PT4-7013	1	
	Transistor, PT4-7059	2	
1.18.5.13	<u>Module Assembly, 0.5-<math>\mu</math>sec Monostable Multivibrator (MV-2), 202216</u>		
	Capacitor, CY10C__J, Mil-C-11272/1E	5	
	Diode, PT4-2010	12	

<u>PRC Index</u>	<u>Item</u>	<u>Quantity</u>	<u>Remarks</u>
1.18.5.13	<u>Module Assembly, 0.5-μsec Monostable Multivibrator (MV-2), 202216 (Continued)</u>		
	Resistor, PT4-7-C___F, 1/8 w, ±1%	15	
	Transistor, PT4-7013	2	
	Transistor, PT4-7059	2	
	Transistor, PT4-7062	1	
1.18.5.14	<u>Module Assembly, Monostable Multivibrator (MV-3), 203161</u>		
	Resistor, PT4-7-C___F, 1/8 w, ±1%	14	
	Diode, PT4-2010	9	
	Capacitor, CY10C___J, Mil-C-11272B	2	
	Transistor, PT4-7059	3	
	Transistor, PT4-7013	1	
1.18.5.16	<u>Module Assembly, Oscillator and Output Buffer (OS-1A), 203734</u>		
	Circuit Board Assembly, 204106	1	N
	Component Assembly, 204129	1	N
	Board Assembly, Temperature Sensing, 208032	1	N
	Crystal Unit, Specification 61-029 Revision B	1	
	Resistor Assembly, Thermal, PT4-6-1	1	
	Capacitor, CY15C___J, Mil-C-11272/2C	2	
1.18.5.17	<u>Module Assembly, Cross-Strap Switch and 0.3-μsec Monostable Multivibrator (OS-1B), 203740</u>		
	Resistor, PT4-7-C___F, 1/8 w, ±1%	20	
	Capacitor, CY10C101F, ±1%, Mil-C-11272B	3	

<u>PRC Index</u>	<u>Item</u>	<u>Quantity</u>	<u>Remarks</u>
1.18.5.17	Module Assembly, Cross-Strap Switch and 0.3-μsec Monostable Multivibrator (OS-1B), 203740 (Continued)		
	Capacitor, CY10C101J, ±5%, Mil-C-11272B	1	
	Diode, PT4-2009	6	
	Diode, PT4-2010	7	
	Transistor, PT4-7013	3	
	Transistor, PT4-7059	3	
1.18.5.18	Module Assembly, 0.3-μsec Monostable Multivibrator Output Buffer (OS-1C), 203738		
	Resistor, PT4-7-C__F, 1/8 w, ±1%	12	
	Capacitor, CY10C__J	3	
	Capacitor, PT4-1010-C103K, .01 μf, 50 v, ±10%	1	
	Transistor, PT4-7013	1	
	Transistor, PT4-7062	4	
	Diode, PT4-2010	12	
1.18.5.19	Module Assembly, 0.9-μsec Monostable Multivibrator (OS-1D), 203736		
	Resistor, PT4-7-C__F, 1/8 w, ±1%	15	
	Capacitor, CY10C__J, ±5%, Mil-C-11272B	4	
	Capacitor, CY10C__F, ±1%, Mil-C-11272B	1	
	Capacitor, PT4-1010-C103K, .01 μf, 50 v, ±10%	1	
	Transistor, PT4-7059	2	
	Transistor, PT4-7013	2	
	Diode, PT4-2009	3	
	Diode, PT4-2010	7	

<u>PRC Index</u>	<u>Item</u>	<u>Quantity</u>	<u>Remarks</u>
1.18.5.20	<u>Module Assembly, Shift Pulse Driver (SP-1), 202218</u>		
	Diode, PT4-2009	8	
	Diode, PT4-2010	2	
	Capacitor, PT4-1010	2	
	Resistor, RC07GF__J, Mil-R-11C	6	
	Resistor, PT4-7-C__F, 1/8 w, $\pm 1\%$	2	
	Transistor, PT4-7059	1	
	Transistor, PT4-7062	2	
	Transformer, PT6-1006	2	
1.18.5.22	<u>Module Assembly, Logic Gate (KG-1), 205364</u>		
	Resistor, PT4-7-C__F, 1/8 w, $\pm 1\%$	5	
	Diode, PT4-2009	16	
1.18.5.23	<u>Module Assembly, High-Frequency Gate (HG-5), 203163</u>		
	Diode, PT4-2009	34	
	Resistor, PT4-7-C__F, 1/8 w, $\pm 1\%$	10	
1.18.5.24	<u>Module Assembly, High-Frequency Gate (HG-6), 205927</u>		
	Resistor, PT4-7-C__F, 1/8 w, $\pm 1\%$	1	
1.18.5.25	<u>Module Assembly, High-Frequency Gate (HG-7), 205929</u>		
	Resistor, PT4-7-C__F, 1/8 w, $\pm 1\%$	6	
	Diode, PT4-2009	16	
1.18.5.30	<u>Module Assembly, Logic Gate (KG-4), 205370</u>		
	Resistor, PT4-7-C__F, 1/8 w, $\pm 1\%$	4	
	Diode, PT4-2009	26	

<u>PRC Index</u>	<u>Item</u>	<u>Quantity</u>	<u>Remarks</u>
1.19	Analog Data Handling Assembly, 201140		
	Spacecraft Submultiplexers Assembly, 202375	1	See 1.19.1
	Main FF and Exp. Multiplexers Assembly, 202349	1	See 1.19.2
	A/D Converter Assembly, 202374	1	See 1.19.3
1.19.1	Spacecraft Submultiplexers Assembly, 202375		
	Module Assembly, 201057, 1st Level Gate	22	See 1.19.1.1
	Module Assembly, 201252, 2nd Level Gate	2	See 1.19.1.2
	Connector, PT2-5-5	7	
1.19.1.1	Module Assembly, 1st Level Gate, 201057		
	Terminal, 201045	11	
	Terminal, 201046	10	
	Transformer, 521500-1, 6-terminal	4	
	Transistor, PT4-7001	1	
	Transistor, PT4-7002, In 8 matched pairs	16	
	Diode, 1N459, Mil-S-19500/193	1	
	Resistor, 7.5 k, $\pm 1\%$ , 1/8 w, Mil-R-10509D	1	
	Resistor, 3.48 k, $\pm 1\%$ , 1/8 w, Mil-R-10509D	16	
1.19.1.2	Module Assembly, 2nd Level Gate, 201252 (from Schematic 201060)		
	Terminal	29	
	Transistor, PT4-7002, In 9 matched pairs	18	
	Transistor, PT4-7001	9	
	Transistor, PT4-7004	2	
	Transistor, PT4-7003	1	

<u>PRC Index</u>	<u>Item</u>	<u>Quantity</u>	<u>Remarks</u>
1.19.1.2	Module Assembly, 2nd Level Gate, 201252 <u>(from Schematic 201060) (Continued)</u>		
	Diode, PT4-2003	9	
	Diode, PT4-2004	1	
	Diode, 1N485B	1	
	Resistors, 1/8 w, $\pm 1\%$	32	
	Capacitors, 2.2 $\mu$ f, 20 v	3	
	Transformers, 521500-2, 4-terminal	9	
1.19.2	Main Flexible Format and Experiment Multiplexers Assembly, 202349		
	Module Assembly, 201057, 1st Level Gate	30	See 1.19.1.1
	Module Assembly, 201252, 2nd Level Gate	3	See 1.19.1.2
	Connector, PT2-5-5	8	
1.19.3	A/D Converter Assembly, 202374		
	Module Assembly, Comparator, ADHA, 201590	1	See 1.19.3.1
	Module Assembly, Ladder Adder, ADHA, 201594	1	See 1.19.3.2
	Module Assembly, D/A Switch, ADHA, 202831	1	See 1.19.3.3
	Module Assembly, D/A Logic, ADHA, 201582	8	See 1.19.3.4
	Module Assembly, Reference, ADHA, 201588	1	See 1.19.3.5
	Connector, PT2-5-1	1	
	Thermistor, PT4-6	1	
	Resistor, 191 k, 1/8 w, $\pm 1\%$ , Mil-R-10509	1	
	Resistor, RC126F J, 5%, 1/4 w, Mil-R-11	2	
	Resistor, $\pm 1\%$ , 1/8 w, Mil-R-10509	3	



<u>PRC Index</u>	<u>Item</u>	<u>Quantity</u>	<u>Remarks</u>
1.19.3.1	Module Assembly, Comparator, ADHA, 201590		
	Capacitor, Mil-C-11272, CY10C7505, 75 $\mu$ f, $\pm 5\%$	1	
	Capacitor, Mil-C-26655, CS13AF010K, 1.0 $\mu$ f, $\pm 10\%$ , 35 v	3	
	Capacitor, Mil-C-26655, CS13HE2R2K, 2.2 $\mu$ f, $\pm 10\%$ , 20 v	3	
	Diode, PT4-2049	1	
	Diode, PT4-2004	1	
	Diode, PT4-2007	6	
	Resistor, Mil-R-10509D (PT4-7- - - -), $\Omega$ , $\pm 1\%$ , 1/8 w	29	
	Resistor, Mil-R-10509D (PT4-7- - - -), $\Omega$ , $\pm 0.1\%$ , 1/8 w	1	
	Transistor, PT4-7007	1	
	Transistor, PT4-7071	1	
	Transistor, PT4-7008	4	
	Transistor, PT4-7072	2	
	Transistor, PT4-7071 or PT4-7072	1	
1.19.3.2	Module Assembly, Ladder Adder, ADHA, 201594		
	Resistor, 19.6 k, $\pm 0.1\%$ , 1/8 w, Mil-R-1509D	9	
	Resistor, 10 k, $\pm 0.1\%$ , 1/8 w, Mil-R-10509D	7	
	Resistor, 34.8 $\Omega$ , $\pm 1\%$ , 1/8 w, Mil-R-10509D	2	
	Resistor, 158 k, $\pm 1\%$ , 1/8 w, Mil-R-10509D	1	
	Capacitor, 47 $\mu$ f, $\pm 5\%$ , Mil-C-11272/1	1	
	Capacitor, 1 $\mu$ f, $\pm 10\%$ , 35 v, Mil-C-26655/2	2	
	Transistor, PT4-7006	1	

<u>PRC Index</u>	<u>Item</u>	<u>Quantity</u>	<u>Remarks</u>
1.19.3.3	Module Assembly, D/A Switch, ADHA, 202831		
	Resistor, 13.0 k, $\pm 1\%$ , 1/8 w, Mil-R-10509	8	
	Diode, PT4-2005	16	
	Diode, PT4-2037	16	
1.19.3.4	Module Assembly, D/A Logic, ADHA, 201582		
	Diode, PT4-2007	1	
	Capacitor, CY10C__J, Mil-C-11272/1	2	
	Capacitor, PT4-1010-D203M, .02 $\mu$ f, $\pm 20\%$	1	
	Transistor, PT4-7005	1	
	Transistor, PT4-7007	1	
	Transistor, PT4-7008	1	
	Resistor, PT4-7-C-__F, 1/8 w, $\pm 1\%$	9	
1.19.3.5	Module Assembly, Reference, ADHA, 201588		
	Resistor, Mil-R-10509D (PT4-7-__B), __ $\Omega$ , $\pm 0.1\%$ , 1/8 w	7	
	Resistor, Mil-R-10509D (PT4-7-__B), __ $\Omega$ , $\pm 1\%$ , 1/8 w	4	
	Capacitor, Mil-C-26655/2, CS13AE2R2K, 2.2 $\mu$ f, $\pm 10\%$ , 20 v	1	
	Capacitor, Mil-C-26655/2, CS13AF010K, 1 $\mu$ f, $\pm 10\%$ , 35 v	1	
	Diode, PT4-2051	1	
	Diode, PT4-2006	1	

<u>PRC Index</u>	<u>Item</u>	<u>Quantity</u>	<u>Remarks</u>
1.20	Spacecraft Performance Sensors (No Information)		

2.0: ACS PARTS COMPLEMENT

Remarks

Quantity

Item

PRC Index

OPEP and Solar Array Drive, 202540  
Motor Assembly, 2° 41' Drive, 202577

1

2.1

<u>PRC Index</u>	<u>Item</u>	<u>Quantity</u>	<u>Remarks</u>
2.2	<u>Sun Sensor Assembly--Radiation Tracking Transducer, 20284</u>	1	See 2.2.1
2.2.1	<u>Sun Sensor Subassembly, 202954 (Potted)</u>		
	<u>Sun Sensor Subassembly, 202954</u>		
	Transducer, PT4-7011	1	
	Harness, 202618	1	See 2.2.1.1
	Thermistor, PT4-6	1	
	Solar Cell, 1 x 50, PT4-2054	3	
2.2.1.1	<u>Harness, Sun Sensor and X Array</u>		
	Junction Board Assembly, 205946	1	
	Terminal Board Assembly, 203292	1	
	Connector, DT2-5-8	1	
	Resistor, PT4-7-C__D, 1/8 w, $\pm 5\%$	4	
	Resistor, PT4-7-C__F, 1/8 w, $\pm 1\%$	3	
	Resistor, PT4-7-P__D, 1/8 w, $\pm 5\%$	1	
	Resistor, PT4-7-E__D, 1/8 w, $\pm 5\%$	1	

<u>PRC Index</u>	<u>Item</u>	<u>Quantity</u>	<u>Remarks</u>
2.3	Sun Sensor Assembly, 202744		
	Harness, 202883	1	
	Solar Cell, 1 x 50, PT4-7012, 51C, Hoffman Laboratories, L.A.	3	See 2.3.1
	Thermistor, PT4-6	1	
2.3.1	Harness, 202883		
	Junction Board Assembly, 205946 (Board with 6 to 18 Post-Type Terminals)	1	
	Terminal Board Assembly, 205965 (Board with 12 Post-Type Terminals)	1	
	Connector, PT2-5-7	1	
	Resistor, 1/8 w, 1%, PT4-18	2	

PRC Index

2.4

<u>Item</u>	<u>Quantity</u>	<u>Remarks</u>
Sun Sensor Electronics and Logic Assembly, 200932		
Low-Level Magnetic Amplifier, 202409-1	3	
Low-Level Magnetic Amplifier, 202409-2	1	
Low-Level Magnetic Amplifier, 202409-3	1	
Terminal Board No. 1, 202416	1	See 2.4.4
Terminal Board No. 2, 203885	1	See 2.4.5
Terminal Board No. 3, 203848	1	See 2.4.6
Timer Oscillator, PT2-3005-1	1	
Timer Divider, PT2-3005-2	1	
Module, 203528	3	See 2.4.9
Module, 203592	2	See 2.4.10
Module, 203665	4	See 2.4.11
Module, 203666	1	See 2.4.12
Module, 203687	1	See 2.4.13
Module, 203705	1	See 2.4.14
Module, 203706	1	See 2.4.15
Module, 203707	1	See 2.4.16
Module, 203708	1	See 2.4.17
Module, 203732	1	See 2.4.18
Module, 203759	1	See 2.4.19
Module, 203760	1	See 2.4.20
Module, 203764	1	See 2.4.21
Module, 203810	1	See 2.4.22
Relay, PT2-1004-2	1	

PRC Index

2.4 Sun Sensor Electronics and Logic Assembly, 200932

(Continued)

<u>Item</u>	<u>Quantity</u>	<u>Remarks</u>
Relay, PT2-1004-1	1	
Relay, PT2-1002-1	3	
Relay, PT2-1005-1	1	
Connector, PT2-5-4	1	
Connector, PT2-5-5	2	
Connector, PT2-5-3	1	
Connector, PT2-5-9	1	
Connector, PT2-5-8	1	
Transformer, PT6-1010, Power	1	
Transformer, PT6-1011, Audio	2	
Transformer, PT6-1012, Audio	3	
Transformer, PT6-1013, Isolation	5	
Bistable Level Detector, PT6-2003	2	
Terminal Board No. 1, 202416		Printed Circuit Board
Board, 202415	1	
Terminal, Insulated, SP0035-2	30	
Feedthrough, Insulated, SP0036-1	25	
Capacitor, PT4-1013-26, 50 $\mu$ f, 20 v, NP	5	
Capacitor, PT4-1013-38, 23 $\mu$ f, 35 v, NP	4	
Capacitor, PT4-1013-100, 50 $\mu$ f, 10 v, NP	2	
Capacitor, PT4-1013-111, 110 $\mu$ f, 10 v, NP	2	
Resistor, PT4-7-C __ F, 1/8 w, 1 $\frac{1}{2}$	30	

2.4.4



<u>PRC Index</u>	<u>Item</u>	<u>Quantity</u>	<u>Remarks</u>
2.4.5	Terminal Board No. 2, 203885		
	Terminal Board, 203886	1	Printed Circuit Board
	Terminal, SP0047-1 (Post Type)	32	
	Terminal, SP0035-2 (Post Type)	17	
	Terminal, SP0036-1 (Post Type)	24	
	Resistor, Mil-R-11, RC07GF J, 1/4 w, 5%	6	
	Resistor, PT4-7, 1/8 w, 1%	1	
	Capacitor, Mil-C-26655, CS13AF220K	1	
	Diode, Mil-S-19500/118, 1N485B	18	
2.4.6	Terminal Board No. 3, 203848		
	Terminal Board, 203821	1	Printed Circuit Board
	Capacitor, PT4-1013-20, 1.1 $\mu$ f, 20 v, NP	4	
	Resistor, PT4-7, 1/8 w, 1%	12	
	Terminal, SP0035-2 (Post Type)	29	
2.4.9	Module, TLM and D/A Converter, 203528		
	Printed Circuit Boards, Mil-P-18177	3	
	Terminal, 203412	9	
	Capacitor, Mil-C-26655A, CS13AE2R2K	1	
	Diode, Mil-S-19500/118, 1N485B	5	
	Resistor, Mil-R-11C, RC07GF J	9	
	Resistor, Mil-R-10509, RN60C D, 1/8 w, .5%, WW	4	
	Resistor, PT4-7-C3012F, 30.1 k, 1/8 w, 1%	4	
	Transistor, Mil-S-19500/63C, 2N358A	4	

<u>PRC Index</u>	<u>Item</u>	<u>Quantity</u>	<u>Remarks</u>
2.4.10	Module Z9, Demodulator--SS and L, 203592		
	Printed Circuit Boards	2	
	Resistor, Mil-R-11, RC07GF512J	16	
	Transistor, PT4-7001, 2N720A	16	
	Terminal, .040 sq x .609, 1/2 Hard Brass, QQ-B-636	31	
2.4.11	Module Z21, Small Earth Discriminator--SS and L, 203665		
	Printed Circuit Boards	2	
	Terminal, .040 sq x .609, 1/2 Hard Brass, QQ-B-636	9	
	Capacitor, Mil-C-26655A, CS13AF___K, 35 v, 10%	5	
	Capacitor, Mil-C-26655A, CS13AD___K, 15 v, 10%	2	
	Diode, Mil-S-19500/118, 1N485B	3	
	Resistor, PT4-7-C___F, 1/8 w, 1%	16	
	Resistor, Mil-R-11, RC07GF___J	5	
	Transistor, PT4-7004, 2N718A	5	
2.4.12	Module Z26, Normal Mode Gate--SS and L, 203666		
	Printed Circuit Boards	2	
	Terminal, .040 sq x .609, 1/2 Hard Brass, QQ-B-636	15	
	Diode, Mil-S-19500/118, 1N485B	36	
2.4.13	Module Z5, Normal Mode Gate Drivers--SS and L, 203687		
	Printed Circuit Boards	2	
	Diode, Mil-S-19500/118, 1N485B	6	

<u>PRC Index</u>	<u>Item</u>	<u>Quantity</u>	<u>Remarks</u>
2.4.13	Module Z5, Normal Mode Gate Drivers--SS and L, 203687 (Continued)		
	Resistor, PT4-7-C___F, 1/8 w, 1%	16	
	Resistor, RC07GF___J, Mil-R-11	12	
	Transistor, PT4-7004, 2N718A	8	
2.4.14	Module Z11, Array and Yaw TLM--SS and L, 203705		
	Printed Circuit Boards	2	
	Terminal, .040 sq x .609, 1/2 Hard Brass, QQ-B-636	(≈11)	
	Capacitor, PT4-1013-20, 1.1 μf, 20v, ±10%, NP	2	
	Capacitor, Mil-C-26655, CS13AB6R8K, 6v, ±10%	2	
	Diode, Mil-S-19500/127, 1N747A	2	
	Diode, Mil-S-19500/118, 1N485B	6	
	Resistor, Mil-R-11, RC07GF5613	2	
	Resistor, PT4-7-C___F, 1/8 w, 1%	10	
2.4.15	Module Z12, Pitch and Roll TLM--SS and L, 203706		
	Printed Circuit Boards	2	
	Terminal, .040 sq x .609, 1/2 Hard Brass, QQ-B-636	(≈11)	
	Capacitor, PT4-1013-32, 35v, ±10%, 2-3 μf	2	
	Capacitor, Mil-C-26655, CS13AB6R8K	2	
	Diode, Mil-S-19500/127, 1N747A	2	
	Diode, Mil-S-19500/118, 1N485B	4	
	Resistor, Mil-R-11, RC07GF___J	2	
	Resistor, PT4-7-C___F, 1/8 w, 1%	10	

<u>PRC Index</u>	<u>Item</u>	<u>Quantity</u>	<u>Remarks</u>
2.4.16	Module Z28, Reacquire Gates--SS and L, 203707		
	Printed Circuit Boards	2	
	Terminal, .040 sq x .609, 1/2 Hard Brass, QQ-B-636	(≈11)	
	Diode, Mil-S-19500/118, 1N485B	26	
	Diode, PT4-2009, 202297 (Called CR2-36, etc.)	10	
	Transistor, PT4-7004, 2N718A	2	
	Transistor, PT4-7001, 2N720A	1	
	Resistor, PT4-7-C__F, 1/8 w, 1%	8	
	Resistor, Mil-R-11, RC07GF__J	3	
2.4.17	Module Z29, Relay Driver No. 1--SS and L, 203708		
	Printed Circuit Boards	2	
	Terminal, .040 sq x .609, 1/2 Hard Brass, QQ-B-636	(≈13)	
	Diode, Mil-S-19500/118, 1N485B	18	
	Transistor, PT4-7001, 2N720A	6	
	Resistor, Mil-R-11, RC07GF__J	6	
	Resistor, PT4-7C1002F, 10 k, 1/8 w, 1%	3	
2.4.18	Module Z8, D.C. Filter--SS and L, 203732		
	Printed Circuit Boards	2	
	Terminal (See 203707 e.g.)	(≈10)	
	Capacitor, Mil-C-26655, CS13AF220K	12	
	Diode, Mil-S-19500/118, 1N485B	3	
	Resistor, Mil-R-11, RC07GF__J	4	
	Resistor, PT4-7C3322F, 33.2 k, 1/8 w, 1%	1	

<u>PRC Index</u>	<u>Item</u>	<u>Quantity</u>	<u>Remarks</u>
2.4.19	Module Z16, Magnetic Amplifier Gates--SS and L, 203759		
	Printed Circuit Boards	2	
	Terminal, 206962 (Look like those on 203707)	31	
	Capacitor, 2.2 $\mu$ f, 35 v	1	
	Capacitor, Mil-C-26655A, CS13AF010K	1	
	Diode Assembly, PT4-2009, 202297	32	
	Diode, Mil-S-19500/127, 1N746A	1	
	Diode, Mil-S-19500/127, 1N758A	1	
	Diode, Mil-S-19500/118, 1N485B	1	
	Resistor, PT4-7-C__F	12	
	Resistor, Mil-R-11, RC07GF__J	10	
	Transistor, Mil-S-19500/63C, 2N358A	1	
	Transistor, PT4-7004, 2N718A	1	
2.4.20	Module Z27, Reacquisition Gates--SS and L, 203760		
	Printed Circuit Boards	2	
	Terminal (See 203707 e.g.)	( $\approx$ 21)	
	Capacitor, Mil-C-26655, CS13AB6R8K	2	
	Capacitor, 550062-AHR33K, .33 $\mu$ f, 75 v	3	
	Transistor, PT4-7004, 2N718A	2	
	Resistor, PT4-7-C__F	7	
	Resistor, Mil-R-11, RC07GF__J, 1/4 w	3	
	Resistor, Mil-R-11, RC20GF__J, 1/2 w	2	
	Diode, Mil-S-19500/118, 1N485B	33	

<u>PRC Index</u>	<u>Item</u>	<u>Quantity</u>	<u>Remarks</u>
2.4.21	Module Z30, Relay Driver No. 2--SS and L, 203764		
	Printed Circuit Boards	2	
	Terminal (See 203707 e.g.)	(≈13)	
	Transistor, PT4-7001, 2N720A	6	
	Resistor, Mil-R-11, RC07GF__J	6	
	Resistor, PT4-7-C__F	3	
	Diode, Mil-S-19500/118, 1N485B	24	
2.4.22	Module Z17, Timer Output--SS and L, 203810		
	Printed Circuit Boards	2	
	Terminal (See 203707 e.g.)	(≈6)	
	Capacitor, Mil-C-11015/19, CK06CW__K	3	
	Capacitor, PT4-1010-O203M, .02 μf, 50 v, ±20%	2	
	Diode, Mil-S-19500/118, 1M485B	2	
	Silicon-Controlled Rectifier, PT4-2052 (3A101)	2	
	Resistor, Mil-R-11, RC07GF__J	4	

<u>PRC Index</u>	<u>Item</u>	<u>Quantity</u>	<u>Remarks</u>
2.5.2	<u>Module, Reacquire Circuitry, 203012</u>		
	Capacitor, CS13AF___K, Mil-C-26655	3	
	Diode, PT4-2003	2	
	Resistor, PT4-7-C___F, 1/8 w, 1%	9	
	Transistor, PT4-7058, 2N946	4	
	Transistor, PT4-7004	1	
2.5.3	<u>Module, Magnetic Amplifier Control Circuitry, 203009</u>		
	Capacitor, CS13AFR47K, 47µf, 35 v, 10%, Mil-C-26655	8	
	Capacitor, CS13AG010K, 1 µf, 50 v, 10%, Mil-C-26655	2	
	Diode, PT4-2001, 1N647	16	
	Resistor, RN70C___F, Mil-R-10509	14	
2.5.5	<u>Terminal Board Assembly, 203008</u>		
	Terminal Board, 203010	1	
	Diode, PT4-2003	10	
	Resistor, 1/8 w, 10%	9	

PRC Index

2.5

<u>Item</u>	<u>Quantity</u>	<u>Remarks</u>
Electronics Assembly, OPEP and Solar Array Drive, 200934		
Module, TLM Demodulator, 203007	1	See 2.5.1
Module, Reacquire Circuitry, 203012	1	See 2.5.2
Module, Magnetic Amplifier Control Circuitry, 203009	1	See 2.5.3
Module, TLM and D/A Converter, 203523	1	See 2.4.9
Terminal Board Assembly, 203008	1	See 2.5.5
Low-Level Magnetic Amplifier, 202409-1	2	
Bistable Magnetic Amplifier, PT6-2003	2	
Motor-Drive Magnetic Amplifier, PT6-2007	2	
Relay, SL11DA, Latching, PT2-1015	3	
Relay, 80GB-5N-4-A-10K, PT2-1005-2	1	
Relay, 90HB-16N-4-A-25K, PT2-1004-1	1	
Connector, 25-Pin Test, PT2-5-8	1	
Connector, 37-Pin Output and Power, PT2-5-4	1	
Connector, 50-Pin Input and Low Level, PT2-5-10	1	
Resistor, 1/8 w, 1%, PT47C___F	8	
Module, TLM Demodulator, 203007		
Capacitor, CS13AE2R2K, Mil-C-26655	4	
Capacitor, CS13AF010K, Mil-C-26655	4	
Diode, PT4-2003	4	
Resistor, PT4-7-C___F, 1/8 w, 1%	16	

2.5.1



<u>PRC Index</u>	<u>Item</u>	<u>Quantity</u>	<u>Remarks</u>
2.6	<u>Pitch Rate Gyro Assembly, 200935</u>		
	Gyro, C201670	1	
	Transformer, PT6-1007	1	
	Relay, PT2-1014-1	1	
	Transformer, PT6-1008	1	
	Non-Polarized Capacitor, 550201-38, 23 $\mu$ f, 35 v	1	
	Resistor, PT4-74991F, 50 $\Omega$ , 5 w, 1%	1	
	Connector, PT2-5-3, Rack and Panel, Subminiaturized	1	
	Connector, PT2-5-8, Rack and Panel, Subminiaturized	1	
	Component Board Assembly, 202920	1	See 2.6.1.
2.6.1	<u>Component Board Assembly, 202920</u>		
	Printed Circuit Board	1	
	Capacitor, Cerafil Ceramic, PT4-1010-E503M, .05 $\mu$ f, 50 v, 20%	1	
	Capacitor, CTM___VAK, Mil-C-27287	2	
	Capacitor, CS13AF___K, Mil-C-26655	7	
	Diode, Mil-S-19500/118, 1N485B	8	
	Resistor, PT4-7-C___F, 1/8 w, 11%	10	
	Resistor, PT4-7, 1/4 w, 1%	2	
	Resistor, RC07GF___J, Mil-R-11C	4	
	Transistor, PT4-7004	5	
	Inductor, PT6-3-11, 240 mh @ 1 kc	1	

<u>PRC Index</u>	<u>Item</u>	<u>Quantity</u>	<u>Remarks</u>
2.7	<u>Assembly Attitude Control Unit, 220833</u>		
	Module Assembly, 202286	1	See 2.7.1
	Module Assembly, 202143	1	See 2.7.2
	Module Assembly, 202144	2	See 2.7.3
	Terminal Board Assembly (Drivers), 202395	1	See 2.7.4
	Magnetic Amplifier (Yaw), PT6-2005	1	
	Magnetic Amplifier (Pitch and Roll), PT6-2004	2	
	Magnetic Amplifier (Bistable), PT6-2003	6	
	Module Assembly, 203951	1	
	Relay, 4PDT28VDC, PT2-1004-1	2	
	Connector, PT2-5-4 (Input)	1	
	Connector, PT2-5-10 (TLM)	1	
	Connector, PT2-5-5 (Power Input)	1	
	Connector, PT2-5-8 (Power Output +28 v)	1	
	Connector, PT2-5-9 (Test)	1	
	Terminal Board Assembly, 202960 (48 Terminals)	1	
	Terminal, SP0046-1	58	
	Module Assembly Z18, 208004	1	N
2.7.1	<u>Module Assembly, 202286 (Z16 Reaction Wheel)</u>		
	Diode, 1N485, Mil-S-19500/118	15	
	Capacitor, PT4-1010__M, Cerafil	15	
	Capacitor, CS13A__K, Mil-C-R6655	6	
	Resistor, PT4-7C__F, 1/8 w, 1%	36	

<u>PRC Index</u>	<u>Item</u>	<u>Quantity</u>	<u>Remarks</u>
2.7.1	Module Assembly, 202286 (Z16 Reaction Wheel) (Continued)		
	Transistor, PT4-7009, 2N930, Mil-S-19500	12	
	Transistor, PT4-7003, 2N722, Mil-S-19500	3	
	Transformer, PT6-1018	3	
2.7.2	Module Assembly, 202143 (Z13, Reaction Wheel Motor Control, Signal Telemetry)		
	Resistor, PT4-7-C___F, 1/8 w, 1%	3	
	Transistor, PT4-7034, 2N910	3	
	Capacitor, CS13AE2R2K, Mil-C-26655A, 2.2 $\mu$ f, 20 v, $\pm$ 10%	1	
2.7.3	Module Assembly, 202144 (Z14 and Z15, Gas Jet Control Telemetry)		
	Capacitor, PT4-1010-C-103M, .01 $\mu$ f, 50 v	3	
	Resistor, PT4-7-C___F, 1/8 w, 1%	24	
	Transistor, PT4-7003, 2N722	3	
	Transistor, PT4-7034, 2N910	3	
	Diode, 1N485B, Mil-S-19500/118	4	
	Capacitor, CS13H___K, Mil-R-26655A	3	
2.7.4	Terminal Board Assembly (Drivers), 202395		
	Resistor, RW57G500, 50 $\Omega$ , 5 w, 1%, Mil-R-26	6	
	Resistor, PT4-7-C___F, Mil-R-10509, 1/8 w, 1%	16	
	Transistor, PT4-7021, 2N1719	6	
	Capacitor, CPV08A1KC105K, 1 $\mu$ f, 200 v, Mil-C-14157B	6	
	Resistor, RC07GF___J, Mil-R-11C	8	

<u>PRC Index</u>	<u>Item</u>	<u>Quantity</u>	<u>Remarks</u>
2.8	OPEP Gyro Electronics Assembly, 202163		
	Module, Spin Motor Monitor, 202287	1	See 2.8.1
	Module, 400-cycle and 2461-cycle Supply, 202290	1	See 2.8.2
	Module, +20 v Regulator, 202292	1	See 2.8.3
	Toroid Assembly, 400-cycle Driver, 203589	1	See 2.8.4
	Toroid Assembly, 2461-cycle Driver, 203590	1	See 2.8.5
	Toroid Assembly, 246-cycle Output, 203593	1	See 2.8.6
	Toroid Assembly, 400-cycle Output, 203612	1	See 2.8.7
	Transformer, SMM Output, PT6-1003-2	1	
	Relay, Non-Latching, 2PDT, PT2-1013	1	
	Choke, 30 mh, PT6-3-12	1	
	Connector, 37-Pin Male, PT2-5-4	1	
	Connector, 37-Pin Female, PT2-5-9	1	
	Connector, 25-Pin Female, PT2-5-8	1	
	Capacitor, $\pm 5\%$ , 200 v, CPV08, Mil-C1451713	4	
	Resistor, 1/4 w, 5%, RC07GF__J, Mil-R-11C	1	
	Resistor, 1/4 w, 1%, RN65C__F, Mil-R-10509	4	
	Diode, 1N647, PT4-2001	1	
2.8.1	Module, Spin Motor Monitor, 202287		
	Capacitor, CS13AF5R6K, 5.6 uf, 35 v, $\pm 10\%$ , Mil-C-26655	2	
	Capacitor, CS13AC101K, 100 uf, 10 v, $\pm 10\%$ , Mil-C-26655	1	

<u>PRC Index</u>	<u>Item</u>	<u>Quantity</u>	<u>Remarks</u>
2.8.1	Module, Spin Motor Monitor, 202287 (Continued)		
	Capacitor, CS13AE100K, 10 $\mu$ f, 20 v, $\pm$ 10%, Mil-C-26655	2	
	Diode, 1N751A, Mil-S-19500	1	
	Diode, 1N647, PT4-2001	7	
	Resistor, RC07GF__J, Mil-R-11C, 1/4 w, $\pm$ 5%	12	
	Transistor, 2N1132, Mil-S-19500/177	2	
	Transistor, 2N720A, PT4-7001	2	
	Inductor, PT6-3-11, 240 mh @ 1 kc	1	
2.8.2	Module, 400-Cycle and 2461-Cycle Supply, 202290		
	Capacitor, .0047 $\mu$ f, 200 v, NP, $\pm$ 10%; Mil-C-11016, CK06CW472K	1	
	Capacitor, 5.6 $\mu$ f, 35 v, $\pm$ 10%, Mil-C-26655, CS13AF5R6K	1	
	Capacitor, .05 $\mu$ f, 50 v, NP, PT4-1010-E503M	2	
	Resistor, RC07GF__J, Mil-R-11, 1/4 w, 5%	9	
	Resistor, RC20GF5625, 1/2 w, 5%, Mil-R-11	1	
	Transistor, 2N720A, PT4-7001	4	
	Transistor, 2N1041, PT4-7048	2	

<u>PRC Index</u>	<u>Item</u>	<u>Quantity</u>	<u>Remarks</u>
2.8.3	Module, +20 v Regulator, 202292		
	Capacitor, CS13AF220K, 22 uf, 35 v, P, 10%, Mil-C-26655	1	
	Capacitor, PT4-1010-E503M, .05 uf, 50 v, ±20%	1	
	Diode, 1N822, Mil-S-19500	1	
	Diode, 1N3155A, PT4-2038	1	
	Diode, 1N759A, Zener, Mil-S-19500/127	2	
	Resistor, RC07GF___J, Mil-R-11, 1/4 w, 5%	4	
	Resistor, RW59V1R0, 3 w, Mil-R-26	1	
	Resistor, RN65C___F, Mil-R-10509	4	
	Transistor, 2N2060, PT4-7052	1	
	Transistor, 2N720A, PT4-7001	3	
	Transistor, 2N1049A, Mil-S-19500/176	1	
2.8.4	Toroid Assembly, 400-Cycle Driver, 203589		
	Terminal, 4535A, Lerco Electronics, Inc., Burbank (Split Lug)	7	
	Toroid, 201554	1	
2.8.5	Toroid Assembly, 2461-Cycle Driver, 203590		
	Terminal, SP0013-5 (Looks same as those in 203589)	7	
	Toroid, 201553	1	

<u>PRC Index</u>	<u>Item</u>	<u>Quantity</u>	<u>Remarks</u>
2.8.6	Toroid Assembly, 400-Cycle Output, 203612		
	Terminal, SP0013-5 (See 203590)	5	
	Toroid, 201845	1	
2.8.7	Toroid Assembly, 2461-Cycle Output, 203593		
	Terminal, SP0013-5 (See 203590)	9	
	Toroid, 201555	1	

PRC Index

2.9

<u>Item</u>	<u>Quantity</u>	<u>Remarks</u>
<u>OPEP Inertial Reference Assembly, 201371</u>		
Module Z2, 202291	1	See 2.9.1
Module Z4, Amplifier and Demodulator, 202289	1	See 2.9.2
Module Z5, Temperature Controller, 202288	1	See 2.9.3
Toroid Assembly, Push-Pull Output, 203611	1	
Gyro Assembly, GG49E16, C200340	2	
Connector, 37-Pin Male, PT2-5-4	1	
Relay, 2PDT Magnetic Latch, PT2-1002	2	
Transistor, 2N1978, PT4-7050	1	
Thermistor, PT4-6	1	
Capacitor, 1.4 $\mu$ f, $\pm 5\%$ , 200 v, PT4-1017	2	
Resistor, RW59-V-1R0, 1 $\Omega$ , 3 w, 5%, Mil-R-26C	1	
Heating Element, PT4-13009-7 (bonded to housing)	1	
Capacitor, PT4-1010	1	
Capacitor, CS13AE__K, Mil-C-26655	2	
<u>Module Z2, 202291</u>		
Capacitor, 2.2 $\mu$ f, 20 v, P, 10%, CS13AE2R2K, Mil-C-26655A	1	
Resistor, 1/4 w, 1%, RN65C__F, Mil-R-10509	5	
Resistor, 1/4 w, 5%, RC07GF__J, Mil-R-11C	4	
Diode, 1N647, PT4-2001	4	
Capacitor, 1 $\mu$ f, 50 v, P, 10%, CS13AC010K, Mil-C-26655A	2	

2.9.1



<u>PRC Index</u>	<u>Item</u>	<u>Quantity</u>	<u>Remarks</u>
2.9.2	Module Z4, Amplifier and Demodulator, 202289		
	Capacitor, CPV08AIKEJ, 400 v	1	
	Capacitor, PT4-1010-F140M, .1 uf, 50 v, NP, 20%	1	
	Capacitor, CS13AC101K, 100 uf, 10 v, P, 10%, Mil-C-26655	1	
	Capacitor, CS13AF, 35 v, P, 10%, Mil-C-26655	3	
	Capacitor, CPV08AIKE103J, .01 uf, 400 v, Mil-C-14157B	1	
	Resistor, RC07GF J, 1/4 w, 5%, Mil-R-11	16	
	Transistor, 2N720A, PT4-7001	7	
	Transistor, 2N1132, Mil-S-19500/177	1	
	Diode, 1N647, PT4-2001	1	
	Diode, 1N751A, Zener, Mil-S-19500/177	1	
	Transformer, PT6-1003-1	1	
	Coil, PT6-3-10, 30 mh @ 3 kc	1	
	Coil, PT6-3-11, 240 mh @ 1 kc	1	
2.9.3	Module Z5, Temperature Controller, 202288		
	Resistor, RN65C F, 1/4 w, 1%, Mil-R-10509	12	
	Resistor, RC32GF751J, 1 w, 5%, Mil-R-11C	1	
	Resistor, RC42GF102J, 2 w, 5%, Mil-R-11C	1	
	Transistor, PT4-7001	2	
	Transistor, 2N2060	1	
	Diode, 1N3155A	1	

<u>PRC Index</u>	<u>Item</u>	<u>Quantity</u>	<u>Remarks</u>
2.9.3	Module Z5, Temperature Controller, 2J2288 (Continued)		
	Diode, 1N759A, Zener	1	
	Diode, 1N757A	1	
	Capacitor, CS13AF1R5K, 1.5 $\mu$ f, 35 v, 10%, Mil-C-26665	1	

<u>PRC Index</u>	<u>Item</u>	<u>Quantity</u>	<u>Remarks</u>
2.10	<u>Horizon Scanners</u>		
	Tracker	4	See 2.10.1
	Summing Amplifier	2	See 2.10.2
	Voltage Regulator	1	See 2.10.3
	Field Current Generator	2	See 2.10.4
	Positor Field Coil Tuning Capacitors, Polystyrene	2	
	Switching Matrix	1	See 2.10.6
	Reference Output Network	1	See 2.10.7
	Field Current Control	1	See 2.10.8
	Logic Tracking Check	1	See 2.10.9
2.10.1	<u>Tracker, ATL-D-837</u>		
	Signal Preamplifier	1	See 2.10.1.1
	Signal Amplifier	1	See 2.10.1.2
	Logic	1	See 2.10.1.3
	Schmitt Trigger and Drive Amplifier	1	See 2.10.1.4
	Position Amplifier	1	See 2.10.1.5
	Positor	1	
	Bolometer	1	
2.10.1.1	<u>Signal Preamplifier, ATL-D-837</u>		
	Capacitor, Mylar	1	
	Capacitor, Solid Tantalum	1	
	Diode, Silicon	2	
	Transistor, Silicon	3	
	Resistor, Metal Film	14	

<u>PRC Index</u>	<u>Item</u>	<u>Quantity</u>	<u>Remarks</u>
2.10.1.2	<u>Signal Amplifier, ATL-D-837</u>		
	Capacitor, Solid Tantalum	4	
	Diode, Silicon	2	
	Transistor, Silicon	3	
	Resistor, Metal Film	6	
	Resistor, Carbon Film	4	
2.10.1.3	<u>Logic, ATL-D-837</u>		
	Capacitor, Solid Tantalum	2	
	Capacitor, Glass	1	
	Capacitor, Mylar	1	
	Diode	4	
	Transistor	5	
	Resistor, Metal Film	22	Three of these also counted in Logic Tracking Check.
2.10.1.4	<u>Schmitt Trigger and Drive Amplifier, ATL-D-837</u>		
	Capacitor, Solid Tantalum	8	
	Diode, Silicon	6	
	Stabistor	1	
	Transistor, Silicon	8	
	Potentiometer, Wirewound	2	
	Resistor, Metal Film	22	
	Resistor, Carbon Film	1	

<u>PRC Index</u>	<u>Item</u>	<u>Quantity</u>	<u>Remarks</u>
2.10.1.5	<u>Position Amplifier, ATL-D-837</u>		
	Capacitor, Polyester	3	
	Capacitor, Mylar	1	
	Capacitor, Solid Tantalum	1	
	Diode, Silicon	1	
	Inductor	1	
	Transistor, Silicon	3	
	Resistor, Metal Film	8	
	Resistor, Wirewound	4	
	Potentiometer, Wirewound	1	
	Thermistor	1	
2.10.2	<u>Summing Amplifier, ATL-D-837</u>		
	Capacitors, Solid Tantalum	3	
	Capacitor, Mylar	1	
	Capacitor, Glass	1	
	Transistor, Silicon	4	
	Resistor, Metal Film	9	
	Transformer	1	
2.10.3	<u>Voltage Regulator, ATL-D-837</u>		
	Capacitor, Mylar	4	
	Diode, Silicon	2	
	Transistor, Silicon	4	
	Resistor, Metal Film	4	

<u>PRC Index</u>	<u>Item</u>	<u>Quantity</u>	<u>Remarks</u>
2.10.8	<u>Field Current Control, ATL-D-837</u>		
	Capacitor, Solid Tantalum	1	
	Inductor	1	
	Potentiometer, Wirewound	1	
	Resistor, Wirewound	1	
	Transformer	1	
2.10.9	<u>Logic Tracking Check, ATL-D-837</u>		
	Capacitor, Mylar	1	
	Capacitor, Solid Tantalum	1	
	Diode, Silicon	2	
	Diode, Germanium	1	
	Transistor, Silicon	4	
	Resistor, Metal Film	9	
	Resistor, Carbon Film	2	

<u>PRC Index</u>	<u>Item</u>	<u>Quantity</u>	<u>Remarks</u>
2.11	Reaction Wheels (Subcontract; No Information)		

<u>PRC Index</u>	<u>Item</u>	<u>Quantity</u>	<u>Remarks</u>
2.12	Pneumatic System Installation--Attitude Control, 100012		
	Pressure Vessel, 100382	1	
	Line Assembly, 100511	1	
	Line Assembly, 100512	1	
	Line Assembly, 100514	1	
	Manifold, 100515-1	2	
	Manifold, 100515-2	4	
	Boom Assembly, 100516-1	2	
	Valve Assembly, 100528-1	1	
	Pressure Switch, 8027, PT2-3003	6	
	Solenoid Valve, PT2-3002, 126465	6	
	Regulator, PT2-3004, 20670	1	
	Transducer, PT2-3001, L-163-6	1	
	Transducer, PT2-300, H202-13	1	
	Thermocouple, Iron-Constantan	1	
	Thermal Resistor Assembly, CPER61-065, T8SB-235	1	



Remarks

Quantity

Item

PRC Index

Transducer--OPEP and Solar Array, C200979

2.13

### 3.0: POWER SUPPLY PARTS COMPLEMENT

<u>PRC Index</u>	<u>Item</u>	<u>Quantity</u>	<u>Remarks</u>
3.1	Solar Array Installation, 100022		
	Solar Paddle Assembly, 100010	2	See 3.1.1
3.1.1	Solar Paddle Assembly, 100010		
	Module Assembly, Solar Cell, 201022-1	142	See 3.1.1.1
	Module Assembly, Solar Cell, 201022-2	2	See 3.1.1.2
3.1.1.1	Module Assembly, Solar Cell, 201022-1		
	Solar Cell, 201021	112	
	Board--PCNo. 2, 201133-1	1	
	Board--PCNo. 2, 201134-1	15	
	Board--PCNo. 3, 201135-1	1	
	Connector Strip, 201136-1	4	
	Terminal, SP0056-2	2	
3.1.1.2	Module Assembly, Solar Cell, 201022-2		
	Solar Cell, 201021	112	
	Board--PCNo. 1, 201133-1	1	
	Board--PCNo. 2, 201134-1	15	
	Board--PCNo. 3, 201135-1	1	
	Connector Strip, 201136-1	4	
	Terminal, SP0056-2	4	
	Thermistor Tab, PT4-14	1	

<u>PRC Index</u>	<u>Item</u>	<u>Quantity</u>	<u>Remarks</u>
3.2	Battery Pack, 204593 Structure Assembly, Battery Pack, 205870	1	

Remarks

Quantity

Item

PRC Index

Harness, P13404

3.3

<u>PRC Index</u>	<u>Item</u>	<u>Quantity</u>	<u>Remarks</u>
3.4	<u>Converters, D13405</u>		
	Converter 1, C206565	1	N
	Converter 2, C206566	1	N
	Converter 3, C206567	1	N
	Converter 4, C206568	1	N
	Converter 5 and 6, C206569	2	N
	Converter 7 and 8, C206805	2	N
	Converter 9, C206570	1	N
	ACS Inverter Assembly, C207540	1	N

<u>PRC Index</u>	<u>Item</u>	<u>Quantity</u>	<u>Remarks</u>
3.5	<u>Junction Boxes, D13407</u>		
	OPEP End Junction Box, 202435	1	N
	Central Junction Box, 202434	1	N
	Forward End Junction Box, 202436	1	See 3.5.3
	OPEP End Junction Box, 207256-1	1	N
	OPEP End Junction Box, 207256-2	1	N
3.5.3	<u>Forward End "J" Box Assembly, 202436</u>		
	Terminal Board Assembly, 202436	1	
	Connector, DBM-9W4_-NM-1, Cannon Electric, 9 pin	2	
	Connector, PT2-5-2, 15 pin	1	
	Connector, PT2-5-3, 25 pin	1	
	Connector, PT2-5-4, 37 pin	2	
	Connector, PT2-5-5, 50 pin	3	
	Connector, PT2-5-6, 9 pin	3	
	Connector, PT2-5-7, 15 pin	1	
	Connector, PT2-5-8, 25 pin	1	
	Connector, PT2-5-9, 37 pin	1	
	Connector, PT2-5-10, 50 pin	2	
	Connector, DBM-13W6_-NM-1, Cannon Electric, 13 pin	2	

<u>PRC Index</u>	<u>Item</u>	<u>Quantity</u>	<u>Remarks</u>
3.6	<u>Power Integration Unit, 201543</u>		
	400-cps Sync Amplifier, 201734	1	See 3.6.1
	2461-cps Sync Amplifier, 201862	1	See 3.6.2
	Current Monitor, Battery, 201929	1	See 3.6.3
	Current Monitor, Driver Inverter, 204323	1	See 3.6.4
	Charge Regulator, Battery, 201931	1	See 3.6.5
	Connector Panel Assembly, 207695	1	See 3.6.6
	Component Subassembly, 207980	1	See 3.6.7
	Relay Assembly, 207983	1	See 3.6.8
	Junction Board Assembly No. 1, 207723	1	N
	Junction Board Assembly No. 2, 207725	1	N
	Junction Board Assembly No. 3, 207727	1	N
	Junction Board Assembly No. 4, 207729	1	N
	Semiconductor Subassembly No. 1, 208191	1	See 3.6.13
	Semiconductor Subassembly No. 2, 208193	1	See 3.6.14
	Telemetry Unit, 207307	1	N
	Power Transformer Assembly, 204218	1	N
3.6.1	<u>400-cps Sync Amplifier, 201734</u>		
	Printed Circuit Boards, Mil-P-18177	5	
	Pulse Transformer, PT6-1000-1	1	
	Transistor, 2N535B, PT4-7033	3	
	Transistor, 2N697, Mil-S-19500/99A	2	
	Diode, 1N270, PT4-2028	3	

<u>PRC Index</u>	<u>Item</u>	<u>Quantity</u>	<u>Remarks</u>
3.6.1	400-cps Sync Amplifier, 201734 (Continued)		
	Diode, 1N459, PT4-2003	2	
	Diode, 1N974B, PT4-2029	2	
	Diode, 1N754A, Mil-S-19500/127	1	
	Diode, 1N3022B, Mil-S-19500/115	1	
	Capacitor, PT4-1010-F104M	1	
	Capacitor, Mil-C-26655A, CS13AF_K	7	
	Capacitor, Mil-C-26655A, 50 v, 20%	5	
	Capacitor, Mil-C-11015B, CK06CW_K	7	
	Capacitor, 550062-AH3R3M	5	
	Resistor, Mil-R-11C, RC07GF_J, 5%, 1/4 w	29	
	Resistor, Mil-R-11C, RC20GF_J, 5%, 1/2 w	2	
	Resistor, Mil-R-11C, RC32GF_J, 5%, 1 w	1	
	Resistor, Mil-R-26, RW59V, 5%, 3 w	1	
	Connector, Pin, .062 Diameter, 1/2 Hard Brass, QQ-B-626, SP0085-3	12	
3.6.2	2461-cps Sync Amplifier, 201862		
	Printed Circuit Boards, Mil-P-18177	5	
	Connector, Pin, SP0085-3	30	
	Transductor, PT6-1000-2	1	
	Resistor, Mil-R-11C, RC07GF_J	47	
	Resistor, Mil-R-11C, RC20GF_J	2	
	Resistor, Mil-R-11C, RC32GF_J	1	



<u>PRC Index</u>	<u>Item</u>	<u>Quantity</u>	<u>Remarks</u>
3.6.2	2461-cps Sync Amplifier, 201862 (Continued)		
	Resistor, Mil-R-26, RW59V	1	
	Capacitor, PT4-1010-D203K	4	
	Capacitor, Mil-C-11015	7	
	Capacitor, 550062, AH3R3K	4	
	Capacitor, Mil-C-26655, CS13AF_K	7	
	Diode, Mil-S-19500/200, 1N270	4	
	Diode, Mil-S-19500/117, 1N974B, Zener	2	
	Diode, Mil-S-19500/115A, 1N3022B	1	
	Diode, PT4-2003, 1N459	2	
	Diode, PT4-2030, 1N754A	1	
	Transistor, Mil-S-19500/99A, 2N697	2	
	Transistor, PT4-7033, 2N535B	3	
3.6.3	Current Monitor, Battery, 201929		
	Printed Circuit Boards, Mil-P-18177	4	
	Transducer Assembly, 203893	1	
	Transducer, D007-1	1	
	Transducer, D008-1	1	
	Transducer, D004-1	1	
	Connector, Pin, SP0085-3	22	
	Transistor, PT4-7001, 2N720A	1	
	Diode, PT4-2001, 1N647	15	

<u>PRC Index</u>	<u>Item</u>	<u>Quantity</u>	<u>Remarks</u>
3.6.3	Current Monitor, Battery, 201929 (Continued)		
	Resistor, Mil-R-26, RW59V	2	
	Resistor, Mil-R-10509, RN65 F	7	
	Resistor, PT4-7-C F	5	
	Capacitor, Mil-C-26655, CS13AD K, 15 v	2	
	Capacitor, Mil-C-26655, CS13AE K, 20 v	1	
	Capacitor, Mil-C-26655, CS13AF K, 35 v	2	
	Capacitor, Mil-C-27287, CTM103VAK	1	
3.6.4	Drive Inverter, Current Monitor, 204323		
	Printed Circuit Boards, Mil-P-18177	4	
	Connector, Pin, SP0085-3	14	
	Resistor, Mil-R-10509D, RN60C F	11	
	Resistor, Mil-R-10509D, RN65B F	1	
	Capacitor, Mil-C-11015B, CK06CW472K	7	
	Capacitor, PT4-1010-F104K	2	
	Diode, PT4-2001, 1N647	5	
	Transistor, PT4-7001, 2N720A	5	
	Transformer, T004-1	1	
	Transformer, T008-1	1	
	Transformer, T010-1	1	
	Choke, L005-1	1	

PRC Index

3.6.5

<u>Item</u>	<u>Quantity</u>	<u>Remarks</u>
Charge Regulator, Battery, 201931		
Printed Circuit Board	6	
Connector, Pin, SP0085-3	30	
Transistor, PT4-7024, 2N1890	4	
Transistor, PT4-7009, 2N930	4	
Transistor, PT4-7001, 2N720A	2	
Transistor, Mil-S-19500/75, Unijunction, 2N490	1	
Diode, PT4-2037, 1N3063, Silicon	3	
Diode, Mil-S-19500/127, 1N758A, Zener	1	
Diode, Mil-S-19500/159, 1N821A, Zener	1	
Diode, Mil-S-19500/127, 1N759A, Zener	2	
Diode, PT4-2001, 1N647	2	
Diode, Mil-S-19500/118, 1N485B	5	
Diode, Mil-S-19500/127, 1N752A	3	
Diode, Mil-S-19500/127, 1N754A	2	
Silicon-Controlled Rectifier, PT4-2052, 3A101	1	
Resistor, Mil-R-10509D, RN65 __ F	8	
Resistor, PT4-13V-1871F, Wirewound, 3 w	1	
Resistor, Mil-R-10509D, RN60 __ F	16	
Resistor, Mil-R-26C, RW59G __, 3 w, 5%, Wirewound	4	
Capacitor, Mil-C-11015B, CK06/5CW __ K	2	

<u>PRC Index</u>	<u>Item</u>	<u>Quantity</u>	<u>Remarks</u>
3.6.6	<u>Connector Panel Assembly, 207695</u>		
	Panel, Connector, 208109-1	1	
	Board Assembly, TB No. 3, 209064-1	1	N
	Connector, PT2-5-5	2	
	Connector, PT2-5-10	6	
3.6.7	<u>Component Subassembly, 207980</u>		
	Board Assembly, TB No. 2, 207330	1	N
	Board Assembly, TB No. 1, 207329	1	N
3.6.8	<u>Relay Assembly, 207983</u>		
	Time Delay Module, PT2-1018	2	
	Relay, 2PDT, PT2-1005	6	
3.6.13	<u>Semiconductor Subassembly No. 1, 208191</u>		
	Diode, MM521B, 1N1204A	10	
	Transistor, Mil-S-19500/180, 2N1486	6	
3.6.14	<u>Semiconductor Subassembly No. 2, 208193</u>		
	Diode, MM521B, 1N1204A	2	
	Diode, PT4-2057, 1N250B	2	
	Diode, PT4-2056, 1N1186	2	

#### 4.0: THERMAL CONTROL PARTS COMPLEMENT

<u>PRC Index</u>	<u>Item</u>	<u>Quantity</u>	<u>Remarks</u>
4.1	<u>Box Structure (Insulation), 100472</u>		

<u>PRC Index</u>	<u>Item</u>	<u>Quantity</u>	<u>Remarks</u>
4.2	Solar Array (Insulation), DL100825		

Remarks

Quantity

Item

PRC Index

External Package T.C., DL100826

4.3

<u>PRC Index</u>	<u>Item</u>	<u>Quantity</u>	<u>Remarks</u>
4.4	<u>Louver Assembly, 100023</u>		
	Louver Installation Temperature Control, 100532	2	See 4.4.1
	Louver Installation Aft, 100728	2	See 4.4.2
4.4.1	<u>Louver Installation Temperature Control, 100532</u>		
	Louver Assembly, 100185-1	41	
	Louver Assembly, 100185-2	5	
	Louver Assembly, 100185-3	5	
	Actuator, Bimetal, 100170	51	
	Bearing, 100178	102	
4.4.2	<u>Louver Installation Aft, 100728</u>		
	Louver Assembly, 100185-4	5	
	Actuator, Bimetal, 100170	5	
	Bearing, 100178-1	10	



5.0: STRUCTURE PARTS COMPLEMENT

Remarks

Quantity

Item

PRC Index

Body Assembly, Spacecraft (Basic Structure), 100004

5.1

Remarks

Quantity

Item

PRC Index

Solar Array (Main Frame), (2 ea.)

5.2

<u>PRC Index</u>	<u>Item</u>	<u>Quantity</u>	<u>Remarks</u>
5.3	<u>Folding Devices</u>		
	Release System Installation, Deployment, 100009	1	See 5.3.1
	Boom Installation, EP No. 1, 100013	1	See 5.3.2
	Boom Installation, EP No. 2, 100017	1	See 5.3.3
	Boom Installation, EP No. 3, 100020	1	See 5.3.4
	Boom Installation, EP No. 4, 100021	1	See 5.3.5
	Boom Installation, EP No. 5, 100015	1	See 5.3.6
	Boom Installation, EP No. 6, 100018	1	See 5.3.7
	Boom Installation, High-Gain Antenna, 100016	1	See 5.3.8
	Drive and Support Assembly, OPEP, 100014	1	See 5.3.9
	Solar Array Installation, 100022	1	See 5.3.10
5.3.1	<u>Release System Installation, Deployment, 100009</u>		
	Valve Assembly, 102445	4	See 5.3.1.1
	Release Assembly, 102114	8	See 5.3.1.2
	Release Assembly, 102113	4	See 5.3.1.2
5.3.1.1	<u>Valve Assembly, 102445</u>		
	Pressure Gauge Assembly, C102125	1	
	Valve, Explosive N.C., C100094	1	
	Tank Assembly, 3183	1	
5.3.1.2	<u>Release Assembly, 102114</u>		
	Piston, 100647-1	2	
	Spring, 100642-1	2	

<u>PRC Index</u>	<u>Item</u>	<u>Quantity</u>	<u>Remarks</u>
5.3.2	<u>Boom Installation, EP No. 1, 100013</u>		
	Switch, PT2-2000	1	
	Spring, 100646	1	
	Spring, 100639	2	
	Hinge Assembly, 100555	1	See 5.3.2.4
	Terminal Strip Assembly, 100346	1	
	Hinge Half, 100543	1	
	Boom, Assembly of, 100537	1	See 5.3.2.7
5.3.2.4	<u>Hinge Assembly, 100555</u>		
	Switch, PT2-2000	1	
	Spring, 100646	1	
	Spring, 100639	1	
	Hinge Half, 100573	1	
	Hinge Half, 100541	1	
	Terminal Strip Assembly, 100346	1	
5.3.2.7	<u>Boom, Assembly of, 100537</u>		
	Hinge Half, 100650	1	
5.3.3	<u>Boom Assembly, EP No. 2, and 120-136-mc</u>		
	<u>Omni Antenna, 100557-1, -2</u>		
	Switch, PT2-2000	2	
	Spring, 100639-1	4	
	Spring, Locking, 100646-1	2	
	Hinge Assembly, 100566	2	See 5.3.3.4

<u>PRC Index</u>	<u>Item</u>	<u>Quantity</u>	<u>Remarks</u>
5.3.3	Boom Assembly, EP No. 2, and 120-136-mc Omni Antenna, 100557-1, -2 (Continued)		
	Hinge Half, 100563	2	
	Boom Assembly, 100558	2	See 5.3.3.6
	Terminal Strip, 100346	2	
5.3.3.4	Hinge Assembly, 100566		
	Switch, PT2-2000	1	
	Spring, Hinge-Locking, 100646	1	
	Spring, Torsional Drive, 100639-3	2	
	Hinge Half, 100561-1	1	
	Hinge Half, 100573-1	1	
5.3.3.6	Boom Assembly, 100558		
	Boom, 100558-2	1	
	Hinge Half Assembly, 100567-1	1	
5.3.4	Boom Assembly, EP No. 3, 100569		
	Hinge Assembly, 100998	1	See 5.3.4.1
	Hinge Assembly, 100576	1	See 5.3.4.2
	Boom, 100570	1	
5.3.4.1	Hinge Assembly, 360-mc Antenna, 100990		
	Switch, PT2-2000	1	
	Terminal Strip, 100346	1	
	Spring, 100646	1	

<u>PRC Index</u>	<u>Item</u>	<u>Quantity</u>	<u>Remarks</u>
5.3.4.1	Hinge Assembly, 360-mc Antenna, 100990 (Continued)		
	Spring, 100639	2	
	Hinge Half, 100993	1	
	Hinge Half, 100991	1	
5.3.4.2	Hinge Assembly, EP No. 3, 100576		
	Switch, PT2-2000	1	
	Terminal Strip Assembly, 100346-1	1	
	Spring, 100646	1	
	Spring, 100639	2	
	Hinge Half, 100573	1	
	Hinge Half, 100572	1	
5.3.5.	Boom Assembly, EP No. 4, 100578		
	Boom, Assembly of, 100579-1	1	
	Boom, Assembly of, 100579-2	1	
	Hinge Assembly, 100585	1	See 5.3.5.3
	Terminal Strip Assembly, 100346	1	
5.3.5.3	Hinge Assembly, 100585		
	Hinge Half, 100581-1	1	
	Hinge Half, 100582-1	1	
	Spring, 100639-2	2	
	Spring, 100646-1	1	
	Switch, PT2-2000	1	

<u>PRC Index</u>	<u>Item</u>	<u>Quantity</u>	<u>Remarks</u>
5.3.6	Boom Assembly, EP No. 5, 100587		
	Terminal Strip, 100346	2	
	Hinge Assembly, 100602	1	See 5.3.6.2
	Hinge Assembly, 100603	1	See 5.3.6.3
	Hinge Assembly, 100617	1	See 5.3.6.4
5.3.6.2	Hinge Assembly, Inboard EP No. 5, Bcom, 100602		
	Switch, PT2-2000	1	
	Spring, 100646	1	
	Spring, 100639	2	
	Hinge Half, 100611	1	
	Hinge Half, 100610	1	
5.3.6.3	Hinge Assembly, Intermediate EP No. 5		
	Switch, PT2-2000	1	
	Spring, 100639-2	2	
	Spring, 100646-1	1	
	Hinge Half, 100612	1	
	Hinge Half, 100594	1	
5.3.6.4	Hinge Assembly, EP No. 5 and No. 6, Boom, 100617		
	Switch, PT2-2000	1	
	Spring, 100639-2	2	
	Spring, 100646-1	1	
	Hinge Half, 100612-1	1	
	Hinge Half, 100613-1	1	

<u>PRC Index</u>	<u>Item</u>	<u>Quantity</u>	<u>Remarks</u>
5.3.7	<u>Boom Assembly, EP No. 6, 100605</u>		
	Hinge Assembly, 100616	1	See 5.3.7.1
	Hinge Assembly, 100617	2	See 5.3.6.4
	Terminal Strip Assembly, 100346	1	
5.3.7.1	<u>Hinge Assembly, Inboard EP No. 6, Boom, 100616</u>		
	Switch, PT2-2000	1	
	Spring, 100639-2	2	
	Spring, 100646-1	1	
	Hinge Half, 100611	1	
	Hinge Half, 100610	1	
5.3.8	<u>Boom Assembly, High-Gain Antenna, 100623</u>		
	Switch, PT2-2000	2	
	Hold-Down, 102176	1	
	Hold-Down, 100969-1	4	
	Spring, 100646	1	
	Hinge Assembly, 100631	1	See 5.3.8.5
	Hinge Assembly, 100628	1	See 5.3.8.6
	Boom Assembly, 100624	1	
	Terminal Assembly, 100346	1	
5.3.8.5	<u>Hinge Assembly, Outboard/High-Gain Antenna, 100631</u>		
	Spring, 100639-1	2	
	Spring, 100646-1	1	



<u>PRC Index</u>	<u>Item</u>	<u>Quantity</u>	<u>Remarks</u>
5.3.8.5	<u>Hinge Assembly, Outboard/High-Gain Antenna, 100631</u> <u>(Continued)</u>		
	Hinge Half, 100630	1	
	Hinge Half, 100629	1	
5.3.8.6	<u>Hinge Assembly, Inboard/High-Gain Antenna, 100628</u>		
	Spring, 100639-1	2	
	Hinge Half, 100627	1	
	Hinge Half, 100626	1	
5.3.9	<u>Drive and Support Assembly, OPEP, 100014</u>		
	Connector, PT2-5-5	4	
	Connector, PT2-5-4	1	
	Connector, PT2-5-3	1	
	Connector, PT2-5-2	1	
	Boom, Assembly of, 102136-1	2	Just Booms
	Spring, 100646-1	2	
	Spring, 100639-3	4	
	Drive System, Assembly of, 100405	1	See 5.3.9.8
5.3.9.8	<u>Drive System Assembly, OPEP, 100405</u>		
	Switch, PT2-2000	3	
	Connector, PT2-5-4	1	
	Connector, PT2-5-5	1	
	Terminal Board Assembly, 102082-1	1	
	Hinge Assembly, 100412	2	

<u>PRC Index</u>	<u>Item</u>	<u>Quantity</u>	<u>Remarks</u>
5.3.10	Solar Array Installation, 100022	2	
	Spring, 102063-1	2	See 5.3.10.1
	Hinge Assembly, Solar Array		
5.3.10.1	Hinge Assembly, Solar Array, 100646	2	
	Switch, PT2-2000 (Micro)	2	
	Terminal Assembly, 100346-1	1	
	Spring, 100662-1	2	
	Spring, 100639-4	1	
	Hinge Half, 100658-1	1	
	Hinge Half, 100657-1		

<u>PRC Index</u>	<u>Item</u>	<u>Quantity</u>	<u>Remarks</u>
5.4	<u>Interstage and Separation, 100002</u>		
	Interstage Assembly, 100691	1	See 5.4.1
	Clamp Assembly, 100696	1	
	Mechanism Assembly and Installation, Interstage Release, 100686	1	
	Spring, Separation/Interstage, 100702	1	
	Release Assembly, Separation, 101966	1	
	Retainer, Spring Separation Band, 102367	1	
	Spring, Separation Band/Interstage, 102375	1	
	Switch Installation, Separation-- Spacecraft/Interstage, 102662	1	
5.4.1	<u>Interstage Assembly, 100691</u>		
	Shear Pin, 100456	8	
	Strut, Assembly of, 100949	2	
	Cable Assembly, 102198	4	
	Support, Spring, 100957	4	
	Strut, Assembly of, 100693-2	4	
	Strut, Assembly of, 100693-1	4	
	Fitting, Interstage, 100692-1	2	
	Fitting, Interstage, 100692-1	2	

### III. SUBSYSTEM ASSESSMENTS

This section consists of the second assessment TAM's for each of the five major spacecraft subsystems. Their order of appearance follows that of the preliminary assessment: TAM No. 9, "Communications and Data Handling Subsystem"; TAM No. 12, "Attitude Control and Stabilization Subsystem"; TAM No. 11, "Power Supply Subsystem"; TAM No. 8, "Thermal Control Subsystem"; and TAM No. 6, "Structure Subsystem."

TECHNICAL ADVISEMENT MEMORANDUM NO. 9

SECOND RELIABILITY ASSESSMENT FOR  
THE OGO COMMUNICATIONS AND  
DATA HANDLING SUBSYSTEM

# TABLE OF CONTENTS

	<u>Page</u>
1. Introduction . . . . .	1
a. General . . . . .	1
b. Value Functions . . . . .	2
2. Subsystem Description . . . . .	2
3. Command Equipment Description . . . . .	3
a. General . . . . .	3
b. Antenna and Dual Diplexer-Coupler . . . . .	6
c. Command Receiver . . . . .	6
d. Tone Decoder . . . . .	9
e. Digital Decoder . . . . .	11
(1) General . . . . .	11
(2) Matrix Command . . . . .	<del>11</del>
(3) Flexible Format Command . . . . .	21
f. Command Distribution Unit . . . . .	22
4. Command Equipment Interrelationships . . . . .	22
a. General . . . . .	22
b. Determination of Initial Conditions . . . . .	24
c. Determination of Time Relationships . . . . .	25
d. Determination of Failure Effects . . . . .	25
e. Power Switching for Experiments . . . . .	27
f. Miscellaneous . . . . .	28
5. CDH Numerical Assessment . . . . .	28
a. Model Equations . . . . .	28
b. Preparation of Reliability Inputs . . . . .	30
c. Calculations . . . . .	39
6. Conclusions . . . . .	39
References . . . . .	43

## LIST OF EXHIBITS

	<u>Page</u>
1. Command Equipment Functional Block Diagram . . . . .	4
2. Antenna and Dual Diplexer Functional Block Diagram (One Dipole) . . . . .	7
3. Command Receiver Functional Block Diagram . . . . .	8
4. Tone Decoder Functional Block Diagram . . . . .	10
5. Digital Decoder Functional Block Diagram--Information, Sync, and Squelch . . . . .	12
6. Digital Decoder Functional Block Diagram--Shift Register and Parity . . . . .	13
7. Digital Decoder Functional Block Diagram--Programmer and Associated Circuits . . . . .	14
8. Digital Decoder Functional Block Diagram--Address Storage, Internal and Decoder . . . . .	15
9. Digital Decoder Functional Block Diagram--Matrix Sampling Pulse and Enable Output Line . . . . .	16
10. Digital Decoder Functional Block Diagram--Matrix Pulser, . . .	17
11. Digital Decoder Functional Block Diagram--Word Command Circuits . . . . .	18
12. Command Distribution Unit Functional Block Diagram . . . . .	23
13. CDH State Probabilities, $P_{CDH}(S_i, t)$ . . . . .	40
14. Classical Reliability Curves for the CDH Subsystem . . . . .	42

## LIST OF ABBREVIATIONS

A	Antenna
a-m	amplitude modulated
CDH	Communications and Data Handling
CDU	Command Distribution Unit
CE	Command Equipment
CR1, 2	Command Receiver 1, 2
D	Dual Diplexer-Coupler
DD1, 2	Digital Decoder 1, 2
DDHA	Digital Data Handling Assembly
DR	Driver
FF	Flexible Format
F-F	Flip-Flop
FSK	Frequency-Shift Keying
G CH B, C, D, E	Gating Channel B, C, D, E
I	Inverter
OS	One-Shot
PR	Power Regulator
r-f	radio frequency
S1, 2	Squelch 1, 2
SP	Special Programmer
SR	Shift Register
TC	Tuned Circuit
TD	Tone Decoder
TR CH A, B, C, D, E	Trigger Channel A, B, C, D, E



## TECHNICAL ADVISEMENT MEMORANDUM NO. 9

To: Assistant OGO Project Manager, GSFC, NASA  
From: PRC OGO Assessment Team  
Subject: Second Reliability Assessment for the OGO Communications and Data Handling Subsystem

### 1. Introduction

#### a. General

When the extent of the second assessment was planned, it was decided that the Communications and Data Handling (CDH) Subsystem would not be fully reassessed. This decision was based on the fact that the CDH is the most complex subsystem and, in addition, the preliminary CDH assessment was actually treated to the depth of a second assessment in some areas. Accordingly, it was expected that the second assessment report for the CDH Subsystem would consist of TAM No. 2 (which treats the Main Commutator Matrix in detail) and the two PRC letters to Messrs. Purcell and Ragland of GSFC--dated 16 July 1962 and 24 July 1962, respectively--together with a slightly revised preliminary assessment (i. e., updated wherever possible without extensive effort). However, because of the delays in receiving information on many of the subsystems, the second assessment schedule slipped accordingly, and the second assessment plans in the CDH area were necessarily revised. Specifically, since the Command Equipment (CE) had not received as much attention in the preliminary assessment as other portions of the CDH Subsystem, and because of its position in Priority Group 1 as Task No. 1, as outlined in the 21 March 1962 progress report, it was decided that this equipment should continue to receive first priority in the second assessment report.

Unfortunately, study of this equipment quickly revealed that a reasonably complete second assessment could not be completed within the time and funds allotted. This is due primarily to the fact that the major

simplifying assumptions made in the first assessment cannot all be justified at this time (considering the greater volume of information now available) in the development of the CE model. Furthermore, justification of a set of assumptions, as well as value functions, has been complicated by incomplete mission profile information (see section 4).

Therefore, it was decided that for the purposes of the second assessment report the study would consist of (1) becoming completely familiar with the CE in terms of its functions and how they are implemented, hardware-wise, (2) identifying those areas within the equipment most affected by incomplete mission profile information, and (3) updating the CDH model where possible based on (1) and (2). Since the third assessment is scheduled to follow the second immediately, it was felt that there would be no delay in beginning the detailed analysis of the CE as a first task in the third assessment.

#### b. Value Functions

~~From Reference 1, it can be seen that figure of merit~~  
analyses are based on integration of the probabilities of particular equipment states with the values of those particular states to the mission. The tasks of assigning these values vary from the obvious and straightforward to the obscure and complex. Nevertheless, all value assignments must be made on the basis of knowledge of the over-all system and mission requirements. If knowledge of the system and mission is incomplete or incorrect for any reason, assumptions must be made the final accuracy of which is grossly dependent upon the total amount of information available. Communication from NASA is hereby solicited regarding the areas identified in section 4, for the purpose of contributing further system and mission knowledge which will result in more realistic assumptions and value assignments.

#### 2. Subsystem Description

For a description of the CDH Subsystem the reader is directed to Reference 1, pages 26 through 32. A detailed description of the CE follows in the next section.

### 3. Command Equipment Description

Before undertaking a description of the CE it is necessary to make a few remarks regarding the functional block diagrams included in this section. The information for developing the diagrams came from References 2 through 23, supplemented by verbal information obtained by asking specific questions. Abbreviations here, as well as elsewhere in this memorandum, can be interpreted from the List of Abbreviations on page ii.

The functional block diagrams represent the system to the same extent as do the reference drawings. That is, only one drawing represents the entire system; the remainder represent only one piece of equipment each, even though this may be a redundant piece. Throughout the diagrams the individual blocks are titled in essentially the same manner as on the reference schematics. The written description of the system uses the same terminology unless further clarity is required.

The level of diagramming and the use of arrowheads is intentionally inconsistent. In general it was not necessary to portray the detailed logic on the functional block diagrams, but such details were shown where they were significant with respect to the over-all analysis. Thus, some AND gates are shown in the normal logical symbology while others are shown only as blocks. Arrowheads are not used except for analog signals, high-level "clock"-type signals (to separate them from the low-level "logic"-type signals), and other significant signals such as counter "Augment" and "Reset" signals. Dashed signal lines represent significant control signals.

#### a. General

The CE is configured and connected together as shown in Exhibit 1. It is composed of the following:

- 1 Antenna (A)
- 1 Dual Diplexer-Coupler (D)
- 2 Command Receivers (CR)
- 2 Digital Command Decoders (DD)

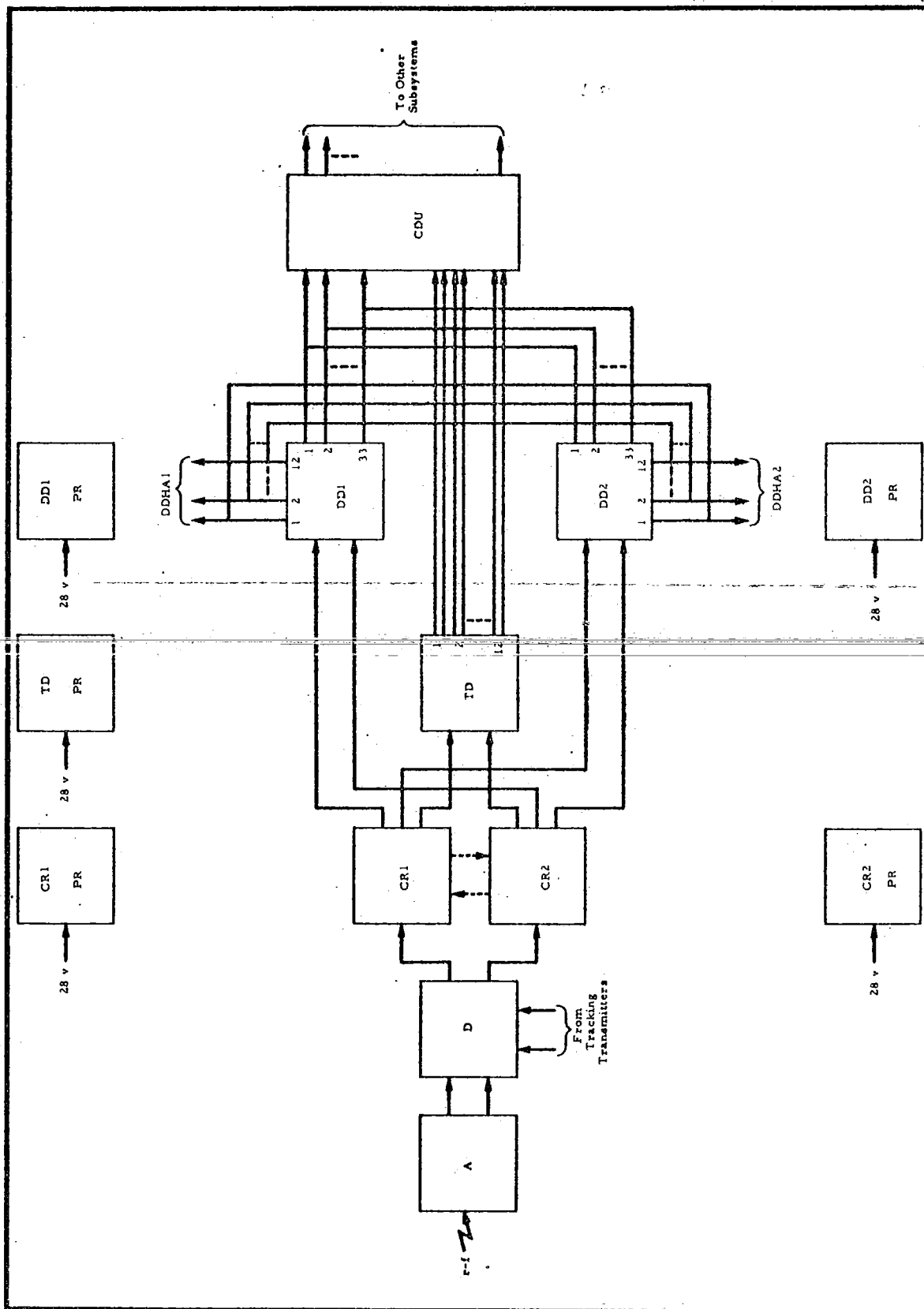


EXHIBIT 1 - COMMAND EQUIPMENT FUNCTIONAL BLOCK DIAGRAM

- 1 Tone Command Decoder (TD)
- 1 Command Distribution Unit (CDU)
- 5 Power Regulators (PR)

All ground-to-space command communications are made via the CE, being transmitted on a nominal 120-mc carrier frequency. "Upon receipt of a command signal the command equipment interprets the signal and issues appropriate control signals to other portions of the CDH Subsystem and to the other subsystems. . . . Since other subsystems require commands for various alternate modes of operation, the CE (in actuality) belongs to, and is an integral part of, every other subsystem as well as this one."

Specific commands are transmitted as amplitude modulated (a-m) signals in one of two possible ways, designated as (1) tone commands or (2) digital commands. The received r-f energy from one antenna in A passes through one diplexer in D to one CR. Each CR operates continuously, and an independent output goes to each decoder from each CR. The CR output is an audio subcarrier (tone). This audio subcarrier with a tone command meant for the TD is amplitude modulated by a sine wave only. With a digital command meant for the DD's, the audio subcarrier is frequency modulated by a digital pulse train using a frequency-shift keying (FSK) technique, in addition to being amplitude modulated by a sine wave.

Whenever the nominal 120-mc signal is not being received by the CR's, and (thus) there is no audio subcarrier output from the CR's to the decoders, the DD is kept in a squelched condition and the TD in an unsquelched condition. When a digital command is being received, the amplitude modulated portion of the CR audio subcarrier is used as a sync signal and a DD squelch removing signal; that is, detection of the sync signal disables the DD squelch circuits. The frequency modulated portion of the audio subcarrier, among other uses, serves to put the TD in a squelched state. When a tone command is being received, there is

---

<sup>1</sup>Quotation marks identify direct quotations from Reference 1.

no sync signal of the proper frequency and, therefore, the DD remains squelched while the TD handles the command.

The command information in a ground-to-space transmission can have one of three final destinations: (1) the CDU Relay Matrix, (2) the Digital Data Handling Assemblies (DDHA), or (3) the Special Programmer (SP). Those commands with a Matrix destination can perform a maximum of 254 different functions. Those with a DDHA destination are used when the CDH is operating in the Flexible Format (FF) mode to determine which of several different experiment sampling sequences is used. The SP is not considered in the subject study. As a function of the command destination, then, a command can be identified as (1) a Matrix Command, (2) an FF Command, or (3) an SP Command.

Whereas digital commands can have any of the three destinations stated in the preceding paragraph, tone commands can only be Matrix Commands with a restricted capability to perform a maximum of 12 of the 254 different functions. As presently configured, only 11 are used and 1 spare is provided.

b. Antenna and Dual Diplexer-Coupler

For the purpose of receiving commands, as opposed to transmitting tracking signals, one antenna and diplexer can be functionally diagrammed as shown in Exhibit 2. The command transmissions are received by two electrically (but not physically) independent antennas. The output from one antenna goes to half of the dual diplexer. The output from each half of the dual diplexer goes to only one CR.

c. Command Receiver

Exhibit 3 provides a functional block diagram of a CR. It can be seen that the basic receiver is a double-conversion a-m receiver. The Signal Present circuit acts as a logical AND; that is, if the Failure Detector detects the presence of the r-f carrier, modulated or not, at the input to the receiver, and the Audio Detector detects the presence of audio (implying modulation), then the Signal Present circuit does not disable the Audio Amplifier and does not boost the redundant CR output. Any other combination of indications from the Failure

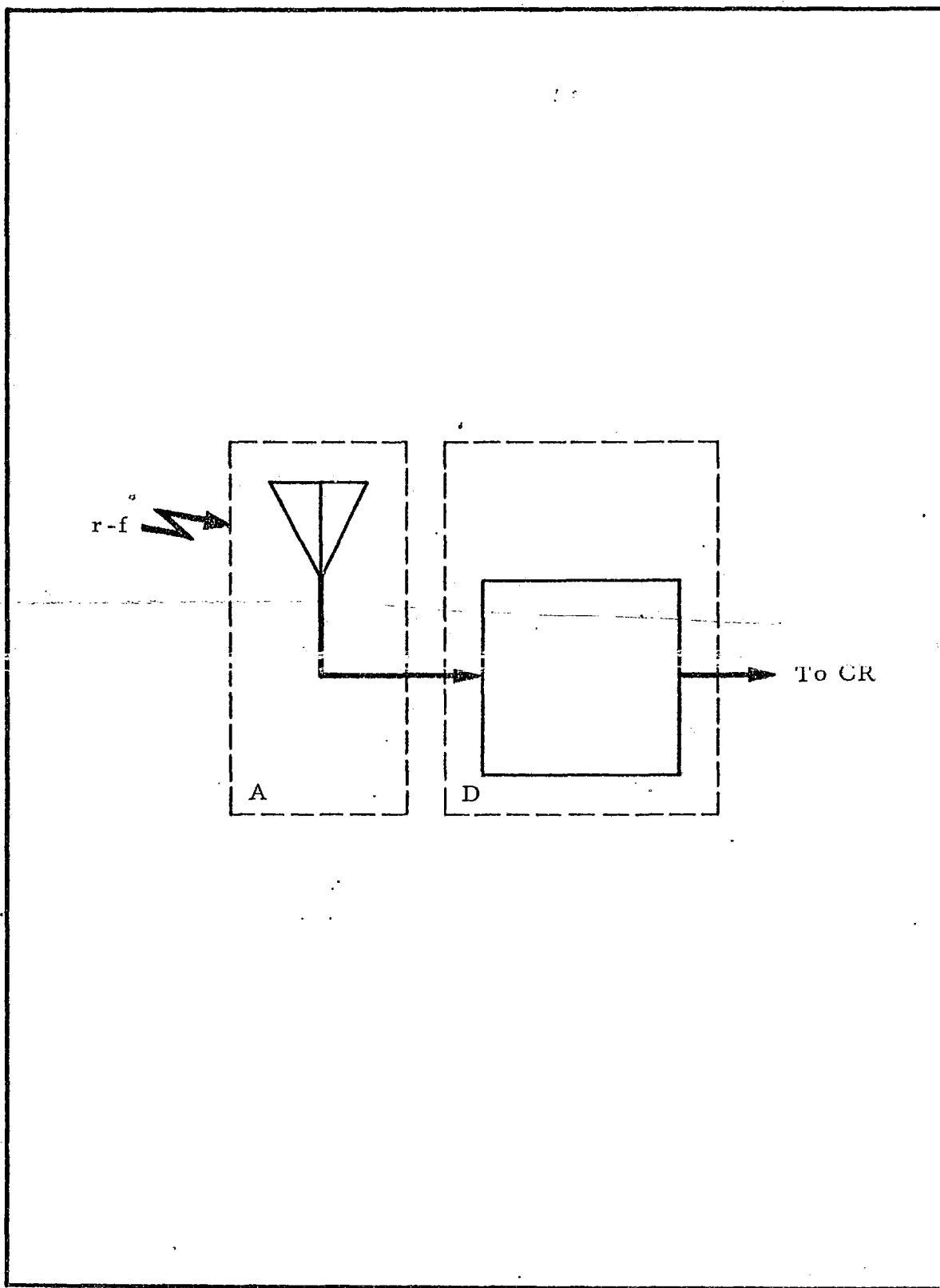


EXHIBIT 2 - ANTENNA AND DUAL DIPLEXER FUNCTIONAL BLOCK  
DIAGRAM (ONE DIPOLE)

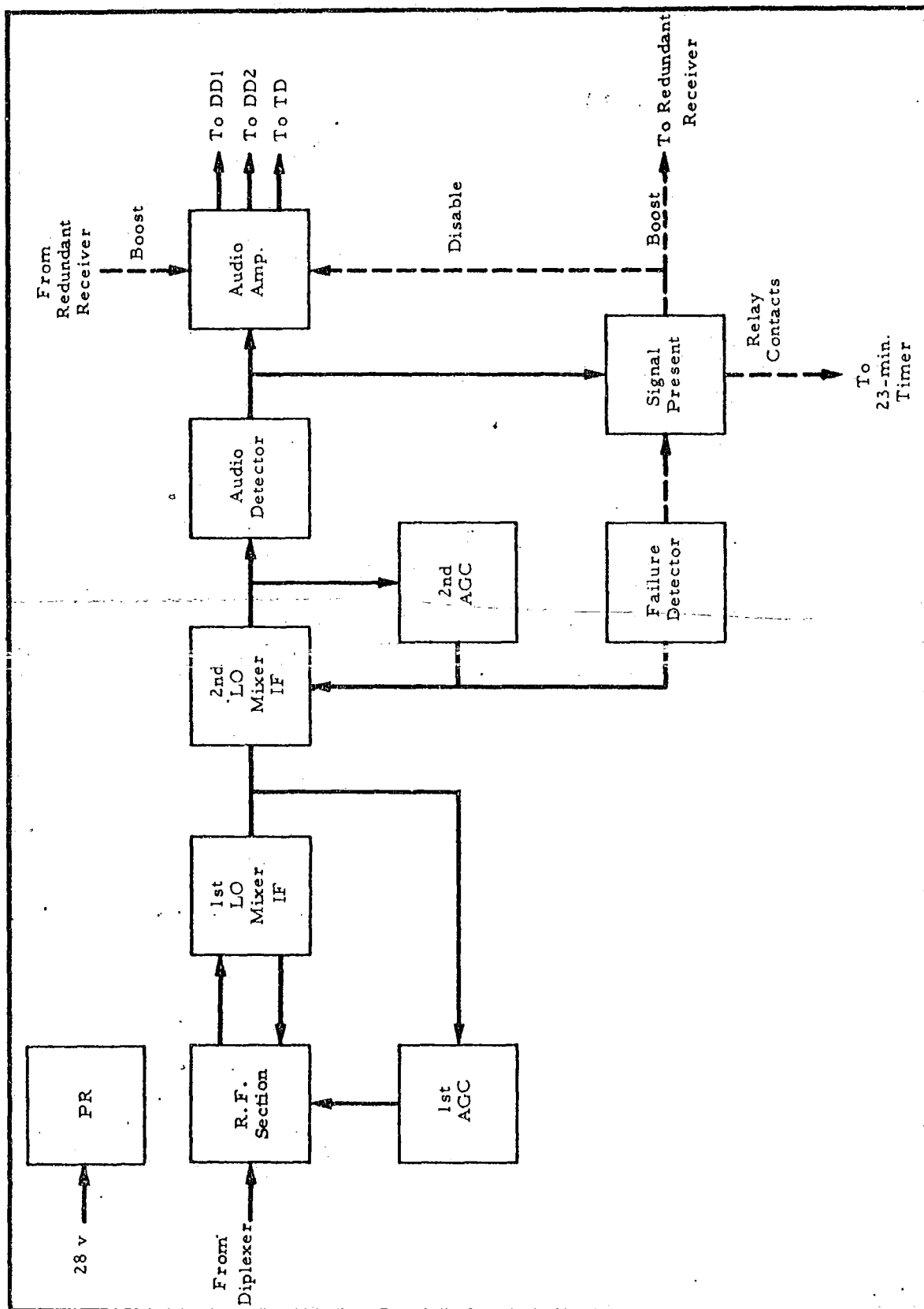


EXHIBIT 3 - COMMAND RECEIVER FUNCTIONAL BLOCK DIAGRAM



Detector and Audio Detector will cause the Signal Present circuit to squelch the Audio Amplifiers and boost the redundant receiver. It can be seen from the diagram and from this description that the output level of an unsquelched Audio Amplifier is a function of the boost signal from the redundant receiver.

d. Tone Decoder

The functional block diagram of the TD is shown in Exhibit 4. At the inputs of the TD are the audio subcarrier outputs from CR1 and CR2. A Driver (DR) circuit is used to drive the Tuned Circuits (TC's), each of which is tuned to a different frequency. The top five TC's shown in the diagram are tuned respectively to the frequencies assigned to the transmission of tone commands. Of the bottom two TC's, one is tuned to the "mark" frequency and the other is tuned to the "space" frequency associated with the frequency-shift keyed digital pulse train (see subsection 3.a). If the output of the CR's contains either the mark or space frequencies, the indication that a digital rather than a tone command is being transmitted, such frequencies are detected by one or the other of the squelch circuits (S1 or S2). The activated squelch circuit generates a signal which inhibits the selection of any of the TD relays.

The execution of a particular TD command (i.e., the operation of a TD relay) requires a reception of the selected tones in a certain sequence. Tone A must always be received first; otherwise, activation of the decoder Flip-Flops (F-F) by any of the remaining tones will be inhibited. Assume that relay K1 is to be energized. This demands that tones A, B, and C be received in ordered sequence, and that no squelch signal be present. Tone A, operating through Trigger Channel A (TR CH A), generates a pulse with the One-Shot (OS) circuit which is inverted by the Inverter (I). The pulse exists for a preset period in the astable state, during which it enables the AND gates associated with the other four channel F-F Set inputs. During the preset period, reception of tone B sets the bistable F-F associated

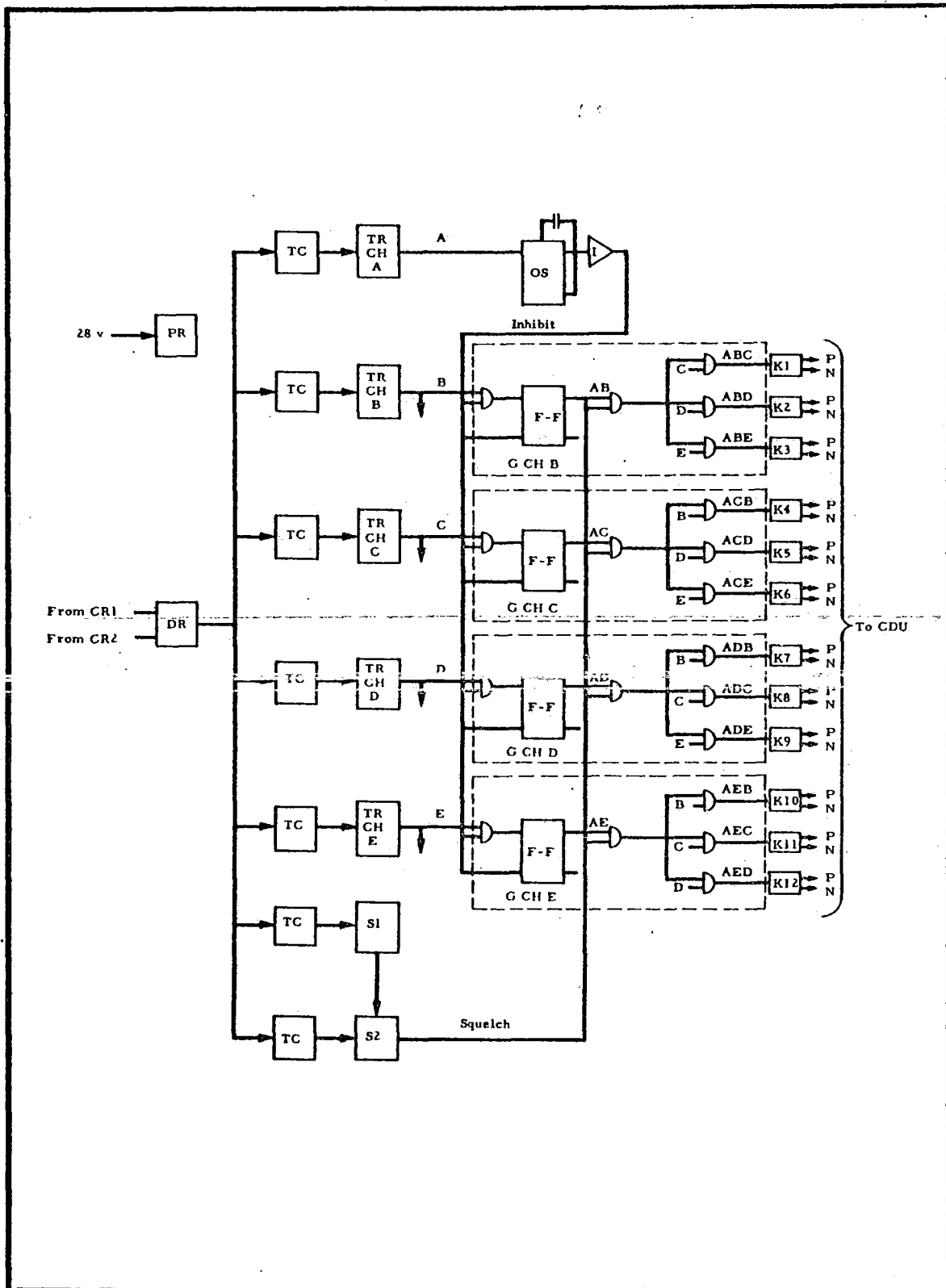


EXHIBIT 4 - TONE DECODER FUNCTIONAL BLOCK DIAGRAM

with channel B. The F-F output, AB, together with the absence of a squelch signal, enables the three AND gates associated with relays K1, K2, and K3. The selection of K1 is finally made when tone C is detected. Such detection must occur before the OS has returned to its stable state.

Note that the reception of tone C, in addition to energizing relay K1, also sets the F-F with output AC. This has no effect, however, because no other tones (including B) are present, and the necessary third term for any of the relay gates remains false. With the end of the preset period the One-Shot returns to its stable state, resetting all F-F's and readying the TD for the next tone command.

e. Digital Decoder

(1) General

For ease of discussion, the DD has been functionally described on several diagrams (see Exhibits 5 through 11). Such diagramming allows a more straightforward analysis, resulting in a better understanding of the operation of the equipment and thereby a better understanding of the possible problems to be encountered.

Depending on the particular type of digital command (Matrix, FF, or SP), the general composition of the DD inputs will differ. The descriptions that follow are based on such a type breakdown and do not discuss the detailed logic, but are more concerned with the functional aspects of the system.

(2) Matrix Command

A Matrix Command requires a 34-bit transmission. The first 24 bits contain digital data while the last 10 are used only for establishing timing periods. The first four bits are referred to as the Synchronization Word, the first bit of which is always a "1." The following three bits of the Synchronization Word are referred to as the Decoder Address bits. These three bits determine which of the two DD's will transfer data to the CDU. The bits can have any configuration except that they cannot all be "0's." (See Exhibit 8.)

The next two bits (fifth and sixth) are referred to as the Internal Address, and indicate which type of command is to follow. These two bits will always be "0's" for a Matrix Command. (See Exhibit 8.)

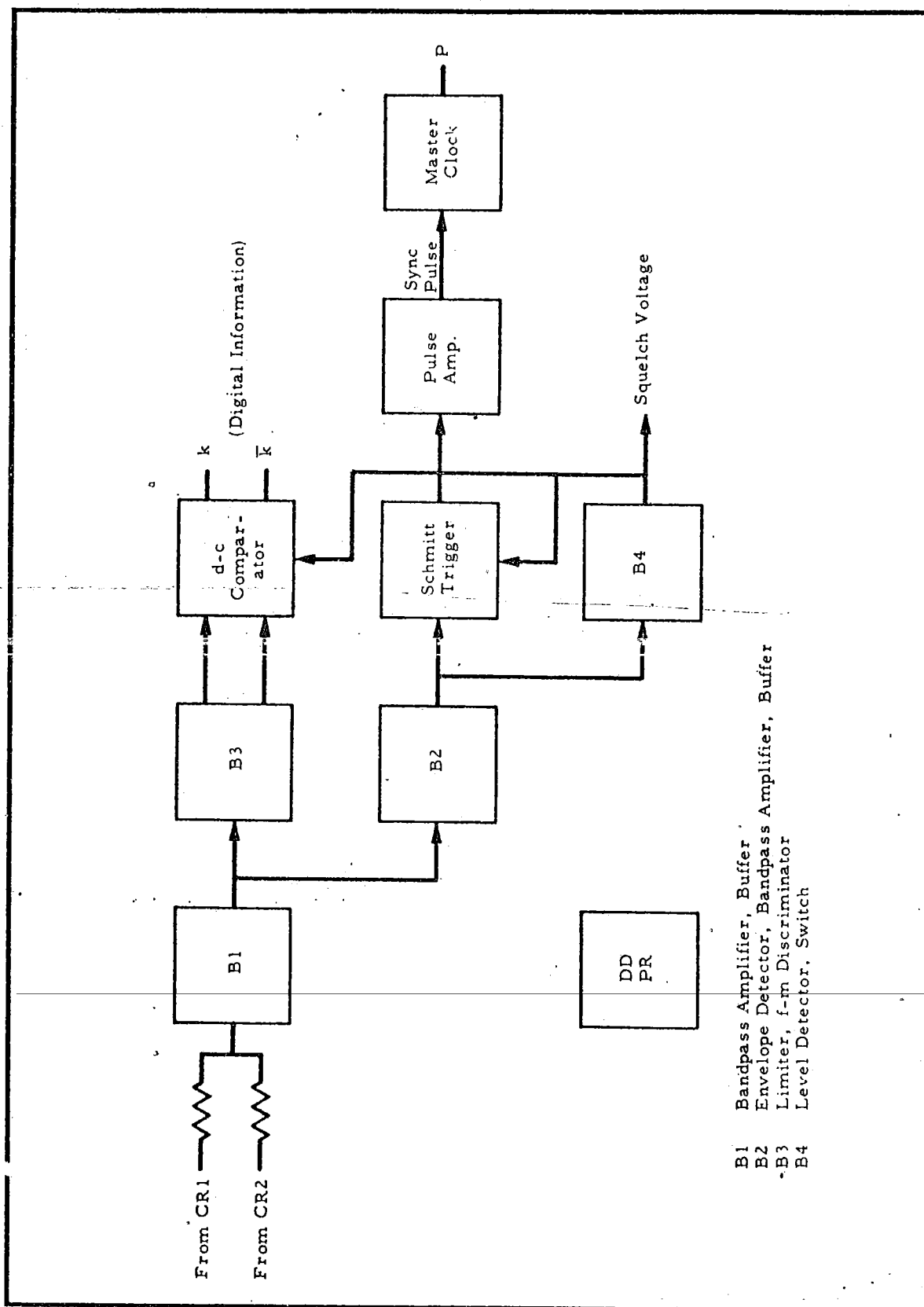


EXHIBIT 5 - DIGITAL DECODER FUNCTION BLOCK DIAGRAM--INFORMATION, SYNC AND SQUELCH

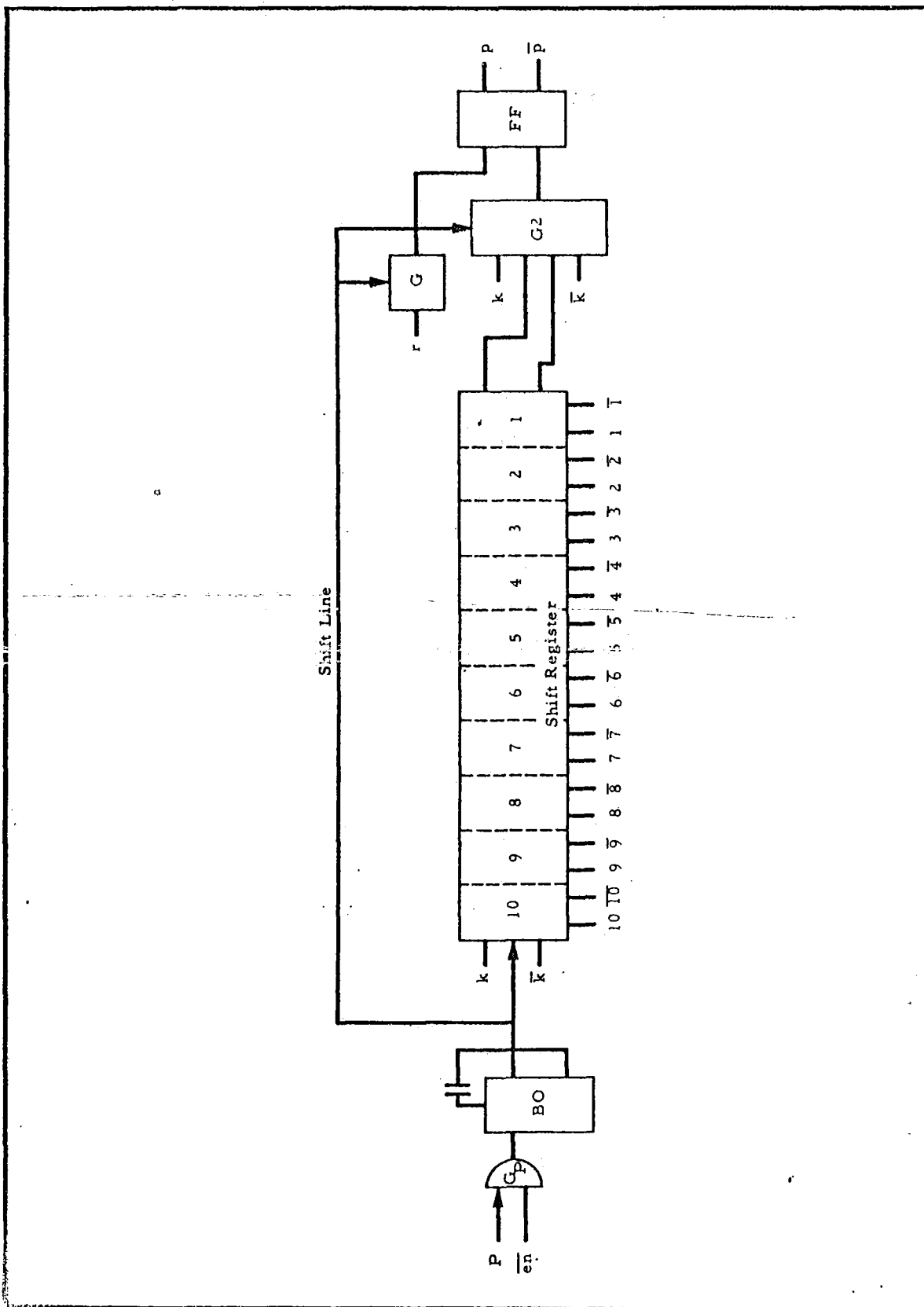


EXHIBIT 6 - DIGITAL DECODER FUNCTIONAL BLOCK DIAGRAM--SHIFT REGISTER AND PARITY

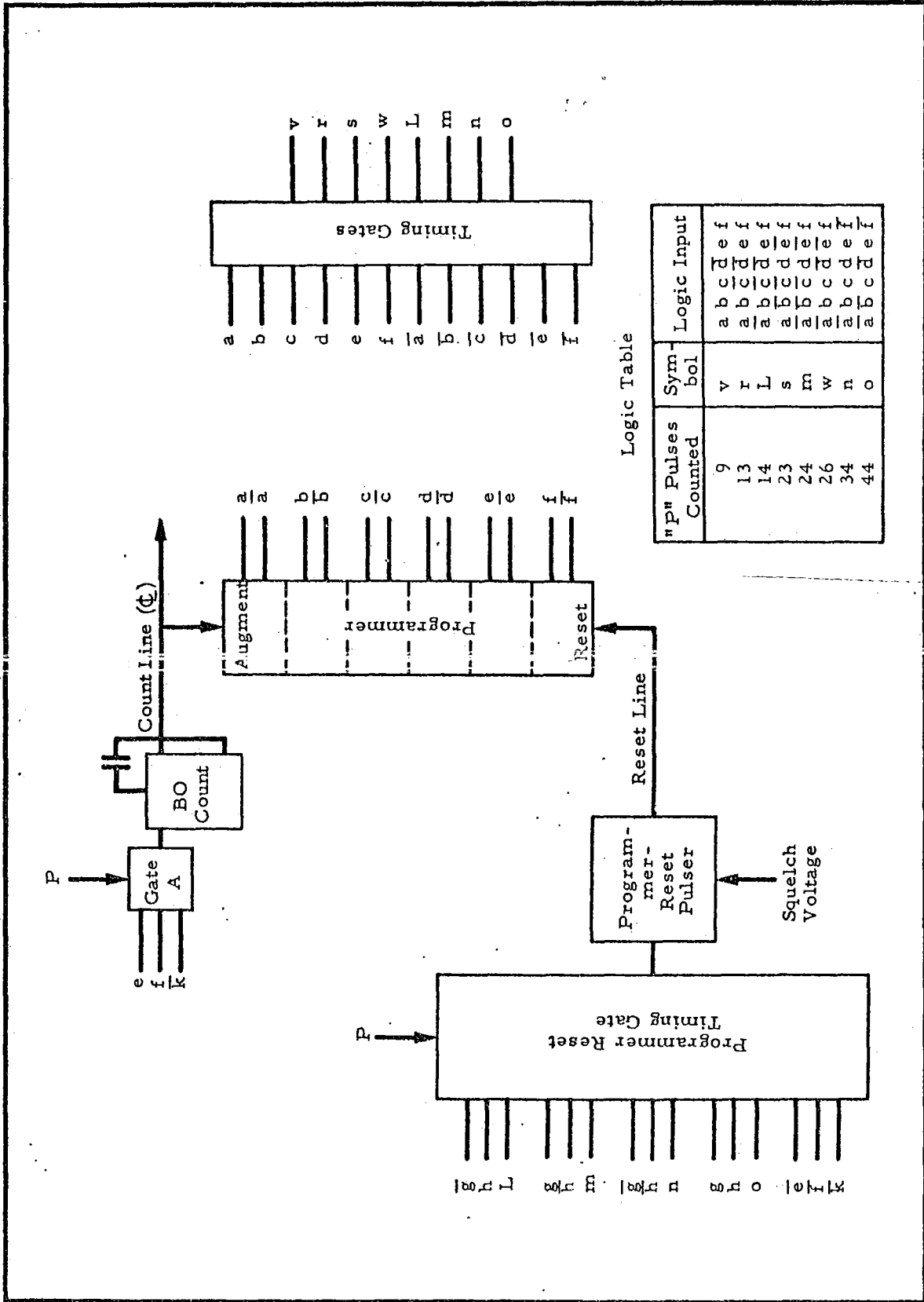


EXHIBIT 7 - DIGITAL DECODER FUNCTIONAL BLOCK DIAGRAM--PROGRAMMER AND ASSOCIATED CIRCUITS.

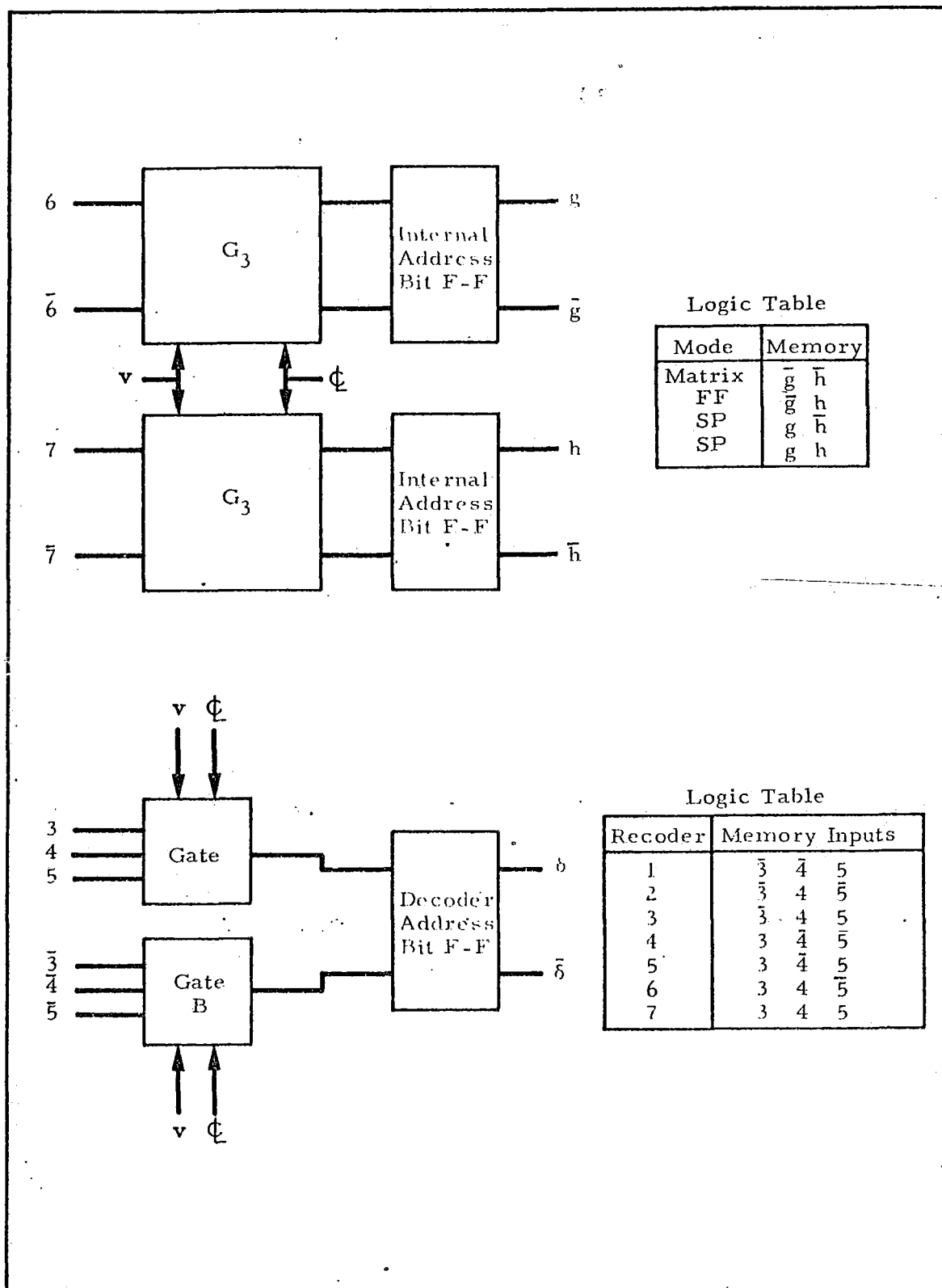


EXHIBIT 8 - DIGITAL DECODER FUNCTIONAL BLOCK DIAGRAM-- ADDRESS STORAGE, INTERNAL AND DECODER

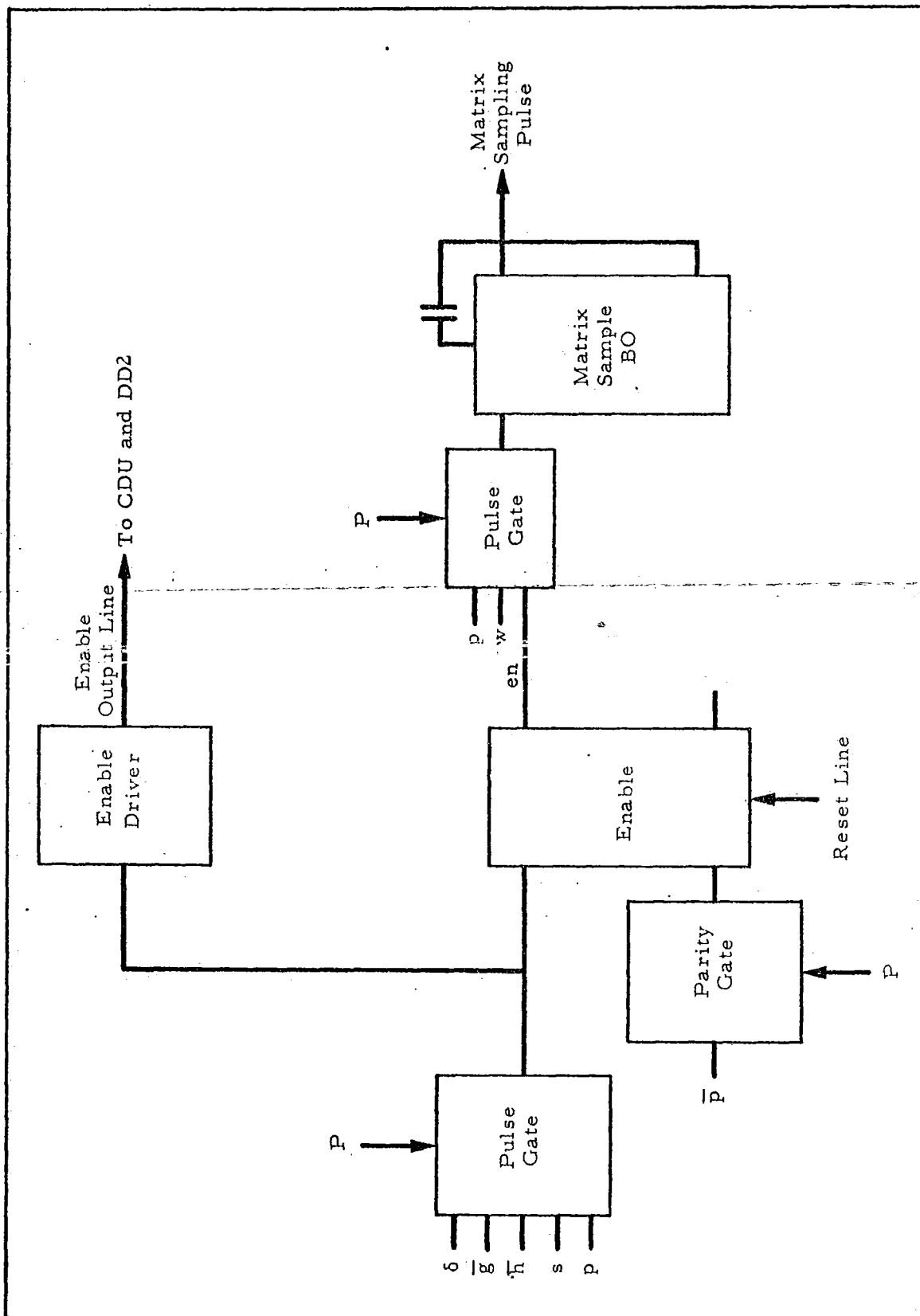


EXHIBIT 9 - DIGITAL DECODER FUNCTIONAL BLOCK DIAGRAM--MATRIX SAMPLING PULSE AND ENABLE OUTPUT LINE



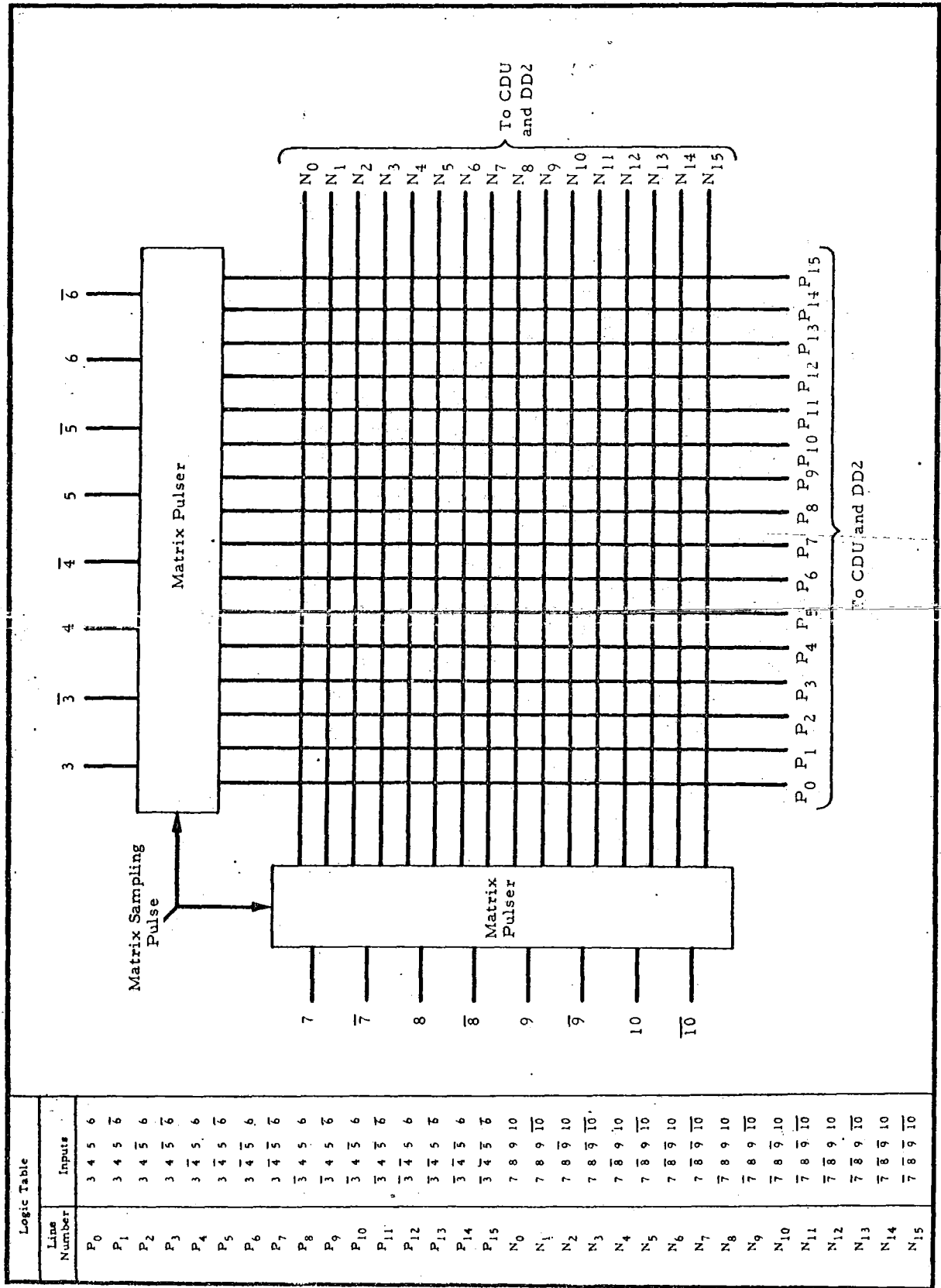


EXHIBIT 10 - DIGITAL DECODER FUNCTIONAL BLOCK DIAGRAM--MATRIX PULSER

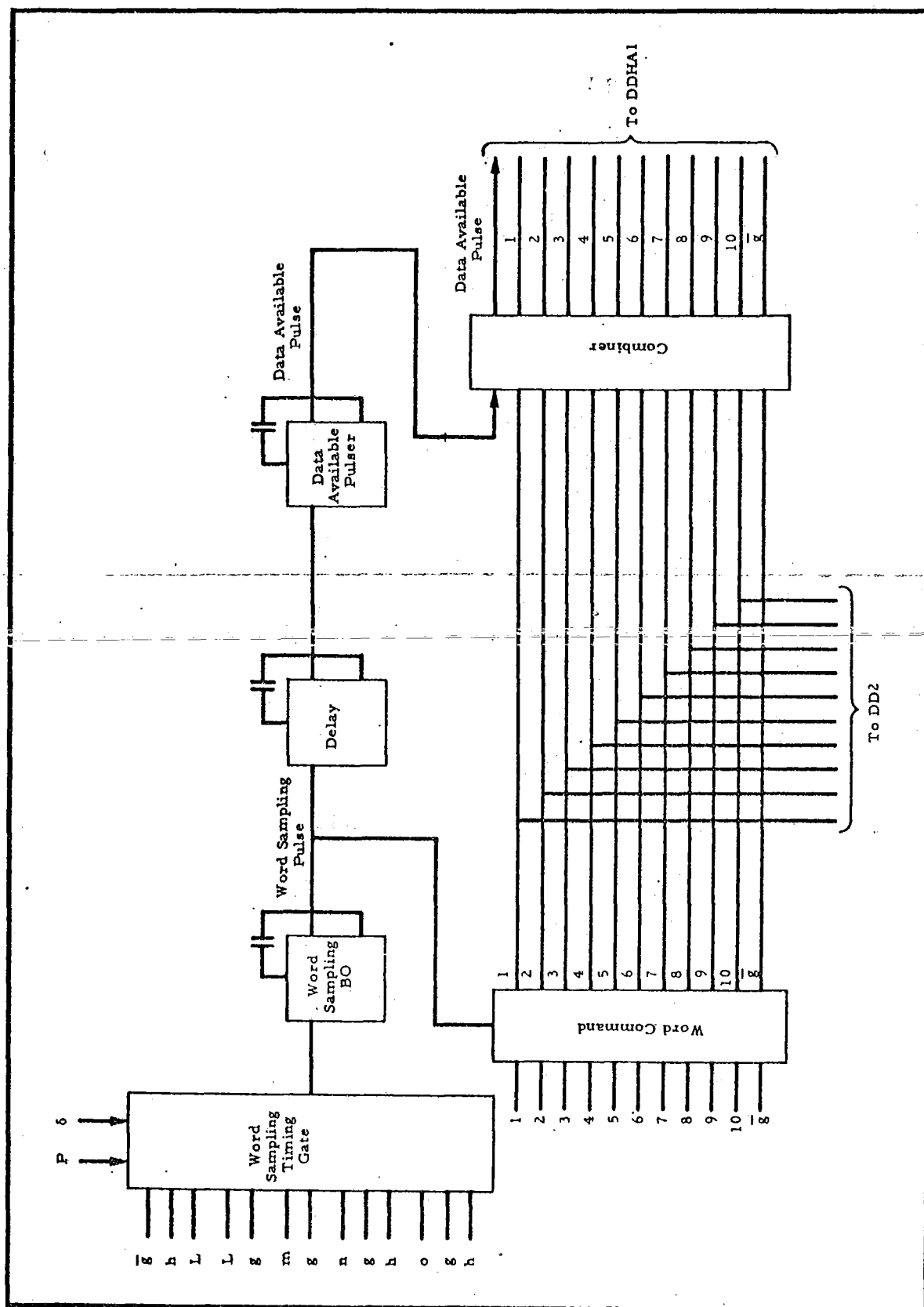


EXHIBIT 11 - DIGITAL DECODER FUNCTIONAL BLOCK DIAGRAM--WORD COMMAND CIRCUITS

The next eight bits are the complements of the binary command which it is desired to execute by means of the CDU. The last 10 data bits are the complements of the preceding 10 bits, meaning that the first 2 of these last 10 will always be "1's" for a Matrix Command and the remaining 8 bits will be the true binary configuration of the command to be executed.

These inputs to the DD are first amplified and buffered in a Band-pass Amplifier and Buffer. (See Exhibit 5.) The digital data are detected and handled through a Limiter, f-m Discriminator, and d-c Comparator. The output from this circuitry is the Digital Information, "k," and its complement, "K."

The a-m sine wave sync signal is detected and handled through an Envelope Detector, a Bandpass Amplifier, a Buffer, a Schmitt Trigger, a Pulse Amplifier, and a blocking oscillator titled Master Clock. The output from these circuits is a clock pulse, "P," which is in sync with the Digital Information and is used for synchronizing the operation of the entire DD.

The signal at the input of the Schmitt Trigger also goes to another Level Detector and Switch. If the signal does not exceed a fixed level, the Squelch Voltage disables the Digital Information and "P" outputs. If the signal exceeds the fixed level, meaning that a digital command is truly being received, the Squelch Voltage enables the Digital Information and "P" pulses to be outputted. Thus, if the CR outputs are not amplitude modulated with the proper sync frequency, but rather with tones such as those meant for the TD, the DD will remain in squelch.

Under control of the clock or sync signal, "P," the Digital Information is shifted into the 10-bit Shift Register (SR). (See Exhibit 6.) Each shift is counted by the Programmer (see Exhibit 7), which is a six-bit binary counter that counts "P" pulses. Particular binary states of the Programmer (indicating a specific number of "P" pulses counted) are decoded by the Timing Gates, providing an indication that specific bit sequences are registered in the SR.

When the ninth "P" pulse has been counted, output "v" of the Timing Gates will come true, indicating the proper time to act upon the Decoder Address bits and the Internal Address bits. This action includes setting the Decoder Address Bit Flip-Flop if--and only if--SR stages 3, 4, and 5 all contain "1's," and loading the Internal Address Bit Flip-Flops with the 2 "0" bits from SR stages 6 and 9, indicating a Matrix Command. (See Exhibit 8.) If stages 3, 4, and 5 are not all "1's," this means that another DD was selected aboard either the same spacecraft or some other OGO.

After 13 "P" pulses have been counted, output "r" of the Timing Gates enables the next "P" pulse (the 14th) to set Parity, meaning "p" is set to a "1." (See Exhibit 6.) The 14th "P" pulse also shifts the 14th Digital Information bit into stage 10 of the SR, meaning that the 4-bit Synchronization Word has been shifted all the way through and out of the SR and that stages 1 and 2 contain the Internal Address bits while stages 3 through 10 contain the complement of the command to be executed.

~~Normal operation requires that the last 10 bits be complementary~~ to those 10 bits already in the SR after the 14th "P" pulse. This allows a parity check before executing a Matrix Command. Thus the last 10 bits are shifted into the SR, and parity is checked bit by bit with the 10 preceding bits which are being shifted out of the SR. If any of the two bits being parity checked are the same, Parity will be reset, making "p" become a "0."

Timing Gates signal "s" indicates that 23 "P" pulses have been counted and that the next "P" pulse will shift the last bit of the 24-bit digital command into the SR, meaning that stages 3 through 10 will then contain the Digital Information to be decoded and transferred to the CDU relay matrix.

For a Matrix Command the Augment and Reset circuits for the Programmer are logically organized to count 34 "P" pulses and then reset as a function of the term " $\bar{g} \bar{h} n$ ," which indicates Matrix Command ( $\bar{g} \bar{h}$ ) and 34 "P" pulses counted (n). (See Exhibits 7 and 8.) The programmer is always reset by the Squelch Voltage when the DD is squelched as described previously.

The 24th "P" pulse generates an Enable Output Line signal to the CDU via the Pulse Gate. (See Exhibit 9.) This signal operates a relay. Allowance for the pull-in time of this relay requires a 3-pulse delay so that the 27th "P" pulse, enabled by Timing Gates signal "w," generates the Matrix Sampling Pulse 3 counts after the Enable Output Line signal.

This pulse goes to the Matrix Pulser (see Exhibit 10), where the Digital Information stored in stages 3 through 10 is decoded in row-column form and transferred to the CDU.

The 35th "P" pulse enabled by Timing Gates signal "n" resets the Programmer and removes the Enable Output Line signal. At this time the DD is ready to receive another digital command.

### (3) Flexible Format Command

A Flexible Format Command requires only a 14-bit transmission with all bits containing digital data. The initial four-bit Synchronization Word is identical to that for a Matrix Command (see the preceding subsection).

The Internal Address bits follow, as for a Matrix Command, and are a "0" and a "1" in order of transmission, indicating that the command is of the FF type. (See Exhibit 8.) The last eight bits represent the binary command that is to be transferred to, and operated on by, the Digital Data Handling Assembly (DDHA).

The Digital Information, Pulse, and Squelch Voltage are separated and used just as for a Matrix Command. Under control of the "P" pulses, the Digital Information is shifted into the SR. The Decoder Address bit and the Internal Address bits are handled in the same manner as with a Matrix Command. The only difference is that the Internal Address Bit Flip-Flops will be loaded with a "0" and a "1," as opposed to the two "0" bits for a Matrix Command.

The Parity gets set by the 14th "P" pulse as for a Matrix Command, but this is of no consequence since parity is not checked for an FF Command. The 14th "P" pulse also shifts the last Digital Information bit into stage 10 of the SR. Occurrence of the 14th "P" pulse is indicated by Timing Gates signal "L." The next "P" pulse, enabled by "L," resets

the Programmer and generates a Word Sampling Pulse. (See Exhibit 11.) The Word Sampling Pulse generates a Data Available Pulse and causes the Word Command circuits (one-shots) to transfer the Digital information stored in the SR to the DDHA. In addition, the Data Available Pulse and one bit of the Internal Address storage are transferred to the DDHA. All transfers to the DDHA are via the Combiner circuits.

At this time the DD is ready to receive another command.

f. Command Distribution Unit

The CDU receives inputs from both the TD and the DD. (See Exhibit 12.) For a decoded command the TD provides a potential (P) and ground (N) to the selected relay in the CDU Relay Matrix.

The enable Output Line signal from the DD occurs before the Matrix Sampling Pulse (see subsection 3.e(2)), so that 28 volts are closed to the Matrix Drivers before one  $P_i$  and one  $N_i$  (both as a function of the Matrix Sampling Pulse) signal occur. When the Matrix Sampling Pulse does occur, it causes one command in the Matrix to be performed. This requires the energization of one or more relay coils in the CDU. Energization of more than one is a function of relay logic within the CDU. Additional circuits within the CDU include timing and time delay circuits and the undervoltage sensor.

4. Command Equipment Interrelationships

a. General

As was pointed out in section 1, the CE has not until now received the same degree of attention as other portions of the CDH such as the Telemetry Equipment. The somewhat detailed functional description of the CE which has been written up in the previous section is a necessary first step toward the inclusion of this equipment in the CDH reliability assessment in a more realistic manner. One approach that might be adopted to accomplish this inclusion would involve a revision of the first assessment model to accommodate the CE function to the same level of detail as characterized the first assessment of the Telemetry Equipment. This is not considered to be desirable at

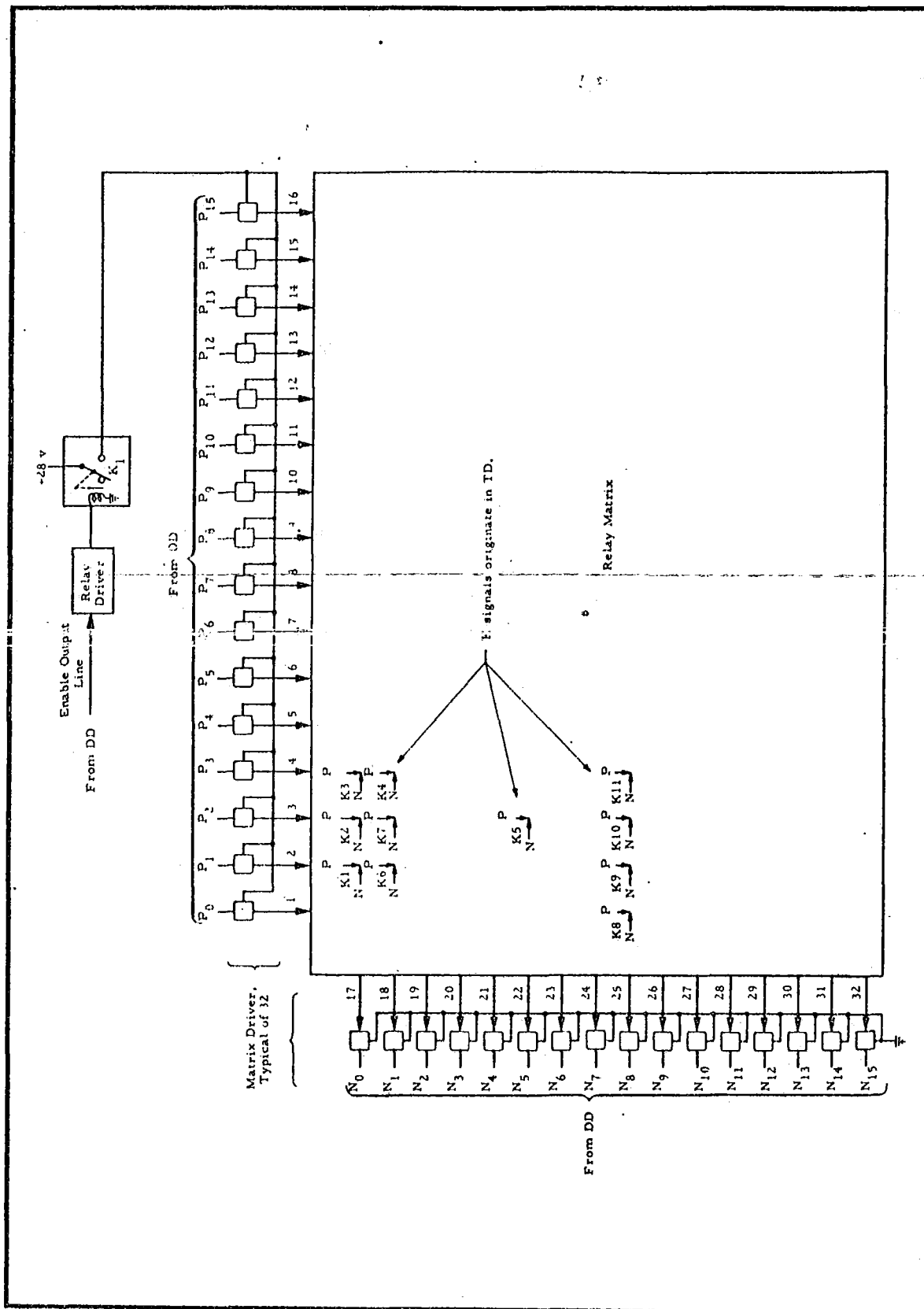


EXHIBIT 12 - COMMAND DISTRIBUTION UNIT FUNCTIONAL BLOCK DIAGRAM

this time because the OGO program is currently advanced enough to provide the necessary additional information for a more searching analysis of the system reliability. An analysis of this kind will demand, among other things, a more thorough knowledge of the relationships which exist between the CE and the other OGO subsystems and between the CE and the OGO mission profile beginning with initial conditions.

The present status of the documentation available to PRC shows a notable deficiency in mission profile information as opposed to block diagrams, schematic diagrams, and parts lists. Subsystem interface relationships are not as well defined as will be necessary for a higher level assessment. Specific areas in which additional information will be elicited include:

1. Initial conditions of the spacecraft systems, particularly the CDU relays.
2. Time profiles of the command occurrences.
3. Failure effects involving the CE.

These areas are not independent, and their interrelationships must be discerned for an accurate analysis. The nature of the information required in each of these areas is discussed below.

b. Determination of Initial Conditions

The initial states of many of the CDU relays can be deduced from available knowledge of the mission and the system functions. Thus, there is little question regarding the initial states of relays associated with Spacecraft Sequencing Commands, ACS Commands, and Experiment Impulse Commands. On the other hand, the initial states of many of the remaining relays cannot be so readily perceived. For example, what functions having both ON and OFF commands are initially in the ON condition, or, conversely, in the OFF condition? It can be presumed that Master Oscillator No. 1 and High Frequency Unit No. 1 are ON, meaning that the No. 2 units of each are OFF. Now, are both Equipment Groups, both Tape Recorders, and both Wideband Transmitters initially OFF? Is the Special-Purpose Transmitter OFF? These few examples can be extended to a complete spectrum of questions concerning the initial states of the command relays.



c. Determination of Time Relationships

The time profile of the command occurrences will weigh heavily in the assignment of state values. It is not necessary, for example, for certain relay commands to be available throughout the entire mission. According to the OGO Data Book (Section 2.1.4, "Initial OGO Sequencing"), if it is necessary to use the Command (Back-Up) Sequence, this action will be completed after approximately 3,460 seconds. Several of the command relays utilized during this period will never again be required. Clearly, an equipment failure affecting the selectability of a particular command relay could have serious consequences if it occurred before or during the period of the Command Sequence, but it would have no degrading effect if it occurred at any time after the Sequence period. In terms of state values, a relay which is no longer required following the Command Sequence will have no effect on mission value after the Sequence, but could well abort the entire mission should it fail prior to the completion of the Sequence. This example illustrates the use of mission profile data for the identification of components or equipment units which are not required beyond a specific time in the mission.

Another application of mission profile data is exemplified by the commands that alter the battery charging regime of the Power Supply Subsystem. In the charge-regulating portion of the subsystem a battery voltage sensing circuit is used to trigger the charge rate between full and trickle. The trigger level can be set by relay command. Considering the variations in battery condition throughout the mission, it is reasonable to expect that the selected trigger level will be a function of some known estimate of time. The effects of failure involving this command are related, therefore, to the mission profile.

d. Determination of Failure Effects

Consideration of the CE includes a large number of states; some of the results of a state will be obvious and straightforward, while others will be very subtle. One fact which tends to obscure certain failure effects is that although there are redundant equipments in the CE, they are not, in all cases, truly in parallel reliability-wise.

For example, the receiving portion of the CE is of the phase diversity reception type, with the crossed dipoles functioning to eliminate the effect of polarization nulls in the received signal. A linearly polarized signal will undergo considerable phase shift in passing through the ionosphere. This Faraday rotation effect, due principally to free electron resonance, can amount to several radians in the 120-Mc/s region. Variations in the ionospheric structure, coupled with the normal orientation changes of the satellite, can potentially produce signal-level degradation of as much as 20 db for a linearly polarized antenna.

Based on these considerations, it is not fully accurate to assume that the loss of a receiver or its associated antenna will not result in some performance degradation. The signal-to-noise ratio that applies to a single receiver fed from one linear dipole will undoubtedly be somewhat less than that which characterizes the fully functioning pair. It may even be that the CR operation will be somewhat oscillatory in nature as the signal strength at the antenna varies as a function of polarization relationships. For the preceding reasons, information regarding the theoretical or expected operating characteristics of the CR's will be useful in developing more meaningful value functions.

The decoders provide another illustration of the necessity for acquiring corollary information about the entire system in order to assess the consequences of CE failures. As indicated in the preceding paragraph, the two DD's are truly in parallel, reliability-wise, with respect to each of the two output signals from the CR's. Each DD is fully capable of selecting all relays in the case of Matrix Commands, or of transferring information to the DDHA upon receipt of an FF Command. The TD, on the other hand, offers command redundancy only under certain circumstances. First it is only in parallel for 11 of the 254 Matrix Commands and exerts no control over transfer of information to the DDHA's, which is a DD function only. Second, it is in parallel with the 11 Matrix Commands only if the spacecraft is in contact with a tracking station that is capable of transmitting both digital and tone commands. Otherwise, nothing is gained reliability-wise. Assuming that the Minitrack stations have only tone command transmission capabilities, the probability of their being

able to command OGO successfully is not related to the DD's. If the TD were not operable or functioning when commanded by a Minitrack station, the probability of being able to execute any command would be zero. If the vehicle were in communication with any tracking station with both digital and tone command transmission capabilities, the probability of executing one of the 11 commands would certainly be greater.

It can be seen from the preceding discussion that true parallel reliability of certain OGO equipment is a function of time (position in orbit), and therefore fits into the broad area of time relationships; hence, it is clear that adequate information regarding the tracking stations and their number, composition, and contact periods with OGO will be useful in making a better determination of the results of any state and, therefore, a better value function for the state.

e. Power Switching for Experiments

A specialized area of great importance concerns the function of switching power to individual experiments by means of the CE. The determination of state values for varying degrees of operability of this function involves simultaneous consideration of the mission profile and the failure-effects relationships.

Additional information is required as to which Power ON/OFF relay is associated with each of the presently assigned experiments. Depending on the assignments, it is possible that a selection circuit failure in the DD and CDU could affect the power control to as many as 16 of the 20 experiments. Therefore, it is important to know the exact relationship so that any particular state can readily be given a value to the mission.

It is important to know or realistically assume (as an initial condition) whether the power to all of the experiments is ON or OFF or some combination of experiments is initially ON and the remainder OFF. It is also necessary to know or assume (as a time relationship) the schedule for commanding Power ON to all of the experiments during a mission. This information is necessary because the mission value of a particular state is dependent on the initial conditions and the time-event

profile. For example, a state that did not allow the Power ON command to be executed for a particular experiment would have a zero value at an early time if that experiment had not yet been energized. Any time after the Power is ON, such a state has a value greater than zero. If the turning ON of Power to each experiment is itself a function of time, the value of certain states at any particular time is related to the number of experiments with Power ON.

f. Miscellaneous

Acquisition of further information in the areas described in the preceding sections will also aid in determining the effects of failures in the DD Shift Register and Parity circuits that would lead to the execution of incorrect Matrix Commands. A large portion of the information required forms what has been referred to as the Mission Profile. It is hoped that such areas can be clarified before final third assessment assumptions are made. If such a Mission Profile has not been generated and definite information cannot be made available, the best possible engineering judgment will be used in making assumptions.

5. CDH Numerical Assessment

a. Model Equations

The following section of this TAM updates subsection IV.A.5 ("Numerical Assessment of the Communications and Data Handling Subsystem") of Reference 1. There are a total of four changes in the second assessment that affect this section. Only one of these changes, the TD redesign, affects the model equations; the other three are concerned with the reliability inputs (see subsection 5.b below).

The TD has been redesigned since the preliminary assessment. Action was taken to improve subsystem reliability by increasing the switching capability between redundant equipments by ground command. (See Reference 1, subsection IV.A.6.a(2), "Possible Increases in Switching Capabilities," and subsection VII.B, Conclusion 5). With its increased switching ability and the original assumption that only four switch-function pairs are required, the TD becomes a truly redundant decoder from a

reliability point of view. This change has the effect of eliminating Equation (IV.A.11) and altering Equation (IV.A.10) to

$$R_{IA}^* = [1 - (1 - R_{MO})^2] [1 - (1 - R_{HFT})^2] [1 - (1 - R_{CR})^2] \\ [1 - (1 - R_{WBT})^2] [1 - (1 - R_{DD})^2 (1 - R_{TD})]$$

where the asterisk indicates the revised term and all other terms in the equation are defined in Reference 1. This change in equations reflects the current situation wherein switching the Equipment Group units, the Master Oscillators, the High-Frequency Timing Units, or the Wideband Transmitters requires only one of the three decoders, as contrasted with the previous situation where the Tone Decoder could switch the Wideband Transmitters only. Thus, the CDH can be in State  $S_1$  in one of three ways (cf. Reference 1, pp. 78-81):

1. Blocks IIA and IIB are both operable; one of the three redundant Digital Decoders and one each of the redundant pairs of Master Oscillators, High-Frequency Timing Units, Command Receivers, and Wideband Telemetry Transmitters is operable; and blocks IIA and IIB, considered redundantly, are in state  $S_1$ .
2. One of each of the redundant DD's, MO's, HFT's, CR's, and WBT's is operable; only one of blocks IIA and IIB is operable; and the block III units associated with the operable block II are in state  $S_1$ .
3. All three decoders are failed; the HFT, the MO, the WBT, and the block II switched in at the time switching capability was lost are operable; and the corresponding block III units are in State  $S_1$ .

Thus, the revised probability that the CDH is in state  $S_i$  is given by:

$$P_{CDH}^*(S_i, t) = R_{IA}^* R_{II}^2 P_i^1 + 2 R_{IA}^* R_{II} (1 - R_{II}) P_i + R_{IC} R_{II} P_i ;$$

where again the asterisk denotes revised terms and the subscripts are defined in the preliminary report (cf. Reference 1, Equation (IV.A.13)).

#### b. Preparation of Reliability Inputs

The three remaining changes are in the category of reliability inputs. The entire reliability inputs section (IV.A.5.b) has been revised herein for the second assessment. One change is in the revised failure rates used (these rates are in accordance with Reference 24); only the revised rates are given in the following revised list. The second change is a new parts complement for the Tone Decoder, reflecting its revised design. The final change is the addition of five coaxial connectors to each Command Receiver in order to account more accurately for the antenna-to-receiver reliability. Only the revised parts complements are given in the following list.

<u>Block I</u>	<u>Number of Parts</u>	<u>Individual Part Failure Rate</u>
Master Oscillator, MO (2 redundant)		
Transistor	15	.30
Resistor	43	.23
Diode	30	.15
Capacitor	18	.01
Transformer	1	.20
	<hr/> 107	<hr/> 19.27

<u>Block I (Continued)</u>	<u>Number of Parts</u>	<u>Individual Part Failure Rate</u>
High-Frequency Timing Unit, HFT (2 redundant)		
Transistor	29	.30
Resistor	96	.23
Diode	75	.15
Capacitor	6	.01
	<u>206</u>	<u>42.09</u>
Command Receiver, CR (2 redundant)		
Connector, Coaxial	5	.20
Transistor, Germanium	13	.30
Transistor, Silicon	9	.30
Diode, Silicon	5	.15
Diode, Zener	4	.26
Transformer, r-f and i-f	17	.20
Transformer, Audio	2	.02
Resistor, Carbon Composition	70	.01
Choke	1	.40
Filter, Feedthrough	2	.06
Coil, Small Size	2	.20
Capacitor, Corning Glass	18	.01
Capacitor, Ceramic	28	.01
Capacitor, Solid Tantalum	11	.08
Capacitor, Paper Equivalent	9	.01
Crystal, Quartz	2	.30
Filter, Quartz	1	.30
	<u>194</u>	<u>16.78</u>
Digital Decoder, DD (2 redundant)		
Resistor, Film	333	.23
Capacitor, Cerafil (Ceramic)	107	.01
Capacitor, Tantalum	11	.08
Diode	245	.15
Transistor	108	.30
Relay	9	.60
Transformer	11	.20
	<u>824</u>	<u>155.29</u>

<u>Block I (Continued)</u>	<u>Number of Parts</u>	<u>Individual Part Failure Rate</u>
Wideband Transmitter, WBT (2 redundant)		
Resistor, Fixed (Carbon Composition)	22	.01
Capacitor, Fixed (Ceramic)	49	.01
Diode, Zener	6	.26
Diode, Varactor	5	1.20
Crystal	1	.30
Transformer, Handwound, Air-Core	4	.20
Inductor, Handwound	12	.40
Transistor, Silicon	9	.30
Capacitor, Variable	13	.15
Resistor, Variable, Wirewound	2	.07
Choke, r-f	8	.40
Connector, Power	1	.20
Connector, Coaxial	6	.20
	<u>138</u>	<u>23.56</u>

#### Tone Decoder, TD (1)

Resistor, Film	173	.23
Capacitor, Cerafil	6	.01
Capacitor, Ceramic	9	.01
Capacitor, Molded Mica	68	.01
Capacitor, Tantalum	18	.08
Diode	28	.15
Transistor	69	.30
Relay	12	.6
Transformer	1	.20
Inductor	15	.40
Connector	2	.20
	<u>401</u>	<u>80.76</u>

#### Command Switching Unit, CSU

##### Matrix Driver No. 1

Rectifier, Silicon-Controlled	1	.45
Diode	1	.15
Resistor	1	.23
Capacitor	1	.01

##### Matrix Driver No. 2

Rectifier, Silicon-Controlled	1	.45
Diode	2	.15
Resistor	1	.23
Capacitor	1	.01



<u>Block I (Continued)</u>	<u>Number of Parts</u>	<u>Individual Part Failure Rate</u>
Relay Driver		
Transistor	2	.30
Resistor	2	.23
Diode	2	.15
Relay (Sensitive)	1	0.60
Relay (Latching)	<u>1</u>	<u>0.60</u>
	17	4.39

## Block II

### Manchester Code Generator, MCG (1)

Transistor	4	.30
Resistor	12	.23
Diode	10	.15
Capacitor	<u>2</u>	<u>.01</u>
	28	5.48

### Main Commutator Enable Circuit, MCEC (1)

Transistor	9	.30
Resistor	28	.23
Diode	24	.15
Capacitor	<u>2</u>	<u>.01</u>
	63	12.76 <sup>1</sup>

### Digital Bit and Word Generator, DBWG (1)

#### Modulo 9 Counter

Transistor	25	.30
Resistor	65	.23
Diode	54	.15
Capacitor	2	.01

<sup>1</sup> The effective failure rate, under the assumptions of the present model, is 12/128 of the failure rate given above, since the system is considered degraded only if the fixed-word transmission memory is stuck in one of the 12 fixed words when the failure occurs. This event has a probability of 12/128; the effective failure rate is therefore 1.20. (See Reference 1, subsection IV.A.2, for a more detailed analysis.)

<u>Block II (Continued)</u>	<u>Number of Parts</u>	<u>Individual Part Failure Rate</u>
Modulo 2 Counter		
Transistor	7	.30
Resistor	19	.23
Diode	13	.15
Capacitor	<u>2</u>	<u>.01</u>
	187	39.01
Main Commutator Counter, MCC (1)		
Flip-Flop Circuit (7)		
Transistor	4	.30
Resistor	11	.23
Diode	5	.15
Capacitor	<u>2</u>	<u>.01</u>
	22	4.50
(Total, MCC)	154	31.50
Frame Sync Coding Circuit, FSCC (1)		
Elements common to at least six bits		
Transistor	4	.30
Resistor	12	.23
Diode	<u>45</u>	<u>.15</u>
	61	10.71
Elements common to each bit		
Resistor	1	.23
Diode	<u>4</u>	<u>.15</u>
	5	.83

	<u>Number of Parts</u>	<u>Individual Part Failure Rate</u>
<u>Block III</u>		
Elements common to all digital words, D (1)		
"OR" Gate		
Transistor	1	.30
Resistor	3	.23
Diode	1	.15
"NAND" Gate (NE-2)		
Transistor	<u>1</u>	<u>.30</u>
	6	1.44
Elements common to each digital word, DW (40)		
NE-1		
Transistor	1	.30
TG-1		
Transistor	1	.30
Resistor	4	.23
Diode	<u>6</u>	<u>.15</u>
	12	2.42
Elements common to each digital column, DC (8)		
AM-5		
Transistor	4	.30
Resistor	8	.23
Diode	5	.15
Capacitor	<u>1</u>	<u>.01</u>
	18	3.80

<u>Block III (Continued)</u>	<u>Number of Parts</u>	<u>Individual Part Failure Rate</u>
AM-4		
Transistor	2	.30
Resistor	7	.23
Diode	6	.15
Capacitor	<u>1</u>	<u>.01</u>
	16	3.12 <sup>1</sup>

Elements common to each  
digital row, DR (8)

#### NE-2

Transistor	1	.30
------------	---	-----

Elements common to 1/4 of  
the digital words, DQ (4)

#### Shift Pulse Driver

Transistor	2	.30
Resistor	5	.23
Diode	4	.15
Capacitor	1	.01
Transformer	<u>1</u>	<u>.20</u>
	13	2.56

Elements common to 1/6 of  
the digital words, OR (6)

#### "OR" Gate

Transistor	1	.30
Resistor	2	.23
Diode	<u>1</u>	<u>.15</u>
	4	.91

<sup>1</sup> Since half of the selectors for columns that have been assigned digital words (see Reference 1, Exhibit IV.A-10) utilize AM-5 circuits and half utilize AM-4 circuits, the failure rate for a DC unit is taken to be an average of the two, viz,

$$\lambda_{DC} = \frac{1}{2} (\lambda_{AM-4} + \lambda_{AM-5}) = 3.46$$

<u>Block III (Continued)</u>	<u>Number of Parts</u>	<u>Individual Part Failure Rate</u>
Elements common to each analog column, AC (8) <sup>1</sup>		
First-Level Driver		
Transistor	1	.30
Resistor	1	.23
Diode	<u>1</u>	<u>.15</u>
	3	.68
Elements common to each row, R (8)		
AM-5		
Transistor	4	.30
Resistor	8	.23
Diode	4	.15
Capacitor	<u>1</u>	<u>.01</u>
	17	3.65
Elements common to each analog row, AR (8)		
Second-Level Gate		
Transistor	3	.30
Resistor	3	.23
Diode	1	.15
Transformer	<u>1</u>	<u>.20</u>
	8	1.94

<sup>1</sup> Each AC unit utilizes either an AM-4 or an AM-5 circuit (see DC units for parts count and failure rate) in addition to a First-Level Driver. According to the assumptions concerning the placement of analog words as shown in Reference 1, Exhibit IV.A-11, five-eighths of the AC units use AM-4 circuits and three-eighths use AM-5 circuits. Thus the average failure rate for an AC unit is

$$\lambda_{AC} = \lambda_{ILD} + \frac{5}{8} \lambda_{AM-4} + \frac{3}{8} \lambda_{AM-5} = 4.05$$

<u>Block III (Continued)</u>	<u>Number of Parts</u>	<u>Individual Part Failure Rate</u>
Elements common to each analog word, AW (30)		
First-Level Switch		
Transistor	2	.30
Resistor	2	.23
Transformer	1	.20
	<u>5</u>	<u>1.26</u>
Elements common to all analog words, A (1)		
Third-Level Driver and Switch		
Transistor	3	.30
Resistor	3	.23
Diode	1	.15
Transformer	1	.20
	<u>8</u>	<u>1.94</u>
Aperture Gating		
Transistor	3	.30
Resistor	7	.23
Diode	2	.15
Capacitor	3	.01
	<u>15</u>	<u>2.84</u>
Shift Register Enable Memory		
Transistor	6	.30
Resistor	15	.23
Diode	12	.15
Capacitor	2	.01
	<u>35</u>	<u>7.07</u>
Bit Rate Generator		
Transistor	38	.30
Resistor	129	.23
Diode	203	.15
Capacitor	8	.01
	<u>378</u>	<u>71.60</u>

<sup>1</sup>The effective failure rate, as in the case of the MCEC, is taken to be 12/128 of the failure rate given above. The engineering analysis for this is given in Reference 1, subsection IV.A.2. The effective failure rate is then 0.66.

<u>Block III (Continued)</u>	<u>Number of Parts</u>	<u>Individual Part Failure Rate</u>
A/D Converter		
Transistor	34	.30
Resistor	156	.23
Diode	84	.15
Capacitor, Glass	61	.01
Capacitor, Tantalum	1	.08
Transformer, Signal	2	.20
	<u>338</u>	<u>59.77</u>
GM-2		
Transistor	1	.30
Resistor	2	.23
Diode	1	.15
	<u>4</u>	<u>.68</u>
GM-1		
Resistor	8	.23
Diode	32	.15
	<u>40</u>	<u>6.64</u>
(Total failure rate of elements common to all analog words)		144.03

c. Calculations

Exactly the same methods are used as in the preliminary report; hence, only the CDH State Probabilities,  $P_{CDH}(S_i, t)$ , and the CDH Subsystem "Classical" Reliability are presented in this assessment (cf. Reference 1, Exhibits IV.A-19 and IV.A-20). These figures are combined in Exhibit 13 of this memorandum.

6. Conclusions

The reassessed classical reliability of this subsystem for 1 year is 0.383; the comparable first assessment figure is 0.059. The main reason for this increase is the use of reduced failure rates for

EXHIBIT 13 - CDH STATE PROBABILITIES,  $P_{CDH}(S_i, t)$

Relative "Value"	State Number, i	Time, t (hours)			
		2190	4380	6570	8760
1	1	.77222	.44296	.21424	.09300
39/40	2	.00547	.00879	.00734	.00465
39/40	3	.01172	.01856	.01579	.01011
9/10	4	.00089	.00131	.00111	.00042
9/10	5	.00626	.00999	.00835	.00532
7/8	6	.00927	.01493	.01259	.00804
13/15	7	.00412	.00614	.00509	.00320
4/5	8	.11395	.22528	.23896	.19127
4/5	9	.00365	.00585	.00488	.00310
11/15	10	.00004	.00013	.00016	.00014
7/10	11	.00036	.00142	.00242	.00263
7/10	12	.00251	.01051	.01758	.01971
7/10	13	.00371	.01555	.02606	.02918
2/3	14	.00158	.00657	.01096	.01222
3/5	15	.00003	.00085	.00054	.00030
3/5	16	.00148	.00618	.01035	.01182
3/5	17	.00013	.00118	.00296	.02873
3/5	18	.00004	.00031	.00079	.00119
3/5	19	.00009	.00074	.00187	.00280
11/30	20	.00006	.00050	.00125	.00187
11/30	21	.00009	.00074	.00186	.00277
8/15	22	.00002	.00015	.00039	.00059
1/2	23	.00005	.00047	.00117	.00176
1/2	24	.00008	.00070	.00174	.00260
7/15	25	.00003	.00029	.00073	.00110
2/5	26	.00001	.00011	.00026	.00039
1/5	27	.00056	.00096	.00087	.00069
0	28	.06158	.21883	.40969	.56040

$$\text{Classical Reliability} = \sum_{i=1}^{14} P_{CDH}(S_i, t) = .93575 \quad .76799 \quad .56553 \quad .38299$$



this assessment. Changing the Tone Decoder design so that it is more fully redundant with the Digital Decoders resulted in a further increase in reliability. The changed (i.e., increased) parts complements in the Tone Decoder and in the Command Receivers have a negligible effect on subsystem reliability.

The change in the Command Receiver parts complement consists of the addition of five coaxial connectors. This results in only a 2-percent increase in the total Command Receiver failure rate, and, hence, is negligible with regard to the over-all subsystem.

The redesigned Tone Decoder has an expanded parts complement (391 total parts for the new Tone Decoder compared with 334 for the initial version), but the total failure rate differs by only 1 percent. This is due to the greater population of low-failure-rate parts and the reduced population of high-failure-rate parts.

Exhibit IV.A-22 of Reference 1 shows the changes in reliability resulting from a more completely redundant Tone Decoder. For convenience, the results of this change are graphed in Exhibit 14.

Use of the revised failure rates given in Reference 24 results in the uppermost reliability curve of Exhibit 14. It is easily seen that this change yields the major reliability increase.

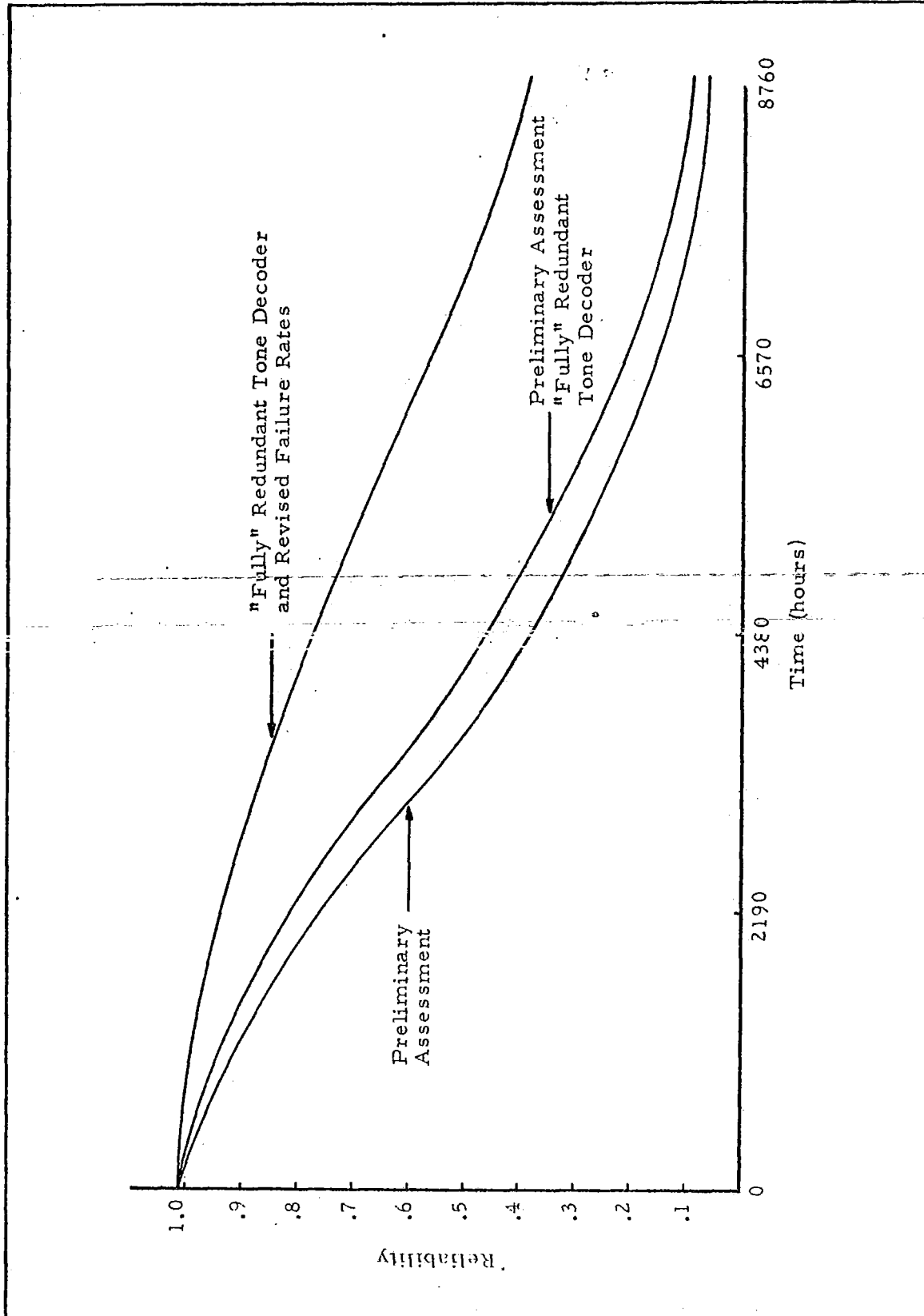


EXHIBIT 14 - CLASSICAL RELIABILITY CURVES FOR THE CDH SUBSYSTEM

## REFERENCES

1. Preliminary Reliability Assessment for the Orbiting Geophysical Observatories, PRC R-243, 1 February 1962.
2. STL Drawing No. X200393C (Block Diagram, OGO Communication Subsystem).
3. STL Drawing No. 201487 (Block Diagram, Command Receiver).
4. STL Drawing No. 201490 (Schematic Diagram, Command Receiver).
5. STL Drawing No. 206997 (Block Diagram, Tone Decoder, Sequential Version).
6. STL Drawing No. 206998 (Schematic Diagram, Tone Decoder, Sequential Version).
7. STL Drawing No. 200478 (Block Diagram, Decoder, Digital Command).
8. STL Drawing No. 201507B (Schematic Diagram, Decoder, Digital Command).
9. STL Drawing No. 201530A (Schematic Diagram, Command Distribution Unit).
10. STL Drawing No. 201540A (Schematic Diagram, Relay Module, 1A).
11. STL Drawing No. 201541A (Schematic Diagram, Relay Module, 1B).
12. STL Drawing No. 201542B (Schematic Diagram, Relay Module, 2A).
13. STL Drawing No. 201447A (Schematic Diagram, Relay Module, 2B).
14. STL Drawing No. 202267 (Schematic Diagram, Relay Module, 6 and 9).
15. STL Drawing No. 201454 (Schematic Diagram, Relay Module, 3, 4, and 7).
16. STL Drawing No. 202268 (Schematic Diagram, Relay Module, 8).

REFERENCES  
(Continued)

17. STL Drawing No. 202269 (Schematic Diagram, Relay Module, 10).
18. STL Specification No. D-13413 (120/136-mc Omni-Directional Antenna).
19. STL Specification No. D-13414, Rev. B (120/136-mc Diplexer-Coupler).
20. STL Specification No. D-13415, Rev. A (Command Receiver).
21. STL Specification No. D-13417, Rev. B (Tone Decoder, Sequential Version).
22. STL Specification No. D-13416 (Digital Decoder)..
23. STL Specification No. D-13406 (Command Distribution Unit).
24. Parts Failure Rates--OGO Second Reliability Assessment, Technical Advisement Memorandum No. 7 (PRC to GSFC),  
24 August 1962.

TECHNICAL ADVISEMENT MEMORANDUM NO. 12

SECOND RELIABILITY ASSESSMENT FOR  
THE OGO ATTITUDE CONTROL AND  
STABILIZATION SUBSYSTEM

## TABLE OF CONTENTS

	<u>Page</u>
1. Introduction . . . . .	1
2. Assessment Summary and Discussion of Models . . . . .	2
3. Solar Array Channel Reliability . . . . .	7
4. Yaw Channel Reliability . . . . .	17
5. Pitch Channel Reliability . . . . .	30
6. Roll Channel Reliability . . . . .	39
7. Common Equipments . . . . .	49
a. Inverter . . . . .	49
b. Converter . . . . .	49
c. Mode Memory Circuits . . . . .	52
8. Special Equipments . . . . .	52
a. Regulator Filter . . . . .	52
b. Rate Gyro Electronics . . . . .	54
c. Small Earth Discrimination Circuits . . . . .	54
d. Horizon Scanner . . . . .	56
9. ACS Subsystem Reliability . . . . .	57
a. Individual Reliabilities, Mode I . . . . .	57
b. Individual Reliabilities, Mode IIa . . . . .	58
c. Individual Reliabilities, Mode IIb . . . . .	58
d. Individual Reliabilities, Mode IIc . . . . .	59
e. Individual Reliabilities, Mode III . . . . .	59
f. Time-Cumulative Reliabilities . . . . .	60
10. Strengths and Weaknesses . . . . .	61
11. Recommendations . . . . .	62

# LIST OF EXHIBITS

	<u>Page</u>
1. ACS Subsystem Reliability by Channel and Mode . . . . .	6
2. Solar Array Channel, Mode I . . . . .	9
3. Solar Array Channel, Modes IIa, IIb, IIc . . . . .	10
4. Solar Array Channel, Mode III . . . . .	11
5. Yaw Channel, Modes I, IIa . . . . .	21
6. Yaw Channel, Modes IIb, IIc . . . . .	22
7. Yaw Channel, Mode III . . . . .	23
8. Box 37, Valve Drivers and Valves . . . . .	24
9. Box 36, "OR" Gate Logic. . . . .	25
10. Pitch Channel, Modes I, IIa . . . . .	33
11. Pitch Channel, Modes IIb, IIc . . . . .	34
12. Pitch Channel, Mode III . . . . .	35
13. Roll Channel, Modes I, IIa . . . . .	43
14. Roll Channel, Modes IIb, IIc . . . . .	44
15. Roll Channel, Mode III . . . . .	45
16. Mode Memory Circuits, Reliability Diagram . . . . .	51
17. -3 Volt Regulator Diagram. . . . .	53
18. Small Earth Discrimination Circuits, Reliability Diagram	55
19. Mode Transition Logic Circuits . . . . .	64
20. Earth Acquisition Logic Circuits. . . . .	67
21. Possible Revised Earth Acquisition Logic Circuits. . . . .	70
22. Possible Revised Earth Acquisition Logic Circuits. . . . .	71
23. Possible Revised Earth Loss Logic Circuits. . . . .	73

## TECHNICAL ADVISEMENT MEMORANDUM NO. 12

To: Assistant OGO Project Manager, GSFC, NASA  
From: PRC OGO Assessment Team  
Subject: Second Reliability Assessment for the OGO Attitude Control and Stabilization Subsystem

### 1. Introduction

Unlike the preliminary reliability assessment (cf. PRC R-243) of the ACS Subsystem, this assessment considers the subsystem in terms of its four axis-orientation servo channels (roll, pitch, yaw, and array). The adoption of this functional approach (which considers each servo channel from its error sensor to its final reaction on the spacecraft) was deemed a necessary change from the preliminary approach in order to allow the inclusion of operating modes (e.g., the sun acquisition mode) other than the normal mode. Using STL's terminology, the five modes of operation pertinent to each channel are as follows: I = boost phase; IIa = array slew; IIb = sun acquisition; IIc = earth acquisition; and III = normal mode. Thus, each servo channel becomes characterized by (1) the axis about which it exerts control and (2) the particular electrical configuration pertinent to a given operating mode.

Since each channel may have several different electrical configurations, a description of each channel in each of its distinct configurations is given in this memorandum. A particular channel and mode configuration might be, for example, "Solar Array, Mode I," as shown in Exhibit 2 (which also presents a tabular listing of failure modes pertinent to that configuration).

A brief discussion of the modelling and a summary of the reliability assessment (i.e., channel as well as total subsystem) is presented in Section 2. The subsystem analysis is based primarily on separate analyses of each of the four servo channels given in later sections: the solar array channel in Section 3, the yaw channel in Section 4, the pitch channel in Section 5, and the roll channel in Section 6.



To complete the preliminaries of the subsystem analysis, Sections 7 and 8 present the respective analyses of common and special channel equipments. Section 9 develops the detailed model equations for ACS Subsystem reliability in each mode, and includes numerical evaluations. The memorandum concludes with a discussion of subsystem strengths and weaknesses together with recommendations for reliability improvement.

## 2. Assessment Summary and Discussion of Models

Some 75 different functional circuit groupings were identified and used in this assessment of the ACS Subsystem. It was recognized that certain failures in certain groupings could occur without subsystem failure if the groupings were part of a particular channel operating in a particular mode. Identification and inclusion of such mitigating considerations in the model have constituted one major effort of the second assessment. That this effort is worthwhile (reliability-wise) can be seen by first defining the zeroth-order subsystem reliability at time  $t$  as the probability that no failure of any of the 75 groups has occurred by time  $t$ . This function is the simple product of 75 individual reliability functions (not necessarily exponential), each of which reflects internal redundancies (such as quads) and failure-effects analyses. Evaluated at  $t = 8760$  hours (or 1 year), the zeroth-order reliability of the ACS Subsystem is 0.0043. Comparison of the second assessment final reliability prediction for the ACS (presented in Exhibit 1 of this TAM) of 0.02854 to the zeroth-order prediction may be considered as comparing a "higher order" to a "zeroth-order" approximation, with the difference in the two predictions providing a measure of the inaccuracy of the zeroth-order prediction. The extent to which such higher order approximations approach the true reliability will be discussed in following paragraphs, but it is deemed illustrative first to present the following modeling example:

Consider a hypothetical servo channel consisting of five equipments. Suppose further that the channel must operate at prescribed times in one of two alternative modes, and that different equipment configurations are necessary to effect each mode, as shown in the following table.

Equipment Number	1	2	3	4	5
Required for Mode I ?	Yes	Yes	No	No	Yes
Required for Mode II ?	No	No	Yes	Yes	Yes

In normal operation it is assumed that the channel will operate in Mode I until  $t = \tau$ , at which time the channel will change to Mode II and continue to operation in Mode II for  $t > \tau$ . Denoting the probability of no failure at time  $t$  of the  $i$ th equipment in the  $j$ th mode by  $P_i^j(t)$  ( $i = 1, 2, 3, 4, 5$ ;  $j = I, II$ ), the probability of no failure of the channel  $P_C^I(t)$  for  $t < \tau$  is therefore

$$P_C^I(t) = P_1^I(t) P_2^I(t) P_5^I(t) . \quad (1)$$

Similarly, for  $t > \tau$ , the probability of no failure of the channel is

$$P_C^{II}(t) = \left[ P_C^I(\tau) \right] \left[ P_3^I(\tau) P_4^I(\tau) \right] \left[ P_3^{II}(t - \tau) P_4^{II}(t - \tau) P_5^{II}(t - \tau) \right] . \quad (2)$$

In general,  $P_i^I(t) \neq P_i^{II}(t)$  ( $i = 1, 2, 3, 4, 5$ ), since equipment internal configurations (and thus the consequences of certain failures) generally differ for each mode. Note that the first major factor in Equation (2) is the probability that the Mode I operation was successful to time  $\tau$ ; the second major factor is the probability of no failure of equipments 3 and 4 (needed for Mode II operation) by time  $\tau$ ; and the third is the conditional probability of no failure in equipments 3, 4, and 5 at time  $t$ , given that Mode II operation is successfully initiated at time  $\tau$ .

Now, if it is assumed that all equipments are needed all of the time, the zeroth-order reliability of the hypothetical channel is given by

$$P_C^{*I}(t) = P_1^I(t) P_2^I(t) P_3^I(t) P_4^I(t) P_5^I(t) \quad (t < \tau) \quad (3)$$

$$P_C^{*II}(t) = P_C^{*I}(\tau) P_1^{II}(t - \tau) \cdots P_5^{II}(t - \tau) \quad (t \geq \tau) \quad (4)$$

Since all the  $P_i^j(t)$ 's lie between 0 and 1 regardless of the underlying reliability law, it follows from comparisons of Equations (1) and (3) and Equations (2) and (4) that

$$\begin{aligned} P_C^{*I}(t) &\leq P_C^I(t) & (t < \tau) \\ P_C^{*II}(t) &\leq P_C^{II}(t) & (t \geq \tau) \end{aligned} \quad (5)$$

In fact, since  $P_i^j(t)$  is strictly less than unity (for all  $t > 0$ ), the ~~inequalities in Equation (5) are strict inequalities, hence, the outlook~~ (or assumption) that all equipments are needed all of the time--i. e., the zeroth-order approximation--is seen to be pessimistic. The degree of pessimism can be quantitatively evaluated, for example, by evaluating the ratio

$$\frac{P_C^I(t)}{P_C^{*I}(t)} = P_3^I(t) P_4^I(t) \quad (6)$$

for  $t < \tau$  (and a similar ratio for  $t \geq \tau$ ).

Certain assumptions were made in order to keep the above illustration simple; however, the inference drawn from the example is appropriate. Indeed, the development of the model equations in the following sections follows the same general approach described in this example. The term "higher order" reliability approximation (as distinguished from an "exact" expression) is used for several reasons. Expressions such as  $P_i^I(t)$  are meant to reflect failure-effects analysis within the  $i$ th equipment. The superscript distinguishes expressions which, individually,

may be appropriate for operation only in a certain mode. An example of this might be an equipment called a "selection-switching relay." The use of such an equipment in a channel in one mode might require that the relay coil be energized, while use of this same equipment for the same channel in another mode might not require that the coil be energized. Thus, the effect of a failure such as an "open" in the first mode is catastrophic, but in the second is nil. The probability expression for the equipment in these two modes must differentiate between the different effects of such failures.

If an "exact" failure-effects analysis could be performed on every one of the 75 equipments of the ACS in each of its modes, the inclusion of the resulting equations in the present ACS analysis model would yield an "exact" expression for reliability. The present assessment is not an exact assessment. For some circuit groupings (such as the delayed-timing-pulse generator) an estimated reliability function was derived because of the lack of design information. For other circuit groupings (such as horizon scanner selection logic) a "parts count" reliability function was used in place of full consideration of failure/success under the many given conditions. For yet other circuit groupings (such as the valve-driver amplifier), relatively complete failure-effects analyses by PRC were used. However, it is felt that the present assessment is a good first approximation, and the analysis model is readily extendable, as more information becomes available, to a still better approximation of the "exact" reliability.

Based on the above modelling concepts, the next seven sections develop the detailed model equations and present the calculations underlying the assessment. These results for the ACS Subsystem are summarized in Exhibit 1. Note that the exhibit gives both channel and ACS Subsystem reliabilities for the various modes of operation. Also, individual as well as cumulative values are presented. That is, each of the numbers in the "(a)" rows represents the probability that the channel (or the ACS) was operable at the beginning of this time period. Each of the numbers in the "(b)" rows, then, is the cumulative probability (i. e., reliability) that the channel (or the ACS) will survive from time 0 to the end of the time period in question.

EXHIBIT 1 - ACS SUBSYSTEM RELIABILITY BY CHANNEL AND MODE

	Mode I ~ 1 hr. 1 hr.	Mode IIa ~ .04 hr. 1.04 hr.	Mode IIb ~ .5 hr. 1.5 hr.	Mode IIc ~ 35 hr. 36 hr.	Mode III			
					2154	4344	6534	8724
Approximate Time in Mode					2190	4380	6570	8760
Approximate Cumulative Time								
Solar Array Channel (a)	.93472	1.00000	.99995	.99634	.79064	.62238	.48989	.38451
(b)	.93472	.92689	.92684	.92345	.72533	.57096	.44943	.35275
Yaw Channel (a)	.93804	1.00000	.99993	.99472	.73708	.53976	.39642	.29169
(b)	.93804	.93804	.89865	.89390	.64486	.47223	.34682	.25519
Pitch Channel (a)	.93804	1.00000	.99993	.99487	.62672	.36970	.21270	.11720
(b)	.93804	.93804	.92815	.92339	.54690	.32261	.18651	.10227
Roll Channel (a)	.93804	1.00000	.99996	.99533	.65105	.40110	.24099	.13711
(b)	.93804	.93804	.93097	.92655	.57329	.35319	.21220	.12073
ACS Subsystem (a)	.93322	1.00000	.99988	.99115	.42220	.19069	.08431	.03561
(b)	.93322	.91772	.86230	.85460	.33843	.15286	.06758	.02854

(a) Individual probabilities

(b) Cumulative probabilities

### 3. Solar Array Channel Reliability

The solar array channel consists of the following equipment and miscellaneous parts. Combinations of various  $R_i(t)$  versus mode are defined in Exhibits 2, 3, and 4.

i	Item	$R_i(t)$
1.	Converter	$e^{-3.76t}$
2.	Inverter	$e^{-20.91t}$
3.	Mode Memory	$e^{-45.93t}(e^{-.3t} + 2e^{-.15t} - 2e^{-.285t}) \cdot (e^{-.3t} + 2e^{-.15t} - 2e^{-.165t})^{27}$
4.	Relay K5	$e^{-.6t}(2e^{-.015t} - e^{-.03t})$
5.	Low-Level d-c Magamp	$e^{-2.52t}$
6.	Bistable d-c Magamp	$e^{-4.18t} \quad R_6^{(1)} = e^{-.418t} \quad R_6^{(2)} = e^{-3.762t}$
7.	Motor Driver Magamp	$e^{-5.33t} \quad R_7^{(1)} = e^{-.533t} \quad R_7^{(2)} = e^{-4.797t}$
8.	Magamp Control Circuitry	$e^{-2.01t} \quad R_8^{(1)} = e^{-.201t} \quad R_8^{(2)} = e^{-1.809t}$
9.	Solar Array Motor	$e^{-4.80t}$
10.	Relay K4	$e^{-.6t}(2e^{-.015t} - e^{-.03t}) \quad R_{10}^{(1)} = e^{-.4t}$
11.	Shaft Resolver	$e^{-.25t}$
12.	Reacquire Circuitry	$e^{-3.58t}(e^{-.3t} + 2e^{-.15t} - 2e^{-.165t}) \cdot (e^{-.16t} + 2e^{-.08t} - 2e^{-.144t})$
13.	Array Coarse Sensors	$e^{-2.8t} + 4\{1 - e^{-0.7t}\}(e^{-0.7t})^3$
14.	Array Fine Sensors	$e^{-.7t}$

i	Item	$R_i(t)$
15.	Intensity Detector	$e^{-.7t}$
16.	Level Detector Magamp	$e^{-2.09t}$
17.	Relay K1	$e^{-.6t}(2e^{-.015t} - e^{-.03t})$ $\cdot (e^{-.46t} + 2e^{-.23t} - 2e^{-.345t})$
18.	Low-Level d-c Magamp	$e^{-2.52t}$
19.	6 Resistors	$e^{-1.38t}$
20.	6 Resistors	$e^{-1.38t}$
21.	2 Resistors, 2 Switches	$e^{-1.86t}$
22.	1 Capacitor	$e^{-.08t}$

Reliability of solar array  
channel in Mode I =  $R_{S,I} = R_1 R_2 R_3 R_4 R_6^{(1)} R_7^{(1)} R_8^{(1)} R_9$

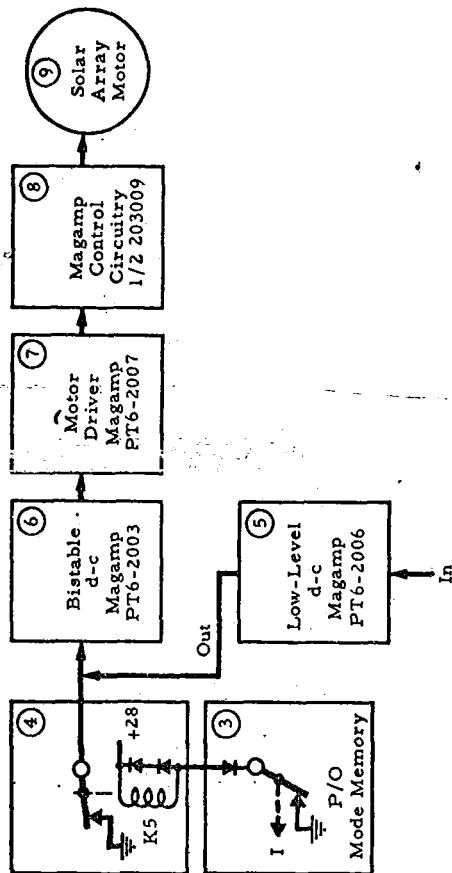
Reliability of solar array  
channel in Mode II =  $R_{S,II} = R_1 R_2 R_3 R_5 R_6 \cdots R_{12} R_{20} R_{21}$

Reliability of solar array  
channel in Mode III =  $R_{S,III} = R_1 R_2 R_3 R_5 \cdots R_{10}^{(1)} R_{13} \cdots R_{21} R_{22}$

Reliability of solar array  
channel through Mode I =  $R_{S,I}^* = R_{S,I}$

Reliability of solar array  
channel through Mode II =  $R_{S,II}^* = R_{S,I}^* (R_5 R_{10} R_{11} R_{12} R_{20} R_{21})' R_{S,II}$

Reliability of solar array  
channel through Mode III =  $R_{S,III}^* = R_{S,II}^* (R_{13} R_{14} \cdots R_{19} R_{22})' R_{S,III}$



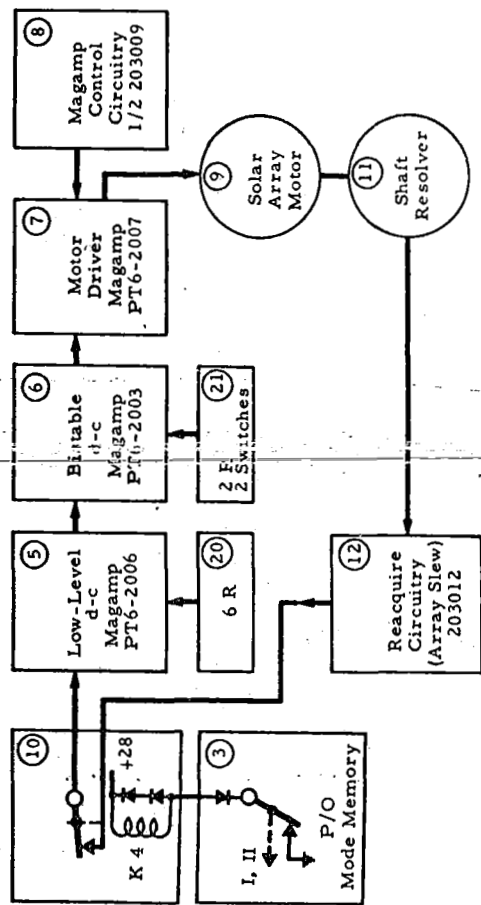
#### Failure Modes, Solar Array Channel, Mode I

A channel failure is implied by any one of the following failures in the numbered boxes below:

- ③ Diode open, or contacts open, or failure in mode memory.
- ④ Relay K5 open or short, or both diodes short.
- ⑥ ⑦ ⑧ Certain types of failures give output with zero input (basic failure rate  $\lambda$  was divided by 10 to represent this condition).
- ⑨ Motor winding open or short.

#### EXHIBIT 2 - SOLAR ARRAY CHANNEL, MODE I





#### Failure Modes, Solar Array Channel, Modes IIa, IIb, IIc

A channel failure is implied by any one of the following failures in the numbered boxes below:

- (3) Diode open, or contacts open, or failure in mode memory.
- (10) Relay K4 open of short, or both diodes short.
- (5) (6) (7) (8) (9) (11) (20) (21) Open or short of any element (see note).

Note: An element (such as a quad diode) is assumed failed when the element no longer functions (as a "diode"); all elements which involve piece-part redundancy were so considered.

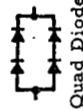
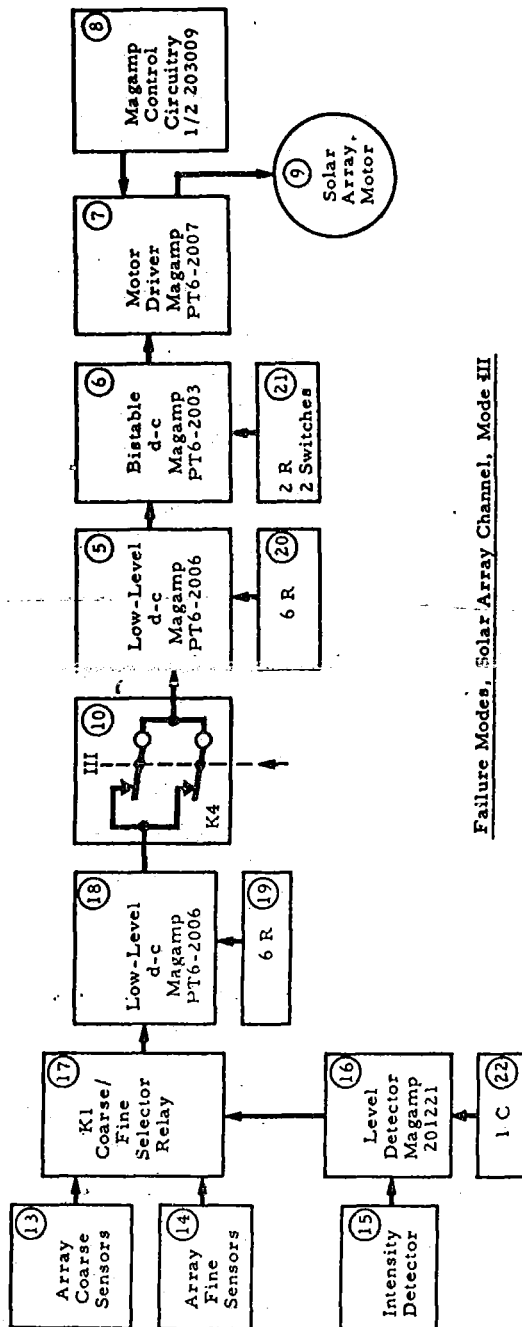


#### EXHIBIT 3 - SOLAR ARRAY CHANNEL, MODES IIa, IIb, IIc



#### Failure Modes, Solar Array Channel, Mode III

A channel failure is implied by any one of the following failures in the numbered boxes below:

- (13) Any one of four "solar cells" shorts (acceptable "states" are (a) no failure (short or open) in four cells, and (b) exactly one failure open).
- (17) A failure which would not permit energizing the coil of K1, i.e., a short across the coil (both diodes short), or an open in series (both resistors open), or a short or open coil.
- (18) Both contacts fail open or failure in mode memory.
- (14) Open or short in any element (see note).
- (15) An element (such as a quad diode) is assumed failed when the element no longer functions (as a "diode"); all elements which involve piece-part redundancy were so considered.
- (16) Quad Diode

Note: An element (such as a quad diode) is assumed failed when the element no longer functions (as a "diode"); all elements which involve piece-part redundancy were so considered.

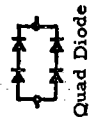


#### EXHIBIT 4 - SOLAR ARRAY CHANNEL, MODE III

$$R_{S,I} = e^{-77.152t}(e^{-.3t} + 2e^{-.15t} - 2e^{-.285t})(e^{-.3t} + 2e^{-.15t} - 2e^{-.165t})^{27} \\ \cdot (2e^{-.015t} - e^{-.03t})$$

t = 1 hour, but a K factor of 800 applies in Mode I, hence,

$$R_{S,I} = e^{-.06172}(e^{-.00024} + 2e^{-.00012} - 2e^{-.000228}) \\ \cdot (e^{-.00024} + 2e^{-.00012} - 2e^{-.000132})^{27} \\ \cdot (2e^{-.000012} - e^{-.000024}) \\ = (.94021)(.99976 + 2(.99988 - .999772)) \\ \cdot (.99976 + 2(.99988 - .999868))^{27}(1.99976 - .99976) \\ = (.94021)(.999976)(.999784)^{27}(1) \\ = (.94019)(99418)$$

$$\underline{R_{S,I} = .93472}$$

$$R_{S,IIa} = e^{-97.11t}(e^{-.3t} + 2e^{-.15t} - 2e^{-.285t})(e^{-.3t} + 2e^{-.15t} - 2e^{-.165t})^{28} \\ \cdot (2e^{-.015t} - e^{-.03t})(e^{-.16t} + 2e^{-.08t} - 2e^{-.144t})$$

t = .04 hour

$$R_{S,IIa} = e^{-.000004}(1)(1)(1)(1)$$

$$\underline{R_{S,IIa} = .999996 \cong 1}$$

$$\begin{aligned}
R_{S, IIb} &= R_{S, IIa}, \text{ with } t = .5 \text{ hour} \\
&= e^{-.000048} (1)(e^{-.3t} + 2e^{-.15t} - 2e^{-.165t})^{28} (1)(1) \\
&= (.999952)(.999996)
\end{aligned}$$

$$\underline{R_{S, IIb} = .99995}$$

$$\begin{aligned}
R_{S, IIc} &= R_{S, IIa}, \text{ with } t = 35 \text{ hours} \\
&= e^{-.0034} (e^{-.0000105} + 2e^{-.00000525} - 2e^{-.000009975}) \\
&\quad \cdot (e^{-.0000105} + 2e^{-.00000525} - 2e^{-.000005775})^{28} (1) \\
&\quad \cdot (e^{-.00000560} + 2e^{-.00000280} - 2e^{-.00000504}) \\
&= (.99660) \left( .9999895 + 2(.99999475 - .999990025) \right) \\
&\quad \cdot \left( .9999895 + 2(.99999475 - .999994225) \right)^{28} \\
&\quad \cdot \left( .9999944 + 2(.9999972 - .99999496) \right) \\
&= (.99660)(.9999895 + .000009450)(.9999895 + .000001050)^{28} \\
&\quad \cdot (.9999944 + .00000448) \\
&= (.9966)(.99999895)(.99999055)^{28} (.99999888) \\
&= (.99659784)(.99974487)
\end{aligned}$$

$$\underline{R_{S, IIc} = .99634}$$

$$R_{S, III} = e^{-104.15t} (e^{-.3t} + 2e^{-.15t} - 2e^{-.285t})$$

$$(e^{-.3t} + 2e^{-.15t} - 2e^{-.165t})^{28} (2e^{-.015t} - e^{-.03t})^2$$

$$(e^{-.16t} + 2e^{-.08t} - 2e^{-.144t})(e^{-.46t} + 2e^{-.23t} - 2e^{-.345t})$$

t = 2154, 4344, 6534, 8724 hours

Term	Time			
	2154	4344	6534	8724
$e^{-104.15t}$	.79905	.63604	.50637	.40309
$e^{-.3t}$	.99935	.99870	.99804	.99738
$e^{-.15t}$	.99968	.99935	.99902	.99869
$e^{-.285t}$	.99939	.99876	.99814	.99751
$e^{-.165t}$	.99964	.99928	.99892	.99856
$e^{-.015t}$	.99997	.99991	.99990	.99987
$e^{-.03t}$	.99994	.99988	.99980	.99974
$e^{-.16t}$	.99966	.99930	.99896	.99860
$e^{-.08t}$	.99983	.99965	.99948	.99930
$e^{-.144t}$	.99969	.99938	.99906	.99874
$e^{-.46t}$	.99901	.99800	.99700	.99600
$e^{-.23t}$	.99950	.99900	.99850	.99799
$e^{-.345t}$	.99926	.99850	.99775	.99699
$(e^{-.3t} + 2e^{-.15t} - 2e^{-.285t})$	.99993	.99988	.99980	.99974
$(e^{-.3t} + 2e^{-.15t} - 2e^{-.165t})$	.99943	.99884	.99824	.99764
$(2e^{-.015t} - e^{-.03t})$	1	1	1	1
$(e^{-.16t} + 2e^{-.08t} - 2e^{-.144t})$	.99994	.99984	.99980	.99972
$(e^{-.46t} + 2e^{-.23t} - 2e^{-.345t})$	.99949	.99900	.99850	.99800
$(e^{-.3t} + 2e^{-.15t} - 2e^{-.165t})^{28}$	.98416	.96800	.95187	.93602
$(2e^{-.015t} - e^{-.03t})^2$	1	1	1	1
$R_{S, III}(t)$	.78589	.61490	.48108	.37531

$$\underline{R_{S,I}^* = R_{S,I} = .93472}$$

$$R_{S,IIa}^* = R_{S,I} R_{S,IIa} (R_5 R_{10} R_{11} R_{12} R_{20} R_{21})'$$

$$\begin{aligned} (R_5 R_{10} R_{11} R_{12} R_{20} R_{21})' &= e^{-10.19t} (2e^{-.015t} - e^{-.03t}) \\ &\quad \cdot (e^{-.3t} + 2e^{-.15t} - 2e^{-.165t}) \\ &\quad \cdot (e^{-.16t} + 2e^{-.08t} - 2e^{-.144t}) \end{aligned}$$

with  $t = 1$  and  $K = 800$ ,

$$\begin{aligned} (R_5 R_{10} R_{11} R_{12} R_{20} R_{21})' &= e^{-.00815} (1) (e^{-.00024} + 2e^{-.00012} - 2e^{-.000132}) \\ &\quad \cdot (e^{-.000128} + 2e^{-.000064} - 2e^{-.0001152}) \end{aligned}$$

$$= (.99138)(.99978)(.99997)$$

$$= .99163$$

$$R_{S,IIa}^* = (.93472)(.999996)(.99163) = .92689$$

$$\underline{R_{S,IIa}^* = .92689}$$

$$\begin{aligned} R_{S,II,b}^* &= R_{S,IIa}^* R_{S,IIb} \\ &= (.92689)(.99995) \end{aligned}$$

$$\underline{R_{S,IIb}^* = .92684}$$

$$R_{S,IIc}^* = R_{S,IIb}^* R_{S,IIc}$$

$$= (.92684)(.99634)$$

$$\underline{R_{S,IIc}^* = .92345}$$

$$R_{S,III}^* = R_{S,IIc}^* R_{S,III}^* (R_{13} R_{14} \cdots R_{19} R_{22})'$$

$$(R_{13} R_{14} \cdots R_{19} R_{22})' = e^{-10.87t} (e^{-.46t} + 2e^{-23t} - 2e^{-.345t})$$

$$\text{with } t = 1, K = 800, \text{ and } t = 36, K = 1$$

$$= e^{-.008696} (e^{-.000368} + 2e^{-.000184} - 2e^{-.000276})$$

$$e^{-.00039} (e^{-.0000166} + 2e^{-.000083} - 2e^{-.000276})$$

$$= .99134(.99982)(.99999)$$

$$= .99115$$

$$R_{S,III}^* = (.99115)(.92345) R_{S,III} = .91528 R_{S,III}$$

$$\underline{R_{S,III}^*(2154) = .71931}$$

$$\underline{R_{S,III}^*(4344) = .56280}$$

$$\underline{R_{S,III}^*(6534) = .44032}$$

$$\underline{R_{S,III}^*(8724) = .34351}$$

#### 4. Yaw Channel Reliability

The yaw channel consists of the following equipment and miscellaneous parts. Combinations of various  $R_i(t)$  versus mode are defined in Exhibits 5, 6, and 7.

i	Item	$R_i(t)$
1.	Converter	$e^{-3.76t}$
2.	Inverter	$e^{-20.91t}$
3.	Mode Memory	$e^{-45.93t}(e^{-.3t} + 2e^{-.15t} - 2e^{-.285t}) \cdot (e^{-.3t} + 2e^{-.15t} - 2e^{-.165t})^{27}$
23.	Small Earth Discriminator Circuits	$e^{-26.81t}$
24.	Relay K1	$e^{-1.80t} \quad R_{24}^{(1)} = e^{-1.60t}$
25.	Relay K2	$e^{-1.80t} \quad R_{25}^{(1)} = e^{-.8t}$
26.	Low-Level Magamp, PT6-2013	$e^{-3.90t}$
27.	6 Resistors, 3 Capacitors	$e^{-1.62t}$
18.	Low-Level d-c Magamp, PT6-2006	$e^{-3.90t}$
29.	3 Resistors	$e^{-.69t}$
17.	Coarse/Fine Selector Relay	$e^{-1.0t}(e^{-.46t} + 2e^{-.23t} - 2e^{-.345t})$
31.	Yaw Coarse Sensors	$e^{-1.4t}$
32.	Yaw Fine Sensors	$e^{-0.7t}$



i	Item	$R_i(t)$
33.	Intensity Detector	$e^{-0.7t}$
16.	Level Detector Magamp, 201221	$e^{-4.37t}$
35.	Bistable Magamp, 201221	$e^{-4.37t}$
36.	8 Diode Quads	1
37.	Valve Drivers and Valves	$e^{-32.22t}(e^{-.46t} + 2e^{-.23t} - 2e^{-.345t})^8$ $R_{37}^{(1)} = \left\{ 1 - \left[ 2e^{-1.50t}(1 - e^{-.115t}) + e^{-1.43t}(1 - e^{-.09t}) + e^{-1.65t}(1 - e^{-.064t}) \right] \right\}^4$
38.	Bistable Magamp, 201221	$e^{-4.37t}$ $R_{38}^{(1)} = e^{-.4t}$
39.	2 Diode Quads	1
40.	Motor Driver Magamp, 201220	$e^{-4.23t}$
41.	Yaw Reaction Wheel Motor	$e^{-4.80t}$
42.	2 Diode Quads, 1 Resistor, 1 Zener Diode	$e^{-.49t}$
43.	Level Detector Magamp (1/2 PT6-2003)	$e^{-2.09t}$ $R_{43}^{(1)} = e^{-.209t}$
44.	Unstable Null and Sun Interference Logic	$e^{-2.98t}$ $R_{44}^{(1)} = e^{-.298t}$
45.	1 Resistor	$e^{-.23t}$
46.	1 Capacitor	$e^{-.08t}$

i	Item	$R_i(t)$
47.	1 Resistor	$e^{-.23t}$
48.	1 Resistor	$e^{-.23t}$
49.	Regulator, Filter	$(e^{-.46t} + 2e^{-.23t} - 23^{-.345t})$ $\cdot (2e^{-.064t} - e^{-.128t})$ $\cdot (2e^{-.675t} - e^{-1.35t})$

Reliability of yaw channel  
in Mode I =  $R_{Y,I} = \{1 - (1 - R_{24})R_{16}R_{17}R_{18}R_{25}R_{26}R_{27}R_{29}R_{31}R_{32}R_{33}R_{35}R_{36}$   
 $\cdot R_{37}R_{45}R_{38}^{(1)}R_{47}R_{48}\} R_1R_2R_3R_{49}R_{37}^{(1)}$

Reliability of yaw channel  
in Mode IIa =  $R_{Y,IIa} = R_{Y,I}$

Reliability of yaw channel  
in Mode IIb =  $R_{Y,IIb} = R_1R_2R_3R_{16}R_{17}R_{18}R_{24}^{(1)}R_{25}R_{26}R_{27}R_{29}R_{31}R_{32}R_{33}R_{35}\dots$   
 $R_{42}R_{43}^{(1)}R_{44}^{(1)}R_{46}\dots R_{49}$

Reliability of yaw channel  
in Mode IIc =  $R_{Y,IIc} = R_{Y,IIb}$

Reliability of yaw channel  
in Mode III =  $R_{Y,III} = R_1R_2R_3R_{16}R_{17}R_{18}R_{24}^{(1)}R_{25}^{(1)}R_{26}R_{27}R_{29}R_{31}R_{32}R_{33}R_{38}$   
 $\cdot R_{39}\dots R_{42}R_{43}^{(1)}R_{44}^{(1)}R_{46}\dots R_{49}$

Reliability of yaw  
channel through Mode I =  $R_{Y,I}^* = R_{Y,I}$

Reliability of yaw  
channel through Mode IIa =  $R_{Y,IIa}^* = R_{Y,I}R_{Y,IIa}$

Reliability of yaw  
channel through Mode IIb =  $R_{Y,IIb}^* = R_{Y,IIa}^* R_{Y,IIb} (R_{35}\dots R_{48})'$

Reliability of yaw

$$\text{channel through Mode IIc} = R_{Y, IIc}^* = R_{Y, IIb}^* R_{IIc}$$

Reliability of yaw

$$\text{channel through Mode III} = R_{Y, III}^* = R_{Y, IIc}^* R_{III} (R_{23})'$$

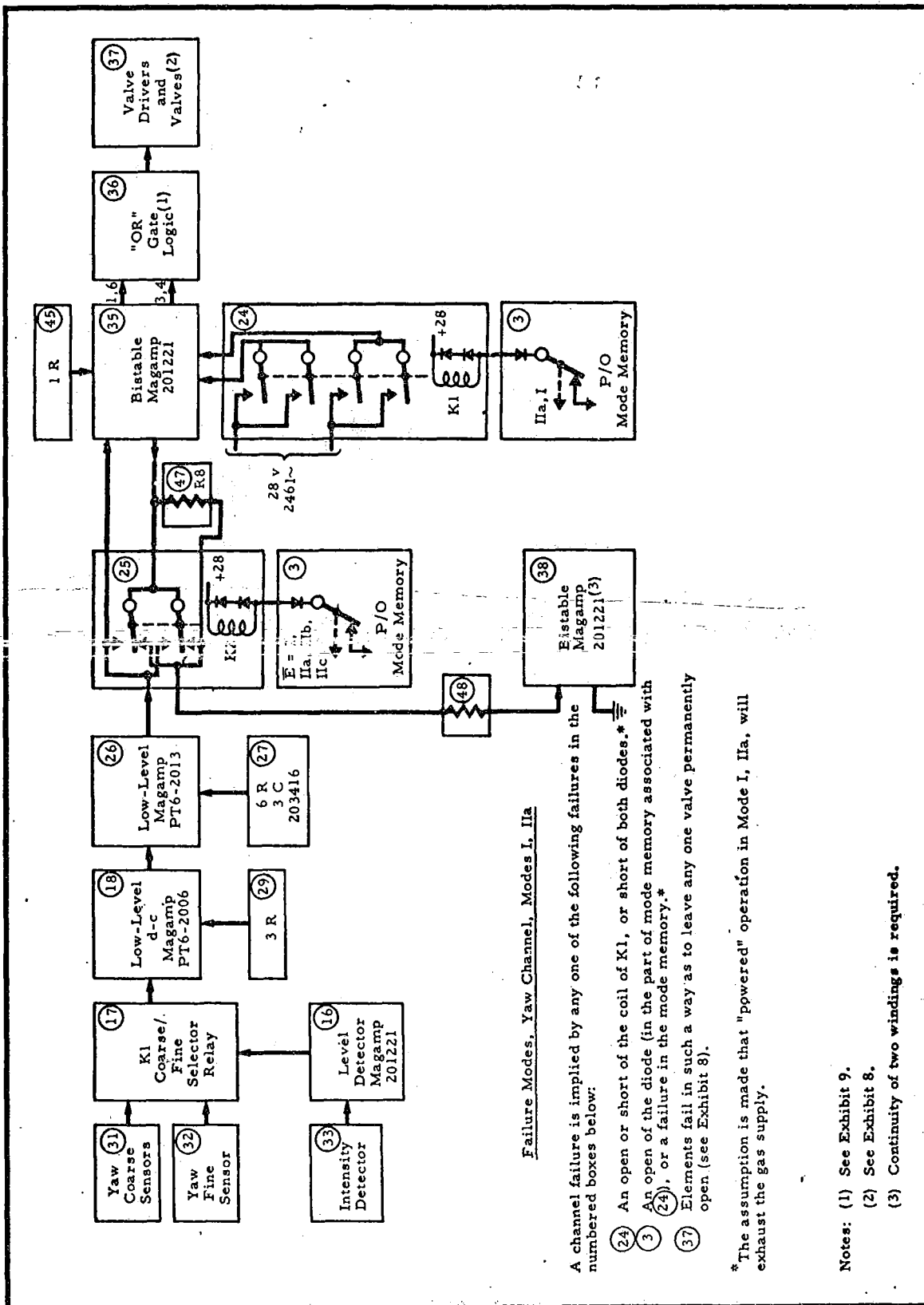
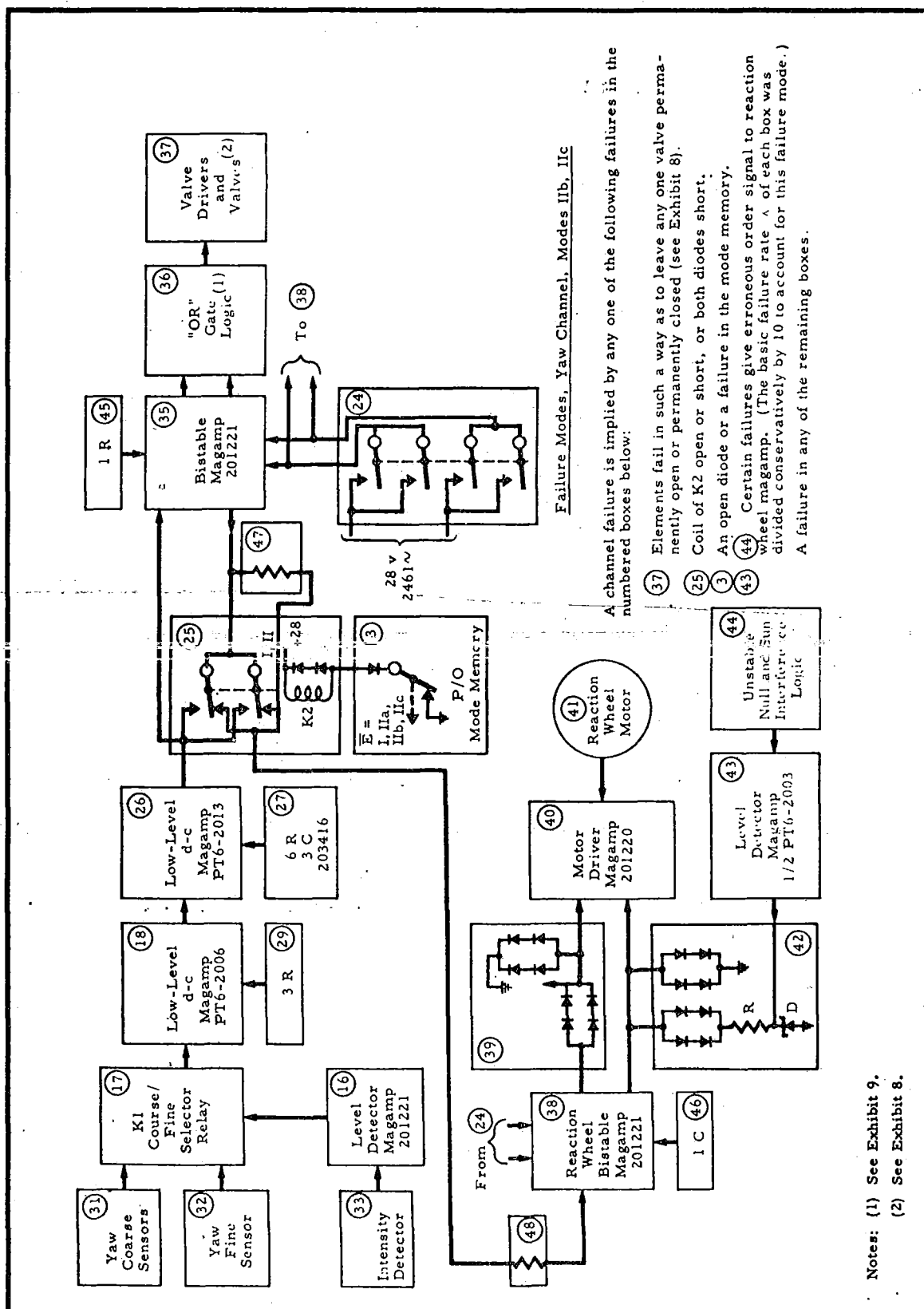


EXHIBIT 5 - YAW CHANNEL, MODES I, IIa



Notes: (1) See Exhibit 9.  
(2) See Exhibit 8.

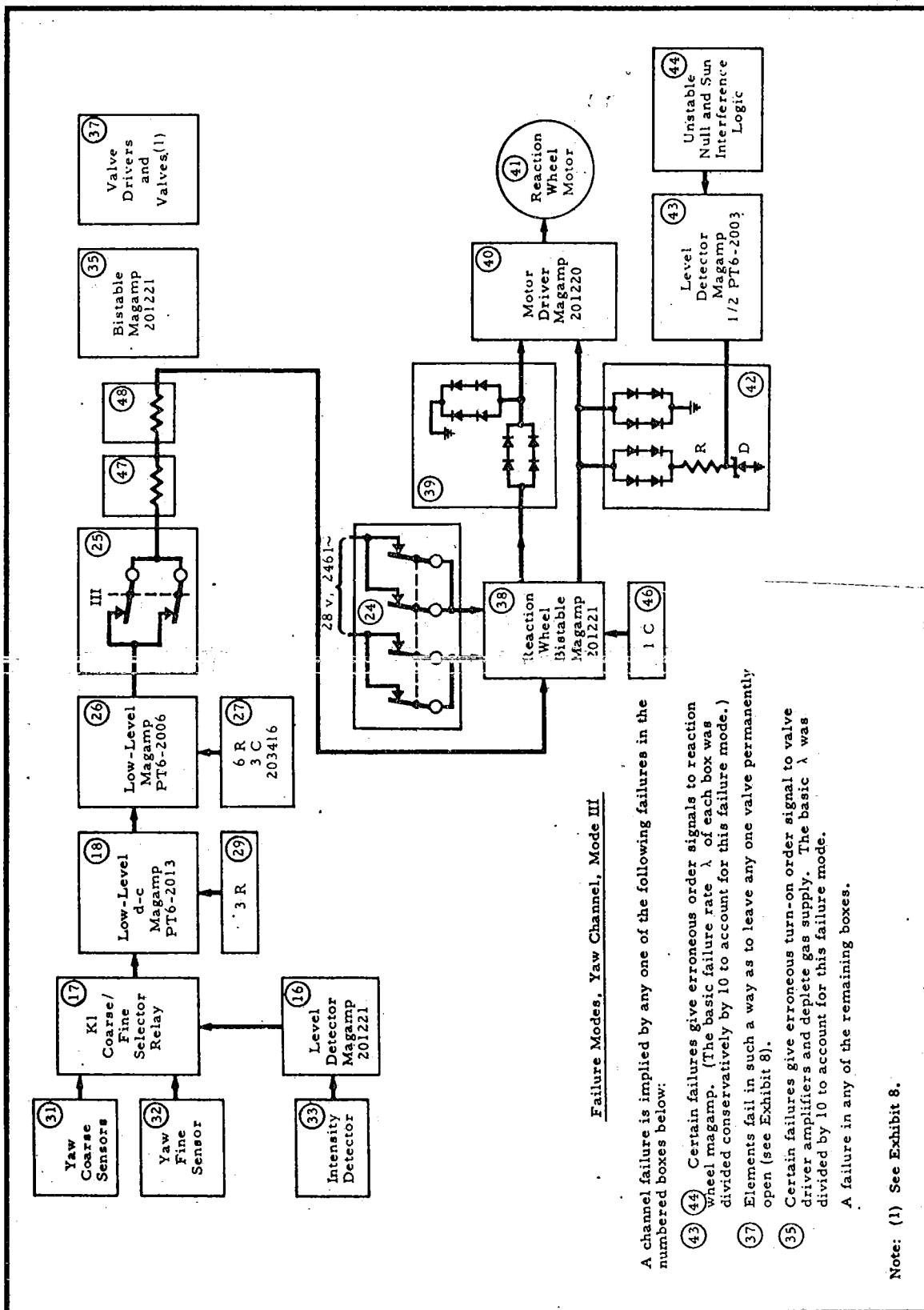
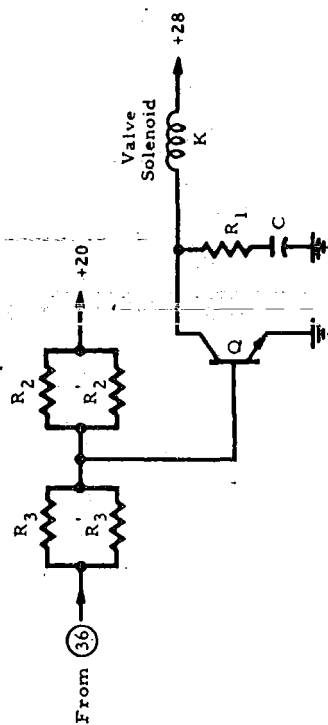


EXHIBIT 7 - YAW CHANNEL, MODE III



There are four (37)'s in pitch and yaw channels and two in roll channel.

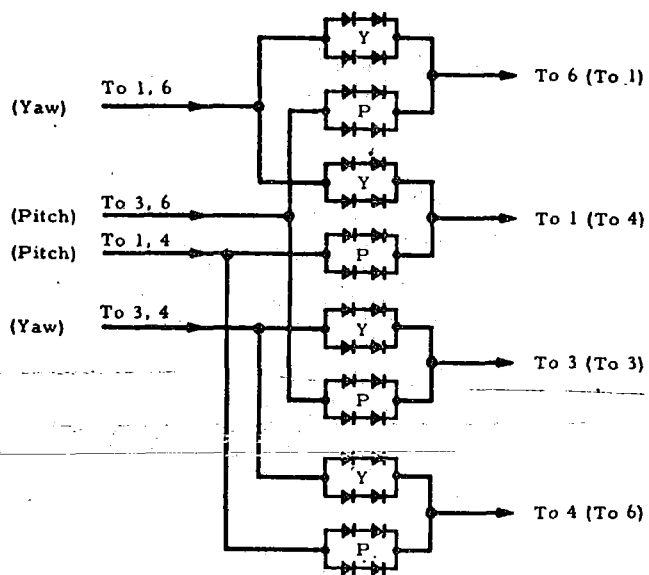
Valve-Fails-Open (Solenoid Energized) Modes

1. C Shorts
2. Q Shorts
3. R<sub>3</sub> and R<sub>3</sub> Open
4. R<sub>2</sub> or R<sub>2</sub> Short

Valve-Fails-Closed (Solenoid De-Energized) Modes

1. Q Opens
2. R<sub>2</sub> and R<sub>2</sub> Open
3. K Shorts
4. K Opens

EXHIBIT 8 - BOX 37, VALVE DRIVERS AND VALVES



Note: P = pitch; Y = yaw. The P quads may fail open with no consequence to the yaw channel; the Y quads may fail open with no consequence to the pitch channel. Short Y or P is catastrophic.

EXHIBIT 9 - BOX 36, "OR" GATE LOGIC



$$\begin{aligned}
R_{Y,I} &= \left\{ 1 - (1 - e^{-1.80t})e^{-20.08t}(e^{-.46t} + 2e^{-.23t} - 2e^{-.345t}) \right\} \\
&\quad \cdot e^{-70.60t}(e^{-.3t} + 2e^{-.15t} - 2e^{-.285t})(e^{-.3t} + 2e^{-.15t} - 2e^{-.165t})^{27} \\
&\quad \cdot (e^{-.46t} + 2e^{-.23t} - 2e^{-.345t})(2e^{-.064t} - e^{-.128t}) \\
&\quad \cdot (2e^{-.675t} - e^{-1.35t})
\end{aligned}$$

with  $t = 1$  hour, but  $K = 800$ ,

$$\begin{aligned}
&= \left\{ 1 - (1 - e^{-.00144})e^{-.016}(.99982) \right\} e^{-.05648}(.999976)(.99418) \\
&\quad \cdot (.99982)(1)(1) \\
&= \left\{ 1 - (.00144)(.98413)(.99982) \right\} (.94506)(.999976)(.97418)(.99982) \\
&= \left\{ .99858 \right\} (.93937)
\end{aligned}$$

$$\underline{R_{Y,I} = .93804}$$

$$\begin{aligned}
R_{Y,IIa} &= \left\{ 1 - (1 - e^{-1.80t})e^{-20.08t}(e^{-.46t} + 2e^{-.23t} - 2e^{-.345t}) \right\} \\
&\quad \cdot e^{-70.60t}(e^{-.3t} + 2e^{-.15t} - 2e^{-.235t})(e^{-.3t} + 2e^{-.15t} - 2e^{-.165t})^{27} \\
&\quad \cdot (e^{-.46t} + 2e^{-.23t} - 2e^{-.345t})(2e^{-.364t} - e^{-.128t})(2e^{-.675t} - e^{-1.35t})
\end{aligned}$$

with  $t = .04$ ,

$$= \left\{ 1 \right\} (1) (1) (1) (1) (1) (1)$$

$$\underline{R_{Y,IIa} = 1}$$

$$R_{Y, IIb} = e^{-144.037t} (e^{-.3t} + 2e^{-.285t}) (e^{-.3t} + 2e^{-.15t} - 2e^{-.165t})^{27} \\ \cdot (e^{-.46t} + 2e^{-.23t} - 2e^{-.345t})^{10} (2e^{-.064t} - e^{-.128t}) \\ \cdot (2e^{-.675t} - e^{-1.35t})$$

with  $t = .5$  hour

$$= e^{-.000072} (1)(1)(1)(1)$$

$$R_{Y, IIb} = .99993$$

$$R_{Y, IIc} = R_{Y, IIb}, \text{ with } t = 35 \text{ hours,}$$

$$= e^{-.00504} (1)(.99925)(.9999)(1)(1)$$

$$= (.99497)(.99975)$$

$$R_{Y, IIc} = .99472$$

$$R_{Y, III} = e^{-132.227t} (e^{-.3t} + 2e^{-.15t} - e^{-.285t}) (e^{-.3t} + 2e^{-.15t} - 2e^{-.165t})^{27} \\ \cdot (2e^{-.015t} - e^{-.03t}) (e^{-.46t} + 2e^{-.23t} - 2e^{-.345t})^9 \\ \cdot (2e^{-.064t} - e^{-.128t}) (2e^{-.675t} - e^{-1.35t})$$

with  $t = 2154, 4344, 6534, 8724$  hours,

Term	Time			
	2154	4344	6534	8724
$e^{-132.227t}$	.75202	.56208	.42148	.31664
$(e^{-.3t} + 2e^{-.15t} - 2e^{-.205t})$	.99993	.99988	.99980	.99974
$(e^{-.3t} + 2e^{-.15t} - 2e^{-.165t})^{27}$	.98472	.96912	.95355	.93823
$(2e^{-0.5t} - e^{-.03t})$	1	1	1	1
$(e^{-.46t} + 2e^{-.23t} - 2e^{-.345t})^9$	.99542	.99103	.98659	.98214
$(2e^{-.064t} - e^{-.128t})$	1	1	1	1
$(2e^{-.675t} - e^{-1.35t})$	.99999	.99998	.99997	.99996
$R_{Y,III}$	.73708	.53976	.39642	.39169

$$\underline{R_{Y,I}^* = R_{Y,I} = .93804}$$

$$\underline{R_{Y,IIa}^* = R_{Y,I}^* R_{Y,IIa} = .93804}$$

$$R_{Y,IIb}^* = R_{Y,IIa}^* R_{Y,IIb} (R_{35} \cdots R_{48})^1$$

$$(R_{35} \cdots R_{48})^1 = e^{-51.757t} (e^{-.46t} + 2e^{-.23t} - 2e^{-.345t})^8$$

$$\text{with } t = 1, K = 800, \text{ and } t = .04,$$

$$= e^{-.0414} (.99982)^8$$

$$= .95945(.99856) = .95807$$

$$R_{Y,IIb}^* = (.95807)(.93804)(.99993)$$

$$\underline{R_{Y,IIb}^* = .89865}$$

$$R_{Y, IIc}^* = R_{Y, IIb}^* R_{IIc}$$

$$= (.89865)(.99472)$$

$$R_{Y, IIc}^* = .89390$$

$$R_{Y, III}^* = R_{Y, IIc}^* R_{Y, III} (R23)'$$

$$R23' = e^{-26.81t}$$

$$\text{where } t = 1, K = 800, \text{ and } t = 36 = e^{-.0215}$$

$$= e^{-.0215} = .97873$$

Term	Time			
	2190	4380	6570	8760
$R_{Y, IIc}^* R_{Y, III}$	.65888	.48249	.35436	.26074
$R_{Y, III}^*$	.64486	.47223	.34682	.25519

## 5. Pitch Channel Reliability

The pitch channel consists of the following equipments and miscellaneous parts. Combinations of the  $R_i(t)$  versus mode are defined in Exhibits 10, 11, and 12.

i	Item	$R_i(t)$
1.	Converter	$e^{-3.76t}$
2.	Inverter	$e^{-20.91t}$
3.	Mode Memory	$e^{-45.93t}(e^{-.3t} + 2e^{-.15t} - 2e^{-.285t}) \cdot (e^{-.3t} + 2e^{-.15t} - 2e^{-.165t})^{27}$
23.	Small Earth Discriminator Circuits	$e^{-26.81t}$
24.	Relay K1	$e^{-1.80t} \quad R_{24}^{(1)} = e^{-1.60t}$
25.	Relay K2	$e^{-1.80t} \quad R_{25}^{(1)} = e^{-.8t}$
36.	Diode Quads	1
37.	Valve Driver and Valve	$e^{-32.22t}(e^{-.46t} + 2e^{-.23t} - 2e^{-.345t})^8$ $R_{37}^{(1)} = (\text{See Yaw Channel List})$
49.	Regulator, Filter	$(e^{-.46t} + 2e^{-.23t} - 2e^{-.345t})$ $(2e^{-.064t} - e^{-.128t})$ $(2e^{-.675t} - e^{-1.35t})$
50.	Bistable Magamp, 201221	$e^{-4.37t}$
51.	Bistable Magamp, 201221	$e^{-4.37t}$
52.	2 Resistors, 1 Capacitor	$e^{-.54t}$

i	Item	$R_i(t)$
53.	Diode Quad	1
54.	Diode Quad	1
55.	Motor Driver Magamp	$e^{-4.23t}$
56.	Reaction Wheel Motor	$e^{-4.80t}$
57.	Low-Level d-c Magamp, 201221	$e^{-4.37t}$
58.	8 Resistors, 5 Capacitors	$e^{-2.24t}$
59.	Z10 Error Demodulator	$e^{-9.48t}$
60.	Horizon Scanner Selection Logic	$e^{-4.83t}(e^{-.46t} + 2e^{-.23t} - 2e^{-.345t})^2$
61.	Horizon Scanner	See Separate Analysis
62.	Rate Gyro Electronics	$e^{-(12.69)t}$

Reliability of pitch channel  
in Mode I =  $R_{P,I} = \left\{ 1 - (1 - R_{24})R_{25}R_{36}R_{37}R_{51}R_{52}R_{62} \right\} R_1R_2R_3R_{37}^{(1)}R_{49}$

Reliability of pitch channel  
in Mode IIa =  $R_{P,IIa} = R_{P,I}$

Reliability of pitch channel  
in Mode IIb =  $R_{P,IIb} = R_1R_2R_3R_{24}^{(1)}R_{25}R_{36}R_{37}R_{49}R_{50} \cdots R_{56}R_{62}$

Reliability of pitch channel  
in Mode IIc =  $R_{P,IIc} = R_{P,IIb}$

Reliability of pitch channel  
in Mode III =  $R_{P,III} = R_1R_2R_3R_{23}R_{24}^{(1)}R_{25}^{(1)}R_{36}R_{37}R_{49}R_{50} \cdots R_{61}$

Reliability of pitch  
channel through Mode I =  $R_{P,I}^* = R_{P,I}$

Reliability of pitch  
channel through Mode IIa =  $R_{P,IIa}^* = P_{P,I}^* R_{P,IIa}$

Reliability of pitch  
channel through Mode IIb =  $R_{P,IIb}^* = R_{P,IIa}^* R_{P,IIb} (R_{26} R_{50} R_{53} \cdots R_{56})'$

Reliability of pitch  
channel through Mode IIc =  $R_{P,IIc}^* = R_{P,IIb}^* R_{P,IIc}$

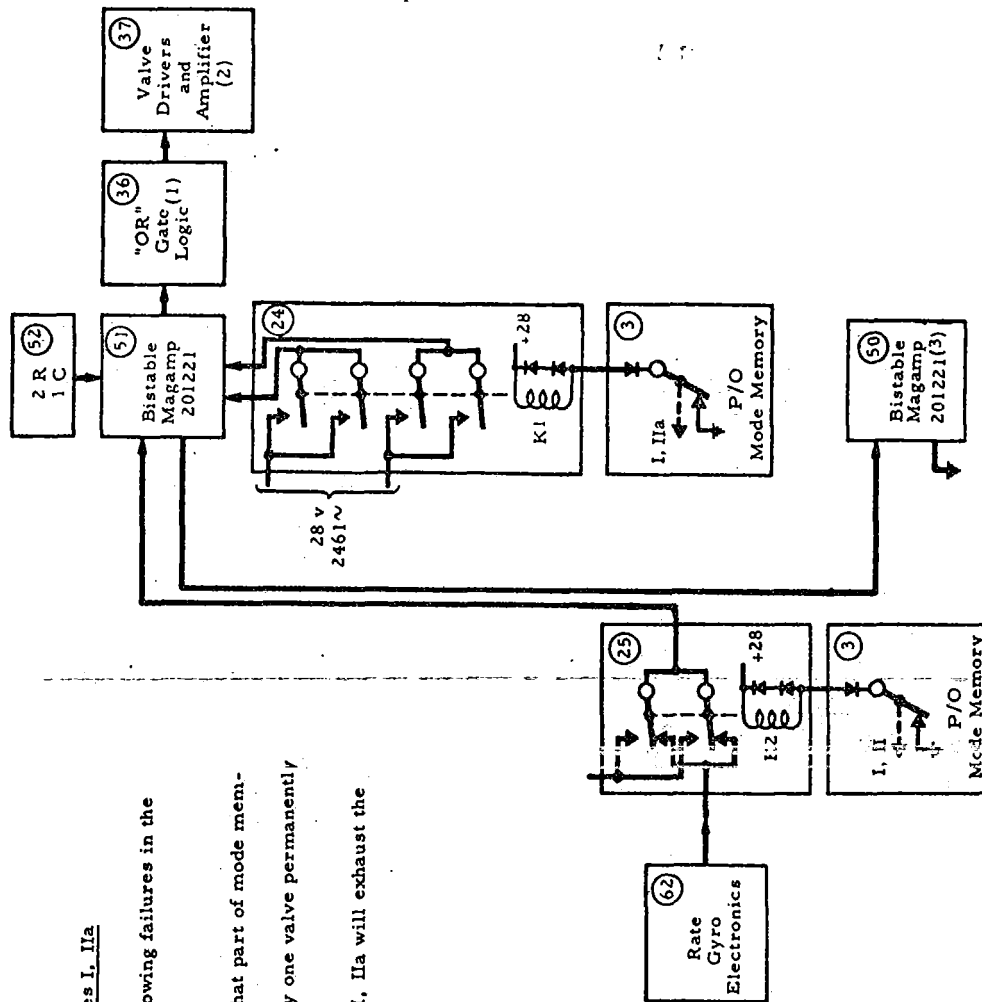
Reliability of pitch  
channel through Mode III =  $R_{P,III}^* = R_{P,IIc}^* R_{P,III} (R_{23} R_{57} R_{58} \cdots R_{61})'$

# Failure Modes, Pitch Channel, Modes I, IIa

A channel failure is implied by any one of the following failures in the numbered boxes below:

- (24) Both diodes short or K1 opens or shorts.\*
- (3) Diode opens or failure in mode memory (that part of mode memory associated with (24)).\*
- (37) Elements fail in such a way as to leave any one valve permanently open (see Exhibit 8).

\*It is assumed that "powered" operation in Mode I, IIa will exhaust the gas supply.



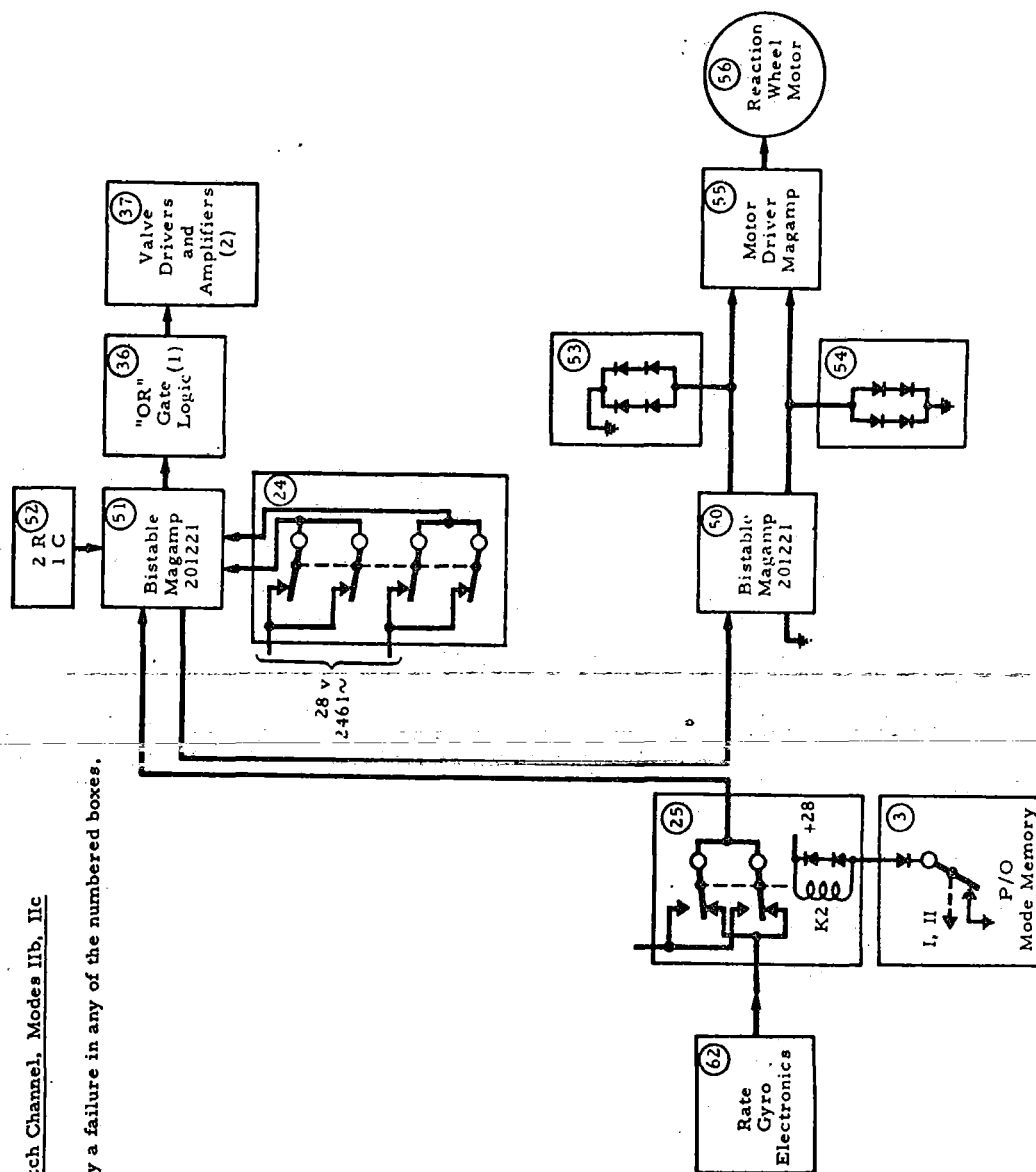
- Notes: (1) See Exhibit 9.  
(2) See Exhibit 8.  
(3) Continuity of two windings is required.

EXHIBIT 10 - PITCH CHANNEL, MODES I, IIa



# Failure Modes, Pitch Channel, Modes Iib, Iic

A channel failure is implied by a failure in any of the numbered boxes.



Notes: (1) See Exhibit 9.  
(2) See Exhibit 8.

EXHIBIT 11 - PITCH CHANNEL, MODES Iib, Iic

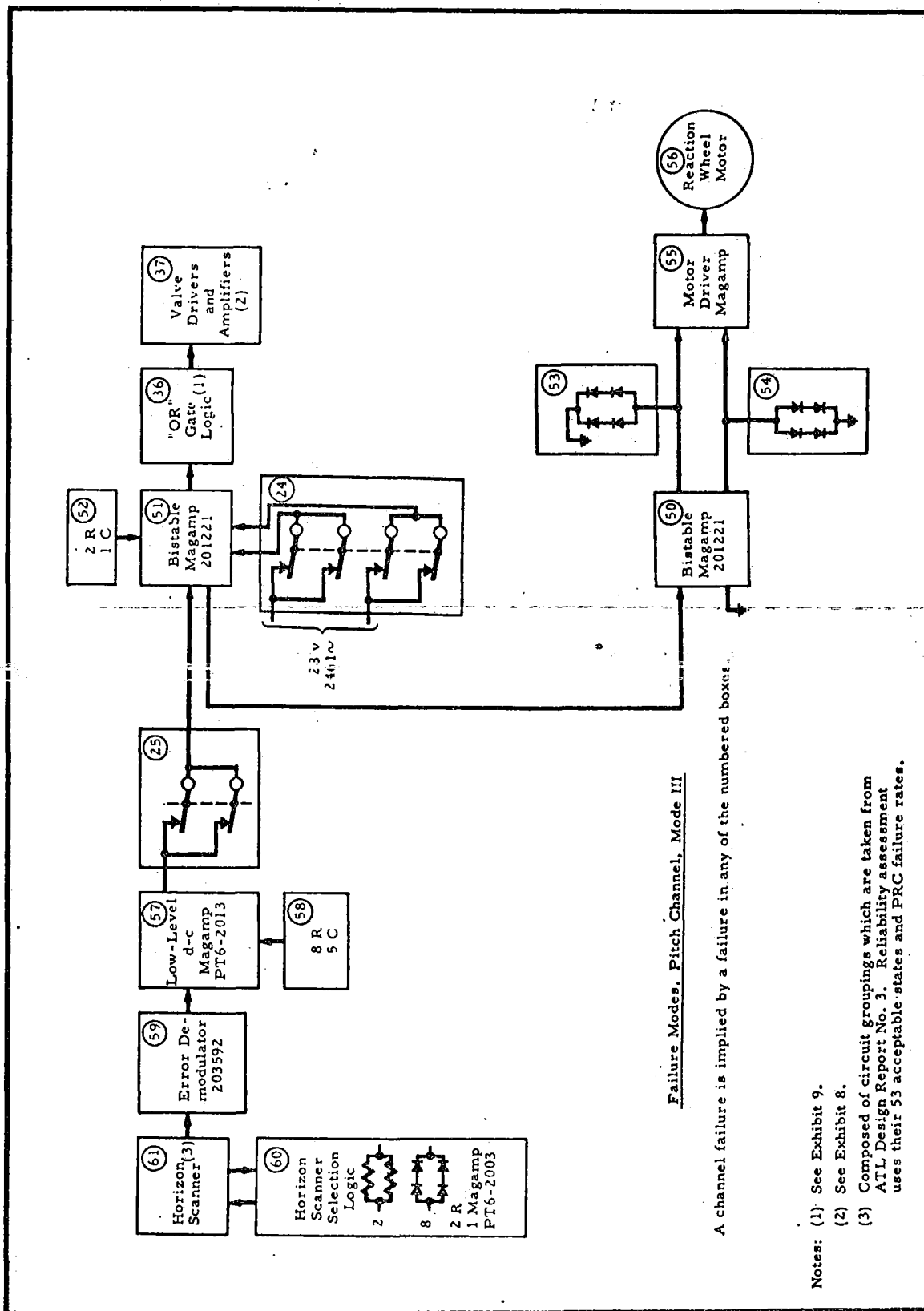


EXHIBIT 12 - PITCH CHANNEL, MODE III

$$R_{P,I} = 1 - (1 - e^{-1.80t}) e^{-14.49t} (.93937)$$

with  $t = 1$ , but  $K = 800$

$$= 1 - (.00144)(.98847) (.93937) = (.99858)(.93937)$$

$$\underline{R_{P,I} = .93804}$$

$$R_{P,IIa} = R_{P,I}, \text{ with } t = .04$$

$$\underline{R_{P,IIa} = 1}$$

$$R_{P,IIb} = e^{-137.22t} (e^{-.3t} + 2e^{-.15t} - 2e^{-.285t}) (e^{-.3t} + 2e^{-.15t} - 2e^{-.165t})^{27} \\ \cdot (e^{-.46t} + 2e^{-.23t} - 2e^{-.345t})^9 \\ \cdot (2e^{-.064t} - e^{-.128t}) (2e^{-.625t} - e^{-1.35t})$$

with  $t = .5$  hours

$$= e^{-.00007} (1) = .99993$$

$$\underline{R_{P,IIb} = .99993}$$

$$R_{P,IIc} = R_{P,IIb}, \text{ with } t = 35 \text{ hours}$$

$$= e^{-.0048} (1)(1)(.99975)(.99991)(1)(1) = (.99521)(.99975)(.99991)$$

$$\underline{R_{P,IIc} = .99487}$$

$$R_{P, III} = e^{-171.26t} R_{\text{Horizon Scanner}} (e^{-.3t} + 2e^{-.15t} - 2e^{-.285t}) \\ \cdot (e^{-.3t} + 2e^{-.15t} - 2e^{-.165t})^{.27} (e^{-.46t} + 2e^{-.23t} - 2e^{-.345t})^{.11} \\ \cdot (2e^{-.064t} - e^{-.128t})(2e^{-.675t} - e^{-1.35t})$$

with  $t = 2154, 4344, 6534, 8724$  hours

Term	Time			
	2154	4344	6534	8724
$e^{-171.26t}$	.69142	.47332	.32637	.22313
$R_{\text{Horizon Scanner}}$	.92574 <sup>‡</sup>	.81500 <sup>‡</sup>	.69500 <sup>‡</sup>	.57250 <sup>‡</sup>
$(e^{-.3t} + 2e^{-.15t} - 2e^{-.235t})$	.99993	.99988	.99980	.99974
$(e^{-.3t} + 2e^{-.15t} - 2e^{-.165t})^{.27}$	.98472	.96912	.95355	.93823
$(e^{-.46t} + 2e^{-.23t} - 2e^{-.345t})^{.11}$	.99440	.98905	.98363	.97822
$(2e^{-.064t} - e^{-.128t})$	1	1	1	1
$(2e^{-.675t} - e^{-1.35t})$	.99999	.99998	.99997	.99996
$R_{P, III}(t)$	.62672	.36970	.21270	.11720

$$R_{P, I}^* = R_{P, I} = .93804$$

$$R_{P, IIa}^* = R_{P, I}^* R_{P, IIa} = .93804$$

<sup>‡</sup> Determined graphically.

$$R_{P, IIb}^* = R_{P, IIa}^* R_{P, IIb} (R_{36} R_{37} R_{50} R_{51} \dots R_{56})'$$

$$(R_{36} R_{37} R_{50} R_{51} \dots R_{56})' = e^{-13.40t}, \text{ with } t = 1, K = 800$$

$$= (.98953)$$

$$\underline{R_{P, IIb}^* = .92815}$$

$$R_{P, IIc}^* = R_{P, IIb}^* R_{P, IIc} = (.92815)(.99487)$$

$$\underline{R_{P, IIc}^* = .92339}$$

$$R_{P, III}^* = R_{P, IIc}^* R_{P, III} (R_{23} R_{54} R_{58} \dots R_{61})'$$

$$(R_{23} R_{54} R_{58} \dots R_{61})' = e^{-47.73t} (e^{-.46t} + 2e^{-.27t} - 23^{-.345t})_{\text{Horizon Scanner}}$$

$$\text{for } t = 1, K = 800, \text{ and } t = 36$$

$$= e^{-.04} (.9996)(.984)^\ddagger$$

$$= (.96079)(.9996)(.984) = .94504$$

$$R_{P, III}^* = (.92339)(.94504)(.62672)$$

$$(.36370)$$

$$(.20447)$$

$$(.11330)$$

$$\underline{R_{P, III}^* = .54690; .32261; .18561; .10227}$$

---

<sup>‡</sup>Determined graphically.

## 6. Roll Channel Reliability

The roll channel consists of the following equipments and miscellaneous parts. Combinations of the  $R_i(t)$  versus mode are defined in Exhibits 13, 14, and 15.

i	Item	$R_i(t)$
1.	Converter	$e^{-3.76t}$
2.	Inverter	$e^{-20.91t}$
3.	Mode Memory	$e^{-45.93t}(e^{-.3t} + 2e^{-.15t} - 2e^{-.285t}) \cdot (e^{-.3t} + 2e^{-.15t} - 2e^{-.165t})^{27}$
13.	Array Coarse Sensor	$e^{-2.8t}$
14.	Array Fine Sensor	$e^{-.7t}$
15.	Intensity Detector	$e^{-.7t}$
16.	Level Detector Magamp	$e^{-2.09t}$
17.	Coarse/Fine Selector	$e^{-.6t}(2e^{-.015t} - e^{-.03t}) \cdot (e^{-.46t} + 2e^{-.23t} - 2e^{-.345t})$
18.	Low-Level d-c Magamp	$e^{-4.37t}$
19.	6 Resistors	$e^{-1.38t}$
22.	2 Capacitors	$e^{-.16t}$
23.	Small Earth Discriminator Circuits	$e^{-26.81t}$
24.	Relay K1	$e^{-1.80t} \quad R_{24}^{(1)} = e^{-1.60t}$

i	Item	$R_i(t)$
75.	Relay K2A	$e^{-1.115t} R_{75}^{(1)} = e^{-1.094t}$
60.	Horizon Scanner Selection Logic	$e^{-4.83t}(e^{-.46t} + 2e^{-.23t} - 2e^{-.345t})^2$
61.	Horizon Scanner	See Separate Analysis
73.	Z9 Error Demodulator	$e^{-9.48t}$
74.	1 Resistor 2 Capacitors	$e^{-.23t}(e^{-.16t} + 2e^{-.08t} - 2e^{-.096t})$
63.	Low-Level d-c Magamp	$e^{-4.37t}$
64.	5 Resistors, 2 Capacitors	$e^{-1.31t}$
65.	Bistable Magamp	$e^{-4.37t}$
66.	2 Resistors 1 Capacitor	$e^{-.54t}$
67.	Valve Driver and Valve (2)	$e^{-16.11t}(e^{-.46t} + 2e^{-.23t} - 2e^{-.345t})^4$ $R_{67}^{(1)} = \left\{ 1 - [2e^{-1.50t}(1 - e^{-.115t}) + e^{-1.43t}(1 - e^{-.09t}) + e^{-1.65t}(1 - e^{-.064t})] \right\}^2$
68.	Bistable Magamp	$e^{-4.37t} R_{68}^{(1)} = e^{-.4t}$
69.	Diode Quad	1
70.	Diode Quad	1
71.	Motor Driver Magamp	$e^{-4.23t}$
72.	Reaction Wheel Motor	$e^{-4.80t}$

i	Item	$R_i(t)$
49.	Regulator, Filter	$(e^{-.46t} + 2e^{-.23t} - 2e^{-.345t})$ $\cdot (2e^{-.064t} - e^{-.128t})$ $\cdot (2e^{-.675t} - e^{-1.35t})$

Reliability of roll

$$\text{channel in Mode I} = R_{R,I} = \{1 - (1 - R_{24})R_{13} \cdots R_{19}R_{22}R_{63} \cdots R_{67}R_{68}^{(1)}R_{74}R_{75}\} \\ \cdot R_1R_2R_3R_{49}R_{67}^{(1)}$$

Reliability of roll

$$\text{channel in Mode IIa} = R_{R,IIa} = R_{R,I}$$

Reliability of roll

$$\text{channel in Mode IIb} = R_{R,IIb} = R_1R_2R_3R_{13} \cdots R_{19}R_{22}R_{24}^{(1)}R_{49}R_{63} \cdots \\ \cdot R_{72}R_{74}R_{75}$$

Reliability of roll

$$\text{channel in Mode IIc} = R_{R,IIc} = R_{R,IIb}$$

Reliability of roll

$$\text{channel in Mode III} = R_{R,III} = R_1R_2R_3R_{23}R_{24}^{(1)}R_{49}R_{60}R_{61}R_{63} \cdots R_{74}R_{75}^{(1)}$$

Reliability of roll

$$\text{channel through Mode I} = R_{R,I}^* = R_{R,I}$$

Reliability of roll

$$\text{channel through Mode IIa} = R_{R,IIa}^* = R_{R,I}^* R_{R,IIa}$$

Reliability of roll

$$\text{channel through Mode IIb} = R_{R,IIb}^* = R_{R,IIa}^* R_{IIb} (R_{68}/R_{68}^{(1)} R_{69}R_{70}R_{71}R_{72})$$



Reliability of roll

channel through Mode IIc =  $R_{R, IIc}^* = R_{R, IIb}^* R_{R, IIc}$

Reliability of roll

channel through Mode III =  $R_{R, III}^* = R_{R, IIc}^* R_{R, III} (R_{23} R_{60} R_{61} R_{73})'$

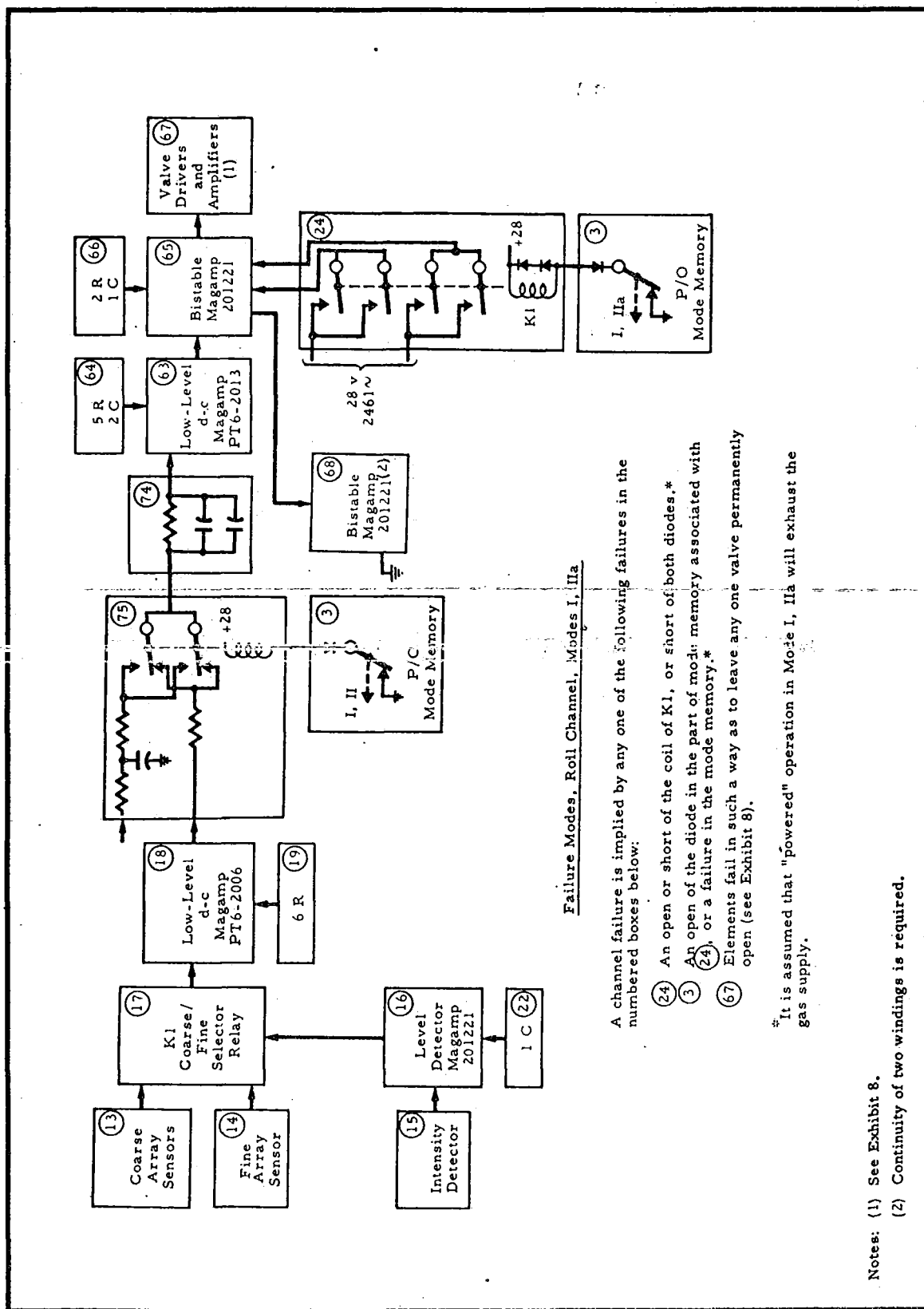


EXHIBIT 13 - ROLL CHANNEL, MODES I, IIa

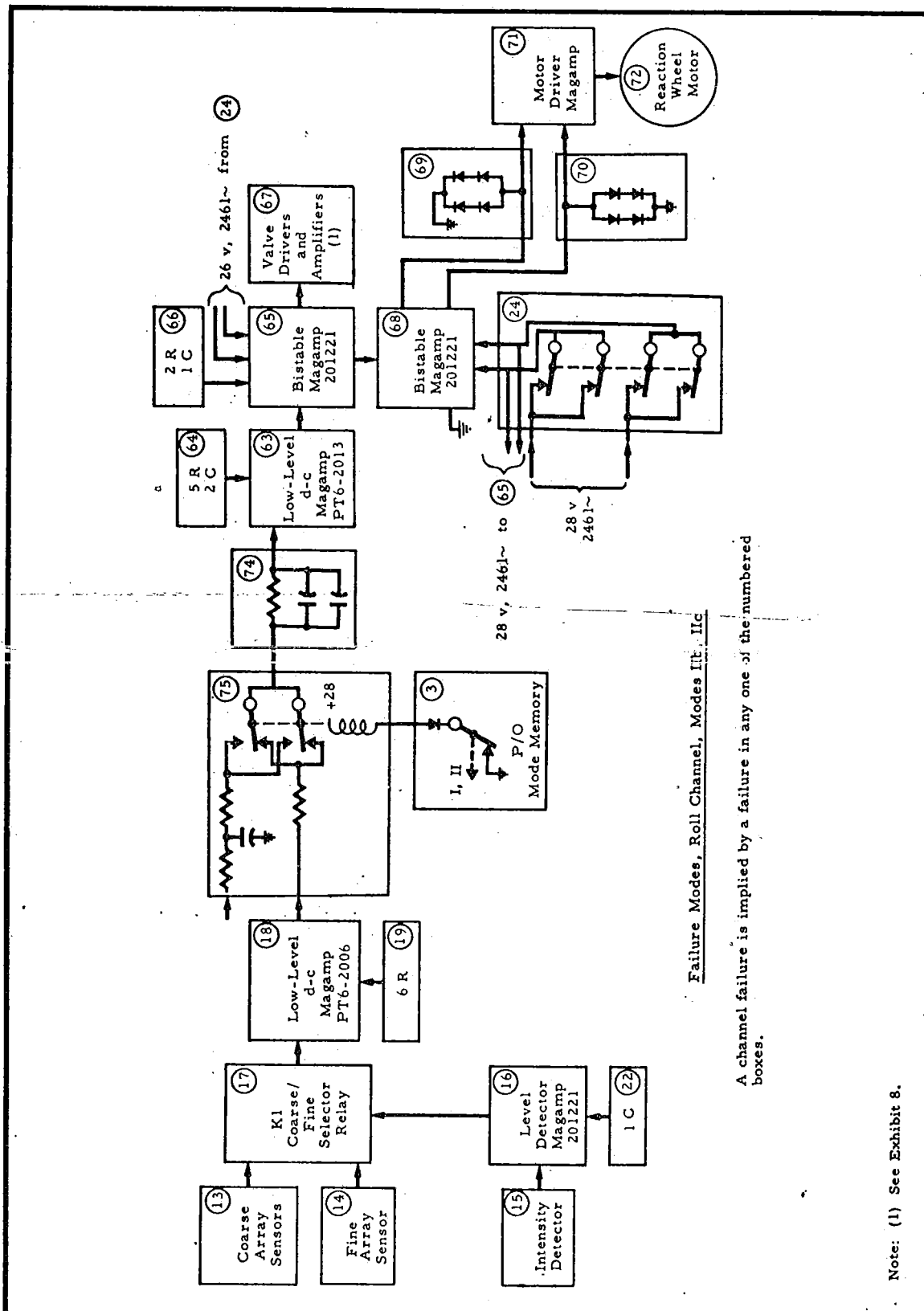
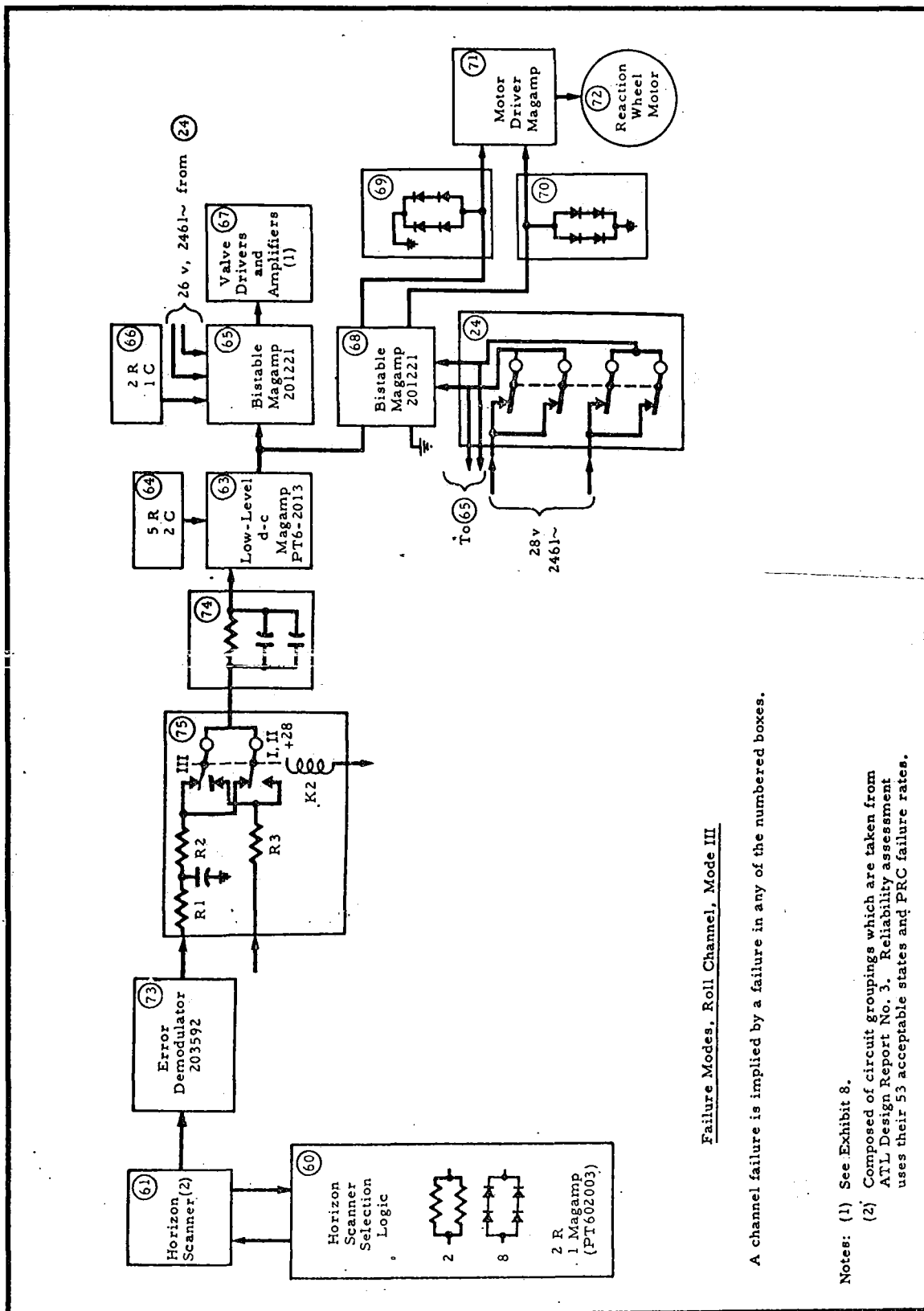


EXHIBIT 14 - ROLL CHANNEL, MODES IIt, IIc



Failure Modes, Roll Channel, Mode III

A channel failure is implied by a failure in any of the numbered boxes.

- Notes: (1) See Exhibit 8.  
 (2) Composed of circuit groupings which are taken from ATL Design Report No. 3. Reliability assessment uses their 53 acceptable states and PRC failure rates.

$$\begin{aligned}
R_{R,I} = & \left\{ 1 - (.00144)e^{-20.51t}(e^{-.16t} + 2e^{.08t} - 2e^{-.096t}) \right. \\
& \cdot (2e^{-.015t} - e^{-.03t})(e^{-.46t} + 2e^{-.23t} - 2e^{-.345t}) \} \\
& \cdot e^{-70.60t}(e^{-.3t} + 2e^{-.150t} - 2e^{-.285t}) \\
& \cdot (e^{-.3t} + 2e^{-.15t} - 2e^{-.165t})^{27} (e^{-.46t} + 2e^{-.23t} - 2e^{-.345t}) \\
& \cdot (2e^{-.064t} - e^{-.128t})(2e^{-.675t} - e^{-1.35t}) ,
\end{aligned}$$

where  $t = 1$ ,  $K = 800$ ,

$$\begin{aligned}
& = \left\{ 1 - (.00144)(.98364)(.99990)(1)(.99982) \right\} (.93937) \\
& = (.99858)(.93937)
\end{aligned}$$

$$R_{R,I} = .93804$$

$$R_{R,IIa} = 1, \text{ for } t = .04$$

$$\begin{aligned}
R_{R,IIb} = & e^{-127.13t}(e^{-.3t} + 2e^{-.15t} - 2e^{-.258t})(e^{-.3t} + 2e^{-.5t} - 2e^{-.165t})^{27} \\
& \cdot (2e^{-.015t} - e^{-.03t})(e^{-.46t} + 2e^{-.23t} - 2e^{-.345t})^6 \\
& \cdot (e^{-.16t} + 2e^{-.08t} - 2e^{-.096t})(2e^{-.064t} - e^{-.128t}) \\
& \cdot (2e^{-.675t} - e^{-1.35t})
\end{aligned}$$

for  $t = 1/2$  hour,

$$= e^{-.00006}(1)(1) \dots (1)$$

$$R_{R,IIb} = .99996$$

$$R_{R, IIc} = e^{-.00445} (1)(.99975)(1)(.99994)(1)(1), \text{ with } t = 35 \text{ hours}$$

$$= (.99556)(.99975)(.99994)$$

$$R_{R, IIc} = .99533$$

$$R_{R, III} = e^{-154.45t} (e^{-.3t} + 2e^{-.15t} - 2e^{-.285t}) \\ \cdot (e^{-.3t} + 2e^{-.15t} - 2e^{-.165t}) (e^{-.46t} + 2e^{-.23t} - 2e^{-.345t})^7 \\ \cdot (e^{-.16t} + 2e^{-.08t} - 2e^{-.096t}) \\ \cdot (2e^{-.064t} - e^{-.128t}) (2e^{-.675t} - e^{-1.35t}) R_{\text{Horizon Scanner}}(t)$$

Term	Time			
	2154	4344	6534	8724
$e^{-154.44t}$	.71700	.51170	.36787	.25924
$R_{\text{Horizon Scanner}}(t)$	.92574	.81500	.69500	.57250
$(e^{-.3t} + 2e^{-.15t} - 2e^{-.285t})$	.99993	.99988	.99980	.99974
$(e^{-.3t} + 2e^{-.15t} - 2e^{-.165t})^{27}$	.98472	.96912	.93555	.93823
$(e^{-.46t} + 2e^{-.23t} - 2e^{-.345t})^7$	.99644	.99302	.98956	.98608
$(e^{-.16t} + 2e^{-.08t} - 2e^{-.096t})$	.99972	.99956	.99916	.99888
$(2e^{-.064t} - e^{-.128t})$	1	1	1	1
$(2e^{-.675t} - e^{-1.35t})$	.99999	.99998	.99997	.99996
$R_{R, III}$	.65105	.40110	.24099	.13711

$$\underline{R_{R,I}^* = R_{R,I} = .93804}$$

$$\underline{R_{R,IIa}^* = R_{R,I}^* R_{IIa} = .93804}$$

$$R_{R,IIb}^* = R_{R,IIa}^* R_{R,IIb} (R_{68}/R_{68}^{(1)} R_{69} R_{70} \cdots R_{72})'$$

$$(R_{68}/R_{68}^{(1)} R_{69} R_{70} \cdots R_{72})' = e^{-9.43t}$$

$$\text{for } t = 1, K = 800$$

$$= (.93804)(.99996)(.93099)$$

$$\underline{R_{R,IIb}^* = .93097}$$

$$\underline{R_{R,IIc}^* = R_{R,IIb}^* R_{R,IIc} = (.93097)(.99525)}$$

$$\underline{R_{R,IIc}^* = .92655}$$

$$R_{R,III}^* = R_{R,IIc}^* R_{R,III} (R_{23} R_{60} R_{61} R_{73})'$$

$$(R_{23} R_{60} R_{61} R_{73})' = e^{-41.12t} R_{\text{Horizon Scanner}}$$

$$\cdot (e^{-.46t} + 2e^{-.23t} - 2e^{-.325t})^2$$

$$\text{with } t = 1, K = 800, \text{ and } t = 36 \text{ hours}$$

$$= e^{-.03438} (.984)(.9996) = (.96623)(.984)(.9996) = .95039$$

$$R_{R,III}^* = (.90756)(.95039)(.65105) = .56155$$

$$(.40110) = .34596$$

$$(.24099) = .20786$$

$$(.13711) = .11826$$

$$\underline{R_{R,III}^* = .57329 \ .35319 \ .21220 \ .12073}$$

## 7. Common Equipments

This section considers those equipments common to all channels.

### a. Inverter

The inverter parts complement, below, is taken from the STL third and fourth assessments (Document 2311-6020-RU-000, 31 July 1962); the failure rates of PRC TAM No. 7 were used.

Item (j)	$n_j$	$\lambda_j$	$n_j \lambda_j$
Transistors	20	.30	6.00
Diodes	23	.15	3.45
Capacitors, Foil Tantalum	3	.09	.27
Capacitors, Solid Tantalum	1	.08	.08
Inductor	1	.40	.40
Resistor, Wirewound	4	1.03	4.12
Resistor, Film	21	.23	4.83
Transformers	7	.20	1.40
Connector Pins	9	.04	.36
			<u>20.91</u>

$$R_2(t) = e^{-(20.91)t}$$

### b. Converter

The converter parts complement, below, is the same as that used in PRC's preliminary assessment, R-243. The failure rates of PRC TAM No. 7 were used.

Item (j)	$n_j$	$\lambda_j$	$n_j \lambda_j$
Resistor, Film	5	.23	1.15
Capacitor, Ceramic	5	.01	.05
Transistor, Silicon	4	.30	1.20
Diode, Silicon	6	.15	.90
Diode, Zener	1	.26	.26
Transformer	1	.20	.20
			<u>3.76</u>

$$R_1(t) = e^{-(3.76)t}$$



c. Mode Memory Circuits

The circuit groups and parts complements of all circuit groups are shown in Exhibit 16. Failure of these circuits was assumed in the event of failure of any block which, in turn, fails if any one of its constituent parts fails. Parts complements were derived from STL Drawing 201523. Parts complements of boxes PT2-1020 and PT2-1021 were conservatively estimated by PRC, since information was not available.

$$R_{D'''} = 1$$

$$R_{D''} = R_D^2 + 2R_D(1 - R_D) = (e^{-.3t} + 2e^{-.15t} - 2e^{-.285t})^2$$

$$R_{D'} = R_D^2 + 2R_D(1 - R_S) = (e^{-.3t} + 2e^{-.15t} - 2e^{-.165t})^{27}$$

Item (j)	$n_j$	$\lambda_j$	$n_j \lambda_j$
Resistor	94	.23	21.62
Capacitor	15	.08	1.20
Diode	80	.15	12.00
Transistor	29	.30	8.70
Transformer	1	.20	.20
Coils	6	.20	1.20
SCR	2	.30	.60
			<u>45.52</u>

$$D' = 27$$

$$D'' = 1$$

$$D''' = 5$$

$$R_{ij}(t) = e^{-45.52t} (e^{-.3t} + 2e^{-.15t} - 2e^{-.285t}) (e^{-.3t} + 2e^{-.15t} - 2e^{-.165t})^{27}$$

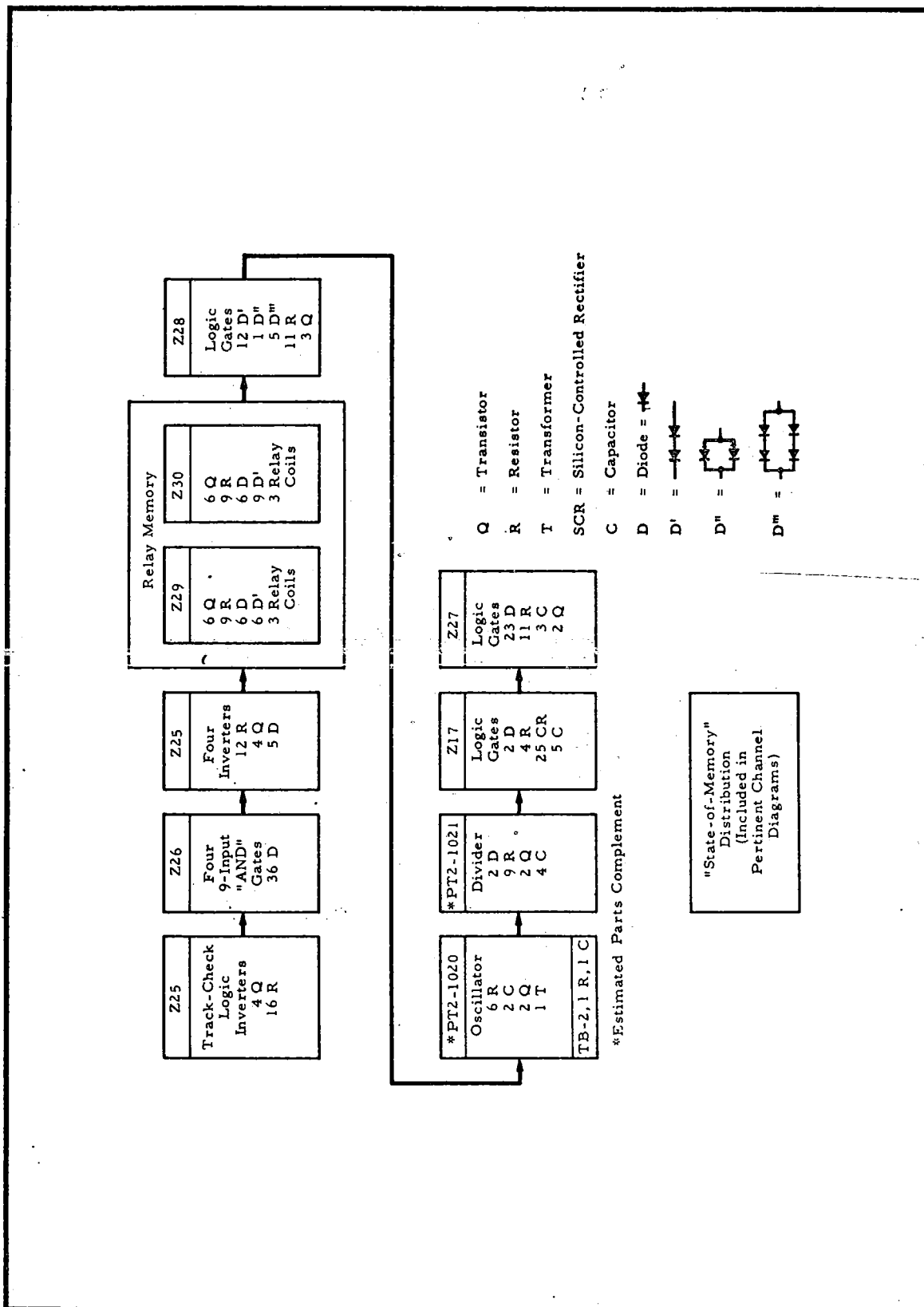


EXHIBIT 16 - MODE MEMORY CIRCUITS, RELIABILITY DIAGRAM

## 8. Special Equipments

This section considers those equipments which may be common to some but not to all channels.

### a. Regulator Filter

This group is composed of the -3 volt regulator circuits, the +10 volt filter capacitance, and the -20 volt filter capacitance. For those applications in which only the -20 volt and/or +10 volt supply voltages were used, these reliability functions were ignored (set to 1.0). For those applications in which the -3 volt and/or the +10 volt and/or the -20 volt supplies were used, as it will be seen, the reliability function is adequately approximated by that of the -3 volt regulator only. The makeup of the -3 volt regulator is shown in Exhibit 17.

$$R_{-3} = (e^{-.46t} + 2e^{-.23t} - 2e^{-.3215t})(2e^{-.064t} - e^{-.128t}) \\ \cdot (2e^{-.675t} - e^{-1.35t})$$

Reliability of +10 volt filter capacitance:

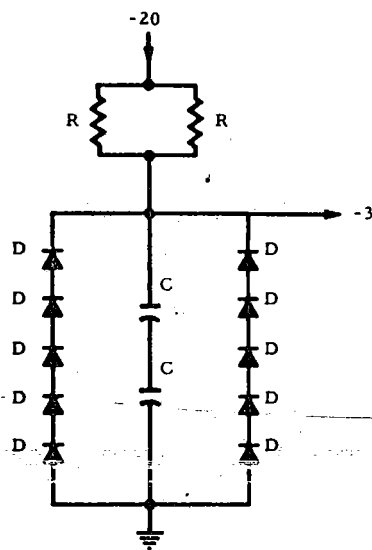
$$R_{+10} = 2e^{-.08 \times 10^{-6}t} - e^{-.16 \times 10^{-6}t}$$

$$\text{for } t = 10,000 = 2(.9992) - .9984 \cong 1.0$$

Reliability of -20 volt filter capacitance:

$$R_{-20} = 2e^{-.08 \times 10^{-6}t} - e^{-.16 \times 10^{-6}t} \cong 1.0$$

$$R_{49}(t) = R_{-3} \cdot R_{+10} \cdot R_{-20} \cong R_{-3}(t)$$



Failure Modes, -3 Volt Regulator

Successful circuit operation if:

1. Neither R short
2. Not both R open
3. Neither diode-leg short  
(i.e., all five diodes)
4. Not both diode-legs open  
(i.e., one diode in each leg)
5. Not both C short

EXHIBIT 17 - -3 VOLT REGULATOR DIAGRAM

b. Rate Gyro Electronics

The parts complement used for the rate gyro electronics is as follows:

Item	Quantity	$x_j$	$n_j \lambda_j$
Resistors	16	.23	3.68
Capacitors	7	.08	.56
Diodes	4	.15	.60
Transistors	3	.30	.90
Transformers	3	.20	.60
Motor	1	4.80	4.80
Relay			<u>1.55</u>
			12.69

$$R_{62}(t) = e^{-(12.69)t}$$

The parts complement was derived from STL Drawing 201545, with telemetry components omitted. The gyro wheel and support structure itself is considered an integral part of the motor in this analysis.

c. Small Earth Discrimination Circuits

Circuit groups and parts complements of all circuit groups are shown in Exhibit 18. Failure is implied by a piece-part failure in any circuit.

Item	$n_j$	$\lambda_j$	$n_j \lambda_j$
Resistor	63	.23	14.49
Capacitor	34	.08	2.72
Diode, Silicon	14	.15	2.10
Transistor	21	.30	6.30
Transformer	6	.20	<u>1.20</u>
			26.81

$$R_{23} = e^{-(26.81)t}$$

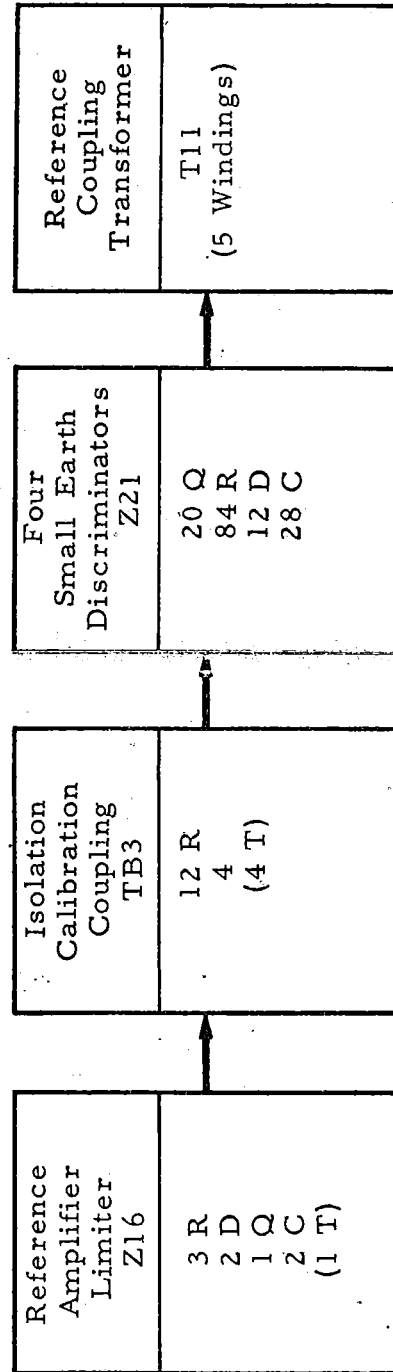


EXHIBIT 18 - SMALL EARTH DISCRIMINATION CIRCUITS, RELIABILITY DIAGRAM

d. Horizon Scanner

The configuration of the horizon scanner was taken from ATL Drawing SK4014, Electronic Schematic, OGO Horizon Scanner, 4/14/62. This drawing, plus others from ATL Design Report No. 3, and the failure-effect analysis set forth in ATL Progress Report D-837, June 1962, were the information inputs. Using PRC failure rates to generate the basic probabilities involved (e. g.,  $R_C$  = reliability of a summing amplifier was computed using parts count of Table VI (D-837), ATL K factor (application factor) and the 53 favorable combinations (acceptable states) in D-837, Table 17, the horizon scanner reliability function evaluated at quarters is as follows:

	<u>1/4 year</u>	<u>1/2 year</u>	<u>3/4 year</u>	<u>1 year</u>
(1)	0.92731	0.81447	0.68987	0.57012
(2)	<del>0.91174</del>	<del>0.78271</del>	<del>0.63448</del>	<del>0.50825</del>

The numbers in row (1) may be considered the "gray-is-white" outlook. By this is meant that ATL, in many instances, recognized that a component failure might reduce the accuracy of the horizon scanner, but, in their opinion, operation would not be considered totally lost. The design review sheets of Design Report No. 3 were reviewed by PRC and, for example, wherever such words as "slight inaccuracy" were associated with a failure (but ignored by ATL), PRC considered such degradation catastrophic and assigned different K factors. Such a "gray-is-black" attitude produced a new set of basic probabilities which were once again combined (as dictated by the 53 combinatorial equations of D-837), and this resultant reliability function evaluated at quarters appears in row (2). This number represents a bounded interval within which (assuming the model is correct) the reliability lies. For use in the roll and pitch channels, the numbers in row (1) were used.

## 9. ACS Subsystem Reliability

The reliability of the subsystem is the product of the independent equipments in each channel times the reliability of the equipment common to each channel.

### a. Individual Reliabilities, Mode I

$$R_{S,I} = R_1 R_2 R_3 R_4 R_6^{(1)} R_7^{(1)} R_8^{(1)} R_9$$

$$R_{Y,I} = \{1 - (1 - R_{24}) R_{16} R_{17} R_{18} R_{25} R_{26} R_{27} R_{29} R_{31} R_{32} R_{33} R_{35} R_{36} \\ \cdot R_{37} R_{45} R_{47} R_{48}\} R_1 R_2 R_3 R_{37}^{(1)} R_{49}$$

$$R_{P,I} = \{1 - (1 - R_{24}) R_{25} R_{36} R_{37} R_{51} R_{52} R_{62}\} R_1 R_2 R_3 R_{37}^{(1)} R_{49}$$

$$R_{R,I} = \{1 - (1 - R_{24}) R_{13} R_{14} R_{15} R_{16} R_{17} R_{18} R_{19} R_{22} R_{63} R_{64} R_{65} R_{66} R_{67} \\ \cdot R_{68}^{(1)} R_{74} R_{75}\} R_1 R_2 R_3 R_{49}^{(1)} R_{67}$$

$$R_{ACS,I} = R_{S,I} R_{37}^{(1)} R_{49} R_{67}^{(1)} \{1 - (1 - R_{24}) (R_{16} R_{17} R_{18}) (R_{25} R_{36} R_{37}) \\ \cdot R_{26} R_{27} R_{29} R_{31} R_{32} R_{33} R_{35} R_{45} R_{47} R_{48} + (R_{25} R_{36} R_{37}) \\ \cdot R_{51} R_{52} R_{62} + (R_{16} R_{17} R_{18}) R_{13} R_{14} R_{15} R_{19} R_{22} R_{63} \dots \\ R_{67} R_{68}^{(1)} R_{74} R_{75} \\ - (R_{16} R_{17} R_{18}) - (R_{25} R_{36} R_{37})\}$$

$$\underline{R_{ACS,I} = .93322}$$



b. Individual Reliabilities, Mode IIa

$$R_{S, IIa} = R_1 R_2 R_3 R_5 R_6 R_7 R_8 R_9 R_{10} R_{11} R_{12} R_{20} R_{21}$$

$$R_{Y, IIa} = R_{Y, I}$$

$$R_{P, IIa} = R_{P, I}$$

$$R_{R, IIa} = R_{R, I}$$

$$R_{ACS, IIa} = R_{S, IIa} R_{ACS, I} / R_{S, I}$$

$$\underline{R_{ACS, IIa} = 1}$$

c. Individual Reliabilities, Mode IIb

$$R_{S, IIb} = R_{S, IIa}$$

$$R_{Y, IIb} = R_1 R_2 R_3 R_{16} R_{17} R_{18} R_{24}^{(1)} R_{25} R_{26} R_{27} R_{29} R_{31} R_{32} R_{33} R_{35} \cdots \\ R_{42} R_{43}^{(1)} R_{44}^{(1)} R_{45} \cdots R_{49}$$

$$R_{P, IIb} = R_1 R_2 R_3 R_{24}^{(1)} R_{25} R_{36} R_{37} R_{49} R_{50} \cdots R_{56} R_{62}$$

$$R_{R, IIb} = R_1 R_2 R_3 R_{13} \cdots R_{19} R_{22} R_{64}^{(1)} R_{49} R_{63} \cdots R_{72} R_{74} R_{75}$$

$$R_{ACS, IIb} = R_{S, IIa} (R_{Y, IIb} / R_1 R_2 R_3) (R_{50} \cdots R_{56} R_{62}) \\ \cdot (R_{13} R_{14} R_{15} R_{19} R_{22} R_{63} \cdots R_{72} R_{74} R_{75})$$

$$\underline{R_{ACS, IIb} = .99988}$$

d. Individual Reliabilities, Mode IIc

$$R_{S,IIc} = R_{S,IIa}$$

$$R_{Y,IIc} = R_{Y,IIb}$$

$$R_{P,IIc} = R_{P,IIb}$$

$$R_{R,IIc} = R_{R,IIb}$$

$$R_{ACS,IIc} = R_{ACS,IIb}$$

$$\underline{R_{ACS,IIc} = .99115}$$

e. Individual Reliabilities, Mode III

$$R_{S,III} = R_1 R_2 R_3 R_5 \cdots R_9 R_{10}^{(i)} R_{13} \cdots R_{21} R_{22}$$

$$R_{Y,III} = R_1 R_2 R_3 R_{16} R_{17} R_{18} R_{24}^{(1)} R_{25}^{(1)} R_{26} R_{27} R_{29} R_{31} R_{32} R_{33} R_{38} R_{39} \cdots \\ R_{42} R_{43}^{(1)} R_{44}^{(1)} R_{46} \cdots R_{49}$$

$$R_{P,III} = R_1 R_2 R_3 R_{23} R_{24}^{(1)} R_{25}^{(1)} R_{36} R_{37} R_{49} R_{50} \cdots R_{61}$$

$$R_{R,III} = R_1 R_2 R_3 R_{23} R_{24}^{(1)} R_{49} R_{60} R_{61} R_{63} \cdots R_{74} R_{75}^{(1)}$$

$$R_{ACS,III} = R_{S,III} (R_{Y,III} / R_1 R_2 R_3 R_{16} R_{17} R_{18}) \\ \cdot (R_{P,III} / R_1 R_2 R_3 R_{24}^{(1)} R_{25}^{(1)} R_{49}) (R_{R,III} / R_1 R_2 R_3 R_{23} R_{24}^{(1)} R_{49})$$

Term	Time			
	2154	4344	6534	8724
$R_{ACS,III}$	.42220	.19069	.08431	.03561

f. Time-Cumulative Reliabilities

$$R_{ACS,I}^* = R_{ACS,I}$$

$$\underline{R_{ACS,I}^* = .93322}$$

$$R_{ACS,IIa}^* = R_{ACS,I}^* R_{ACS,IIa} (R_5 R_6 R_7 R_8 R_{10} R_{11} R_{12} R_{20} R_{21})'$$

$$\underline{R_{ACS,IIa}^* = .91772}$$

$$R_{ACS,IIb}^* = R_{ACS,IIa}^* R_{ACS,IIb} (R_{38} \cdots R_{44} R_{46} R_{50} R_{53} \cdots R_{56} R_{69} \cdots R_{72})'$$

$$\underline{R_{ACS,IIb}^* = .86230}$$

$$R_{ACS,IIc}^* = R_{ACS,IIb}^* R_{ACS,IIc}$$

$$\underline{R_{ACS,IIc}^* = .85460}$$

$$R_{ACS,III}^* = R_{ACS,IIc}^* R_{ACS,III} (R_{23} R_{57} R_{58} R_{59} R_{60} R_{61} R_{73})'$$

Term	Time			
	2190	4380	6570	8760
$R_{ACS,III}^*$	.33843	.15286	.06758	.02854

## 10. Strengths and Weaknesses

The nature of reliability assessment is to allow recognition of "weak" links. Within the ACS subsystem, the question of which servo channel is weakest must be considered. Also, within the individual servo channels, the circuit groupings may be inspected for relative weakness.

In the opinion of the writer, the meanings of the questions and their answers must be considered. Certainly the yaw, pitch, and roll channels have roughly the same mission (i. e., to orient one of the spacecraft's body axes). In addition, the orientation of the normal to the array is equally important. Thus, the four channels are adjudged to be like entities, for which a comparison is justified. However, within a channel, the question of comparison loses meaning when trying to compare, for example, the reliability of the roll channel magamps and valve drivers (in the attitude control unit, STL Drawing 200834) with the reliability of the horizon scanner. Certainly both assemblies must function, but the function of the horizon scanner is considerably more complex than that of the channel magamps and valve drivers.

Within the individual channel analyses (i. e., Sections 3, 4, 5, and 6, along with associated Sections 7 and 8), the numbers, functions, etc., are presented and comparisons may be made, but the meaning of each comparison is dubious.

Exhibit 1 represents the four channels versus mode versus time. It is seen that the weaker channels are the pitch and roll channels. However, these weaker channels do not unduly compromise the subsystem reliability, since the other channels are not "pillars of strength."

There are several design weaknesses which could be corrected. These weaknesses will be discussed in the following section.

## 11. Recommendations

### a. Recommendation 1

The four inverter stages on Z25 in the sensor electronics and logic assembly (Drawing 201523) seem unnecessary when it is considered that each "track-check" signal in the horizon scanner assembly is derived from a "trigger" circuit which could just as readily provide both track-check and its logical complement. The track-check trigger circuit of Q6 and Q7 on ATL Drawing 3771 seems easily alterable to pick up and bring out both of these signals. Such a change would allow elimination of Z25 (circuit board Drawing 203687, which uses 16 resistors and 4 transistors), with improved reliability and weight reduction.

### b. Recommendation 2

Within the present sensor electronics and logic assembly, the use of redundant piece parts is nonuniformly applied, with the resultant compromise of intended reliability. Specifically, in Z28 (Drawing 203707), there are four 3-input "diode" AND gates. Each diode is actually two 1N485-B diodes in electrical series connection. The output of each AND gate is fed to one input of a five-input diode OR gate. Each diode is actually two 1N485-B series-connected diode chains in parallel, using a total of four diodes. The output of this OR gate (through an inverter stage consisting of Q53 and associated resistors) drives one input of a three-input diode AND gate. These diodes are bona fide single diodes of type 1N485-B. The observation here is that the diodes of logic gates driving logic gates should individually have the same strength (reliability-wise) or the chain strength is essentially that of the weakest link.

### c. Recommendation 3

There are two outputs of Z28. One is a control signal to relay K3 to start the generation of a delayed pulse. The second is to an AND gate. The relay K3 is actuated, and the input signal to diode CR269 in Z27 is positive, when the following condition is true:

$$E(\overline{A}\overline{B} + \overline{A}\overline{C} + \overline{A}\overline{D} + \overline{B}\overline{C} + \overline{B}\overline{D} + \overline{C}\overline{D}) \quad (1)$$

The parenthetical expression means "Two Heads Are Not Tracking" (THANT). The E symbol implies that the system is in Mode III. This composite signal into the three-input AND gate (consisting of CR269, CR146, CR147, and R179) is "ANDed" with E again (through CR147), and if the THANT signal remains true for the delay-time interval, the delayed pulse into CR146 produces a true condition at the output. (Through Q51 and Q52, the mode memory and, therefore, the ACS are set back to Mode IIa.) It is intended to keep relay K3 from operating except when  $E(\overline{A}\overline{B} + \overline{A}\overline{C} + \overline{A}\overline{D} + \overline{B}\overline{C} + \overline{B}\overline{D} + \overline{C}\overline{D})$  is true. This condition implies that diode CR147 is of no use and should be removed.

d. Recommendation 4.

It is recommended that use of redundancy on a "piece parts" basis should be investigated for all the diodes and resistors on the TB2 (203885) board. These elements function to distribute the "states" of the mode memory to various addresses; they are crucial elements. Also, use of redundancy in mode-sequencing logic should be investigated. Exhibit 19 shows three portions of the mode-sequencing logic. The upper box shows the circuits which produce a "true" output pulse when in Mode I (i. e.,  $\overline{E} \cdot \overline{F} \cdot \overline{G}$ ) and the ACS start pulse appears. This pulse advances the mode memory to Mode IIa (i. e.,  $\overline{E} \cdot \overline{F} \cdot G$ ). When the array slew operation is completed, the  $(180^\circ)$  signal arrival produces a true output pulse to advance the mode memory to Mode IIb (i. e.,  $\overline{E} \cdot F \cdot G$ ). When the pulse  $t_1$  is produced 29 minutes (nominal) later, a true output pulse advances the mode memory to Mode IIc (i. e.,  $\overline{E} \cdot F \cdot \overline{G}$ ). Since the present IIc  $\rightarrow$  III sequencing logic will be discussed later, the reason for suggesting the use of piece-parts redundancy in the basic circuitry of Exhibit 19 is as follows: The logic discussed in Recommendation 3 (i. e., the THANT logic) is, reliability-wise, "strong." This strength is twofold. First, the probability of the THANT logic producing a true output (when "true" is logically valid) is high. Second, the probability of not producing a true output (when "untrue" is logically valid) is very small. Yet, the strong THANT logic only initiates a reacquisition cycle. The subsequent mode-sequencing progression

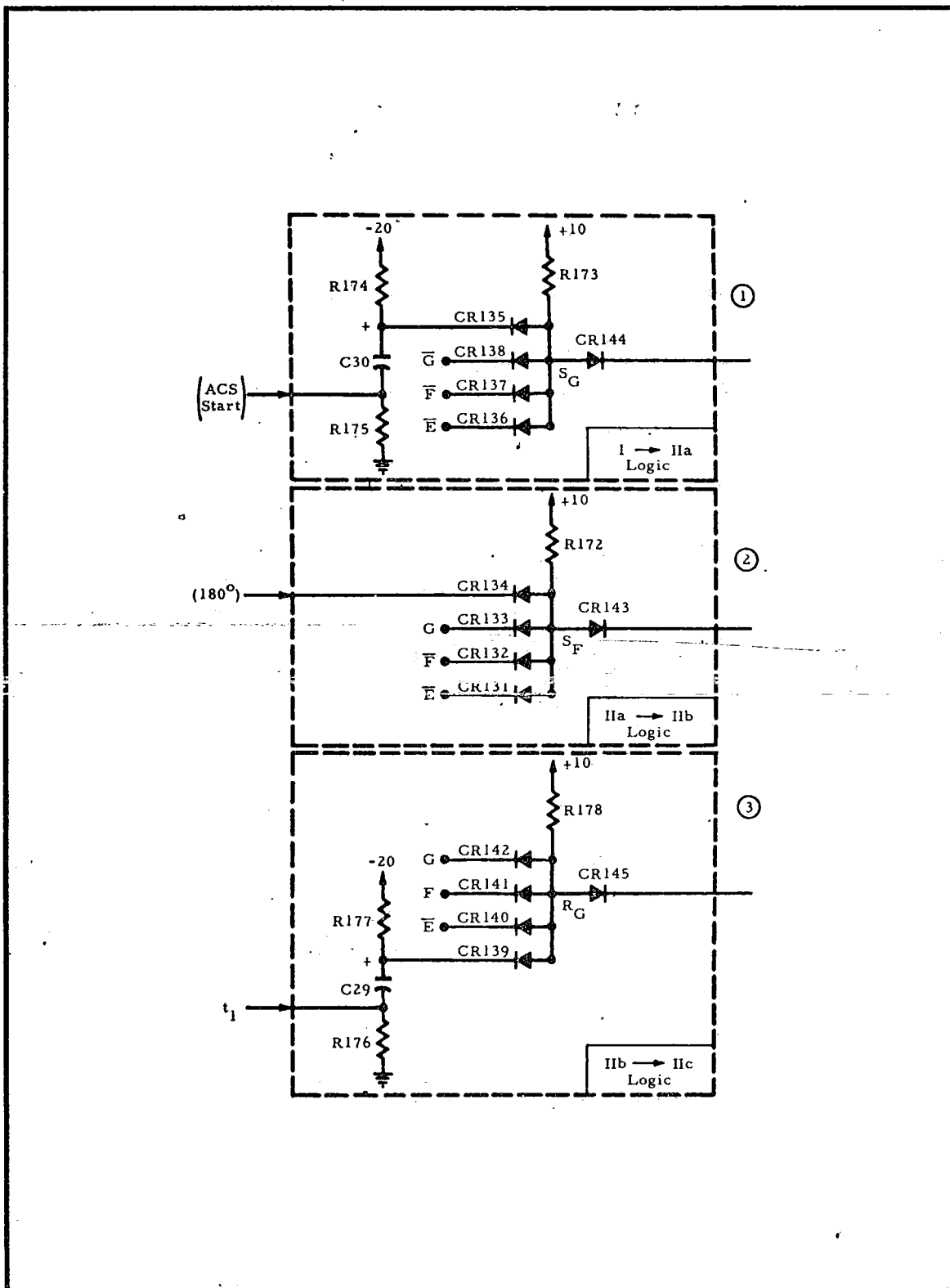


EXHIBIT 19 - MODE TRANSITION LOGIC CIRCUITS

through the circuits of Exhibit 19 is just as important as initiation when desired. Thus, there is a second nonuniform use of redundancy as discussed in Recommendation 3.

e. Recommendation 5

The mode-sequencing logic circuitry, which advances the mode memory from Mode IIc (i. e.,  $\bar{E} \cdot F \cdot \bar{G}$ ) to Mode III (i. e., E), is shown in Exhibit 20. A criticism of the existing configuration is that the state, IIc (i. e.,  $\bar{E} \cdot F \cdot \bar{G}$ ) (actually, its logical complement), is brought into each of four 9-input OR gates of Z26. Removal of diodes CR100, 101, 102, 91, 92, 93, 109, 110, 111, 118, 119, and 120 would make the logic condition of the output bus "true" only for ALTHATALE, which stands for "At Least Three Heads Are Tracking A Large Earth." The addition of the simple AND gate shown in the box would require reversal of CR66, addition of resistor R, and addition of diodes D1, D2, and D3, driven by memory states  $\bar{E}$ , F, and  $\bar{G}$ , respectively. In summary, 12 diodes are "out" and 3 diodes and 1 resistor are "in."

f. Recommendation 6

Exhibit 20 shows the four small earth discriminator circuits, Z21 (Drawing 203665). Also shown are the four coupling calibration circuits for each of the position signals from the four position amplifiers in the horizon scanner assembly. For tracker head A, for example, C75, T7, and R99A form the coupling calibration circuits. In addition, the 2461-cps reference signal is introduced by T6 into the four Z21's and also by T11 into the four Z21's. The circuit of Z16 provides limiting/buffering for driving T6.

The essence of this recommendation is to question the need for Z16, the position-signal coupling circuits, and the Z21's. To develop the argument, consider the collector signal of Q48. If the logical term  $(A\alpha)(B\beta)(D\delta) \cdot (\bar{E} \cdot F \cdot \bar{G})$  is "true," then collector voltage is high. The meaning of each parenthesized factor in the term, using  $(A\alpha)$ , for example, is as follows:



(1) Head A is "locked on" and tracking a thermal gradient (because of the design of the scanner, only "down" scans are valid, and the first thermal gradient of interest is the space-horizon interface), and (2) the angular position of its axis is greater than  $4.4^{\circ}$  with respect to the yaw axis of the spacecraft.

The preceding statement must be true for head B and head D as well, and the mode memory must be in Mode IIc for the collector of Q48 to swing (from false to true) positively and generate a pulse to advance the mode memory from Mode IIc to Mode III.

The indented statement in the preceding paragraph describes a condition on a tracker-head position output signal which could just as well be qualified by the presence of A, for example, alone, provided a particular head search-angle interval was permitted to range cyclically only from  $4.4^{\circ}$  to  $90^{\circ}$  (instead of  $0^{\circ}$  to  $90^{\circ}$  as at present). For the IIc  $\rightarrow$  III logic, then, the term (A $\alpha$ ) would be replaced only by A, (B $\beta$ ) only by B, and (D $\delta$ ) only by D. If the OR gates of Z26 (Exhibit 20) are retained, the complements A, B, and D would be used (see Recommendation 1) and, in each of the four OR gates, three diodes could be removed. This is in addition to removal of four Z21's, Z16, and the coupling/calibration circuits.

The natural question is, "What 'price' must be paid to alter the scan-angle interval from  $0^{\circ}$ - $90^{\circ}$  to  $4.4^{\circ}$ - $90^{\circ}$ ?" The sawtooth current waveform in each tracker head is generated and controlled in the Schmitt Trigger and Drive Amplifier (ATL Drawing D-3767). One peak of this waveform, corresponding to  $0^{\circ}$  at present, could be moved to correspond to  $4.4^{\circ}$  by a simple "clamp circuit," using perhaps two diodes and two resistors. The intention here is to recommend an easily implementable "electronics change" to move the  $0^{\circ}$  point to  $4.4^{\circ}$ . No physical change of the positor is thus required. A physical change, of course, actually limiting angular excursion to  $4.4^{\circ}$ , would be a second method of moving the  $0^{\circ}$  point to  $4.4^{\circ}$ .

The argument may be advanced that position signals corresponding to angles less than  $4.4^{\circ}$  may be encountered during the natural

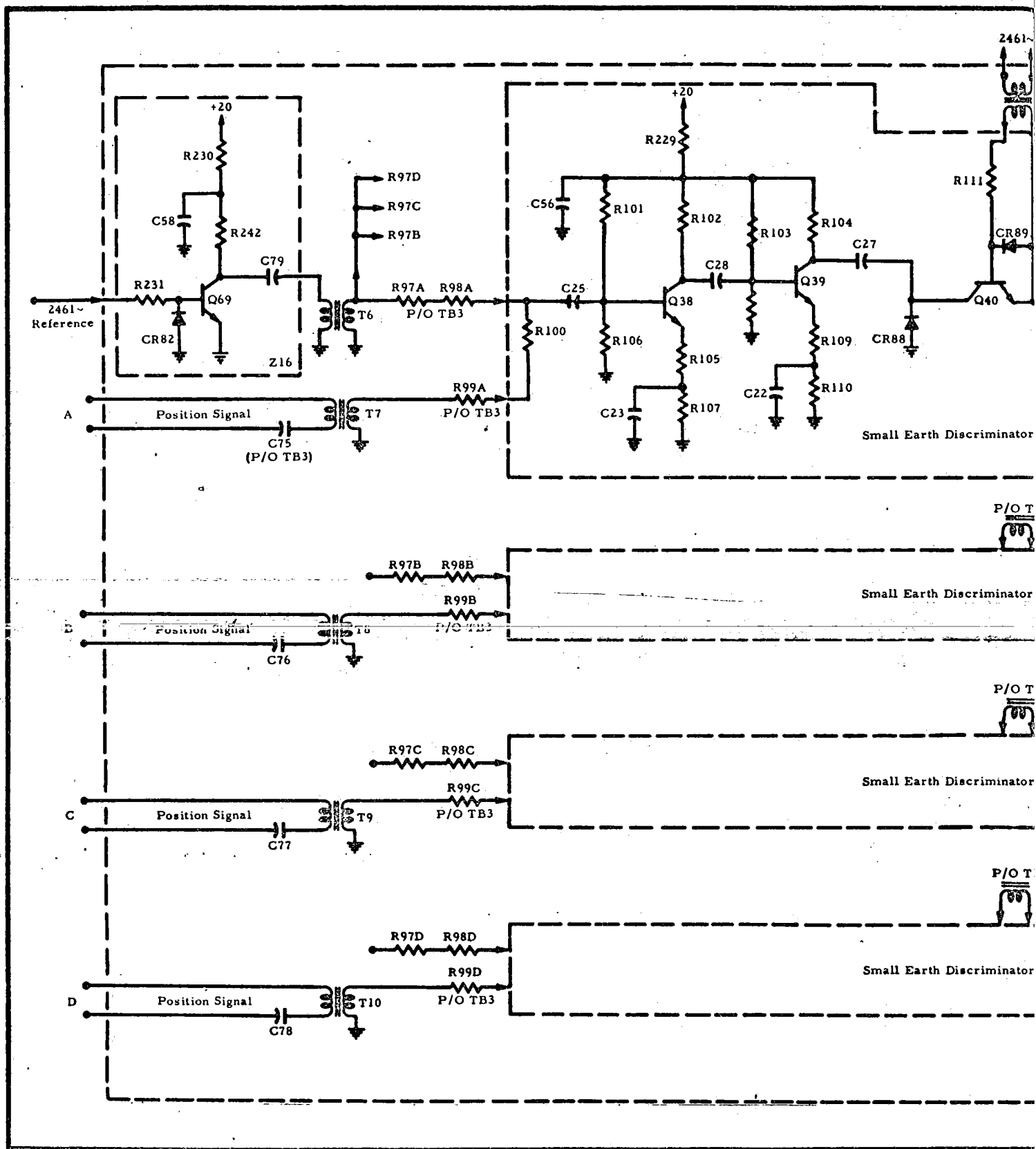
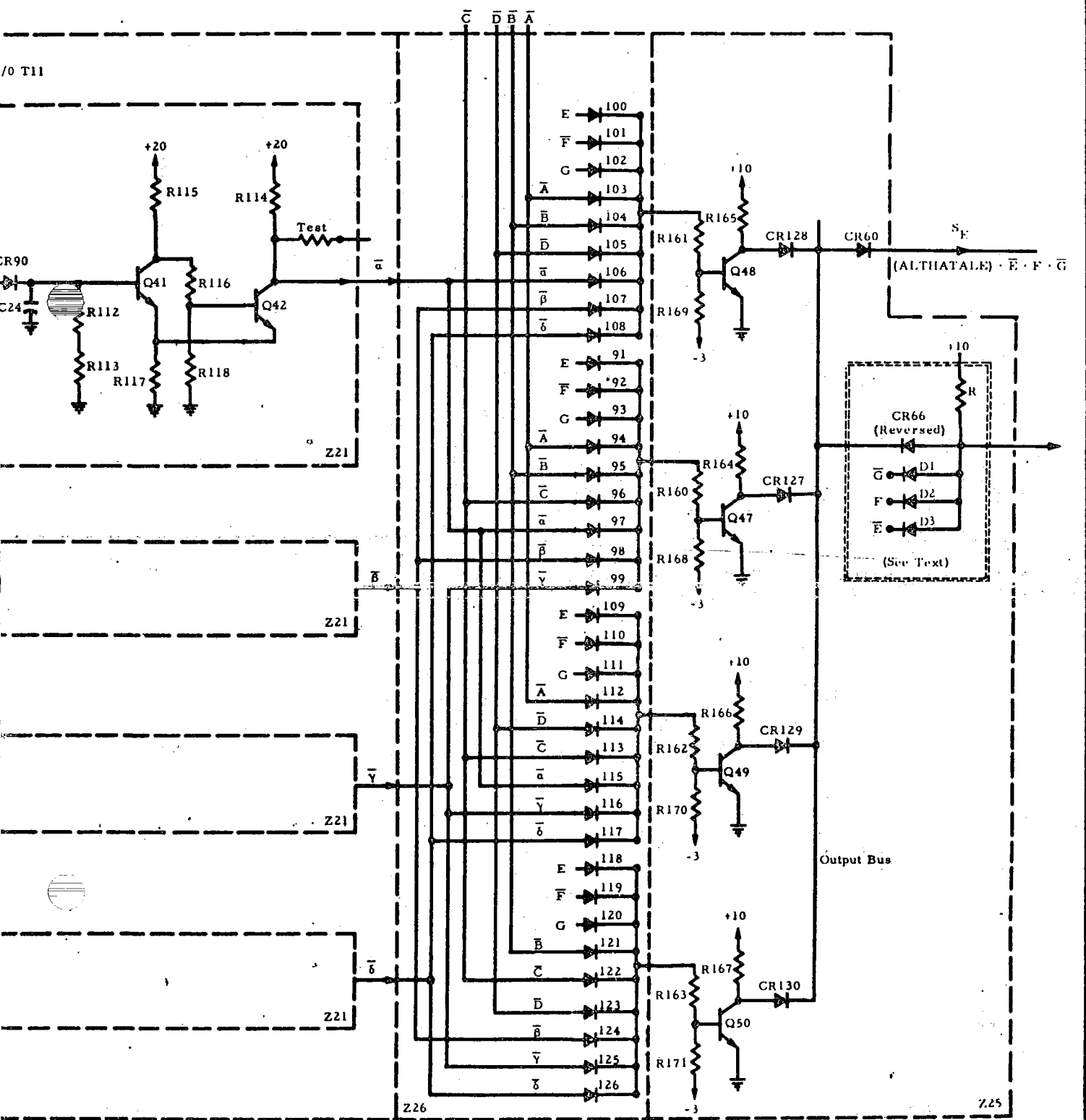


EXHIBIT 20 - EARTH

70 T11



ACQUISITION LOGIC CIRCUITS

earth-track mode. From the OGO data book, the pitch and roll maximum offset angle is  $\pm 0.4^\circ$ . Thus, "locked on," even in OGO orbit at 60,000-mile apogee (total intercept angle of approximately  $8^\circ$ ), a head is generating approximately a  $4^\circ$  signal. When designing to preclude "locking on" the moon (i. e., a small earth) by  $4.4^\circ$  thresholding, much lower angle thresholds could suffice. First-order calculations show that under "worst" (i. e., biggest angle) conditions, total moon-intercept angle is about  $0.7^\circ$ .

In summary, it appears that most of the circuitry of Exhibit 20 could be eliminated if tracking-check signal A (and, of course, B, C, and D) meant "Head A is tracking at an angle  $\geq 4.4^\circ$ ." Thus, only part of Z26 and Z25 would be left.

g. Recommendation 7

Recommendation 6 is considered feasible to implement, with the attendant simplification and weight reduction. For the sake of discussion, assume that Recommendations 5 and 6 have been followed. Exhibit 21 results. As mechanized, the output swings true when  $Y(\bar{E} \cdot F \cdot \bar{G})$  is true. The boxed-in circuitry now resembles the mode-sequencing logic of IIa  $\rightarrow$  IIb in Exhibit 19. A further simplification results when it is realized that

$$[(ABD) + (ABC) + (ACD) + (BCD)] = (\overline{AB} + \overline{AC} + \overline{AD} + \overline{BD} + \overline{CD}) = \bar{Y}$$

Therefore, it would seem that, except for the function of the boxed-in circuits, the remainder of the circuits (see Exhibit 21) could be eliminated if two relatively simple changes are made as follows:

First, instead of  $\bar{E}$ ,  $F$ ,  $\bar{G}$ , pick up  $E$ ,  $\bar{F}$ ,  $G$  in the mode memory and (for the moment assume it possible) bring in  $\bar{Y}$ . Reverse CR66 again and D1, D2, D3. The OR gate of Exhibit 22 results. Retention of one inverter stage (such as Q48, R161, R169, and R165) provides an output pulse when  $Y(\bar{E} \cdot F \cdot \bar{G})$  is true. Alternatively stated, given

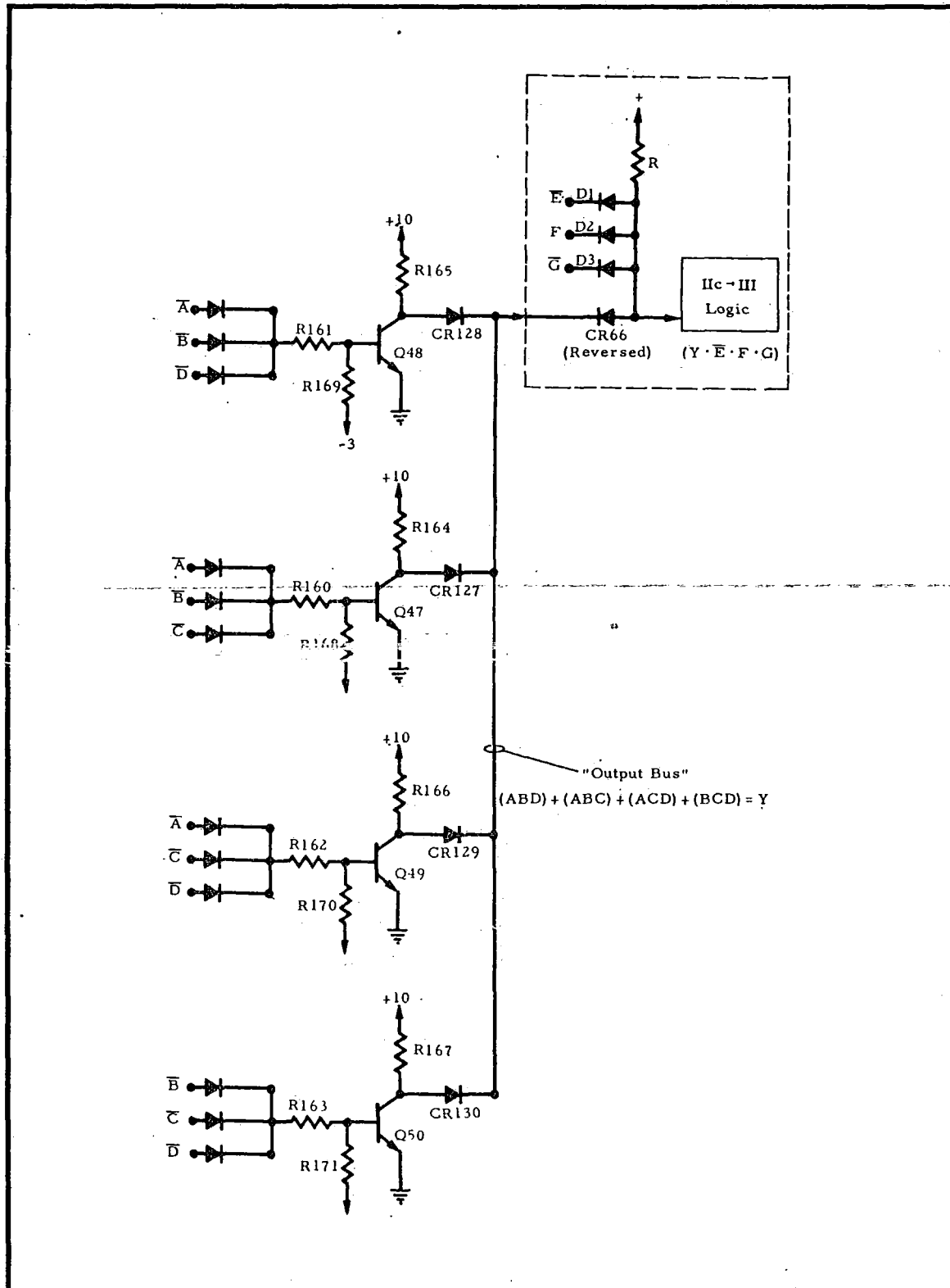


EXHIBIT 21 - POSSIBLE REVISED EARTH ACQUISITION LOGIC CIRCUITS

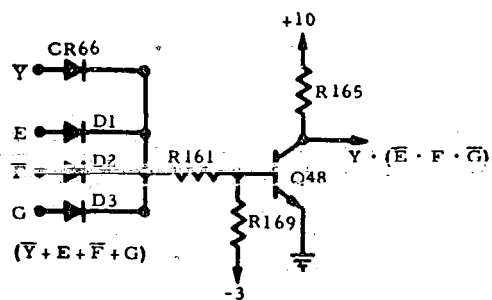


EXHIBIT 22 - POSSIBLE REVISED EARTH ACQUISITION  
LOGIC CIRCUITS

that Mode IIc exists, advance the mode memory when  $Y$  is true. This is the function of the IIc  $\rightarrow$  III mode-sequencing logic.

The only unanswered question is, "Where does  $\bar{Y}$  appear?" Exhibit 23 shows a possible simple revision of the functional circuitry of Z28 (Drawing 203707). D17, a diode quad which at present brings in  $\bar{E}$ , is removed and (in reverse) inserted as one of the inputs to a two-input AND gate. Drive is now supplied to this gate from  $E$  (in the mode memory). Diode  $D_X$  is added, along with resistor  $R_X$ , to form the two-input AND gate, and  $\bar{Y}$  is now available at the collector of Q53.  $E(\bar{Y})$  at the output of the AND gate is the usual drive signal to R123, etc., which controls the time-delay-pulse generating circuits.

h. Recommendation 8

The parts count for the time-delayed-pulse generator circuits was assumed. Without benefit of knowledge of the makeup of PT6-1020 and PT6-1021, an estimate was made. Since the time delays (according to the OGO data book) are  $29 \pm 4 \text{ min} = t_1$  and  $2.9 \pm 0.3 \text{ min} = t_3$ , it would appear that a simple time delay relay would suffice. This suggestion should be seriously considered if the clock-counter system presently used is inordinately complex. More will be said concerning this suggestion in the third assessment or as information becomes available.

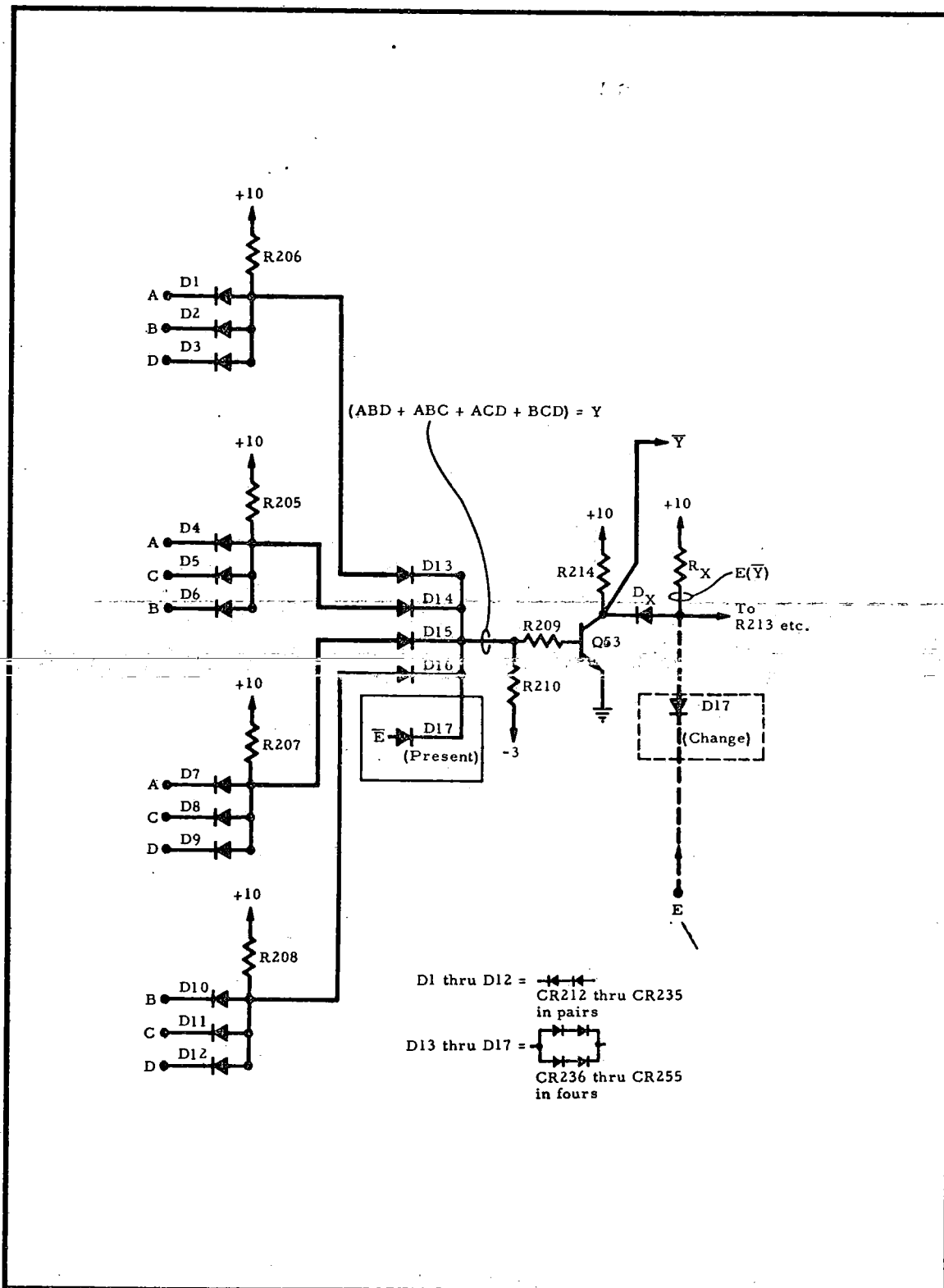


EXHIBIT 23 - POSSIBLE REVISED EARTH LOSS LOGIC CIRCUITS



TECHNICAL ADVISEMENT MEMORANDUM NO. 11

SECOND RELIABILITY ASSESSMENT,  
POWER SUPPLY SUBSYSTEM

# LIST OF EXHIBITS

## Page

1.	Schematic Block Diagram, Power Supply Subsystem . . .	3
2.	Solar Array Output @ 80° C . . . . .	5
3.	Load Profile, POGO Orbit, 37-Minute Eclipse . . . . .	13
4.	Parameters Underlying Calculation of Required Charge Time . . . . .	14
5.	Maximum Allowable Eclipse Time, POGO Orbit, as Function of $I_{SA}$ and Mission Time . . . . .	18
6.	Simplified Reliability Block Diagram for Power Supply Subsystem . . . . .	25
7.	Summary of Power Supply Subsystem Reliability and State Probabilities . . . . .	29
8.	Power Supply Subsystem Reliability Versus Time . . . . .	30

## TECHNICAL ADVISEMENT MEMORANDUM NO. 11

To: Assistant OGO Project Manager, GSFC, NASA  
From: PRC OGO Reliability Assessment Team  
Subject: Second Reliability Assessment, Power Supply Subsystem

### 1. Introduction

The second reliability assessment of the OGO Power Supply Subsystem utilizes very little of the preliminary assessment (cf. Reference 1) because the subsystem has been substantially redesigned since that time. Therefore, the description of the subsystem in Section 2 is considerably more complete than would otherwise be the case in a second assessment. In the event of failures in the subsystem, some automatic correction ability is included; however, failure correction is very much dependent on the diagnosis of subsystem telemetry data at ground stations, the selection of proper corrective commands, and the transmission, reception, and successful completion of these commands. In addition, the effects of the POGO orbit on the subsystem (e.g., solar cell deterioration due to radiation, the stringent charge requirements due to limited sunlight time, etc.) are included. The effect of long EGO eclipse time on the subsystem is also considered.

It is seen that, due to solar cell deterioration during a 1-year mission in a POGO orbit, the battery recharge capability of the solar array is marginal at the end of the mission. Also, the many cycles of battery charge and discharge, as well as the depth of discharge in the worst-case POGO orbit ( $82^{\circ}$  orbit inclination and noon launch) may cause battery deterioration to a point where one battery is no longer able to handle the load. This possibility needs to be thoroughly evaluated in a comprehensive testing program.

Modes of failure are identified and subsystem states are defined in Section 3. Section 4 presents the reliability assessment using the figure-of-merit approach. Strengths and weaknesses of the present design are discussed in Section 5. The final section delineates the recommendations for overcoming these weaknesses.

## 2. Subsystem Description and Assumptions

### a. Description

Exhibit 1, redrawn from STL Drawing M205897, is a simplified schematic block diagram of the Power Supply Subsystem. It will be helpful in the discussion that follows, much of which is drawn from a yet unpublished STL description (Reference 2).

The solar array is basically as described in subsection IV.C.1.a of Reference 1. However, the number and arrangement of diodes and controlling transistors (or power amplifiers) have been changed. The 48 strings of 96 series groups of 7 solar cells in parallel are still divided into 24 strings per paddle. The 24 strings on each paddle are now divided into 3 equal sections of 8 strings, with the output of the paddle being used, in the normal (or primary) mode, to recharge independent batteries and to supply power to the load bus through isolating individual power transistors in shunt from the midpoints of their minus diodes. Two of the three sections on each paddle are controlled by terminals; these, in turn, are controlled by charge regulators deriving input data from the respective batteries. The third section of cell strings on each paddle consists of uncontrolled strings that are connected to the load bus, and to their respective battery charging buses, through separate isolating diodes. The power supplied by the uncontrolled section is less than the average load power; thus, additional power is required from the controlled sections to supply the remaining load and to charge the batteries. When the power transistors shunting the controlled solar array sections are saturated, the maximum array voltage is reduced to less than the normal battery voltage. Thus the battery charge current can be controlled from "full on" to zero, giving complete control of the battery charge current for normal loads and solar array temperatures.

STL states in Reference 2 that, when the array is cold (after eclipse) and the battery voltage is low, the array voltage is higher than the battery voltage, even though the shunting power transistors are driven to their minimum impedance condition. In this situation, full control is not possible until the array warms up (approximately 20 minutes for the

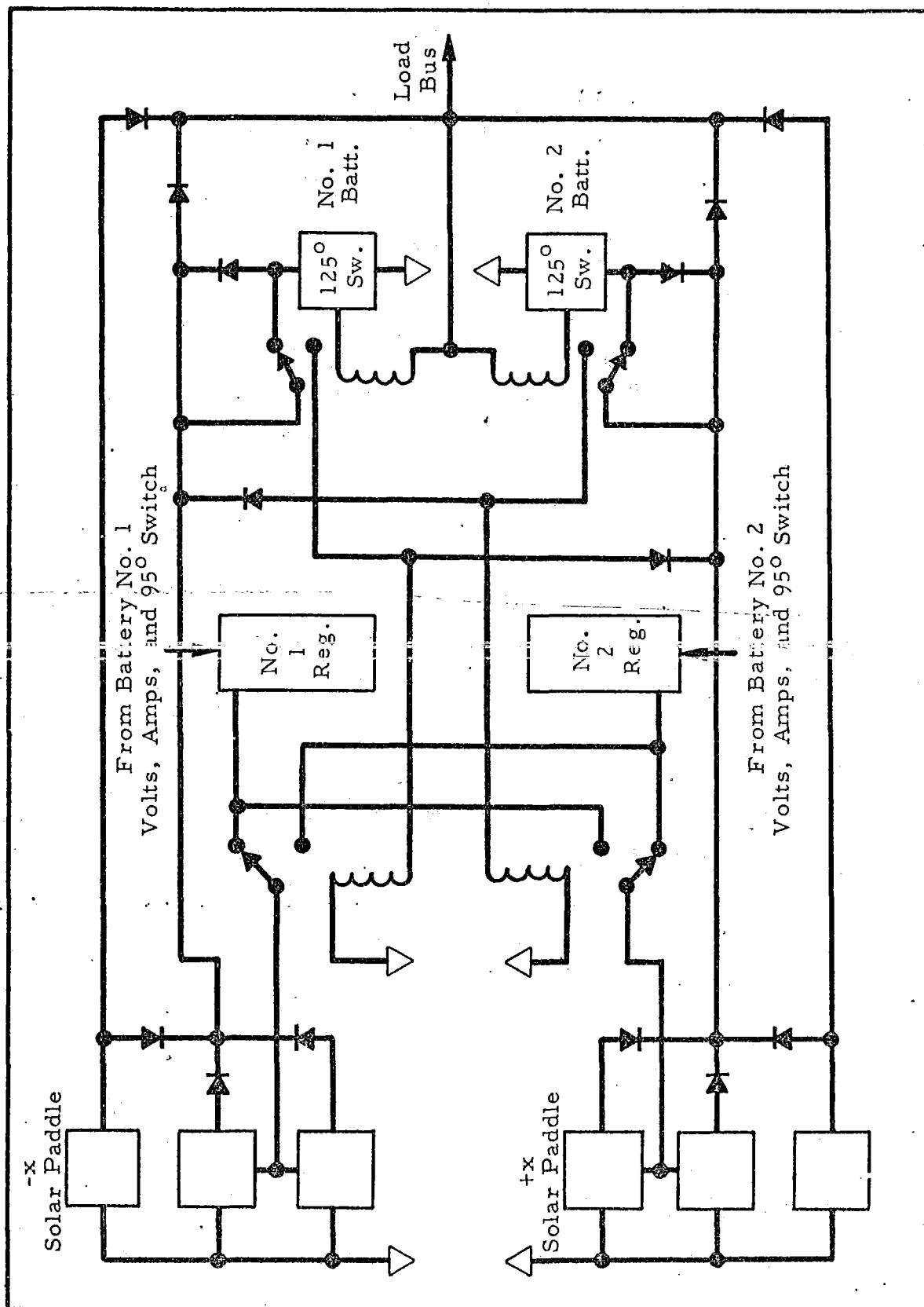


EXHIBIT 1 - SCHEMATIC BLOCK DIAGRAM, POWER SUPPLY SUBSYSTEM

longest eclipse). The transistors do, however, dissipate one-third of the cold array output; therefore, solar array current would not be as high as that resulting if no control were attempted. In a POGO orbit this is not the problem that it is in an EGO orbit, since the array does not reach as low a temperature during its shorter eclipse time.

Exhibit 2 presents the solar array output at 80°C for a new array and for one which has been exposed to the radiation effects of 1 year in a POGO orbit (cf. References 3 and 4). Deterioration data are confirmed by statements in Reference 5 concerning the array used in the Telstar communications satellite.

In the normal operating mode the subsystem is configured as shown in Exhibit 1. The following is a description of the manner in which the subsystem functions under the condition that there are no failures in the over-all subsystem. The changes which can be effected either by automatic sensing and switchover or by means of ground command through the Command Distribution Unit (CDU) will be discussed in Section 3.

During eclipse, each battery supplies approximately one-half of the load through isolating diodes to the load bus. At the end of the eclipse/discharge period the terminal voltages of the two batteries are equal and their depths of discharge are also about equal, maintained that way during the discharge time by action of the diodes. Though both batteries may discharge at about the same rate, there is no simple, good way to assure that each will charge at about the same rate without providing independent charge regulators. This fact, coupled with the need to provide redundancy in the subsystem, is the obvious reason for the use of two regulators in OGO.

At the end of eclipse, the batteries are recharged at a rate compatible with the depth of discharge (a function of eclipse time) and the amount of sunlight time available before the next eclipse. Four charge rates, including a trickle rate maximum, and two intermediate rates can be selected by ground command. Eclipse and sunlight time can be predetermined and do not change very rapidly (cf. Reference 6). For a 90° POGO orbit, the charge rate might be changed only four times in a 1-year mission. To preserve the batteries, the minimum rate that

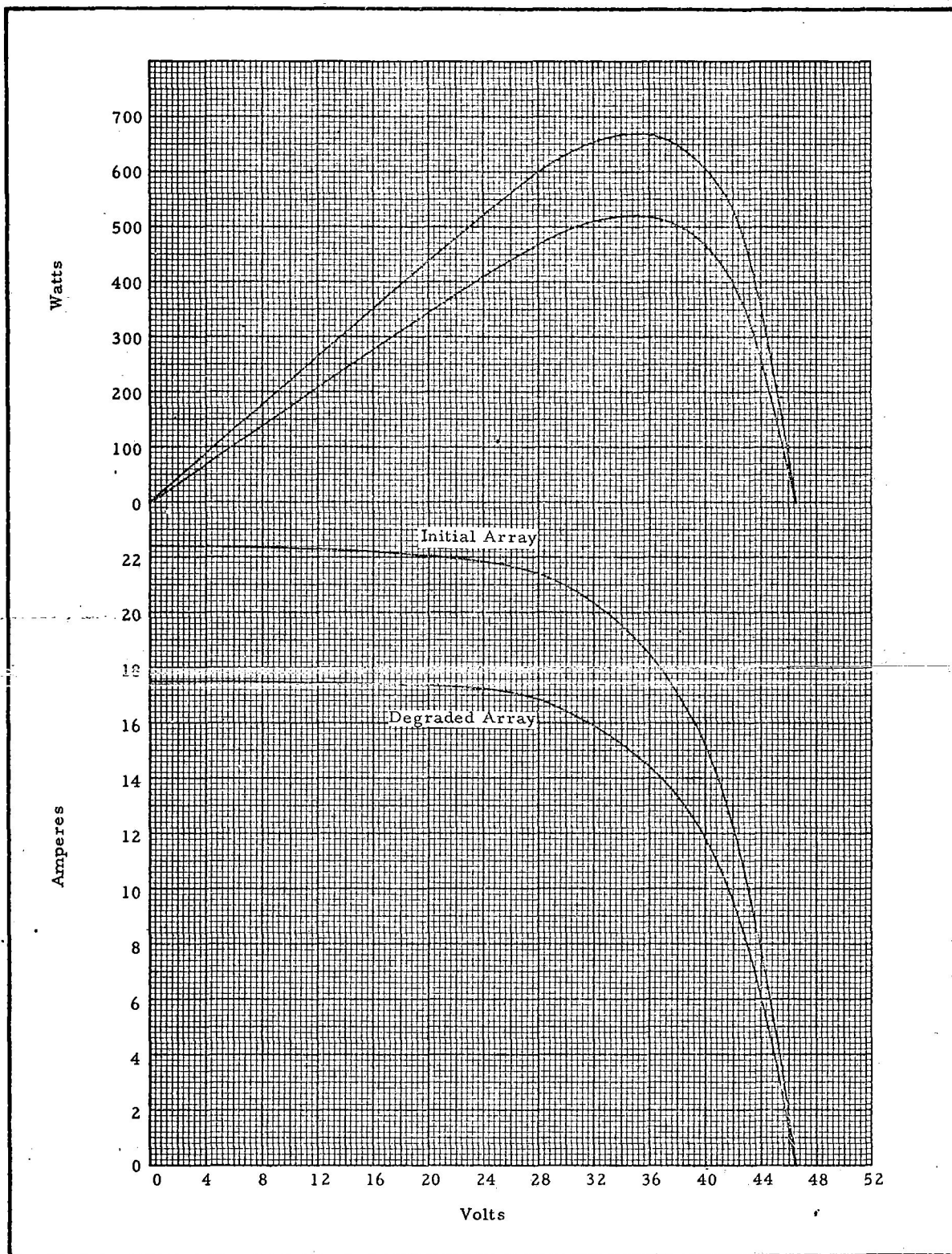


EXHIBIT 2 - SOLAR ARRAY OUTPUT @ 80°C

would assure full recharge should be selected. The charge regulator functions as a servomechanism to control the charge current at the selected level. The output of the regulator drives the power amplifiers (power transistors), which shunt the array, as previously described, so as to furnish the required load current and selected charge current. A battery current monitor determines both the level and sense of battery current (i. e., whether the battery is charging or discharging). Should the battery discharge for any reason the array is turned full on. Should the rate of charge fall below the selected level, the shunt impedance across the array will be increased and the array will deliver an increased charge current. The reverse situation also holds. The charge current level is maintained constant until the battery approaches full charge. Approach to full charge is indicated by increasing battery terminal voltage and battery case temperature as backup.

At a preselected level of battery terminal voltage, one of two selected by ground command (lower for a new battery and higher for an older battery), the battery charge current is switched to a trickle charge of 330 ma. by action of the voltage monitor in a bistable time-delay circuit. After a time delay of from 5 to 15 seconds (set before launch), during which time the terminal voltage drops somewhat, the bistable circuit switches the charge current back to the preselected charge level. When the battery terminal voltage again triggers the bistable circuit, the cycle is repeated. As the battery charge approaches its maximum capacity the time required for the terminal voltage to again reach the selected level decreases, with the result that the average charge current during the charge cycling is only slightly higher than the trickle charge current. For the balance of the sunlight period of the orbit, this equilibrium charge current is maintained by the cycling of the bistable circuit, and the array is set to furnish the sum of the load current and this equilibrium charge current. If for any reason the battery temperature should exceed 95°F, either before or during the operation of the bistable circuit cycling, the charge level is switched to the trickle level by the action of thermostats mounted on the battery cases. As the temperature falls below the differential temperature of the thermostat, the



charge level is returned to the control of the voltage monitor and the bistable circuit.

Another thermoswitch will cause a battery to be switched entirely out of its charging circuit if, for any reason, the battery temperature exceeds 125°F. This situation will be discussed more fully in Section 3.

The foregoing charge regime takes place in each independent battery circuit. A certain degree of interrelationship exists between one battery and the other, since each is connected to the load bus through diodes. Continuous interchange of load current takes place so that both battery circuits effectively recharge at the same rate and handle one-half of the load. It is beyond the scope of this report to analyze these balance conditions.

The capability of changing, by ground command, the configuration of the power subsystem to compensate for several potential failure modes and degraded states of performance is built into the subsystem. To supply the information concerning subsystem performance needed by ground stations to assure that the proper reconfiguration commands are selected, many data points are entered into the telemetry subsystem. Among these are (1) the position of all command relays, such as trigger voltage level, charge current level, etc., (2) the position of failure transfer relays, (3) solar array current, (4) battery current, (5) battery current direction, (6) the voltage of controlled portions of the solar array, (7) individual battery temperature, (8) individual battery terminal voltage, and (9) load bus voltage. A discussion of the use of these data and commands to correct for malfunctions will be included in Section 3.

b. Detailed Assumptions

The reader is referred to Reference 1, subsection IV.C.1.b, for a discussion of the assumptions made for the preliminary assessment. Some of these assumptions must necessarily be changed in view of the new subsystem design and/or information. Specifically, assumptions (1), (2), (4), (5), and (6) of Reference 1 remain unchanged and are equally valid for the second assessment. The remaining assumptions, appropriately changed, are now presented:

Assumption (3): Solar cell efficiency is assumed to decay exponentially. The concept of half-life rather than mean-time-to-failure is used in the mathematical expression which describes this decay.

In the first assessment a linear decay of solar cell efficiency was assumed. Mean-time-to-failure in terms of reduced efficiency would, at most, have to be defined in rather empirical terms. On the other hand, if the concept of half-life is introduced into the consideration of quantifying decay of efficiency, an explicit mathematical expression can be stated to describe that decay. As was stated in the preliminary assessment, one expects an exponential decay. By definition, the time in life  $T$  at which the output of a solar cell decays to one-half of its initial output is its half-life. A cell's output at any time  $t$  can then be stated by the usual exponential expression

$$I(t) = I_o e^{-.693 \frac{t}{T}}, \quad (1)$$

where  $t$  = any arbitrary time  
 $T$  = the time at which  $I/I_o = 0.5$   
 $I(t)$  = the cell's current output at time  $t$   
 $I_o$  = the cell's initial current output

Assuming the average battery voltage during charge to be 30.5 volts, initial and 1-year solar array currents from Exhibit 2 are  $I_o = 20.8$  amperes and  $I(1 \text{ yr}) = 16.2$  amperes. Based on these values, the half-life of the solar array can be calculated by solving for  $T$  in Equation (1); namely,

$$T = \frac{(.693)(8760)}{\ln(16.2/20.8)} = 24,300 \text{ hours} \quad (2)$$

Using this half-life value, the output current at any time  $t$  can then be determined via Equation (1).

The further reduction of output current to be expected from the random opening of random cells of the array is insignificant, as can be seen by considering the expected failure rate per cell and the number of hours in a year. Using the failure rate for solar cells of  $0.7 \times 10^{-6}$  (cf. Reference 1), the expected fraction failing in 1 year's time is 0.006132, or about 200 cells. Thus, the reduction in output current in a year's time due to open solar cells can be ignored.

Assumption (7): The opening or shorting of battery cells, either singly or in combination, results in complete battery failure.

In discussions with STL subsystem engineers it was determined that, considering the actual construction of the battery pack, it is not now certain that a battery can successfully withstand the shortening of even one cell. Should one cell short, its temperature would very probably increase to a point where the thermostats mounted in the battery pack would be activated. This event can be negated by the ability to override these switches. However, the overheating of one cell could result in the overheating of its neighbors, leading to the ultimate destruction of the entire string of cells. The likelihood of occurrence of shorted cells must, therefore, be established with high confidence. Since this is primarily a function of manufacturing technique, and not a characteristic inherent in Ni-Cad batteries, the determination of the probability of short circuits must come as the result of an extensive testing and development program. PRC understands that such programs are underway, and is quite strong in its feeling that the full results of these programs should be made available to PRC for inclusion in the third reliability assessment of this subsystem. Any gross inaccuracy in the selection of battery cell failure rate can lead to completely erroneous conclusions concerning Power Supply Subsystem reliability.

Assumption (8): The power storage capacity of the subsystem is assumed to be that of one battery, not both.

The full effects of the number of charge and discharge cycles, depth of discharge, rates of charge and discharge, and battery temperature on battery capacity decay have not been divulged to PRC either by the manufacturer or by STL. Perhaps these effects are not yet fully known to them. However, statements in the literature, by both STL and others (cf. References 7 and 8), indicate that battery capacity definitely decays as a function of these parameters. This information, along with that discussed in assumption (7), should be available to PRC by the time of the third assessment.

As will be seen in Section 4, it is necessary to consider the batteries as redundant in order to achieve a reasonable subsystem reliability level. Under this consideration, it then necessarily follows that subsystem power storage capacity is that of one battery, not two, since the probability of the subsystem's having to function with only one battery is appreciable. The influence of this situation on OGO differs according to whether it is being considered for use in POGO or EGO orbits.

In a POGO orbit of maximum eclipse duration (37 minutes, as given in Reference 6, at a load of 240.96 watts at 28 volts, per Reference 9), the depth of discharge for each battery, when two are being used, is of the order of 22 percent. The operational requirement stated in the STL battery specification, Reference 10, calls for a depth of discharge of 26 percent. This situation is all right. However, should only one battery be available to handle the load (i.e., one branch has failed), its depth of discharge would obviously be 44 percent. Although this is an "out-of-specification" operational requirement, it is assumed, for this assessment, that the subsystem will function satisfactorily at this depth of discharge. This point will be included as a subsystem weakness in subsection 5. b.

For the EGO orbit, Reference 10 permits a depth of discharge of 75 percent (because there are fewer charge/discharge cycles during the mission). For a one-battery-capacity subsystem, this permits an EGO discharge load of  $0.75 \times 12 = 9.0$  ampere hours. At a load current of

approximately 8 amperes (cf. Reference 9<sup>1</sup>), the maximum permissible EGO eclipse is 9/8 hours. In Reference 6 it is seen that EGO orbits can have eclipses in excess of 3 hours, depending on the time of day and time of year of the launching. By judicious selection of launch time, the maximum eclipse time can be maintained lower than 9/8 hours. It appears to PRC that the 2-hour EGO eclipse time mentioned in various OGO documents depends on the ability of both batteries to continue operation for a year. The probability of this event's occurring is estimated to be only 0.50 (assuming a nonredundant, two-battery Power Supply Subsystem).

Assumption (9): It can be verified that the solar array is capable of supplying the power requirements of both EGO and POGO orbits.

In Reference 1 it was reasoned that the spacecraft could function satisfactorily in an EGO orbit if the solar array could deliver 280 watts. Decay of the solar cells after a year in an EGO orbit still permits the solar array to develop 300 watts, as indicated in References 3 and 4. STL is accepted as an authority on solar cell performance in space environments (cf. References 11 and 12).

The margin of solar cell performance after a year in a POGO orbit, however, requires close scrutiny because of the relatively short sunlight time available to recharge batteries following an eclipse. Based on the following data and calculations, it is concluded that, after a period of 1 year in a worst-case POGO orbit (37-minute eclipse), the solar array is capable of producing the power required to supply spacecraft loads and to recharge the batteries after periods of eclipse discharge.

#### Data Sources

1. Exhibit 2 presents the initial and 1-year output of the solar array as given in References 3 and 4. The total output voltage and amperage of the array are based on an effective electrical configuration of 96 series groups of 336 paralleled solar cells.

---

<sup>1</sup> Although this reference covers POGO only, 8 amperes will be assumed for EGO in order to illustrate this point.

2. Exhibit 3, derived from Reference 9, is the spacecraft load profile during periods of maximum eclipse in a POGO orbit.
3. An average battery charge voltage of 30.5 volts is derived from Reference 13.
4. Reference 14 states: "The total lack of sun on the array due to a worst-case eclipse and noon turn occurring in one orbit (including array errors) will be less than the equivalent of 5.0 minutes of eclipse (dark time)." This reduces effective charging time (sunlight) by 5.0 minutes.
5. Charge AH = 1.2 x discharge AH, per Reference 10. (The factor 1.2 accounts for battery losses during charge and discharge.)

To verify that the solar array is adequate at the end of (and hence throughout) a 1-year POGO mission, it is necessary to determine the required charge time following an eclipse and compare this time with the available daylight time. Exhibit 4 presents the parameters necessary to calculate the required charge time for a POGO orbit.

The condition to be met during each orbital period is that the charge AH = 1.2 x discharge AH. This can be expressed by the relation

$$(I_{SA} - I_T)(t_T - 5) + (I_{SA} - I_D)(t_C - t_T) = 1.2 I_E t_E \quad (3)$$

Rearranged, Equation (3) yields the time required for reaching full charge,

$$t_C = \frac{1.2 I_E t_E - (I_{SA} - I_T)(t_T - 5)}{(I_{SA} - I_D)} + t_T \quad (4)$$

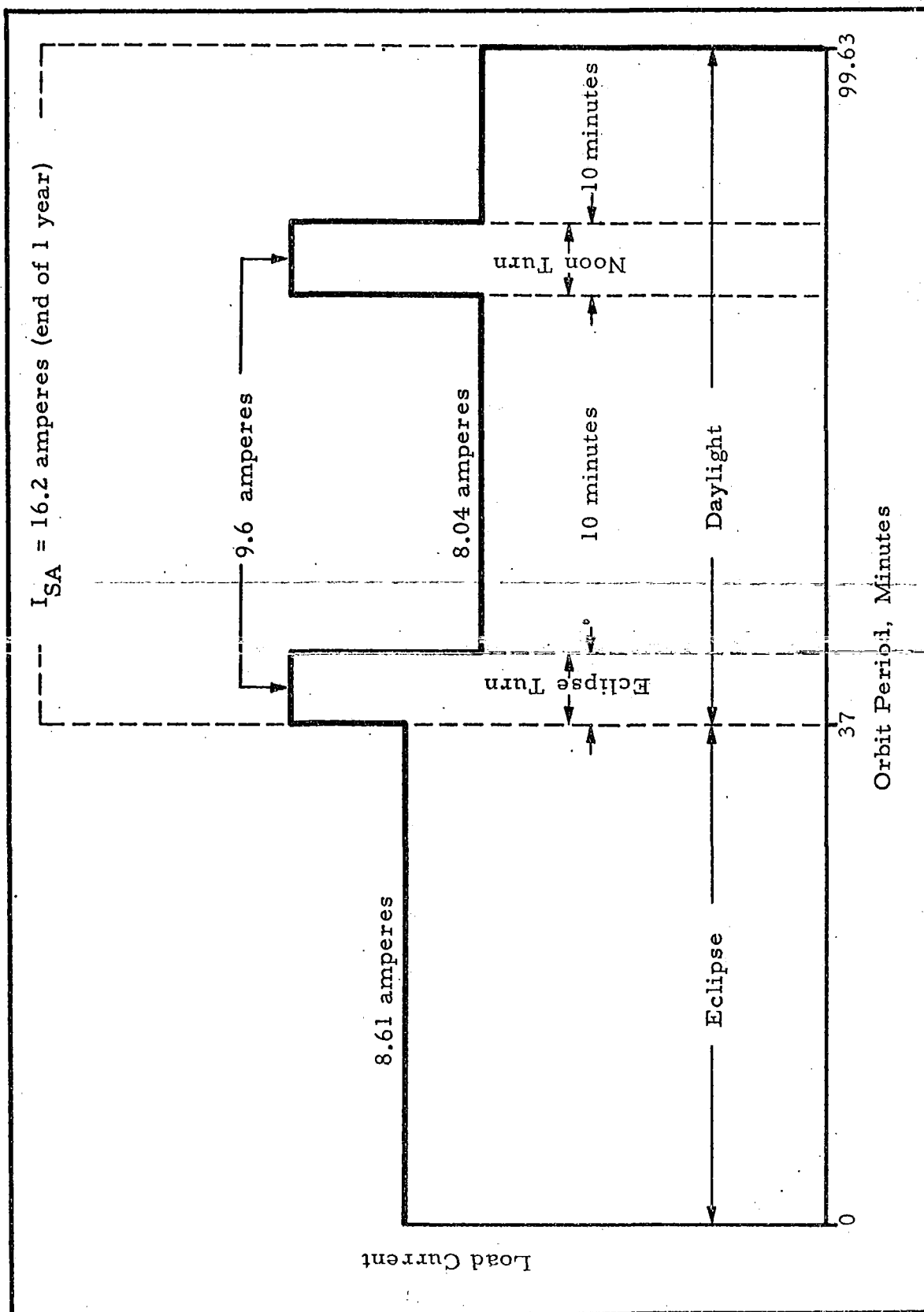


EXHIBIT 3 - LOAD PROFILE, POGO ORBIT, 37-MINUTE ECLIPSE

EXHIBIT 4 - PARAMETERS UNDERLYING CALCULATION OF  
REQUIRED CHARGE TIME

Parameters	Value	Definition
$I_{SA}$	16.2 amps (at 30.5 volts)	Maximum solar array current at 1 year
$I_E$	8.61 amps	Load current during eclipse
$I_D$	8.04 amps	Load current during daylight (nonturning)
$I_T$	9.6 amps	Load current during turns
P	99.63 min.	POGO orbit period
$t_E$	37 min.	Maximum eclipse time
$t_D$	62.63 min.	Daylight time (equal to maximum charging time)
$t_T$	20 min.	Sum of moon and eclipse turn times
$t_C$	To be calculated	Required charging time



Substitution of the values given in Exhibit 4 yields

$$t_C = \frac{(1.2)(8.61)(37) - (16.2 - 9.6)(20 - 5)}{(16.2 - 8.04)} + 20 \quad (5)$$

$$t_C = 54.72 \text{ minutes}$$

Since  $t_D$  exceeds  $t_C$  by 7.91 minutes, the batteries can be completely recharged during the daylight period of the orbit and are on trickle charge level for 7.91 minutes. The decrease of the charge rate during the operation of the bistable circuit should be thoroughly evaluated in the testing program to assure that full charge is reached in the time available.

Assumption (10): In Reference 1, assumption (10) stated that the failure probability of the telemetry circuits and all but one of the current monitors could be ignored. All reconfigurations of the power subsystem (as it is now designed), with the exception of those subject to actuation of the 95°F and 135°F thermostats, must be established by ground command. Certain telemetry data are needed at ground stations to assure that correctable failures are not overlooked and that inoperable configurations are not commanded. Therefore, those portions of the telemetry system located within the power subsystem needed to supply these minimum data points should be included in the assessment of subsystem reliability. It is assumed here that such portions have perfect reliability. Their inclusion (with the proper reliability prediction) must await the assessment, however, since drawings concerned with the contents of the TLM module within the power integration unit have not been received by PRC.

### 3. Modes of Failure and Subsystem States

Each of the components used in the Power Supply Subsystem has a certain probability of failure. Whether the subsystem itself fails when individual components fail is a function of the way in which the particular component is used. The subsystem may continue functioning with

the full capability of meeting all system loads; it may continue functioning but not be able to continue to the end of the mission; or it may suffer catastrophic failure.

In this section the several types (or modes) of failure and their consequences will be discussed. They will then be exhaustively grouped into the various resulting subsystem operability states preparatory to the development of the model equations and numerical evaluation of reliability in Section 4. Certain assumptions and approximations concerning even probabilities will be stated and used in the process of exhausting each state.

a. Modes of Failure

The Power Supply Subsystem design being considered in this assessment, like the one considered in the preliminary reliability assessment, is highly redundant. Unlike the first design, however, there are a few components in the present design whose failure, combined with solar array deterioration, will cause the outright failure of the entire subsystem during the latter portion of the mission. Their combined failure probability, as will be seen in the next section, does not seriously reduce subsystem reliability. For the most part, combined failures of assemblies such as regulators and batteries must occur in order for the over-all subsystem to be in a failed state. Thus, catastrophic failure of the subsystem occurs primarily when either the solar array fails or both battery/charge regulator circuits fail.

The extent to which the solar array can be expected to deteriorate in a year's time has been discussed. It was shown that, including the probability of a solar cell opening, the performance of the array after 1 year in POGO orbit is sufficient both to supply the load requirements and to recharge the batteries. However, if any one of the four diodes in series with the controlled sections of the array and the load fails open, or any one of the four transistors controlling sections of the array fails short, the array power available to the load is five-sixths of the full array power. After about 7 months in orbit this amount is not sufficient

both to supply the load bus and to recharge the batteries. The length of time for which an array delivering only five-sixths of its full power output is capable of supplying both system loads and battery charge requirements can be determined by combining Equations (1) and (3) as developed below.

If the required battery charging time  $t_C$  is allowed to equal the entire available daylight time in a POGO orbit, then  $t_C = P - t_E$ , where  $P$  is the POGO orbit period (cf. Exhibit 3). By substituting this relation in Equation (3) for  $t_C$ , the maximum allowable eclipse or discharge time  $t_E$  can be expressed<sup>1</sup> in terms of available solar array current,  $I_{SA}$ , namely,

$$t_E = \frac{94.63 I_{SA} - 784}{2.3 + I_{SA}} \quad (6)$$

Next, from Equation (1), the expected solar array output current,  $I_{SA}$ , can be determined for any time  $t$  during the 1-year mission for full and five-sixths capacity. First, if no series diodes or shunt transistors have failed, full power output  $I_{SA_{6/6}}$  is achievable, given by

$$I_{SA_{6/6}} = 20.8 e^{-.693t/24,300} \quad (7)$$

Second, if any one of the diodes or transistors has failed, only five-sixths  $I_{SA_{5/6}}$  full power output is achievable, given by

$$I_{SA_{5/6}} = (5/6)(20.8)e^{-.693t/24,300} \quad (8)$$

Exhibit 5 is a plot of maximum allowable eclipse time, or battery discharge time,  $t_E$ , for any time during the 1-year mission,  $t$ , for

---

<sup>1</sup>After substitution of the values of the other parameters given in Exhibit 4.

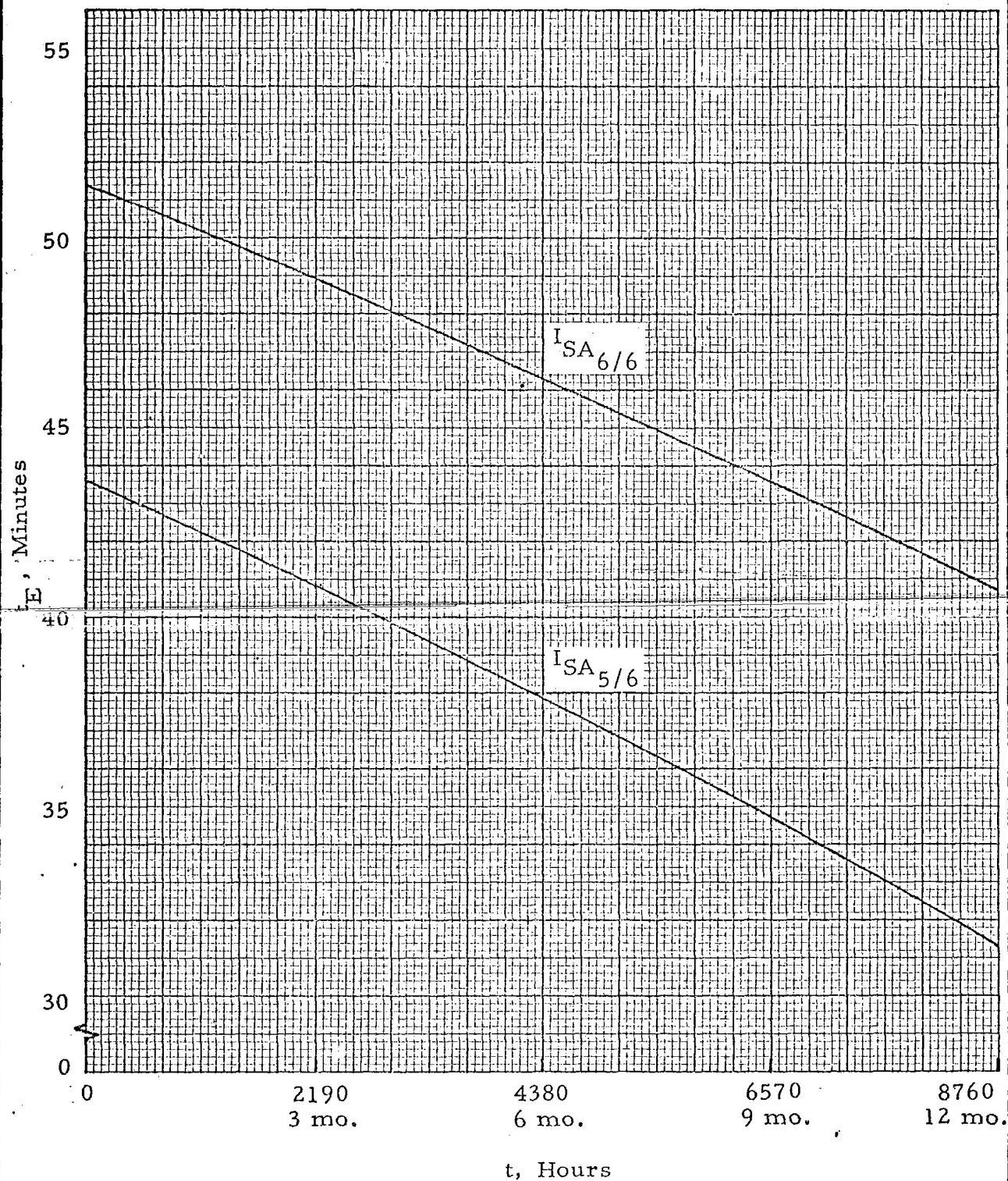


EXHIBIT 5 - MAXIMUM ALLOWABLE ECLIPSE TIME, POGO ORBIT,  
AS FUNCTION OF  $I_{SA}$  AND MISSION TIME

these two levels of solar array performance. Since the maximum eclipse time is 37 minutes, it is seen that the array has the ability to supply all load requirements throughout the year. It can also be seen that, with one failed diode or one failed transistor, the array can supply load requirements for approximately 7 months of the mission. In a  $90^\circ$  POGO orbit the eclipse time varies with the mission time (cf. Reference 6). If OGO is launched so as to provide a reducing eclipse time at 7 months, and a diode or transistor has failed, the spacecraft can be expected to live for approximately another 100 days. In this condition the charge requirements fall off faster than the solar array deterioration, and the spacecraft can continue to live (barring any catastrophic failure) until the eclipse time; thus the charge requirement, when added to system loads, exceeds the output of the degraded array.

The modes of failure of the batteries were essentially discussed under assumptions (7) and (8) of subsection 2.b. If battery capacity decay with the number of charge/discharge cycles and other parameters were known, the ability of one battery to handle the load could be developed in a manner similar to the half-life method used in the discussion of the solar array when it can deliver only five-sixths of its full power. Since these data are not known, a battery will be considered to have failed if one cell either opens or shorts. In addition, it will also be assumed that in POGO orbits one battery is capable of functioning to the end of the mission with a depth of discharge of approximately 50 percent. In EGO orbits, a maximum eclipse not exceeding 1 hour and a depth of discharge not exceeding 75 percent are assumed. Under these conditions, the failure of one battery will not cause the failure of the entire Power Supply Subsystem; both batteries must fail for this event to occur. Experience at Gulton Industries, Inc., on a NASA-sponsored Ni-Cad battery project, indicates good progress in the development of batteries having the required life (cf. Reference 7).

The remaining major portions of the Power Supply Subsystem are the two charge regulators and associated drive inverters and current monitors. As in the case of the batteries, the failure of one regulator

will not cause the entire subsystem to fail; both regulators must fail for this event to occur. The current-regulating part of a regulator can fail in such a manner as to turn off the solar array or to turn the array full on. The voltage-limiting or monitoring (bistable) part of the regulator can fail in a manner such that the charge current will not be reduced to the trickle level, or such that charging at the level required to reach full battery charge will be prohibited.

The major portions of the Power Supply Subsystem can be interconnected in several different configurations to offset the effects of the various individual failures described above. Certain combined failures can also be prevented from causing catastrophic subsystem failure. Some configurations can be established automatically; others must be established through the proper diagnosis of telemetry data and the successful response to ground commands.

Failure situations and the automatic means for eliminating their effects are as follows:

1. Either a shorted battery or a regulator fails so as to turn the solar array full on, resulting in an overheated battery. In this situation, a thermoswitch set to actuate when the battery case temperature exceeds 125°F closes, actuating relay switching circuits which (a) open the charge circuit to that battery while allowing it to discharge into the load bus, (b) turn control of the associated solar array paddle over to the other regulator, (c) transfer the output of the associated solar array paddle to the charging circuit of the other battery, (d) trigger the under-voltage bus relays (unless inhibited by ground command), (e) set the battery charge current level to maximum (unless inhibited by ground command), (f) set up the associated charge regulator to function as a solar array voltage regulator in the event that the other battery also fails, and (g) give telemetric indication of the rearranged configuration. Return to normal configuration if and when the battery case temperature falls below 125°F can be accomplished only by means of ground command.

2. The voltage monitor or bistable fails to reduce the charge current to the trickle level as full charge is approached, resulting in increasing battery case temperature. In this situation, a thermoswitch

set to actuate when the battery case temperature reaches 95°F opens, causing the charge current to be reduced to, and remain at, the trickle level. When the battery case temperature falls below the temperature differential inherent in the thermoswitch, the switch closes and the charging current returns to the preselected level. This feature provides a backup to the normal method of charge control by monitoring battery terminal voltage.

Failure situations and the ground commands for eliminating their effects are as follows:

1. Either an open battery or its regulator fails so as to turn off one solar array paddle, resulting in the battery's having zero terminal voltage or a terminal voltage too low to permit the battery to remain on the load bus. This failure situation must be discerned at a ground station by noting solar array current and midpoint voltage, battery current, and battery terminal voltage. With the realization that this failure situation exists, the ground command that actuates the same relay circuits as does the 125°F thermoswitch can be transmitted with the result that the faulty battery/charge regulator is switched out of operation and the subsystem configured to operate with the remaining battery/charge regulator powered by the full array.

2. Aging batteries exhibit higher terminal voltages than do new ones upon reaching full charge. If the voltage level at which the voltage monitor triggers the bistable circuit is not increased, an aging battery may not reach its full charge capacity during the available sunlight time. This could eventually cause the mission to fail. This failure situation can be discerned at a ground station by noting battery terminal voltage variation during the period of bistable circuit operation. By ground command, the voltage level at which the voltage monitor circuit triggers the bistable circuit can be set to the higher of two possible levels.

The automatic switching initiated by the actuation of the thermoswitches can be completely overridden by ground commands. Thus, if it is believed that automatic switching has incorrectly occurred, or if "last-ditch" attempts to keep the subsystem functioning are desirable, all possible reconfigurations of the subsystem including those establishable by automatic means can be commanded from the ground.

b. Power Supply Subsystem States

In the above discussion it is seen that the subsystem can be in any of several different states of operation, from full operability (even though a certain component or assembly of components has actually failed) to degraded operability (capable of functioning with full output for a determinable period of time, however, barring additional failures) to inoperability (incapable of supplying subsystem loads and recharging the batteries). Each of these three operability states is defined below in terms of one or more substates.

(1)  $S_1$  (Fully Operable State)

The fully operable state  $S_1$  is defined as existing when any one of seven substates  $S_{1j}$  ( $1 \leq j \leq 7$ ) exists:

$S_{11}$ : All components and assemblies operable; normal configuration of two branches, each consisting of one paddle, one battery, and one charge regulator; each branch handling approximately half of the load requirements.

$S_{12}$ : One battery shorted, or its regulator incapable of turning off its paddle, or both. Subsystem automatically switched to operation with the other battery/charge regulator powered by full solar array.

$S_{13}$ : Inverse of  $S_{12}$  (i.e., the other battery shorted, or its regulator incapable of turning off its paddle, or both).

$S_{14}$ : One battery or one of two diodes between battery and load bus open, or associated regulator maintaining continuous solar array cutoff (includes malfunctioning voltage monitor/bistable). Subsystem commanded from ground to operate with the other battery/charge regulator powered by full solar array.

$S_{15}$ : Inverse of  $S_{14}$ .

$S_{16}$ : One or the other or both regulators having a failed voltage monitor/bistable circuit; charge current reduced to trickle level at full charge by action of 95°F thermoswitch.

$S_{17}$ : Any one of four transistors controlling solar array in open condition, with regulators and remaining three transistors automatically



compensating for loss of control over the one section of the solar array. In this case each transistor is considered to be an ensemble of three components (a transistor plus two resistors).

(2)  $S_2$  (Degraded Operability State)

The degraded operability state  $S_2$  is defined via a single substate  $S_{21}$ :

$S_{21}$ : The open failure of any one of the diodes in series with the four controlled sections of the solar array, or the short failure of any one of the four transistors controlling the solar array, after mission time  $t$  (as determined in Equation (8) in conjunction with curves in Reference 6), reduces the value of the experimental data, since these data will not be available for the entire year.

(3)  $S_3$  (Inoperable State)

The inoperable state  $S_3$  is realized when the subsystem is in any one of four substates  $S_{3j}$  ( $1 \leq j \leq 4$ ):

$S_{31}$ : Both batteries failed.

$S_{32}$ : Both regulators failed.

$S_{33}$ : One battery and the other regulator failed.

$S_{34}$ : The inverse of  $S_{33}$ .

4. Numerical Assessment

a. Model Equations

The equations for the present configuration are much simpler than those derived in the previous assessment, primarily because of the deletion of the blocking diodes from each string of solar cells. The simplification results in only three state equations, corresponding respectively to the fully operable, degraded operability, and inoperable states defined in the preceding section. General assumptions were made in order to render the computations more tractable, but these can be shown to have negligible effect on subsystem reliability predictions. The assumptions are listed on the following page.

1. Since the reliabilities of the telemetry and command circuits external to the Power Supply Subsystem are considered in the discussion of the Communications and Data Handling Subsystem, they are not included in the present subsystem assessment.

2. The probability of short failures (to ground or across terminals) of solar cells is negligible relative to the probability of open failures.

3. If the blocking diode of a solar cell section fails short there is no significant effect, since the probability of the solar cell section's also failing short (to ground) is negligible.

4. The probability of failure of synchronization amplifiers is not included in the assessment because the Power Supply Subsystem contains a free-running oscillator in each battery/charge regulator.

5. The effects of switching failures in substates  $S_{12}$ ,  $S_{13}$ ,  $S_{14}$ ,  $S_{15}$ , and  $S_{16}$  are negligible, since (a) the switching mechanism is highly reliable and (b) a loss in switching capability has a detrimental effect on the system only if the regulator or battery in that branch has also failed.

The numerics to substantiate the above assumptions will be presented in subsection 4.c, containing the reliability calculations.

Exhibit 6 depicts the reliability block diagram for the Power Supply Subsystem. The two branches, each consisting of a battery and a regulator plus a few diodes and transformers, are treated as redundant. For state  $S_1$ , all four controlled sections and both uncontrolled sections must be operable, while for state  $S_2$  one of the six sections is inoperable with the other five operable (a section includes the blocking diodes, power transistor, and associated resistors in addition to the solar cells). The reliability of a branch will be denoted by  $R_B$ , that of a controlled section by  $R_{CS}$ , and that of an uncontrolled section by  $R_{US}$ . The probability that the subsystem is in state  $S_1$ , then, with all sections and at least one branch operable, is

$$P(S_1) = P_{CS}^4 R_{US}^2 \left[ 1 - (1 - R_B)^2 \right] \quad (9)$$

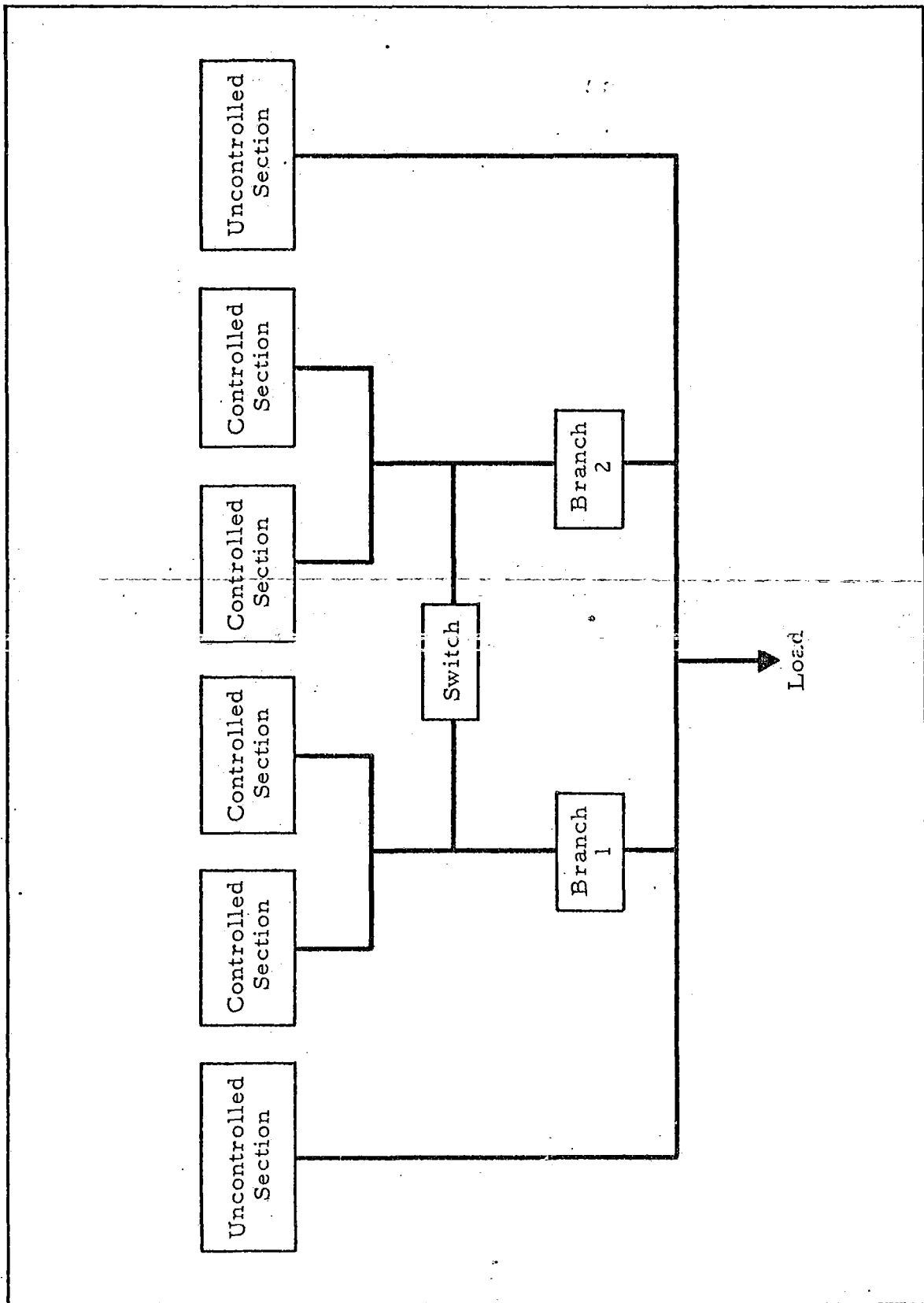


EXHIBIT 6 - SIMPLIFIED RELIABILITY BLOCK DIAGRAM FOR POWER SUPPLY SUBSYSTEM

The probability that the subsystem is in state  $S_2$ , with five out of six sections and at least one branch operable, is

$$P(S_2) = \left\{ 4R_{CS}^3(1 - R_{CS})R_{US}^2 + 2R_{CS}^4(1 - R_{US})R_{US} \right\} R_{US} \left\{ 1 - (1 - R_B)^2 \right\}. \quad (10)$$

The probability that the system is in state  $S_3$  is, of course,

$$P(S_3) = 1 - P(S_1) - P(S_2) \quad (11)$$

As was stated in the preceding section, state  $S_2$  is detrimental to spacecraft operability only when the solar array has degraded to a point where the required recharge time exceeds the available daylight time. This occurs at some time between 7 and 10 months (depending on the particular orbit) after launch. It follows, then, that Power Supply Subsystem reliability  $R_{PS}(t)$  is equal to the sum of  $P(S_1)$  and  $P(S_2)$  up to that point in time and to  $P(S_1)$  only thereafter.

#### b. Preparation of Reliability Inputs

In this subsection the component parts and associated failure rates are listed. When short and open failures result in a different substate they are listed separately. The failure rates for diodes, transistors, resistors, and capacitors were taken from Reference 15, and the rates for the rest of the components, with the exception of battery cells, were taken from Reference 1; for battery cells the STL failure rates were used.

The parts lists for the regulator include those parts whose failure causes branch failure such that the regulator cannot turn the array off (substates  $S_{12}$  and  $S_{13}$ ), as well as those parts whose failure renders the regulator incapable of turning the array on (substates  $S_{14}$  and  $S_{15}$ ).

The parts complements and associated failure rates, then, are as follows:

<u>Regulator</u>	<u>Branch</u>	<u>Failures Per Million Hours</u>
<u>Branches (each)</u>		
Transistors, Silicon	9	0.30
	10 (short)	0.15
	8 (open)	0.15
Diodes, Silicon	4	0.15
Diodes, Zener	3	0.26
	1 (short)	0.03
Silicon-Controlled Rectifier	2 (short)	0.15
Resistors, Film	20	0.23
	12	0.23
Capacitors, Paper	15	0.01
Transformers, Signal	3	0.20
<u>Other Branch Components</u>		
Transformers	4 (open)	0.26
Control Sets	4	
Coils	2	0.80
Diodes, Silicon	2 (open)	0.15
Battery Cells	22	1.00
<u>Controlled Sections (each)</u>		
Transistor, Silicon Power	1 (short)	0.12
Diode, Silicon	1	0.15
<u>Uncontrolled Sections (each)</u>		
Diodes, Silicon	2 (redundant)	0.15
<u>Switching, for Substates <math>S_{12}</math> and <math>S_{13}</math></u>		
Thermoswitch ( $125^{\circ}$ )	1	0.16
Relay, Latch, Redundant Contact Sets	1	0.00
Relay, Sensitive, Single Contact Sets	1	0.60

<u>Regulator</u>	<u>Branch</u>	<u>Failures Per Millions Hours</u>
<u>Switching, for Substates <math>S_{14}</math> and <math>S_{15}</math></u>		
Relay, Latch, Redundant Contact Sets	1	0.00
Relay, Sensitive, Single Contact Sets	1	0.60
<u>Switch for Charge Current Reduced to Trickle (Substate <math>S_{16}</math>)</u>		
Thermoswitch ( $95^{\circ}$ )	2 (redundant)	0.16

### c. Calculations

The first consideration is to determine the negligible terms of the subsystem reliability equations. As was stated in the assumptions, switching reliabilities are not included in the system equations because of their negligible effects.

For example, the probability that the switching mechanism for substate  $S_{12}$  will not be operable at the end of 1 year (which is the worst case) is simply its unreliability; viz,

$$1 - R_{\text{Switch}} = .0067$$

Similarly, the probability that switching is required (that is, that the parts corresponding to substate  $S_{12}$  have failed by the end of the year) is

$$1 - R_{12} = .085$$

It follows that the probability of both occurrences is then equal to .00057. This, of course, is an upper bound, since both switch unreliability and  $1 - R_{12}$  are lower earlier in the year. Thus, to the accuracy desired, this term is of little significance. Similarly, considerations of switching reliability for substates  $S_{13}$ ,  $S_{14}$ ,  $S_{15}$ , and  $S_{16}$  are unnecessary. In retrospect, if all switching were included in the model

equations they would require a number of additional terms which, when numerically evaluated, would not significantly affect subsystem reliability predictions.

The terms of the subsystem state equations are computed using the failure rates listed for a branch and for the sections, and setting switching reliability equal to unity. As in the preliminary assessment, the reliability degradation of the solar cells is predicted to be such that it does not significantly affect subsystem reliability as long as the rest of the subsystem is operable. If one of the six array sections is inoperable, however, the degradation of the cells in the other five may cause problems in recharging after an eclipse. This factor, which was discussed more completely in a previous subsection, is taken into account in determining which states are operable and in defining subsystem reliability. Exhibit 7 gives the state probabilities for each of the three states at four time periods. The last column of this exhibit gives the predicted values of Power Supply Subsystem reliability at the four time periods, each calculated as defined in the paragraph immediately following Equation (11). (For the reader's convenience,  $R_{PS}$  is presented in graphic form in Exhibit 8.)

Time (hours)	State Probabilities			Subsystem Reliability
	$P(S_1)$	$P(S_2)$	$P(S_3)$	
2190	.9908	.0018	.0074	.9926
4380	.9703	.0035	.0262	.9738
6570	.9413	.0051	.0536	.9413
8760	.9095	.0066	.0839	.9095

EXHIBIT 7 - SUMMARY OF POWER SUPPLY SUBSYSTEM RELIABILITY AND STATE PROBABILITIES

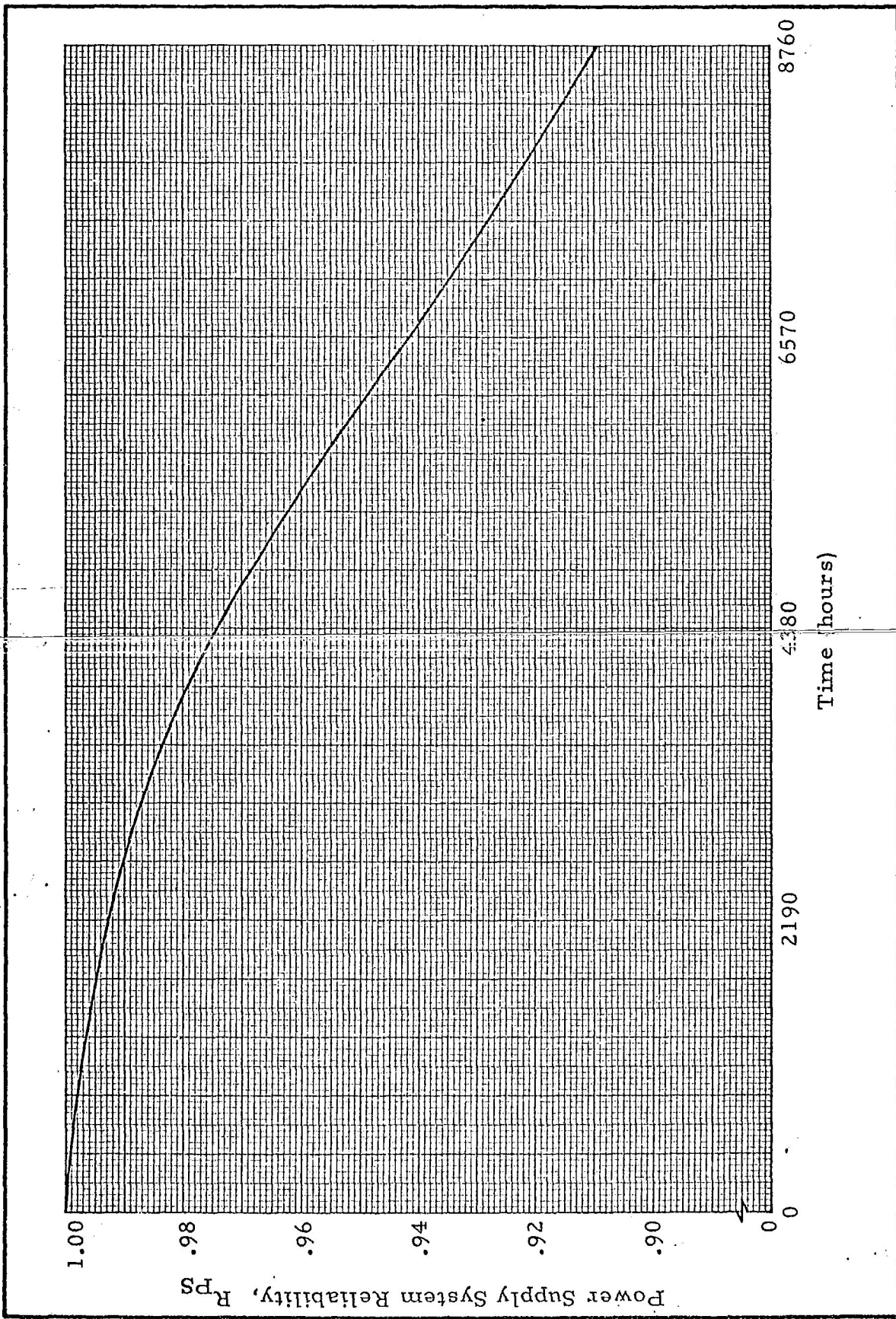


EXHIBIT 8 - POWER SUPPLY SUBSYSTEM RELIABILITY VERSUS TIME



## 5. Strengths and Weaknesses

### a. Strengths

There are several features of this design which make it excellent from both performance and reliability points of view:

(1) The batteries are charged at a constant rate of current controlled by servo action. This feature practically eliminates the possibility of thermal runaway.

(2) Bistable control of the charging rate as full capacity is approached assures that maximum charge is returned to the battery in the limited time available.

(3) Backup to the control of the charge rate by means of temperature sensing (a 95°F thermoswitch) assures full charge within the restraints of temperature.

(4) The ability to charge at lower rates when orbital conditions permit contributes to the longevity of the batteries.

(5) Shunt control of the solar array assures that full solar array power is available to supply the load and charge the batteries. No power is wasted when it is needed the most.

(6) Solar array isolating diodes are minimized. Their failure is more significant, but there are not as many of them to fail.

(7) The most damaging type of potential failure, battery temperature in excess of 125°F, is under automatic control. By ground command, many different configurations of the Power Supply Subsystem are possible.

(8) Impending or actual component failures can be detected at ground stations through the telemetry system, and their effects negated by ground control of the subsystem. Automatic methods beyond those included would cause a detrimental increase in complexity, with a resultant decrease in reliability.

### b. Weaknesses

(1) As might be expected, the batteries are the weakest link in the entire subsystem. With 22 cells in series the

probability that at least one of them will become either opened or shorted is appreciable. There is not much that can be done about the number of cells in series; there is no other practical way of obtaining the required working voltage. It was pointed out in subsection 3.a that a battery handling the entire load actually operates outside the limits established by the battery specification (cf. Reference 10). While the necessity that a battery handle the entire load arises only in the event of failure of one of the subsystem branches, acceptable reliability can be achieved only through redundant battery branches. For example, if redundancy were not included, the estimate of Power Supply Subsystem reliability made in this assessment would be approximately 0.50. Subsystem reliability thus depends on the ability of one battery to handle the entire load. Equipment performance should not be allowed to depend on any component parameters that are uncontrolled in the component specification.

(2) Batteries and regulators are not individually redundant. As presently designed, a battery and its regulator are redundant with another battery and its regulator; regulators cannot be interchanged once the subsystem is assembled. The switching required to achieve individual redundancy can be accomplished with four DPDT switches. It is considered that sufficient telemetry data are available at ground stations to permit diagnosis of subsystem failures involving the regulators and batteries. As a first approximation, the probability of subsystem failure at the end of a year in orbit is reduced from 0.99 to 0.06, or by 33-1/3 percent, when the regulators and batteries are fully redundant. In terms of predicted subsystem reliability, the level is increased from about 0.91 to 0.94, a sizable increase.

(3) Several failure modes are correctable only from the ground through the command system. In addition to the complexity involved in such a failure detection, decision, and correction method, lack of contact with ground stations during portions of each orbit or possibly for several complete orbits may create serious problems in maintaining a properly functioning Power Supply Subsystem. Analysis of the effects of ground station location on the reliability of this subsystem is beyond the scope of the second assessment. Sufficient

information concerning the location of ground stations may be available in time for inclusion in the third assessment.

(4) For a sizable portion of a 1-year mission in a POGO orbit, the ratio of eclipse time to daylight time is sufficiently high to require that the charge current level must be set at maximum. For maximum charge level, both charge select relays must be energized; if the coil on one of these relays should fail, maximum charge level could not be selected. From this point of view it would seem desirable that these switching circuits be designed so that, in the event of coil failure, a maximum rather than a lesser charging level would be the result. Perhaps latching-type relays should be used throughout the Power Supply Subsystem.

(5) In the new design of the subsystem it would appear that full advantage has not been taken of strength (5) above. The 30 watts, or more, that were necessarily dissipated in the series regulator transistors of the original design when full current was needed are not wasted or needed in the present design. Unless new estimates of OGO load requirements are 10 to 15 percent higher than those stated in Reference 9, it is PRC's opinion that the solar array power output margin of safety is unnecessarily high. This is especially true if the interconnections of the solar cells are changed to provide maximum power output at a voltage equal to the average terminal voltage of the batteries during the charging phase. If the solar array output power were to be reduced by 30 watts, 1840 solar cells could be eliminated (each cell produces 0.0163 watts at its maximum power output point after 1 year in a POGO orbit). Since there are 32,256 cells in the array as presently designed, the elimination of 1840 cells represents a weight saving of 5.7 percent of the total array weight, assuming that it can be reduced linearly. The total weight of the solar array, excluding wiring harness, sun sensor, charger regulators, and sun experiment, is estimated at 101 pounds (cf. Reference 3). A 5.7-percent reduction in weight would thus be approximately 5.7 pounds, a sizable amount when booster requirements are considered.

## 6. Recommendations

a. The capability of one battery to handle the entire load should be established with statistical confidence; this cannot be left to chance. Capacity decay as a function of depth of discharge, number of charge/discharge cycles, battery temperature, charge rate, discharge rate, etc., should be established in a development evaluation and acceptance program mutually acceptable to NASA, STL, and the battery supplier. Battery specifications must be written to cover more accurately the operational situations, both POGO and EGO, for two batteries sharing the load as well as for one battery handling the entire load.

Launch restraints for both POGO and EGO orbits imposed by the limitations of the batteries (including the single-battery situation) should be explicitly determined and described by STL for the benefit of NASA and all experimenter's.

Methods of bypassing opened or shorted cells should be investigated in an attempt to increase battery reliability.

b. Switching circuits to provide full redundancy of regulators and batteries should be developed. The gain in subsystem reliability should be traded against the cost in switching unreliability and weight and power requirements.

c. The design feature that many failure modes are correctable only through the telemetry and command paths should be included in the over-all OGO system ground-station location studies.

d. The use of latching-type relays throughout the subsystem should be considered. Reliability gain should be traded against increased complexity in any other circuits.

e. Reconfiguration of the solar array should be studied by STL in order to make more efficient use of its power output. If power requirements have not increased excessively, potential weight savings exist. For the latest design of the subsystem, maximum solar array power output should occur at a lower array voltage than was the case for the first design. This is occasioned by the replacement of the series regulator by a shunt regulator which wastes no power (thus requiring

no voltage drop) when maximum load occurs. If increased load is now estimated, it may be possible to meet the increase in this manner rather than by adding more solar cells with a resultant increase in system weight.

## REFERENCES

1. Planning Research Corporation, R-243, Preliminary Reliability Assessment for the Orbiting Geophysical Observatories, 1 February 1962.
2. Space Technology Laboratories, Unpublished description of electrical power subsystem (undated).
3. Space Technology Laboratories, 2311-0010-OU-000, Section 6.0 of the Data Book ("Electrical Power Subsystem"), 5 January 1962.
4. Space Technology Laboratories, D-13401, Specification, Solar Array Power, OGO, 22 January 1962.
5. "Telstar To Be First Active ComSat," Missiles and Rockets, 9 July 1962, p. 14.
6. Space Technology Laboratories, 8100.1-10, Eclipse Distribution for Various Possible OGO Orbits, 15 February 1961.
7. "New Cells Due for Heavy Space Duty," Missiles and Rockets, 11 June 1962, p. 34.
8. Space Technology Laboratories, 9312.6-150, A Study of Satellite Power Supply (undated).
9. Space Technology Laboratories, SK 201070-B, Power Data, POGO, 1 February 1962.
10. Space Technology Laboratories, PT-3-1004, Specification, Sealed, Sintered Plate, Nickel-Cadmium Secondary Cells, 27 April 1962.
11. Space Technology Laboratories, 8987-0001-RU-000, Final Report, Charged Particle Radiation Damage in Semiconductors (I: Experimental Proton Irradiation of Solar Cells), 15 September 1961.
12. Space Technology Laboratories, 8987-0009-RU-001, Charged Particle Radiation Damage in Semiconductors (II: Minority Carrier Diffusion Analysis in Photovoltaic Devices), 19 February 1962.
13. Space Technology Laboratories, Status of OGO Battery Program (undated and unnumbered; contains curves dated June 1962, by P. Bauer).
14. Space Technology Laboratories, 2313-0004-RU-000, OGO Attitude Control Subsystem Description, Logic, and Specification, 4 December 1961, p. 28.
15. Planning Research Corporation, TAM No. 7, Parts Failure Rates -- OGO Second Reliability Assessment, G. E. Monroe, R. G. Salter, and J. D. Andrew, 24 August 1962.

TECHNICAL ADVISEMENT MEMORANDUM NO. 8

SECOND RELIABILITY ASSESSMENT

FOR THE OGO THERMAL

CONTROL SUBSYSTEM

## TABLE OF CONTENTS

	<u>Page</u>
1. Subsystem Description . . . . .	1
2. Subsystem States and Modes of Failure . . . . .	2
a. Subsystem States . . . . .	2
b. Modes of Failure . . . . .	2
3. Numerical Assessment . . . . .	6
a. Model Equations . . . . .	6
b. Component Parts Complement of the Thermal Control Subsystem . . . . .	7
c. Numerical Evaluation of State Probabilities and Reliability . . . . .	7
4. Strengths and Weaknesses of the Subsystem . . . . .	8
5. Quantitative Assessment of Thermal Control Subsystem Under Tumbling Conditions . . . . .	10
6. Summary . . . . .	21
References . . . . .	22



TECHNICAL ADVISEMENT MEMORANDUM NO. 8

To: Assistant OGO Project Manager, GSFC, NASA  
From: PRC OGO Assessment Team  
Subject: Second Reliability Assessment for the OGO Thermal Control Subsystem

1. Subsystem Description

For a description of the Thermal Control Subsystem the reader is referred to PRC R-243, Preliminary Reliability Assessment for the Orbiting Geophysical Observatories (Reference 1). Where the description of the present configuration differs significantly from that of Reference 1, the latest configuration will be described herein. Specifically, the following changes (or more detailed descriptions) are noted:

a. The controlling actuators for the louvers of columns<sup>1</sup> 1, 2, 3, 4, 5, 6, and 8 will be adjusted so that the louvers will be fully open at 75°F and fully closed at 50°F.

b. The controlling actuators for the louvers of column 7 will be adjusted so that the louvers will be fully open at 65°F and fully closed at 40°F. Column 7 is directly over the two 4-watt transmitters, and the heat balance analysis conducted by STL (cf. Reference 2) indicates that the transmitter baseplate temperatures would reach as high as 110°F during normal orbit operation. The reduction in actuating temperature will help to alleviate this problem.

c. An RTV elastomer has been selected and successfully tested for the interface conductance filler material. This material allows interface conductances of approximately 25 Btu/hr ft<sup>2</sup>°F, thereby offering considerable improvement over the 2-3 Btu/hr ft<sup>2</sup>°F interface conductance experienced without filler.

---

<sup>1</sup>The terminology of Reference 1 is used here.

d. Mylar sunshades have been added to protect one radiating side panel from exposure to sunlight due to a  $4-1/2^{\circ}$  offset in attitude control incorporated in sun sensors. The sunshades are arranged so that sunlight will not strike any portion of the radiating panel during the normal offset attitude condition.

e. Angle sensors which had been planned for the louvers have been deleted.

f. A large percentage of the previously exposed bracketry will now be insulated with Mylar tape in order to reduce the number of uncontrolled heat paths on the vehicle.

g. The bimetal actuators have been surface-oxidized in order to insulate them more fully from heat inputs other than conductance from the radiating panels.

h. Anodizing has been selected as the surface finishing process for the radiating panels. An anodizing process has been developed which provides a solar absorptivity of approximately 0.3 and an emissivity of 0.8.

i. Potassium silicate paint has been selected as the coating material for the back of the solar cell substrates. This paint exhibits a solar absorptivity of approximately 0.2 and an emissivity of 0.85.

## 2. Subsystem States and Modes of Failure

### a. Subsystem States

Since sufficient information for the determination of meaningful degraded states for the Thermal Control Subsystem still does not exist, the same two states,  $S_1$  and  $S_2$ , defined in Reference 1, will be used for this assessment. As before,  $S_1$  corresponds to subsystem success while  $S_2$  corresponds to subsystem failure.

### b. Modes of Failure

The STL memorandum entitled "OGO Louver System Reliability" (Reference 3) has been reviewed by PRC to determine whether or not it contains an accurate, up-to-date delineation of failure

modes for the Thermal Control Subsystem. The memorandum explicitly defines 36 failure modes for the subsystem, each in terms of a combination of failed louvers. Individual louver failure is defined as occurring in three ways: stuck open, stuck closed, and stuck half open. More precisely, these three failure conditions correspond respectively to a louver stuck in the  $30^{\circ}$ - $90^{\circ}$ ,  $0^{\circ}$ - $20^{\circ}$ , and  $20^{\circ}$ - $30^{\circ}$  arcs of the  $90^{\circ}$  through which a louver is designed to operate.

Three other STL documents (References 4, 5, and 6) that preceded Reference 3 provide the historical or evolutionary background underlying the delineation of the 36 failure modes in Reference 3. Based on rational, technical judgment and on consideration of, for example, the distribution of OGO components, consequences of localized temperature extremes, and the total thermal environment during a complete orbit, STL first defined a basic set of failure modes. Then, later on, the concept of "intermediate" or "half open" louver failure was introduced and the number of subsystem failure modes increased accordingly.

Now, it is important to note that the 36 failure modes delineated to date do not constitute all possible failure modes, although it is possible (but not stated by STL in Reference 3) that they constitute all important (i. e., occurring with non-negligible probability) failure modes. It is easy to construct additional failure modes. For example, the mode tabulated<sup>1</sup> in Exhibit 1 is a candidate for mode number 37.

<u>Louver Failure Condition</u>	<u>Side 1 Column Number</u>		
	<u>1</u>	<u>2</u>	<u>3</u>
Closed	2	5	7
Open	9	5	2
Half open	6	7	8

#### EXHIBIT 1 - FAILURE MODE 37

For the reader who is more familiar with the STL designations of louver position, Side 1 may be identified with, say, the +X panel, and

<sup>1</sup>Using the terminology of Reference 1.

column 1, column 2, and column 3 identified respectively with Zone III, Zone II, and Zone I. The numbers given in the exhibit mean "any combination of"; e. g., the entry in the upper left-hand corner means "any two of the louvers in column 1 failed closed."

Next, failure mode 38 might be the Side 2 (i. e., the -X panel) counterpart of failure mode 37, while modes 39, 40, etc., might be defined by selecting other specific combinations of louver failures that do exist and are not included in the 36 modes given in Reference 3.

Review of the reliability expressions given in Reference 3 reveals that they are essentially correct, as qualified therein, particularly if they are adjusted (and/or qualified) to account for the non-exhaustiveness of failure modes. The equation for  $R_2$ , for example, might be written more precisely as

$$R_2 = 1 - \sum_{\substack{\text{All} \\ \text{modes}}} P_j,$$

where the summation exhausts all mutually exclusive<sup>1</sup> failure modes. It may be true that this sum can be approximated by the one given in Reference 3, namely,

$$\sum_{\substack{\text{All} \\ \text{modes}}} P_j \cong \sum_{j=1}^{36} P_j.$$

However, no comparison of the magnitudes of these is presented in Reference 3.

It appears, then, the one-by-one enumeration of failure modes does not guarantee that all important failure modes are exhausted.

---

<sup>1</sup> An assumption made preceding the STL expression for  $R_2$  to assist in the argument.

Furthermore, since conducting a heat balance analysis of each potential failure mode to determine its importance (or even existence) as a failure mode would involve a prohibitive amount of effort, it appears that an alternative approach to failure mode enumeration, also based on engineering judgment, is desirable.

For the second assessment, it is felt that the failure modes of Reference 1, slightly modified, provide a more logical and accurate delineation of failure modes. The reader will recall that the modes given in Reference 1 were based on the concepts of critical areas (i. e., portions of the panels near high heat sources) and on the likelihood of their occurrence.

As regards the modification of the modes defined in Reference 1, it is felt that the thermal control problem is better understood at this time, primarily because of the more accurate heat balance analysis (Reference 2), and that the refinement of individual louver failure into "stuck closed" and "not stuck closed" is of importance.<sup>1</sup> More explicitly, since the effects of these two failure conditions are quite different, it is felt that the failure modes given in Reference 1 must, to be more realistic, be modified as follows:

- M<sub>1</sub>: Loss of operation of any 12 (or more) louver/actuators in any position.
- M<sub>2</sub>: Loss of operation of any four (or more) contiguous louver/actuators in any one panel column in the closed position.
- M<sub>3</sub>: Loss of operation of any two (or more) louver/actuators in any one of the three critical areas in the closed position.

Modes M<sub>2</sub> and M<sub>3</sub>, as defined above, account for the fact that the loss of four (or more) contiguous louver/actuators in a column in the closed position will cause subsystem failure, whereas the loss of four (or more) contiguous louver/actuators in a column in the not closed position will not cause subsystem failure. To be precise, one should include the cases where a large number (i. e., many more than four) of louver/actuators in a column are failed in the not closed position; however,

---

<sup>1</sup> Here, "stuck closed" means stuck within 0°-20° of arc and "not stuck closed" means stuck within 20°-90° of arc.

consideration of the probability of occurrence of such cases makes their inclusion unnecessary.

### 3. Numerical Assessment

#### a. Model Equations

The model equations developed in Reference 1 apply without modification (except for the new interpretation of the failure modes) and are used in this assessment. For the reader's convenience the key model equations are repeated herein; namely,

$$P_{TC}(S_2, t) = P(M_1) + P(M_2) + P(M_3) - P(M_1)P(M_2) - P(M_1)P(M_3) - P(M_2)P(M_3) + P(M_1)P(M_2)P(M_3) \quad (IV.D.1)$$

$$P_{TC}(S_1, t) = 1 - P_{TC}(S_2, t) \quad (IV.D.2)$$

$$R_{TC}(t) = P_{TC}(S_1, t) \quad (IV.D.3)$$

$$P(M_1) = 1 - \sum_{n=0}^{11} \frac{(112\lambda_a t)^n e^{-112\lambda_a t}}{n!} \quad (IV.D.5)$$

$$P(M_2) = 6 \sum_{m=4}^{17} (17 - m + 1) (1 - e^{-\lambda_a t})^m \quad (IV.D.8)$$

$$+ 2 \sum_{m=4}^5 (5 - m + 1) (1 - e^{-\lambda_a t})^m$$

$$P(M_3) = 3 - 10e^{-4\lambda_a t} + 8e^{-5\lambda_a t} - 10e^{-9\lambda_a t} + 9e^{-10\lambda_a t} \quad (IV.D.11)$$

The first two of these express, respectively, the probability of subsystem failure and success at any time,  $t$ . The third equation shows

that the reliability  $R_{TC}(t)$  of the subsystem is simply the probability that it is in state  $S_1$ . The last three equations express the probabilities that the subsystem is in each of the failure modes defined above. For more detailed definition of the notation derivation of the equations, etc., the reader is referred to Reference 1 (pp. 176-179).

b. Component Parts Complement of the Thermal Control Subsystem

The elements of the subsystem are identical to those of Reference 1, and, along with their associated failure rates, are tabulated below.

<u>Element</u>	<u>Failure Rate</u>
Insulating shield	0
Louver	$0.5 \times 10^{-6}/\text{hour}$
Pivots and bearings	$1.5 \times 10^{-6}/\text{hour}$
Bimetallic actuator	$1.0 \times 10^{-6}/\text{hour}$

It is well to note that the rates used in this assessment differ from those used in the preliminary assessment. The changes reflect the test experience thus far, and take into account the damage that may be inflicted during the launch phase due to dynamic and thermal stresses. In addition, the tabled failure rates apply to either closed or not closed failure.

c. Numerical Evaluation of State Probabilities and Reliability

Utilizing the failure rates and model equations of the preceding section, the desired quantities are determined by calculating, first, the failure rate  $\lambda_a$  of an individual louver/actuator; then the mode probabilities  $P(M_1)$ ,  $P(M_2)$ , and  $P(M_3)$ ; and finally  $P_{TC}(S_2, t)$  and  $P_{TC}(S_1, t)$ , which equals  $R_{TC}(t)$ .

In view of the modifications of the definitions of  $M_1$ ,  $M_2$ , and  $M_3$  and the tabulation of failure rates given in the preceding section, it follows that the  $\lambda_a$  to be used in calculating  $P(M_2)$  and  $P(M_3)$  is simply the sum of these rates; namely,

$$\lambda_a = \lambda_{\text{louver}} + \lambda_{\text{pivots and bearings}} + \lambda_{\text{actuator}} = 3.0 \times 10^{-6}.$$

Furthermore, since  $M_1$  includes both closed and not closed failures, the  $\lambda_a$  used in calculating  $P(M_1)$  should be double that used in calculating  $P(M_2)$  and  $P(M_3)$ ; i. e.,  $\lambda_a$  equals  $6.0 \times 10^{-6}$  in this case.

Substituting the appropriate value of  $\lambda_a$  in the key model equations yields the values shown in Exhibit 2. Not that calculations were carried out, as in Reference 1, for four operating times,  $t = 2190, 4380, 6570,$  and 8760 hours.

Comparing the values of  $R_{TC}(t)$  given in Exhibit 2 with the corresponding values derived in Reference 1 (cf. Exhibit IV.D-3, p. 182) reveals a general lowering of subsystem reliability. The primary reason for this is the increased value assigned to  $\lambda_a$ . The higher rate, as stated above, reflects test experience gained thus far in the OGO development program and takes into account the dynamic and thermal stresses to which the louver/actuators are subjected during launch.

#### 4. Strengths and Weaknesses of the Subsystem

The results of the louver bearing tests being performed by STL seem to indicate that the lubrication by  $\text{MoS}_2$  in vacuum will be sufficient for this application. It is estimated that the average louver will experience 10,000 cycles of operation over a 1-year period. The tests conducted thus far have demonstrated a louver bearing reliability, operating in hard vacuum with varying duty cycles, of approximately 0.99 with 95-percent confidence. The vibration tests of the bearings have not yet been completed.

The results of the louver vibration tests (Reference 7) indicate that considerable modification of the louvers themselves was incorporated to increase the structural rigidity of the louvers and the mounting brackets. Several failures occurred prior to the modification, but the modified louvers exhibited no failures during vibration. The major modifications to the louvers were (1) redesign of the louver ends to increase the rigidity at the connections to the pivot pins, (2) decrease of the spot-weld spacing



EXHIBIT 2 - CALCULATIONS SUMMARY.

<u>Time (hours)</u>	<u>P(M<sub>1</sub>)</u>	<u>P(M<sub>2</sub>)</u>	<u>P(M<sub>3</sub>)</u>	<u>P<sub>TC</sub>(S<sub>2</sub>, t)</u>	<u>P<sub>TC</sub>(S<sub>1</sub>, t)</u>	<u>R<sub>TC</sub>(t)</u>
2190	0	0	0.00455	0.00465	0.99535	0.995
4380	0.00005	0	0.01235	0.01230	0.98770	0.988
6570	0.00201	0.00001	0.02635	0.02832	0.97168	0.972
8760	0.01645	0.00004	0.03976	0.05619	0.94381	0.944

to 0.25 inch from 0.7 inch, and (3) redesign of the beaded edges of the louver to increase the section modulus and thereby the rigidity of the louver. The above discussion indicates that the louvers can be expected to have a reasonable probability of surviving the launch-phase vibration environment.

The use of the RTV filler material, Mylar tape on the bracketry, and the more accurate determination of material thermal properties and subsystem and experiment locations allow a more realistic heat balance analysis by STL. The more accurate the analysis, of course, the less likely are gross malfunctions of the subsystem such as the louver operating temperatures being "off" by a factor of  $10^0$ . This is evidenced by the decision to change the temperature operating settings of the -X side aft louver panel (i. e., column 7).

The most critical areas are still the areas over the battery packs and the 100-mw and 4-w transmitters. STL analyses indicate that temperatures of  $98^{\circ}\text{F}$  may be reached for the worst-case POGO orbit by the battery baseplates during orbital operation, and that  $98^{\circ}\text{F}$  may also be reached for periods of short duration (20 minutes) during and immediately after requisition in the EGO orbit. As stated earlier, it is felt that these results (based on considerations of the critical areas) further justify the retention of the PRC First Assessment failure modes and model equations.

5. Quantitative Assessment of Thermal Control Subsystem Under Tumbling Conditions

One of the subjects discussed during the NASA/PRC meeting held on 22 June 1962 at PRC was TAM No. 3 (cf. Reference 8). This TAM deals with the possibility of operating the spacecraft in a degraded mode in the event that attitude control and stabilization are lost and the spacecraft assumes a random tumbling condition. The TAM determined that sufficient power generation capability persists to allow operation in a degraded mode while the spacecraft is tumbling and that, if this degraded mode is of value, further study of the tumbling case--from a power supply viewpoint--is warranted.

During discussions at STL after issuance of the TAM and prior to the above-mentioned meeting at PRC, it was pointed out that the electronic assemblies of the spacecraft would become inoperable because of inadequate thermal control of a tumbling spacecraft. Specifically, proper control would not be possible because whenever the louvers were exposed to the sun they would open in an attempt to cool the spacecraft, thus exposing the electronic assemblies to direct sunlight.

Discussions held prior to and during the 22 June 1962 meeting at PRC, then, were directed toward the need, if any, to continue study of the tumbling case. One possibility is that a quantitative evaluation of the maximum steady-state temperature(s) assumed by the tumbling spacecraft might indicate the feasibility of continued operation of the necessary assemblies. Another possibility is that the design might incorporate a mechanism for snapping shut the louvers upon loss of attitude control and stabilization.<sup>1</sup> Both of these possibilities have been explored and are presented in the sequel.

To pursue the former possibility, assume a randomly tumbling spacecraft in a POGO orbit. Since the position of the spacecraft is random, the six surfaces will essentially face the sun an equal percentage of the time. The worst case occurs when the spacecraft is in full sun and one of the radiating panels is facing the sun and the other faces the earth. This is a severe condition because the exposed radiating panels present the largest area of relatively high solar absorptivity and exhibit a hemispherical infrared emissivity equal to that of the insulated surfaces. It seems reasonable to assume that attitude control failure would occur in such a way that no high moments would be imparted to the spacecraft; therefore, it can be considered to be tumbling very slowly, and a steady-state thermal analysis can be used as an approximation for the purpose of this investigation.

---

<sup>1</sup> Or, perhaps, a mechanism which would close the louvers whenever they are exposed to the sun, and otherwise allow them to operate normally.

A simple heat balance equation for the spacecraft is given by:

$$A_T \epsilon \sigma T^4 = Q_S + Q_{RS} + Q_E + Q_I ,$$

or,

$$T^4 = (Q_S + Q_{RS} + Q_E + Q_I) / \epsilon \sigma A_T$$

where

- $A_T$  = total area of the surface of the spacecraft in  $\text{ft}^2$
- $\epsilon$  = average emissivity of area  $A_T$
- $\sigma$  = Stefan-Boltzmann constant =  $1.734 \times 10^{-9} \text{ Btu/hr ft}^2 \text{ } ^\circ\text{R}^4$
- $T$  = average temperature of area  $A_T$  in degrees Rankine
- $Q_S$  = heat absorbed by spacecraft from solar radiation in Btu/hr
- $Q_{RS}$  = heat absorbed by spacecraft from solar radiation reflected from earth in Btu/hr
- $Q_E$  = heat absorbed by spacecraft from earth radiation in Btu/hr
- $Q_I$  = internal heat dissipation of spacecraft in Btu/hr

Each of the Q's is further defined as follows:

$$Q_S = A_S \alpha S ,$$

where

- $A_S$  = surface area of spacecraft exposed to sun in  $\text{ft}^2$
- $\alpha$  = average absorptivity of area  $A_S$
- $S$  = solar constant =  $443 \text{ Btu/hr ft}^2$

$$Q_{RS} \approx 2 A_E \alpha \beta S (1 - \cos \theta_0) D ,$$

where

- $A_E$  = surface area of spacecraft exposed to earth radiation  
in  $\text{ft}^2$   
 $a$  = average absorptivity of area  $A_E$   
 $\beta$  = albedo of earth = 0.34  
 $\theta_0$  = angle between the line joining the spacecraft to earth  
center and a line from the spacecraft to earth horizon  
 $D$  = 1 when earth's surface area seen by spacecraft is within  
sunlit hemisphere<sup>1</sup>  
 = 0 when earth's surface area seen by spacecraft is not  
within sunlit hemisphere

$$Q_E \approx 2 A_E \epsilon E (1 - \cos \theta_0) ,$$

where

- $\epsilon$  = average emissivity of surface area  $A_E$   
 $E$  = earth's thermal radiation constant =  $76.5 \text{ Btu/hr ft}^2$

$$Q_I = 410 \text{ Btu/hr}$$

where the value of 410 Btu/hr. is based on an average power dissipation of 120 watts.

The expressions for  $Q_S$  and  $Q_I$  are well known and need no further explanation;<sup>2</sup> however, the derivation of the expressions for  $Q_{RS}$  and  $Q_E$

<sup>1</sup> D essentially differentiates between the cases when the spacecraft is in eclipse and when it is not.  $Q_{RS}$  is zero in the former case, and otherwise follows the equation given.

<sup>2</sup> A trivial generalization of the expression for  $Q_S$  is used later on; namely, if the surface area exposed to the sun consists of, say, two areas  $S_1$  and  $S_2$  with corresponding average absorptivities  $a_1$  and  $a_2$  respectively, then  $Q_S$  is given by

$$Q_S = (a_1 A_{S_1} + a_2 A_{S_2}) S$$

may be of interest since they are not readily available. Furthermore, since the desired expressions are but particular cases of a more general situation, it is well to consider the general derivation. Exhibit 3 portrays the geometry underlying the general case. Here  $\theta$  represents the angle between the line joining the spacecraft to earth center and the line from the spacecraft to an element of earth surface area,  $dA$ . The incremental area  $dA$  lies within the area swept out as  $\theta$  varies between 0 and  $\theta_0$  (i. e., out to the earth horizon) and as the angle  $\gamma$  (measured, as shown in Exhibit 3, relative to any convenient coordinate system) varies between 0 and  $2\pi$ . The variable distance between the spacecraft and the incremental area is denoted by  $\rho$ .

Now, if  $J$  denotes the intensity of radiation (either earth radiation or solar radiation reflected from earth) at the earth's surface and  $\varphi$  denotes the radiant flux impinging upon the spacecraft, the incremental flux  $d\varphi$  impinging on the spacecraft, considered as a point receiver, from the incremental area  $dA$  is given by

$$d\varphi = \frac{J \rho \sin \theta \rho d\theta d\gamma}{\pi \rho^2}.$$

Integrating over the earth surface swept out by  $\theta$  and  $\gamma$  yields

$$\begin{aligned} \varphi &= \frac{J}{\pi} \int_0^{2\pi} \int_0^{\theta_0} \sin \theta d\theta d\gamma \\ &= 2 J (1 - \cos \theta_0) . \end{aligned}$$

Next, considering the spacecraft as a body having surface area  $A_E$  exposed to radiation from the earth's surface, the total flux received,  $\varphi_R$ , is approximately given by

$$\varphi_R = 2 J A_E (1 - \cos \theta_0) .$$

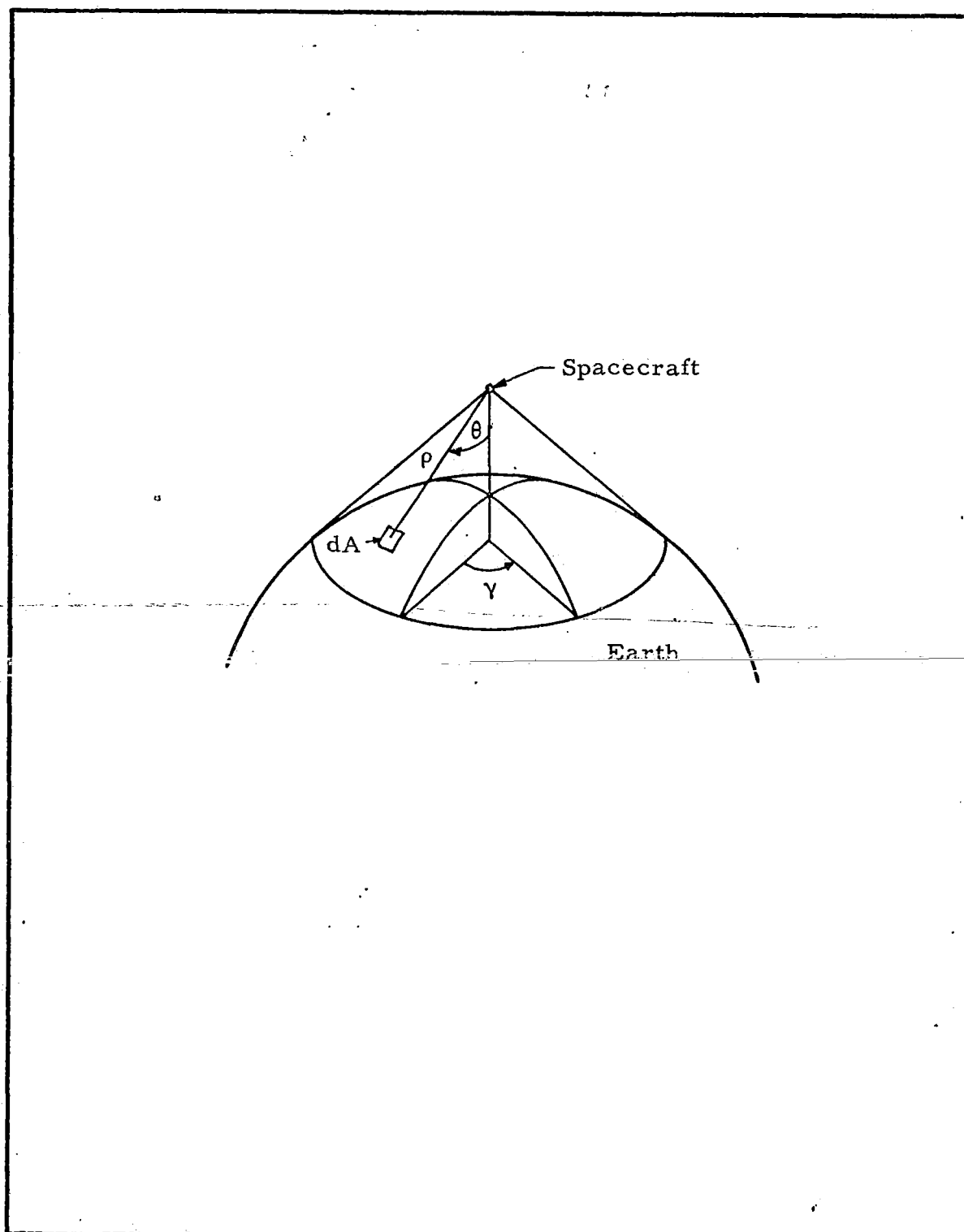


EXHIBIT 3 - GEOMETRY OF THE GENERAL CASE

From this expression the desired expressions for  $Q_{RS}$  and  $Q_E$  are readily derived, since  $J$  equals  $\alpha\beta S$  in the former case and  $\epsilon E$  in the latter. The addition of the factor  $D$  in the expression for  $Q_{RS}$  is clearly necessary to account for eclipses.

Next, utilizing the preceding expressions and assumptions, the spacecraft steady-state temperature  $T$  is calculated. Prior to calculating  $T$ , certain supporting calculations and input assignments must be accomplished.

First, the value of  $\cos \theta_0$  (i. e., cosine of the maximum value of  $\theta$ ) is determined. From Exhibit 4, which assumes that the average altitude of the spacecraft in a POGO orbit is 300 nautical miles,  $\cos \theta_0$  is calculated as follows:

$$\begin{aligned}\cos \theta_0 &= \cos (90^\circ - \cos^{-1} (4000/4300)) \\ &= \cos (90^\circ - \cos^{-1} 0.93) \\ &= 0.367\end{aligned}$$

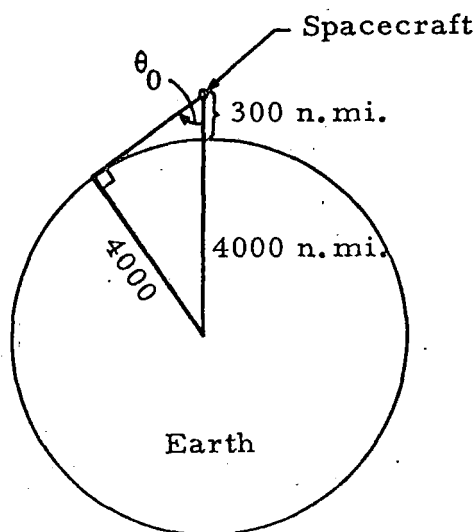


EXHIBIT 4 - GEOMETRY UNDERLYING CALCULATION OF  $\cos \theta_0$



Next, the values of  $\alpha$  and  $\epsilon$  are assigned as shown<sup>1</sup> below:

<u>Material</u>	<u><math>\alpha</math></u>	<u><math>\epsilon</math></u>
Mylar	0.32	0.8
Radiating panel	0.40	0.8

Finally, after determining the required numerical values of surface area, the spacecraft steady-state temperature is calculated as follows:

$$Q_S = [(10) (0.4) + (4.5) (0.32)] [443] \\ = 2409.9 \text{ Btu/hr}^{(2)}$$

$$Q_{RS} = 2 [(10) (0.4) + (4.5) (0.32)] [0.34] [443] [1 - .367] \\ = 1036.6 \text{ Btu/hr}^{(3)}$$

$$Q_E = 2 (14.5) (0.8) (76.5) (1 - .367) \\ = 1116.9 \text{ Btu/hr}$$

$$Q_I = 410 \text{ Btu/hr}$$

$$T^4 = \frac{(2409.9 + 1036.6 + 1116.9 + 410)}{(0.8) (1.734 \times 10^{-9}) (71.4)}$$

<sup>1</sup> The  $\alpha$  for a radiating panel degrades to approximately 0.4 after a 50-day exposure to the sun.

<sup>2</sup> Here the generalization of  $Q_S$  mentioned in a preceding footnote is used. Note also that the radiating panel surface area exposed to the sun is 10 ft<sup>2</sup> and the Mylar-covered area exposed to the sun is 4.5 ft<sup>2</sup>.

<sup>3</sup> Note the use of a generalization of  $Q_{RS}$  similar to that used for  $Q_S$ .

$$T = \left( \frac{4973.4}{9.88 \times 10^{-8}} \right)^{1/4}$$

$$= 474^{\circ}\text{R}$$

$$= 14^{\circ}\text{F}$$

It is important, at this juncture, to point out that in the above calculations of steady-state temperature of the spacecraft surface it was assumed that the spacecraft is tumbling very slowly, and the louvers were assumed to be open at all times.<sup>1</sup> The resulting temperature of 14°F, then, indicates that adequate thermal control could possibly be attained.

Now, since 14°F represents the average temperature of the spacecraft surface, an important next step in the analysis is to calculate the local temperature under the same conditions at, say, a suspected "hot spot" on the spacecraft surface. Such calculations would be unnecessary if the 14° were higher than maximum allowable temperature specified.

Two likely "hot spots" are the radiating panel areas directly over the battery packs and the transmitters. The local temperature over a battery pack will be investigated since (1) each battery pack is a critical spacecraft component and (2) it is likely that little, if any, heat received from the sun's radiation will be conducted away by the radiating panel (due, as discussed below, to the need to conduct away the heat generated by the packs themselves) over the pack.

Consider, now, the heat-conducting capability of the radiating panel over the battery pack. The heat,  $Q_C$ , that can be conducted away from the battery packs by this panel is approximately given by

$$Q_C = P_B \cdot t \cdot K ,$$

---

<sup>1</sup> This assumption is implied by the values of the radiating panel surface area and solar absorptivity used in the calculations.

where

- $P_B$  = perimeter (measured in ft) of the battery pack surface affixed to the radiating panel
- $t$  = thickness of the radiating panel (in ft)
- $K$  = conductivity of the radiating panel (in Btu/hr ft<sup>2</sup> °F/ft)  
= 90 Btu/hr ft<sup>2</sup> °F/ft for 2014 aluminum

Calculating  $Q_C$  yields

$$\begin{aligned} Q_C &= (3.08) (0.00375) (90) \\ &= 1.04 \text{ Btu/hr } ^\circ\text{F/ft} . \end{aligned}$$

Since the maximum heat output from the battery pack is on the order of 35 Btu/hr, it follows that, if this heat output were dissipated solely by conduction through the radiating panel, the necessary temperature differential in the panel would have to be approximately 36<sup>°</sup>F/ft. It is evident, therefore, that the radiating panel's conducting capability could be fully utilized to conduct away the heat output from the battery pack.

Thus, optimistically assuming that this is possible, and assuming also that the radiating panel must dissipate (by radiation) the heat received from the sun,<sup>1</sup> the panel's steady-state temperature can be calculated using the expressions developed above; viz,

$$\begin{aligned} T^4 &= Q_S / \epsilon \sigma A_S = A_S a S E \sigma A_S \\ &= a S / \epsilon \sigma \\ &= (0.4 \times 443) / (0.8) (1.73 \times 10^{-9}) \end{aligned}$$

---

<sup>1</sup> That is, considering only  $Q_S$  or, equivalently, ignoring  $Q_{RS}$  and  $Q_E$  and setting  $Q_I$  equal to 0 because of the assumption that the battery pack heat output is conducted away.

$$\begin{aligned}
 T &= (1.279 \times 10^{11})^{1/4} \\
 &= 598^{\circ}\text{R} \\
 &= 138^{\circ}\text{F}
 \end{aligned}$$

Therefore, the battery baseplate temperature is considerably above the temperature ( $125^{\circ}\text{F}$ ) at which the batteries become inoperative.

Although the above calculations represent very rough approximations, it seems reasonable to conclude that loss of attitude control would, after a reasonably short time, result in loss of the spacecraft in the sense that useful information could no longer be obtained. It is re-emphasized that this conclusion is based on a macroscopic examination of a single hot spot (i. e., the battery pack) and on the assumption of a slowly tumbling spacecraft. Steps to remove this hot spot problem could be taken; however, this approach would necessitate the elimination, if possible, of all remaining problem hot spots.

As regards the rate of tumbling, it appears that if this rate were increased (accidentally or deliberately) the likelihood of an acceptable thermal condition would be much greater. However, evaluation of this situation would require a thorough dynamic heat balance analysis, which, at this time is of questionable value to the OGO program.

A brief investigation of the second possibility mentioned earlier (i. e., incorporation of a special mechanism for closing louvers upon loss of attitude stabilization and control) leads to the conclusion that this is infeasible considering the many constraints (e. g., maximum weight) imposed on the spacecraft design. Indeed, it appears that the introduction of a mechanism which would preserve the independence of the louvers, while still providing the necessary override when needed, would be difficult to implement, and would prohibitively increase the weight of the spacecraft. On the other hand, introduction of an override mechanism that groups all the louvers in a panel is relatively easy to implement; however, it would negate the existing desirable characteristics (e. g., independence) of the louver design.

5. Summary

THE FOLLOWING PRIMARY FINDINGS (OVER THOSE ALREADY DISCUSSED IN REFERENCE 1) CAN BE REPORTED AS A RESULT OF SECOND ASSESSMENT RELIABILITY STUDY OF THE OGO THERMAL CONTROL SUBSYSTEM:

a. DESCRIPTION OF THE SYSTEM HAS CHANGED IN SOME SPECIFIC AREAS. THE CHANGES ARE NOTED IN THIS TAM.

b. PRC HAS MODIFIED THE ORIGINAL MODES OF FAILURE, BASED ON CONSIDERATIONS OF THE DIFFERENCES IN THE EFFECTS ON THE SUBSYSTEM ARISING FROM A "STUCK CLOSED" LOUVER/ACTUATOR AND FROM A "NOT CLOSED" ONE. THESE MODIFICATIONS ARE ALSO REPORTED HEREIN.

c. COMPONENT PART FAILURE RATES HAVE BEEN INCREASED TO ACCOUNT FOR THE EFFECTS OF THE LAUNCH ENVIRONMENT AND TO REFLECT THE LATEST TEST RESULTS. THE REVISED FAILURE RATES ARE GIVEN IN THIS TAM.

d. THE ABOVE CHANGES RESULT IN A SECOND ASSESSMENT RELIABILITY ESTIMATE FOR THE THERMAL CONTROL SUBSYSTEM OF 0.944 (FOR 1 YEAR OF OPERATION)..

e. THE CRITICAL AREAS REMAINING IN THE SUBSYSTEM ARE DISCUSSED; THESE ARE THE BATTERY PACKS, THE TWO 100-MW TRANSMITTERS, AND THE TWO 4-W TRANSMITTERS.

f. A SPECIAL QUANTITATIVE ANALYSIS TO DETERMINE THE INTERFACE EFFECTS BETWEEN THE POWER SUPPLY SUBSYSTEM, IN THE EVENT OF LOSS OF ATTITUDE STABILIZATION AND CONTROL, IS REPORTED IN THIS TAM. THE RESULTS OF THIS PRELIMINARY INVESTIGATION INDICATE THAT LOSS OF ATTITUDE CONTROL WOULD SOON NEGATE THE POSSIBILITY OF OBTAINING USEFUL EXPERIMENT INFORMATION.

## REFERENCES

1. Preliminary Reliability Assessment for the Orbiting Geophysical Observatories (Section IV.D), Planning Research Corporation, R-243, 1 February 1962.
2. OGO Program Monthly Progress Report, 16 January - 15 February 1962, Space Technology Laboratories, 2311-6008-CU-000, 28 February 1962.
3. OGO Louver System Reliability, Space Technology Laboratories, 62-9700.3-28, 9 April 1962.
4. Reliability Model for OGO Louver System, Space Technology Laboratories, 62-9700.3-21, 16 March 1962.
5. Inputs for OGO Louver System Reliability Assessment Plan, Space Technology Laboratories, 9723.1-31, 19 March 1962.
6. Inputs for OGO Louver System Reliability Assessment Plan, Amendment I, Space Technology Laboratories, 9723.1-38, 30 March 1962.
7. Louver Vibration Test Results, Space Technology Laboratories, 9715.1-50, 5 June 1962.
8. Determination of Average Power Generated by Solar Cells Under Conditions of Random Tumbling of the Spacecraft, Planning Research Corporation, Technical Advisement Memorandum No. 3, 1962.
9. Strengths of Metal Aircraft Elements, Armed Forces Supply Support Center, MIL-HDBK-5, March 1961.
10. Solar Array Temperature--Revision, Space Technology Laboratories, 2318-6005-MU-000, 23 January 1962.
11. Gerhard Heller (ABMA), "Thermal Control of Explorer Satellites," American Rocket Society Journal, Vol. 30, No. 4, April 1960.
12. F. G. Cunningham (NASA, GSFC), Power Input to a Small Flat Plate From a Diffusely Radiating Sphere, With Application to Spherical Satellites, TN D-1099, October 1961.
13. F. G. Cunningham (NASA, GSFC), Earth Reflected Solar Radiation Input to Spherical Satellites, TN D-1099, October 1961.

14. E. C. Hastings, Jr., R. E. Turner, and K. C. Spugle (NASA, LRC), Thermal Design of Explorer XIII Micrometeoroid Satellite, TN D-1001, May 1962.
15. OGO Spacecraft Restraints on Launch Vehicle and Launch Stand Operation, Revision I, Space Technology Laboratories, 2311-0015-RU-001, 3 May 1962.
16. OGO Program Monthly Progress Reports, Space Technology Laboratories, January 1962 through June 1962.
17. Various thermal control subsystem specifications and drawings, Space Technology Laboratories.

TECHNICAL ADVISEMENT MEMORANDUM NO. 6

SECOND RELIABILITY ASSESSMENT FOR  
THE OGO STRUCTURE SUBSYSTEM



# TABLE OF CONTENTS

	<u>Page</u>
1. Subsystem Description . . . . .	1
a. General . . . . .	1
(1) Interstaging Function . . . . .	1
(2) Appendage Deployment . . . . .	2
(3) Appendages . . . . .	2
b. Detailed Assumptions . . . . .	2
2. Modes of Failure . . . . .	2
3. Numerical Assessment . . . . .	2
a. Model Equations . . . . .	2
b. Component Parts Complement of the Structure Subsystem . . . . .	3
c. Calculations . . . . .	4
4. Strengths and Weaknesses of the Subsystem . . . . .	4
a. STL Specifications . . . . .	4
b. STL Test Reports . . . . .	6
(1) OGO Boom Hinge Deployment Tests, Deployment Test of OGO Single Element Straight Boom (EP-1), and Proof Test of Boom Deployment Springs . . . . .	6
(2) OGO Deployment Release Mechanism Test . . . . .	7
(3) OGO Panel Development Tests and Various Structural Drawings . . . . .	7
5. Summary . . . . .	7
References . . . . .	9

## TECHNICAL ADVISEMENT MEMO NUMBER 6

To: Assistant OGO Project Manager, GSFC, NASA  
From: PRC OGO Assessment Team  
Subject: Second Reliability Assessment for the OGO Structure Subsystem

### 1. Subsystem Description

#### a. General

For a description of the Structure Subsystem the reader is referred to PRC R-243, Preliminary Reliability Assessment for the Orbiting Geophysical Observatories (Reference 1). In individual cases where the description of the present configuration differs significantly from that of Reference 1, the latest configuration will be described below in a paragraph designated to correspond to an identically numbered paragraph of Subsection E, Section IV, Reference 1.

#### (1) Interstaging Function

The description of the interstaging function now differs in that the active elements which release the clamp have been changed from double-ended explosive bolts to hermetically sealed release mechanisms actuated by redundant explosive charges. Two advantages accrue from this change, (a) the outgassing problem associated with the explosive bolts is relieved and (b) the redundant charges in the hermetically sealed mechanism are arranged so that in the case of the failure of one bridge wire and a low order detonation of the other charge (the primary cause of failure for ordnance devices), the charge with the failed bridge wire may be detonated by the low order detonation of the second charge. This allows one combination of "degraded" events leading to successful separation of the clamp which did not exist with the explosive bolts.

(2) Appendage Deployment

The description of the gas-actuated appendage release mechanism portion of the appendage deployment system has changed. The latest version was described in Technical Advisement Memorandum No. 5, which will be bound herewith in the Second Assessment final report.

(3) Appendages

The description of the appendages has changed in that the antennas have been arranged so that they do not require the three extra hinge joints described in Reference 1. Thus, the total number of deployment hinges to be considered now is 17.

b. Detailed Assumptions

(1) Interstaging Function

The first assumption of Reference 1 has been deleted.

2. Modes of Failure

The possible modes of failure have been changed to the following:

- a. The interstaging function can fail if both hermetically sealed release mechanisms fail or if the remainder of the staging system fails.
- b. The appendage deployment operation can fail if either deployment release assembly fails. Each assembly can fail in the following modes:

- Both gas bottles fail
- Both explosive valves fail
- Any double-ended release latch associated with one boom fails
- Any boom fails to deploy

3. Numerical Assessment

a. Model Equations

Only those model equations which have changed since the preliminary assessment are presented on the next page:

$$P_s(S_1) = P(\text{Interstaging Function}) P(\text{Basic Structure}) P(\text{Appendage Deployment}) \quad (\text{IV.E.2})$$

$$P(\text{Interstaging Function}) = \left\{ 1 - \left[ 1 - P(\text{Release Mechanism}) \right]^4 \right\} \left\{ P(\text{Remainder of Staging System}) \right\} \quad (\text{IV.E.4})$$

$$P(\text{Appendage Deployment}) = P(\text{Release Assembly "A"}) P(\text{Release Assembly "B"}) P(\text{Hinges}) \quad (\text{IV.E.5})$$

$$P(\text{Appendage Deployment}) = \left\{ 2P(V)Q(V)P(L)^6 + P(V)^2[1-Q(L)^2]^6 \right\}^2 \left\{ 17P(\text{Joint}) [1-Q(\text{Spring})^2] \right\} \quad (\text{IV.E.6})$$

where: (V) is an explosive valve

(L) is a single end of a double-ended release latch

Delete: (IV.E.7), (IV.E.8), (IV.E.9), and (IV.E.10)

#### b. Component Parts Complement of the Structure Subsystem

The component parts complement of the subsystem and their failure probabilities are as follows:

<u>Component Part</u>	<u>Number of Parts</u>	<u>Failure Probability<sup>1</sup></u>
Release Latch (One End)	24	0.007
Mechanical Joint	17	0.0004
Torsion Spring	34	0.0004
Explosive Valve	4	0.008
Sealed Release Mechanism (One charge)	4	0.05
Remainder of Staging System	1	0.005
Basic Structure	1	0.001

<sup>1</sup> These will be recognized as the failure probabilities used by STL in their assessment of OGO Reliability. As explained in PRC's Progress Report for the period ending 15 April 1962, STL's failure rates for structural items are being adopted by PRC until such time as test results, stress analysis, etc., may indicate that revision is desirable. Adoption of STL's larger failure rates was motivated primarily by the inclusion in this assessment of the effects of launch phase dynamics.

c. Calculations

The calculated probabilities of success are listed below. Recalling the detailed assumptions for this subsystem, it is seen that the probabilities remain the same throughout the mission time, and subsystem reliabilities versus time need not be presented.

<u>Item</u>	<u>Symbol</u>	<u>Probability of Success</u>
Interstaging	$P(\text{Interstaging Function})$	0.995
Basic Structure	$P(\text{Basic Structure})$	0.999
Appendage Deployment Operation	$P(\text{Appendage Deployment})$	0.991
Structure Subsystem	$P_s(S_1)$	0.985

4. Strengths and Weaknesses of the Subsystem

Additional findings (over those of Reference 1) concerning the strengths and weaknesses of the structures subsystem are drawn entirely from review of STL specifications and reports.

a. STL Specifications

(1) The following STL Specifications have been reviewed:

<u>STL Number</u>	<u>Revision</u>	<u>Date</u>	<u>Title</u>
D13357	A	7/27/61	Specification Spacecraft/Launch Vehicle Interface OGO
D13360		12/5/61	Specification Structure Subsystem OGO
D13361		1/24/62	Specification Basic Frame OGO
D13362		1/29/62	Specification Solar Array Structure OGO
D13363		2/2/62	Specification OPEP Support OGO
D13364		1/24/62	Specification Folding Devices OGO

<u>STL Number</u>	<u>Revision</u>	<u>Date</u>	<u>Title</u>
D13351	A	1/16/62	Specification Environmental Design Qualification Test Electronic and Mechanical Assemblies OGO
D13353		6/1/62	Environmental Type Test OGO/Spacecraft
		12/28/61	Preliminary Environmental Test Levels for OGO Experiments

(2) The conclusions drawn from the review of the above specifications and Reference 9, are as follows:

- If Reference 2 accurately predicts the maximum acceleration, shock and vibration loads, then the specifications and qualification test requirements adequately provide for the design of a highly reliable structure subsystem. This conditional conclusion is drawn by PRC although an acceleration test is not included, nor its exclusion justified, in the Environmental Type Test. It is PRC's judgment that the exclusion of the acceleration test is a low order risk.

- It is certain that variations around the maximum acceleration, shock and vibration loads called out in Reference 2 will exist with some, hopefully small, but finite probability of occurrence.

- The above conclusion notwithstanding, it is felt, that the two environmental qualification test specifications, D13351 and D13353, are sufficiently severe to adequately define most significant structural problem areas during the performance of the prescribed tests, if these problem areas have not already been located during the development testing.

(3) During study of these specifications, the need for consideration of unexpected load variation became apparent. Hence, as an aid to quantitative prediction of the probability of occurrence of damage due to unexpected loads, an approach to a methodology for predicting the probability of occurrence of unexpected loads has been formulated and will be developed and applied during the third assessment.

b. STL Test Reports

The results of reviewing available STL development test reports are presented below:

- (1) OGO Boom Hinge Deployment Tests (Reference 3),  
Deployment Test of OGO Single Element Straight Boom  
(EP-1) (Reference 4) and Proof Test of Boom Deploy-  
ment Springs (Reference 5)

- The design of the boom deployment hinges and springs appears to be adequate.

- With the looped cable method (the STL selected method) it appears from the test results that, in all cases, deployment could be accomplished with a single power spring at each hinge. Discussions with the responsible STL engineers, however, indicate that they are reluctant to go to one spring per hinge because they fear that the loss of the two spring redundancy and the torque safety margin might raise difficulties with the 40-wire cables at the 0° C temperature. It is felt by PRC, however, that this possibility should be further investigated, since the springs can be shown to exhibit at least 0.9993 reliability with 95 percent confidence at ambient temperatures and little loss of reliability may result at the low temperature. Now, if only one spring with 0.9993 reliability is substituted in each of the 17 hinge joints and  $P(\text{Appendage Deployment})$  is computed on this basis, it is found that  $P(\text{Appendage Deployment}) = .0982$ , rather than the previous 0.991. The over-all effect on the Structure Subsystem reliability is to reduce  $P_g(S_1)$  to 0.976 rather than 0.985. In view of the fact that this approach would allow a weight decrease of approximately two pounds, the modest decrease in reliability may prove to be an acceptable risk.

- In lieu of the above recommendations, if it is preferred to retain two springs per hinge, it is suggested that the spring design be optimized for each hinge type when the final selection of wire size is firm. Such optimization will result in a nonnegligible weight savings.

(2) OGO Deployment Release Mechanism Test (Reference 6)

- The results of this test indicate that the deployment release mechanism is adequately designed and, although galling and deformation occurred after 90 to 100 actuations, these wearout phenomena can be expected to have little effect on the reliability for one actuation. Thus, a high reliability can be expected.

(3) OGO Panel Development Tests (References 7 and 8), and Various Structural Drawings

From the review of this information, the following expected problem areas have been defined on the basis of experience and engineering judgment:

- It is felt that vibration inputs to the spacecraft during the launch phase will very likely be transmitted through the experiment mounting panels at levels which will expose the experiment packages to acceleration levels higher than their design specifications require. Several approaches to relieving this problem exist and will be analyzed if this situation is verified during testing.

- It is considered possible that the vibration levels experienced by the folded solar arrays during the launch phase will be high enough to cause damage to the arrays due to large elastic excursions. The most probable failure mode is expected to be the loosening or damaging of the solar cells due to twisting or bowing of the substrates. As with the experiment panels, several avenues of approach to the solution of the problem exist and will be studied if the problem is verified by testing.

- It would be unwise to apply solutions to these problems before the problems themselves are verified, since the solutions will invariably result in a weight penalty.

5. SUMMARY

TO SUMMARIZE, THE FOLLOWING PRIMARY FINDINGS (OVER THOSE ALREADY REPORTED IN REFERENCE 1 AND IN TAM NO. 5) CAN BE REPORTED AS A RESULT OF SECOND ASSESSMENT RELIABILITY STUDY OF THE OGO STRUCTURE SUBSYSTEM:



a. DESCRIPTION OF THE SUBSYSTEM HAS CHANGED TO SOME EXTENT. THESE CHANGES ARE STATED IN THIS TAM.

b. PRC HAS MADE SOME CHANGES IN MODES OF FAILURE. THESE ARE ALSO REPORTED IN THIS TAM.

c. CHANGES IN THE SUBSYSTEM HAVE NECESSITATED SOME CHANGES IN THE MODEL EQUATIONS AND PARTS COMPLEMENTS. THESE ARE GIVEN IN THIS TAM.

d. THE ABOVE CHANGES, COMBINED WITH ADOPTION OF STL'S HIGHER FAILURE RATES FOR STRUCTURAL PARTS, RESULT IN A SECOND ASSESSMENT RELIABILITY ESTIMATE FOR THE STRUCTURE SUBSYSTEM OF 0.985.

e. REVIEW OF STL SPECIFICATIONS, DRAWINGS, AND TEST REPORTS INDICATE THAT A HIGHLY RELIABLE STRUCTURE SUBSYSTEM MAY BE EXPECTED. HOWEVER, POSSIBLE PROBLEM AREAS HAVE BEEN IDENTIFIED, WITH THE PROBLEMS RESULTING FROM LAUNCH AND BOOST INDUCED VIBRATIONS. THESE PROBLEMS MAY EXIST IN THE EXPERIMENT MOUNTING PANELS AND THE SOLAR ARRAYS.

f. A WEIGHT SAVING OF ABOUT TWO POUNDS MAY BE REALIZED BY ELIMINATING REDUNDANT HINGE SPRINGS. PRELIMINARY INVESTIGATIONS INDICATE THAT A REDUCTION IN SUBSYSTEM RELIABILITY FROM 0.985 TO ABOUT 0.976 WOULD RESULT.

## REFERENCES

1. Preliminary Reliability Assessment for the Orbiting Geophysical Observatories, PRC R-243, 1 February 1962.
2. Estimated Shock, Acceleration and Vibration Environments for Atlas-Agena B and Thor-Agena B Spacecraft, AGENA-SAV-1, NASA, Revised 1 August 1961 by G. D. Hinshelwood.
3. OGO Boom Hinge Deployment Tests, 9711.1-33, STL, 8 December 1961.
4. Deployment Test of OGO Single Element Straight Boom, 9711.1-3, STL, 8 January 1962.
5. Proof Test of Boom Deployment Springs, 62-9711.1-9, STL, 8 February 1962.
6. Test Report OGO-D19-4, OGO Deployment Release Mechanism Test, 9521.18-17, 2319-6006-MU-000, STL, 27 February 1962.
7. OGO Panel Development Tests, 2319-0003-MU-001, STL, 22 November 1961.
8. OGO Panel Development Tests, 2319-6009-MU-000, 23 March 1962.
9. Detailed Test Plan for Vibration Survey of the OGO Spacecraft and Interstage-Structural Model, 2319-6011-RU-000, STL, 26 March 1962.

TECHNICAL ADVISEMENT MEMORANDUM NO. 13

OGO SPACECRAFT  
SYSTEM RELIABILITY

## TABLE OF CONTENTS

	<u>Page</u>
1. Summary . . . . .	1
2. FOM and Classifical Reliability Evaluations . . . . .	1

## LIST OF EXHIBITS

	<u>Page</u>
1. List of Defining Subsystem 4-tuples and Relative Values for Each System State . . . . .	3
2. Subsystem State Probabilities Summary . . . . .	5
3. System State Probabilities and Classical System Reliabilities for Each Mission Time . . . . .	6
4. Graph of $V(t)$ , Spacecraft FOM System Reliability . . . . .	7
5. Graph of $\bar{V}(\tau)$ , Spacecraft Time-Averaged FOM System Reliability . . . . .	8
6. Graph of $R(t)$ , Spacecraft Classical System Reliability . . . . .	10

## TECHNICAL ADVISEMENT MEMORANDUM NO. 13

To: Assistant OGO Project Manager, GSFC, NASA  
From: PRC OGO Assessment Team  
Subject: OGO Spacecraft System Reliability

### 1. Summary

This TAM presents the results of the second assessment of OGO spacecraft system reliability. In Section 2 the figure-of-merit (FOM) and classical system reliability model formulations established in the first assessment report, PRC R-243, will be restated, and the numerical evaluations of spacecraft system reliability conducted from the two points of view will be presented.

### 2. FOM and Classical Reliability Evaluations

The basic FOM formulation derived in R-243 is that of the expected relative value,  $V(t)$ , of spacecraft performance. This expresses the value that can be expected from an average OGO mission's experimental information from an initial time point to any given one,  $t$ , relative to the value that would be obtained if no spacecraft equipments failed to this time  $t$ . The degraded expectation thus arises from the probabilities of spacecraft equipments failing.

The defining equation is

$$V(t) = \sum_{i=1}^M P(S_i, t) V(S_i, t) \quad , \quad (1)$$

where  $M$  = the number of possible equipment states of the spacecraft  
 $P(S_i, t)$  = the probability that spacecraft system state  $S_i$  will occur at time  $t$

$V(S_i, t)$  = the relative value of the spacecraft's output at time  $t$  (or, rather, a small time interval about  $t$ ) given that it is in state  $S_i$  at that time. This relative value is the ratio of the output value (as appropriately defined, e.g., the number of performable experiments) of the spacecraft in state  $S_i$  to this value in the perfect state

As in the first assessment,  $V(S_i, t)$  is now defined as

$$V(S_i, t) = n_i / N \quad , \quad (2)$$

where  $N$  is the total number of experiments performable in the perfect state, and  $n_i$  is the number of experiments performable in system state  $S_i$ . The values of  $n_i/N$  used in the numerical assessments to follow are listed in Exhibit 1.

The state probability  $P(S_i, t)$  is written, also as in the first assessment, as the product of certain subsystem state probabilities:

$$P(S_i, t) = .985 P_{CDH}(S_{i_1}, t) P_{ACS}(S_{i_2}, t) P_{PS}(S_{i_3}, t) P_{TC}(S_{i_4}, t) \quad . \quad (3)$$

Here CDH denotes the Communications and Data Handling Subsystem, ACS the Attitude Control and Stabilization Subsystem, PS the Power Supply Subsystem, and TC the Thermal Control Subsystem. Structure Subsystem reliability is taken as a constant value of .985, reflecting only launch failure possibilities and assuming that it then remains in the initial state during the remainder of the mission, except with negligible probability.

The subscripts on the  $i$ 's denote the components of the index 4-tuples  $(i_1, i_2, i_3, i_4)$  that represent the subsystem state combinations giving each system state. These correspondencies are also listed in Exhibit 1.

EXHIBIT 1 - LIST OF DEFINING SUBSYSTEM 4-TUPLES AND  
RELATIVE VALUES FOR EACH SYSTEM STATE

System State Index, i	Subsystems 4-Tuple	State Relative Value, $n_i/N$
1	(1, 1, 1, 1)	1
2	(2, 1, 1, 1)	39/40
3	(3, 1, 1, 1)	39/40
4	(4, 1, 1, 1)	9/10
5	(5, 1, 1, 1)	9/10
6	(6, 1, 1, 1)	7/8
7	(7, 1, 1, 1)	13/15
8	(8, 1, 1, 1)	4/5
9	(9, 1, 1, 1)	4/5
10	(10, 1, 1, 1)	11/15
11	(11, 1, 1, 1)	7/10
12	(12, 1, 1, 1)	7/10
13	(13, 1, 1, 1)	7/10
14	(14, 1, 1, 1)	2/3
15	(15, 1, 1, 1)	3/5
16	(16, 1, 1, 1)	3/5
17	(17, 1, 1, 1)	3/5
18	(18, 1, 1, 1)	3/5
19	(19, 1, 1, 1)	3/5
20	(20, 1, 1, 1)	11/30
21	(21, 1, 1, 1)	11/30
22	(22, 1, 1, 1)	8/15
23	(23, 1, 1, 1)	1/2
24	(24, 1, 1, 1)	1/2
25	(25, 1, 1, 1)	7/15
26	(26, 1, 1, 1)	2/5
27	(27, 1, 1, 1)	1/5
28	All Others	0



Since output value is effectively zero if any of the subsystems except the CDH is in other than a perfect state, only the various degraded states of the CDH subsystem give rise to degraded states of interest for the system. The probabilities of such system states are, therefore, the products of the probabilities that the ACS, PS, and TC Subsystems are in their satisfactory (non-zero output producing) states times the probability of occurrence of each of the 28 CDH states (the last of which is the dead state). These subsystem state probabilities are listed in Exhibit 2. The system state probabilities to which they give rise upon multiplication according to Equation (3), as has been discussed, are listed in Exhibit 3.

Finally, the results of computing  $V(t)$  from Equation (1) for four values of time  $t$  during the mission form the base points for the interpolated graph of  $V(t)$  in Exhibit 4.

A second figure-of-merit is the time average of the expected relative value,  $\bar{V}(\tau)$ . In a mission time interval of length  $\tau$ ,

$$\bar{V}(\tau) = \frac{1}{\tau} \int_0^{\tau} V(t) dt \quad . \quad (4)$$

Its merits are also discussed in R-243. It is graphed in Exhibit 5 from a numerical integration,  $V(t)$ , given in Exhibit 4.

The classical spacecraft reliability measure  $R(t)$ , the probability that the spacecraft will be in a "satisfactory state" at time  $t$ , is obtainable by simply defining the meaning of "satisfactory state," in terms of the  $S_i$  that have been listed, and then adding the probabilities that the system will be in each such state. This gives as a sum the probability that the system will be in some satisfactory state; i. e., its reliability in the classical sense.

As in R-243, satisfactory system states are here selected to be those corresponding to the CDH subsystem's being in one of its first 14 states, and the remaining subsystems' being in their individual

# EXHIBIT 2 - SUBSYSTEM STATE PROBABILITIES SUMMARY

Communications and Data Handling State Probabilities, $P_{CDH}(S_{i_2}, t)$				
$i_1$	Time (hours)			
	2190	4380	6570	8760
1	.77222	.44296	.21424	.09300
2	.00547	.00879	.00734	.00465
3	.01172	.01856	.01579	.01011
4	.00089	.00131	.00111	.00042
5	.00626	.00999	.00835	.00532
6	.00927	.01493	.01259	.00804
7	.00412	.00614	.00509	.00320
8	.11395	.22528	.23896	.19127
9	.00365	.00585	.00488	.00310
10	.00004	.00013	.00016	.00014
11	.00036	.00142	.00242	.00263
12	.00251	.01051	.01758	.01971
13	.00371	.01555	.02606	.02918
14	.00158	.00657	.01096	.01222
15	.00003	.00085	.00054	.00030
16	.00148	.00618	.01035	.01182
17	.00013	.00118	.00296	.02873
18	.00004	.00031	.00079	.00119
19	.00009	.00074	.00187	.00280
20	.00006	.00050	.00125	.00187
21	.00009	.00074	.00186	.00277
22	.00002	.00015	.00039	.00059
23	.00005	.00047	.00117	.00176
24	.00008	.00070	.00174	.00260
25	.00003	.00029	.00073	.00110
26	.00001	.00011	.00026	.00039
27	.00056	.00096	.00087	.00069
28 <sup>(1)</sup>	.06158	.21883	.40969	.56040

Attitude Control and Stabilization State Probabilities, $P_{ACS}(S_{i_2}, t)$				
$i_2$	Time (hours)			
	2190	4380	6570	8760
1	.338	.153	.068	.028
2 <sup>(1)</sup>	.662	.847	.932	.972

Power Supply State Probabilities, $P_{PS}(S_{i_3}, t)$				
$i_3$	Time (hours)			
	2190	4380	6570	8760
1	.9926	.9738	.9413	.9095
2 <sup>(1)</sup>	.0074	.0262	.0587	.0905

Thermal Control State Probabilities, $P_{TC}(S_{i_4}, t)$				
$i_4$	Time (hours)			
	2190	4380	6570	8760
1	.995	.988	.972	.944
2 <sup>(1)</sup>	.005	.012	.028	.056

Note: (1) Subsystem failure states.

EXHIBIT 3 - SYSTEM STATE PROBABILITIES AND CLASSICAL  
SYSTEM RELIABILITIES FOR EACH MISSION TIME

System State Index, i	System State Probabilities, $P(S_i, t)$			
	Time, t (hours)			
	2190	4380	6570	8760
1	.24641	.06213	.01274	.00220
2	.00175	.00123	.00044	.00011
3	.00374	.00260	.00094	.00024
4	.00028	.00018	.00006	.00001
5	.00200	.00140	.00050	.00013
6	.00295	.00209	.00075	.00019
7	.00132	.00086	.00030	.00008
8	.03636	.03160	.01421	.00452
9	.00117	.00082	.00029	.00008
10	.00001	.00002	.00001	--
11	.00011	.00019	.00014	.00006
12	.00030	.00147	.00104	.00047
13	.00096	.00218	.00155	.00068
14	.00050	.00092	.00065	.00029
15	.00001	.00012	.00003	.00001
16	.00047	.00086	.00062	.00028
17	.00004	.00016	.00017	.00068
18	.00001	.00004	.00004	.00003
19	.00003	.00010	.00011	.00006
20	.00002	.00007	.00007	.00004
21	.00003	.00010	.00011	.00006
22	.00001	.00002	.00002	.00001
23	.00002	.00006	.00006	.00004
24	.00003	.00010	.00011	.00006
25	.00001	.00004	.00004	.00002
26	.00000	.00001	.00001	.00001
27	.00018	.00013	.00005	.00002
28 <sup>(1)</sup>	.70078	.89050	.96494	.98962
Classical System Reliability <sup>(2)</sup>	.298	.108	.034	.009

Notes: (1) Failed state (some subsystem failed).

(2) Sum of probabilities of states 1 through 14.

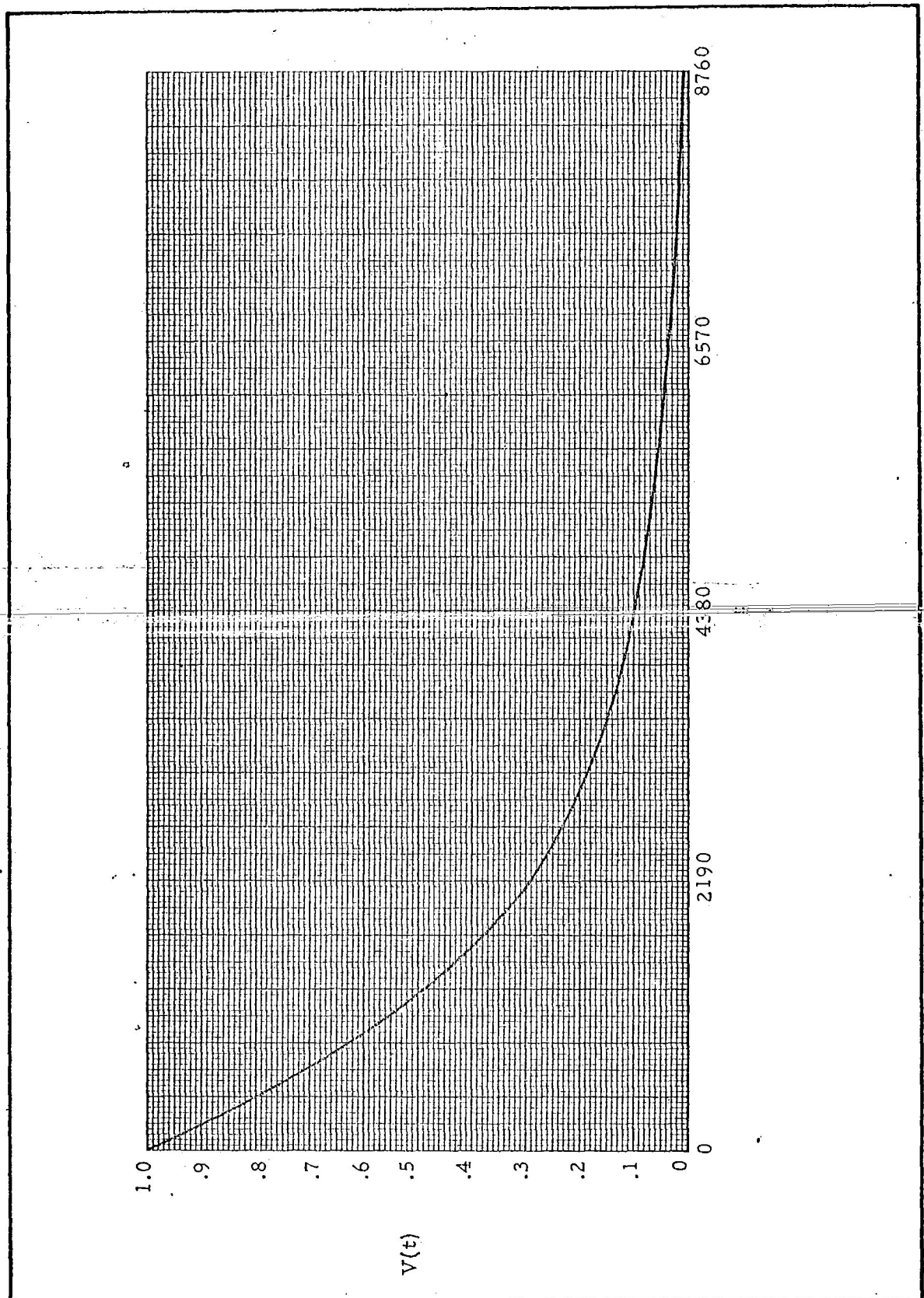


EXHIBIT 4 - GRAPH OF  $V(t)$ , SPACECRAFT FOM SYSTEM RELIABILITY

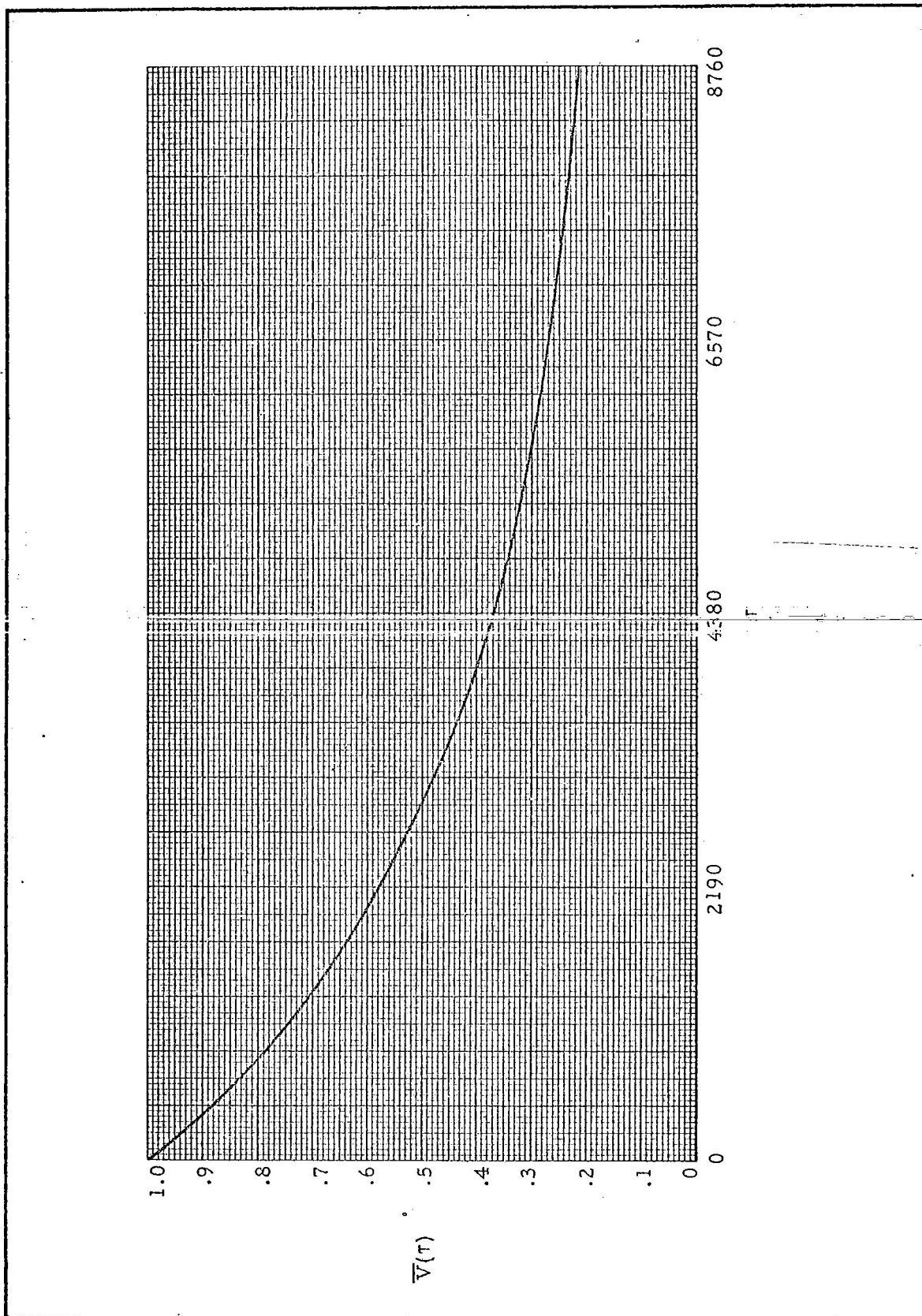


EXHIBIT 5 - GRAPH OF  $\bar{V}(\tau)$ , SPACECRAFT TIME-AVERAGED FOM SYSTEM RELIABILITY

subsystem satisfactory states. That is, system states 1 through 14 in Exhibit 3 are satisfactory. Spacecraft classical reliability  $R(t)$ , then, is given by

$$R(t) = \sum_{i=1}^{14} P(S_i, t) \quad (5)$$

The last row of Exhibit 3 presents numerical values of  $R(t)$  for four mission times of interest. Also, Exhibit 6 presents an interpolated graph of  $R(t)$ .

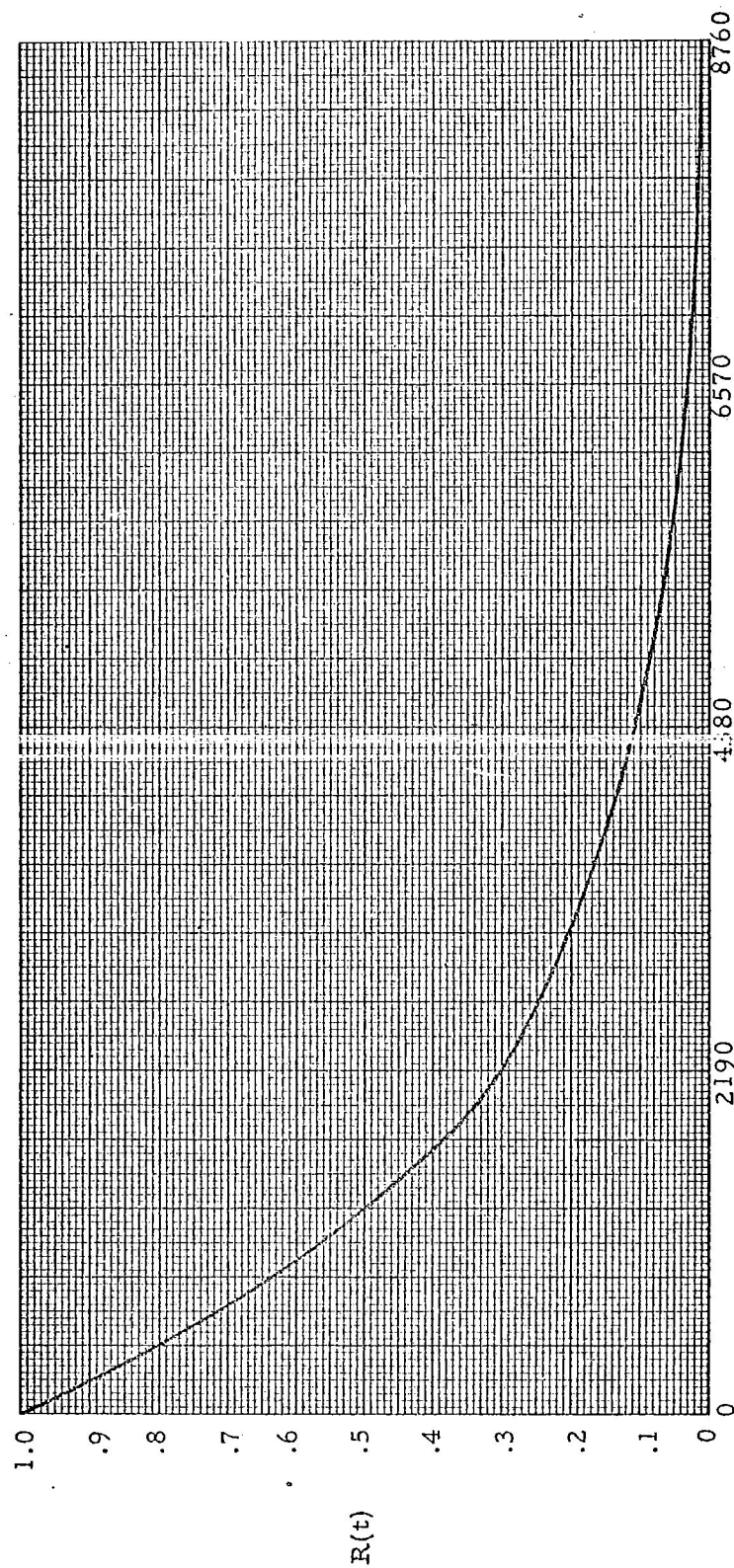


EXHIBIT 6 - GRAPH OF  $R(t)$ , SPACECRAFT CLASSICAL SYSTEM RELIABILITY

## V. CONCLUSIONS AND RECOMMENDATIONS

The second assessment effort has increased the scope of the OGO reliability study and, accordingly, has led to a number of conclusions which supplement or, in some instances, more strongly confirm those that resulted from the first assessment. The analyses and reasoned judgments incorporated into the TAM's that constitute this report set forth the most recent conclusions that have been reached regarding OGO reliability. To facilitate the review and study of these more important inferences, they have been abstracted from the appropriate sections of the report and are presented here in a concise fashion. Certain conclusions lead rather naturally to corresponding recommendations; these have been presented in the TAM's and are not readily susceptible of condensation. Accordingly, the source (or sources) of each conclusion is given in terms of reference TAM numbers.

### A. General System Conclusions

1. The classical reliability goal of 0.70 for 1 year in orbit, established by NASA for OGO, is not likely to be realized. It must be noted that this conclusion is based on the probability that random failures of component parts will not impair the satellite to the extent of losing more than one-third of the experimental data channels prior to 1 year of operation. TAM No. 13 is the source of this conclusion.

2. The probability of completing the launch and acquisition phases without a serious loss due to random failures is relatively high, and there is approximately a 66-percent chance that OGO will conclude its first month of operation with sufficient equipment intact to return at least two-thirds of the experimental data. The graphs in TAM No. 13 bear this out.

3. The Attitude Control and Stabilization Subsystem is the weakest of the five major subsystems from a reliability standpoint. This conclusion must be qualified by noting that the second assessment effort did not include a detailed revision of the CDH Subsystem reliability estimate. The ACS Subsystem reliability estimate of 0.0285 for 1 year reflects a



greater depth of analysis and the inclusion of more failure modes than was possible in the first assessment study of this subsystem. TAM No. 12 provides the detailed reasoning behind this judgment.

4. It is unlikely that the system reliability goals can be met without a drastic revision of the mission objectives and a corresponding simplification of subsystem complexity. There remains some possibility that the use of special, high-reliability piece parts would effect a significant upward change in the reliability estimate; however, the magnitude of this effect cannot be predicted accurately without further study. This somewhat general comment arises from consideration of all of the second assessment work.

5. The failure rates used in this assessment are considerably lower, on the average, than those employed in the first assessment; however, the effects of the rate reductions have been largely offset by the more stringent reliability analysis resulting from the greater depth of the study. Failure rate philosophy is presented in TAM No. 7.

#### B. Communications and Data Handling Subsystem Specific Conclusions

1. The relative increase in the reliability estimate for this subsystem over that resulting from the first assessment reflects the generally lower failure rates used. It should not be inferred that substantial reliability improvements were obtained by subsystem redesign. TAM No. 9 is the source of this conclusion.

2. The main commutator matrix (MCM), as currently implemented, does not constitute the most reliable configuration when viewed on a figure-of-merit basis. The criterion of an economical parts budget is not always a suitable indicator of reliability when the consequences of failure are weighed. Other methods of gating the states of the main commutator counter (MCC) to the MCM should be employed. A generalized approach to the analysis will be found in TAM No. 2, which suggests two alternative gating schemes and points the way to further analysis.

### C. Attitude Control and Stabilization Subsystem Specific Conclusions

1. The pitch and roll channels are less reliable than the array and yaw channels, principally because of the influence of the horizon scanner. TAM No. 12 illustrates this in detail.

2. Redundant piece parts have been applied nonuniformly throughout various areas of the ACS. This is observed particularly in the apparently inconsistent attempts to use semiconductor quads or pairs. Recommendations 2 and 4 of TAM No. 7 are the sources of this conclusion.

3. The logical circuitry implementing many of the ACS functions has not been optimized to achieve the simplicity that would undoubtedly improve reliability. Notably, the earth acquisition circuits and small earth discriminator logic are susceptible of considerable simplification, as is brought out in recommendations 5, 6, and 7 of TAM No. 12. Recommendations 1 and 3 provide further evidence of the basis for this conclusion.

### D. Power Supply Subsystem Specific Conclusions

1. The redesign of the Power Supply Subsystem has eliminated a number of subsystem weaknesses and has significantly improved the subsystem's reliability over that which was estimated in the first assessment. TAM No. 11 documents this conclusion.

2. Batteries remain the weakest link in the Power Supply Subsystem. Although redundancy has been provided in this area, it is effective under all conditions of operation only if the batteries are not discharged beyond the specified limits. The potential redundancy of the charge regulators has not been fully employed, in that each regulator is constrained to operate with only one particular battery. TAM No. 11 furnishes more details for these conclusions.

3. The short-term reliability of the Power Supply Subsystem is relatively high because of the significant degree of redundancy that exists in this subsystem. This is based on a comparison with a non-redundant system that would have an equivalent 1-year reliability. The

graphs of reliability in TAM No. 11 show the redundancy effects in the form of a noticeable departure from the classic exponential form.

E. Thermal Control Subsystem Specific Conclusions

1. The inclusion of the effects of launch environment and the incorporation of test results have significantly lowered the reliability estimate for the Thermal Control Subsystem below the estimate reported in the first assessment. TAM No. 8 is the basis for this conclusion. The reliability of this subsystem continues to be high, however, relative to some of the other subsystems.

2. The transmitters and battery packs are the critical spacecraft locations from the standpoint of thermal control. These heat sources are less tolerant of high temperatures and more difficult to cool. This is discussed in TAM No. 8.

F. Structure Subsystem Specific Conclusions

1. The second assessment, together with a review of STL specifications, drawings, and test reports, indicates that a highly reliable Structure Subsystem may be expected. Launch-induced vibrations, however, may reveal problem areas in the experiment mounting panels and in the folded solar arrays. TAM No. 6 is the source of this conclusion.

2. A decrease in the degree of redundancy within the appendage deployment release mechanism will effect a weight saving of about 0.78 pounds, and, if explosive valves with redundant charges can be employed, the weight reduction can be accomplished with little sacrifice in reliability. TAM No. 5 analyzes the details on which this conclusion is based.

G. Additional Specific Conclusions

1. The loss of attitude control and stabilization, with resultant random tumbling of the satellite, will seriously affect the power supply, but there is reason to believe that some spacecraft functions could be maintained by means of the average incident solar radiation.

A distinct hazard exists, however, in that the uncontrolled thermal situation might allow the batteries to exceed the design temperature limit. This problem is analyzed in TAM No. 3 and TAM No. 8.

2. Comparison of STL's OGO Reliability Report Number II with the PRC first assessment results discloses that differences in failure-rate assignments are a major cause of disagreement in numerical reliability estimates. It is known, however, that other differences between the two studies exist, and most of these involve the more optimistic modeling assumptions governing the STL approach. This conclusion is based on the material in TAM No. 4.